UNIVERSITÀ DEGLI STUDI DI TRIESTE

Dipartimento di Fisica

XXII CICLO DEL
DOTTORATO DI RICERCA IN

NANOTECNOLOGIE

NANOCOMPOSITE SYSTEMS BASED ON METAL NANOPARTICLES AND POLYSACCHARIDES FOR BIOMEDICAL APPLICATIONS

(SSD BIO/10 – Biochimica)

DOTTORANDO

Andrea Travan

DIRETTORE DELLA SCUOLA
Chiar.mo Prof. **Maurizio Fermeglia**
Università degli Studi di Trieste

RELATORE
Chiar. mo Prof. **Sergio Paoletti**
Università degli Studi di Trieste

CORRELATORE
Dott. **Ivan Donati**
Università degli Studi di Trieste

ANNO ACCADEMICO 2008/2009

To my family

Acknowledgements

I would like to thank all the people who have supported me along the whole PhD. I especially acknowledge my supervisor Prof. Sergio Paoletti, my co-supervisor Dr. Ivan Donati, Eleonora Marsich, Gianluca Turco and everyone I worked with during these years. I owe a lot to all of them for all the things they have taught me and for making me feel part of this beautiful group. Finally I thank my family, Giulia, and my friends, for what they meant to me during this adventure.

Table of Contents

Preface

This thesis is submitted in accordance to the requirements of the Graduate School of Nanotechnology for the academic title of Ph.D in Nanotechnology at the University of Trieste. The work has been carried out mainly at the Department of Life Sciences at the University of Trieste, and by the Swiss Research Center CSEM (Centre Suisse d' Electronique et Microtechnique) of Neuchâtel, under the supervision of Prof. Sergio Paoletti and co-supervised by Dr. Ivan Donati. This study was supported by grants from the Italian Ministry for University and Research (PRIN 2007), the Friuli Venezia Giulia Region (LR 26/2005, art. 23 for the R3A2 network), and the EU-FP6 Project “NEWBONE” (Contract Number 026279-2).

The thesis consists of a general introduction, aims of the study, summary and general discussion of the scientific papers given in the appendix.

Summary

The present work is focused on the development of nanocomposite systems for biomedical applications and has been carried out in the framework of the European Project called “Newbone” (EU-FP6); in particular, the main goal of the thesis was to realize biocompatible coatings for orthopedic prosthesis endowed with antimicrobial properties. Nanocomposite systems based on a chitosan-derived polysaccharide (Chitlac) that stabilizes metal nanoparticles (silver and gold) have been prepared in colloidal solutions which possess broad spectrum antibacterial properties. As a complementary work, it was studied and defined a particular chemical mechanism of silver ions reduction carried out by the lactose moieties of Chitlac; the optical properties of the metallic nanoparticles obtained through this mechanism were tested by means of Raman spectroscopy, thus detecting considerable enhancements of the signal due to the SERS effect (Surface Enhanced Raman Scattering). Given the better biological properties of silver-based systems (Chitlac-nAg) with respect to gold in terms of antimicrobial efficacy and biocompatibility, only the former metal was chosen in the following steps towards the preparation of the nanocomposite coating for the prosthesis. Studies on the biocidal mechanism of the Chitlac-nAg solution ascribed the activity to the interaction metal-bacteria membrane. On the other hand, since the lack of physical barriers to nanoparticle diffusion into eukaryotic cells determines the risk of a massive uptake with cytotoxic outcomes, we focused our attention toward the preparation of Chitlac-based three-dimensional structures entrapping silver nanoparticles. To this end, the gel forming properties of the polysaccharide alginate were exploited allowing the production of a semi-solid system in a mixture with Chitlac-nAg: this material displays potent antibacterial properties without showing cytotoxic effects towards eukaryotic cells, as verified by *in vitro* and *in vivo* tests. Such result was particularly important in relation to the state of the art in this research field. Since the core material of the prosthesis is made of methacrylic thermosets, in order to coat this substrate material we have devised a technique based on surface activation followed by deposition of the Chitlac-based layer. Such technique allows obtaining a nanocomposite coating where silver nanoparticles are entrapped within the Chitlac matrix. This bioactive layer endows the thermoset surface with considerable antimicrobial properties, as bacteria are rapidly killed upon direct contact with the material. At the same time, *in vitro* tests proved that eukaryotic cells adhere and proliferate on the nanocomposite coating, which indicates the possibility to have good integration of the material in the tissues surrounding the implant. The combination of these properties determined the choice of our coating for the final *in vivo* test in a minipig model as a conclusion of the European project; this test is in progress at the moment and it will hopefully confirm the encouraging studies *in vitro*.

Sommario

Questo lavoro riguarda lo sviluppo di materiali nanocompositi per applicazioni biomediche e si configura all' interno del progetto europeo "Newbone" (EU-FP6); in particolare, lo scopo principale della tesi era realizzare un rivestimento biocompatibile e dotato di proprietà antibatteriche per protesi ortopediche. Sono stati preparati sistemi nanocompositi basati su un polisaccaride derivato dal chitosano (Chitlac) che permette di ottenere soluzioni colloidali di nanoparticelle (argento e oro) con proprietà antibatteriche. Parallelamente, è stato studiato un particolare meccanismo chimico di riduzione degli ioni argento ad opera dei residui di lattitolo del Chitlac; le proprietà ottiche delle nanoparticelle ottenute attraverso questo meccanismo sono state valutate attraverso spettroscopia Raman, evidenziando la possibilità di avere un incremento del segnale grazie al verificarsi dell' effetto SERS. Essendo state riscontrate migliori proprietà biologiche del sistema a base di argento (Chitlac-nAg) rispetto a quello a base di oro in termini di efficacia antimicrobica e biocompatibilità, Chitlac-nAg è stato scelto per i successivi studi di realizzazione del rivestimento per la protesi. Test sul meccanismo antimicrobico della soluzione Chitlac-nAg hanno dimostrato l'interazione tra le nanoparticelle e la membrana batterica. Allo stesso tempo, poiché la mancanza di barriere fisiche può favorire la diffusione delle nanoparticelle all' interno delle cellule eucariote con rischio di effetti citotossici causati dalla loro internalizzazione, si è voluto realizzare delle strutture tridimensionali a base di Chitlac in grado di intrappolare le nanoparticelle. A questo scopo, sono state sfruttate le proprietà di gelificazione del polisaccaride alginato in modo da ottenere un sistema semi-solido in miscela con Chitlac-nAg; il materiale ottenuto possiede marcate proprietà antibatteriche senza però risultare tossico per le cellule eucariote, come dimostrato da test *in vitro* e *in vivo*. Questo risultato è particolarmente importante in relazione allo stato dell' arte sull' argomento. Poiché la parte portante della protesi è costituita da un polimero metacrilico, al fine di rivestire questo materiale di substrato è stata messa a punto una tecnica basata sull' attivazione della superficie e successiva deposizione del rivestimento a base di Chitlac. Questa tecnica permette di ottenere un rivestimento nanocomposito costituito da nanoparticelle di argento incorporate nella matrice di Chitlac. Grazie a questo strato bioattivo la superficie della protesi acquisisce un' efficace attività antibatterica che si manifesta quando i batteri entrano in diretto contatto con il materiale. Inoltre, test *in vitro* hanno dimostrato che le cellule eucariote aderiscono e proliferano sul rivestimento nanocomposito, suggerendo quindi una buona integrazione del materiale nei tessuti attorno all' impianto. La combinazione di tali proprietà ha determinato la scelta di questo rivestimento per il test *in vivo* su "minipig" a conclusione del progetto europeo: questo test è al momento in via di svolgimento e da esso ci si può attendere una conferma degli incoraggianti risultati ottenuti dagli studi *in vitro*.

ARTICLE PUBLISHED ON THE NANOTECHNOLOGY PORTAL

“NANOWERK”

NANOWERK SPOTLIGHT

(http://www.nanowerk.com/spotlight/spotid=11406.php)

Posted: June 29, 2009

“How to make nanosilver non-cytotoxic with sugar “

(Michael Berger)

This on-line article posted on the website www.nanowerk.com was based on the scientific results discussed by the author in Paper 2 (Travan *et al.*, “Non-cytotoxic Silver Nanoparticle-Polysaccharide Nanocomposites with Antimicrobial Activity”. *Biomacromolecules* 2009, 10, 1429–1435).

.

List of Appendix Papers

1. Ivan Donati, **Andrea Travan**, Chiara Pelillo, Anna Coslovi, Alois Bonifacio, Valter Sergo, Sergio Paoletti. Polyol Synthesis of Silver Nanoparticles: Mechanism of Reduction by Alditol Bearing Polysaccharides. *Biomacromolecules*, 2009, 10 (2), 210-213

2. **Andrea Travan**, Chiara Pelillo, Ivan Donati, Eleonora Marsich, Monica Benincasa, Tommaso Scarpa, Sabrina Semeraro, Gianluca Turco, Renato Gennaro, Sergio Paoletti. Non-Cytotoxic Silver Nanoparticle – Polysaccharide Nanocomposites with Antimicrobial Activity. *Biomacromolecules* 2009, 10, 1429–1435

3. **Andrea Travan**, Ivan Donati, Eleonora Marsich, Francesca Bellomo, Satish Achanta, Sabrina Semeraro, Tommaso Scarpa, Mila Toppazzini, Vittorio Spreafico, Sergio Paoletti. Surface Modification and Polysaccharide Deposition on BisGMA/TEGDMA Thermoset. *Biomacromolecules* 2010, 11, 3, 583-592

4. **Andrea Travan**, Eleonora Marsich, Ivan Donati, Monica Benincasa, Marta Giazzon, Laura Felisari, Sergio Paoletti. Silver-Polysaccharide Nanocomposite Antimicrobial Coatings for Methacrylic Thermosets. Submitted to *European Cells and Materials Journal* (2010)

5. Eleonora Marsich, **Andrea Travan**, Ivan Donati, Andrea Di Luca, Monica Benincasa, Sergio Paoletti. Cytotoxicity Evaluation of Hydrogels Embedding Gold Nanoparticles. Manuscript in preparation

6. **Andrea Travan**, Eleonora Marsich, Ivan Donati, Sergio Paoletti. Silver nanocomposites and their biomedical applications. Chapter of the peer-reviewed Book entitled "Nanocomposites for the Life Sciences". In press, *Wiley-VCH* (2010)

Contributions to other publications not included in the thesis:

- Francesco Brun, **Andrea Travan**, Agostino Accardo, Sergio Paoletti. Characterization of Silver Nanoparticles For Biomedical Applications By Means Of Quantitative Analysis of TEM Micrographs. *Biomedical Sciences Instrumentation* 2010 (In press).

Patents filed:

- **Andrea Travan**, Ivan Donati, Eleonora Marsich, Sergio Paoletti. Materiali nanocompositi basati su nanoparticelle metalliche stabilizzate con polisaccaridi a struttura ramificata (Italian Patent 8853 PTIT 2009)
- **Andrea Travan**, Ivan Donati, Eleonora Marsich, Sergio Paoletti. Materiali nanocompositi formati da una matrice polisaccaridica e nanoparticelle metalliche, loro preparazione ed uso (Italian Patent 8981 PTIT 2009)
- **Andrea Travan**, Ivan Donati, Elonora Marsich, Sergio Paoletti. Nanocomposite materials based on metallic nanoparticles stabilized with branched polysaccharides. PCT Patent extension (2010)
- **Andrea Travan**, Ivan Donati, Elonora Marsich, Sergio Paoletti. Three-dimensional nanocomposite materials consisting of a polysaccharidic matrix and metallic nanoparticles, preparation and use thereof. PCT Patent extension (2010)

1. INTRODUCTION

1.1 SILVER NANOCOMPOSITES

By definition, nanocomposites are materials containing domains or inclusions that are of nanometer size scale[1]. Nanocomposite materials that exploit the properties of silver at the nanoscale for biomedical applications are of increasing interest in the scientific literature (Figure 1) and today they can be found in many commercial products, like wound dressings and creams.

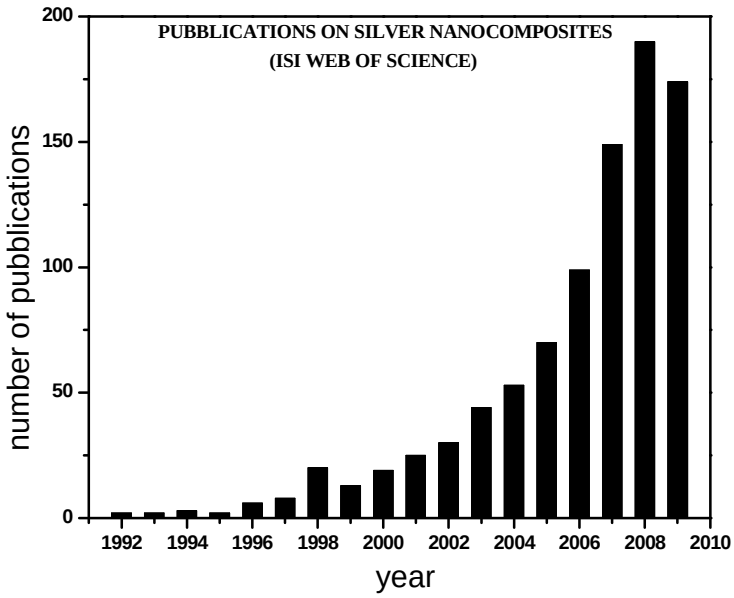

Figure 1. Publication counts derived from the Thompson ISI Web of Science database on October 2009, using the key word “silver nanocomposites”.

The idea behind these novel materials is that silver at the nanometer scale displays unique properties that can be used for different purposes, ranging from antimicrobial to optical and catalytic applications[2;3].

1.2 PREPARATION AND CHARACTERIZATION OF SILVER NANOCOMPOSITES

1.2.1 Preparation Techniques

Since silver nanocomposite constructs are meant to exploit the properties of silver at the nano-scale, many efforts are aimed at finding efficient and reproducible routes to produce silver nanoparticles (hereafter AgNPs). Many potential uses for these novel materials are being explored, ranging from antimicrobial purposes to molecular imaging.

When preparing homogeneous nanocomposite materials containing AgNPs, a crucial issue is the tendency of nanoparticles to aggregate, which leads to the loss of the peculiar properties associated with the nano-scale. For instance, in the antimicrobial field, studies by Lok *et al.*[4] revealed that non-stabilized AgNPs prepared by standard chemical methods (reduction of silver salt solutions) tend to aggregate in culture media and biological buffers which have high salt contents (chloride and phosphate being considered the most problematic anions): the aggregation leads to a decrease in the effective surface of the nanoparticles or the degree to which they can associate to bacteria.

The so called "*ex situ*" preparation methods consist in the synthesis of nanoparticles as a first step, and then in mixing the pre-formed nanoparticles with a matrix (typically a polymer); however with this conventional technique it is difficult to disperse homogeneously the nanoparticles[5]. At variance, an "*in situ*" approach aims at synthesizing the nanoparticles within a suitable matrix in order to achieve a homogeneous dispersion in the composite materials.

To date, the preparation and stabilization of metal nanoparticles represent an open challenge. The methods for preparing non-aggregated AgNPs for biomedical applications can be divided into two groups[6]:

- wet chemical synthesis in the presence of a reducing agent and a stabilizing agent;
- synthesis through physical processes

The chemical approach is based on the use of a silver salt in an aqueous environment; silver ions are then reduced to zeroth-valent silver in the presence of a stabilizing agent in order to limit aggregation of the so-formed nanoparticles. The stabilizing agent is meant to cap the particles and prevent further growth. The most accepted mechanism for the synthesis of a particle suggests a two-step process, *i.e.*, nucleation followed by successive growth. In the first step, part of the metal ions in solution is reduced by a suitable reducing agent. The atoms thus produced

act as nucleation centres and catalyze the reduction of the remaining metal ions present in the bulk solution. The atomic coalescence leads to the formation of metal clusters whose dimensions can be controlled by ligands, surfactants or polymers; in the absence of a stabilizer, clusters in aqueous solution undergo further growth leading ultimately to precipitation of the metal[7].

Polymers and more generally many organic molecules can bind to the particle surface and thus serve the role of stabilizer. In general, the stabilization of metal nanoparticles is explained by the electronic interaction of the polymer functional groups with the metal particles. In fact, nucleophilic groups can bind the metal particles by donating electrons[8]. A common approach to prepare stable AgNPs involves the use of polymer solutions: to this end, a variety of polymers can be used, ranging from synthetic to natural ones. Nitrogen-containing stabilizing polymers, such as poly-(ethyleneimine) and poly(vinylpyrrolidone), act *via* lone electron pairs. Protective polymers can coordinate metal ions before reduction, forming a polymer-ion complex; such a complex can then be reduced under mild conditions, resulting in metal particles of smaller dimensions and a narrower size distribution than those obtained without protective polymers[9]. Once the reduction occurred, the stabilizing effect of these macromolecules is attributable to the fact that either the particles are attached to the much larger protecting polymers or the protecting molecules cover or encapsulate the metal particles[10]. This chemical approach can be generalized in Figure 2.

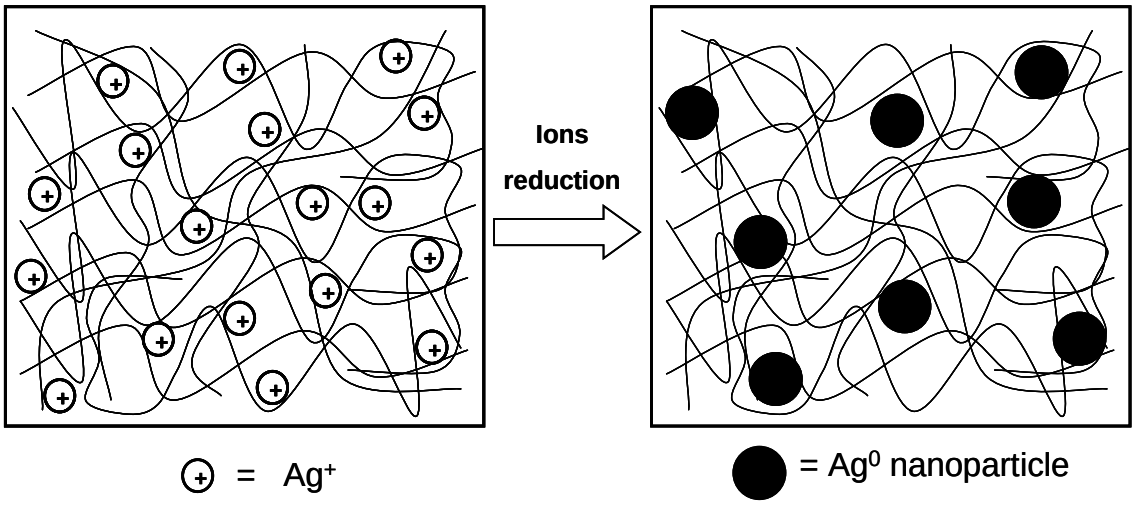

Figure 2. Preparation of AgNPs in the presence of a stabilizing polymer (wet synthesis)

In particular, owing to the presence of many different functional groups, polyelectrolytes are successfully used in the preparation of stable AgNPs. Polyelectrolytes at low concentrations (such as polyphosphate, polyacrylate, poly-(vinyl-sulfate), poly-(ethylene-imine)[2;11;12], poly-(allyl-amine)[10], and chitosan[13-15]) have been used with different outcomes to stabilize

nanoparticles preventing the growth of aggregates. As already mentioned, poly-(vinyl-pyrrolidone)[5;16], a neutral polymer, has been widely used for the stabilization of silver nanoparticles. It must be noticed that in order to find applications in the field of biomaterials, both the stabilizing and the reducing agents must not represent a biological hazard[17].

Considering the reduction step, various exogenous agents can be used, such as ascorbic acid[18;19], sodium borohydride[20], sodium citrate[21;22], alcohols[23], hydrogen[24], polyols, hydroxyalkyl radicals, and aldehyde groups of reducing sugars[25-27]. For a "green synthesis" of nanoparticles[28], reducing saccharides can be used as non-toxic and environmental-friendly reducing agents. In this case the synthesis is based on a Tollens reaction that involves the reduction of a silver ammoniacal solution with a reducing sugar (*e.g.,* glucose, maltose, xylose…)[29].

By the choice of the stabilizer and the reducing agent, one can control the growth process and manipulate shape and size of the metal nanoparticles in the nanocomposites. For instance, a lactose-substituted chitosan (1-deoxylactit-1-yl chitosan, shortly named "Chitlac") was successfully used to prepare stable silver nanoparticles using this particular polymer either as stabilizing agent only, or as both reducing and stabilizing agent at the same time[30;31]. In the first case, the nanoparticles are obtained in a polysaccharide solution with silver ions reduced by ascorbic acid ($C_6H_8O_6$) according to the following stoichiometry[32;33]:

$$2Ag^{+} + C_6H_8O_6 \rightleftharpoons 2Ag^{0} + C_6H_6O_6 + 2H^{+}$$

The nanoparticles thus obtained were mostly round-shaped and well dispersed with an average diameter of 30 nm as revealed by image analysis based on transmission electron micrographs.

This polysaccharide acts as an efficient stabilizing ligand for silver ions and AgNPs thanks to the presence of amino groups. Esumi *et al.*[34] demonstrated that metal nanoparticles can be protected by the exterior amino groups of dendrimers which act as stabilizers.

Huang *et al.*[35]discussed the preparation of silver-chitosan nanocomposites obtained by chemical synthesis from a chitosan solution in the presence of $AgNO_3$ reduced by $NaBH_4$; the evaporation of the solvent in this colloidal solution brings to the formation of a nanocomposite film. The morphology of the film shows a rod-like structure, whose formation is attributed to the presence of the silver clusters that act as an accelerant to the precipitation of polymer crystallites.

Silver nanocomposites can be prepared in the form of nanofibres by means of the electrospinning technique, a process by which a suspended droplet of polymer solution is charged to high voltage to produce fibres with a diameter typically smaller than 500 nm. If the solution contains AgNPs

stabilized by the polymer, it is possible to obtain nanocomposite fibres. Wang *et al.*[5] successfully prepared AgNPs through reduction of $AgNO_3$ by ethanol in PVP/ethanol solution and managed to obtain nanocomposite fibres with AgNPs smaller than 10 nm.

The need to obtain antimicrobial coatings and films can be fulfilled by incorporating AgNPs into polymeric matrixes by means of the so-called "layer-by-layer" technique. This is a simple and straightforward approach based on the alternate deposition on a substrate of layers of polyelectrolytes with opposite charges through a dipping process (Figure 3, left).

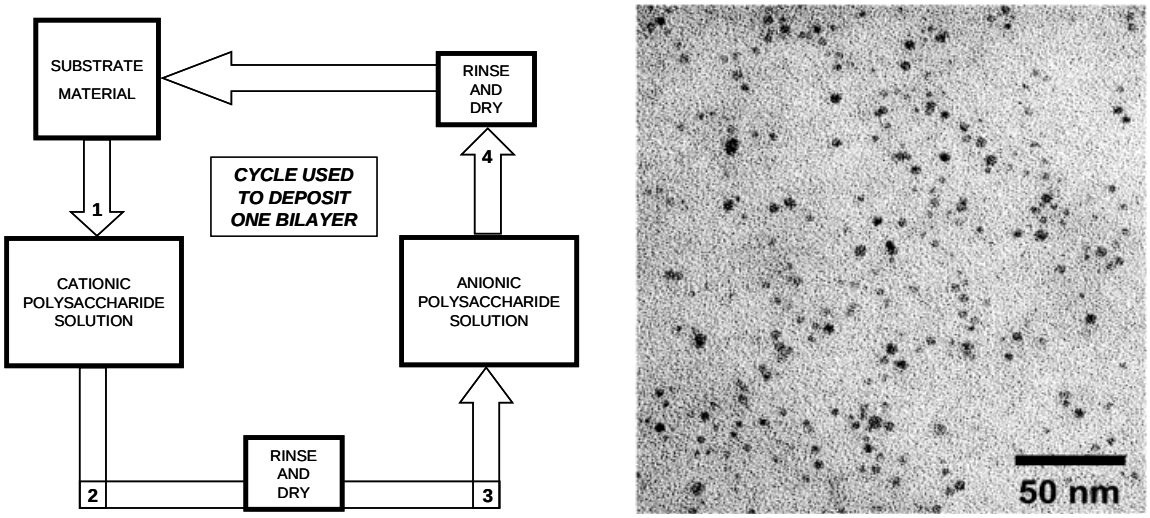

Figure 3. Left) Schematics of the layer-by-layer self-assembly procedure for creating polymeric thin films, adapted from Grunlan *et al.* (2005). Right) TEM image of a silver-PEI-PAA film that shows the dispersion of spherical AgNPs with a mean diameter of 4 nm. From Dai *et al.* (2002), reproduced with permission.

The dipping process is repeated until a desired number of layers is obtained, each layer having a thickness in the range of a few nanometers. With this method it is possible to incorporate in one or more layers bioactive agents like silver. According to this approach, Grunlan *et al.*[36] prepared polyelectrolyte multilayers using silver nitrate and/or cetrimide (antiseptic agent) as antimicrobial agents. The films were prepared by alternately dipping poly(ethylene terephtalate) (PET) substrate into solutions of poly(acrylic acid) (PAA) and poly(ethylene imine) in mixture with the bioactive agents. Dai *et al.*[2] followed the layer-by-layer approach to obtain multilayered polyelectrolyte films that incorporate homogeneously dispersed AgNPs; in this work a polyethyleneimmine (PEI) solution was used to prepare stabilized silver ions from $AgNO_3$. Then, the alternated deposition on a substrate of the PEI-silver layer and of a poly(acrylic acid) (PAA) solution followed by reduction with $NaBH_4$ led to the formation of a multilayered film based on the two oppositely charged polysaccharides containing finely dispersed AgNPs (Figure 3, right).

Multilayers can be fabricated by means of the layer-by-layer technique not only on planar substrates, but also on three-dimensional templates. In the case of a spherical template, its eventual dissolution after the film formation allows obtaining multlayered capsules that can embed bioactive agents like AgNPs; Choi *et al.*[37]synthesised polyelectrolyte capsules with two types of nanoparticles embedded: AgNPs for the antimicrobial activity and goethite nanoparticles to endow the capsules with the possibility to be moved by external magnetic fields. The capsules were prepared by means of copolymerized polyelectrolytes composed of poly(styrene sulfonate) (PSS) and poly(acrylic acid) (PAA) in addition to poly(allylamine hydrochloride) (PAH). Then, metal ions were loaded from aqueous solution into the capsules and were finally let react to create the two different types of nanoparticles. Ho *et al.*[38]developed a nanocomposite film where a polymer network based on poly(ethylene imine) derivatized with double bonds was copolymerized with 2-hydroxyethyl acrylate; after a UV-initiated polymerization the film was loaded with silver ions that were subsequently reduced to form AgNPs. After immersing the film in $AgNO_3$ solution, the chemical reduction of Ag^+ complexed within the polymer network occurred by treating the film in ascorbic acid solution until the film turned to yellowish-brown, which suggests the formation of well dispersed nanoparticles.

Polyols can be used as reducing agents for silver ions: in this case, the silver-reduction mechanism typically involves a heat treatment. Wiley *et al.*[39;40] prepared AgNPs with different shapes (quasi-spherical particles, single-crystal cubes, tetrahedrons, rods, triangular nanoplates, nanowires with pentagonal cross sections, twinned structures…) by reducing $AgNO_3$ with ethylene glycol at high temperature in the presence of PVP.

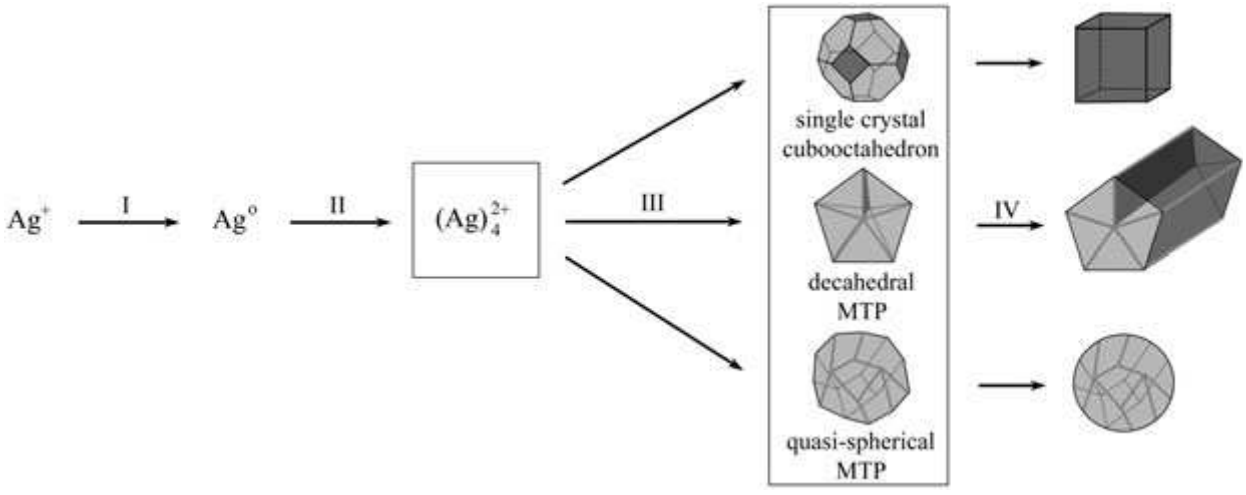

Figure 4. Schematic showing the reduction of silver ions by ethylene glycol (I); the formation of silver clusters (II); the nucleation of seeds (III); and the growth of seeds into nanocubes, nanorods or nanowires, and nanospheres (IV). From Wiley *et al.* (2005), reproduced with permission.

These studies showed how the crystallinity of seeds was determined by the molar ratio between the capping agent (PVP) and $AgNO_3$ as well as by the strength of the chemical interaction between the polymer and various crystallographic planes of silver (Figure 4).

Silver nanocomposites can be prepared using polymeric dendrimers as stabilizing agents. In fact dendrimers are branched macromolecules that possess architecture and ligand sites that allow the pre-organization of metal ions and an effective stabilization of silver owing to the formation of stable complexes at atomic/molecular level dispersion. Balogh *et al.*[41] discussed the preparation of silver complexes within poly(amidoamine) dendrimers for antimicrobial applications. Kuo *et al.*[10] reported the formation of AgNPs stabilized in pseudo-dendritic poly(allylamine) derivates.

Following the same strategy, other organic macromolecules can be used to stabilize AgNPs: for instance Lok *et al.*[42] reported the preparation of antimicrobial AgNPs stabilized by bovine serum albumin (BSA).

Inorganic stabilizers are also being explored for the preparation of silver nanocomposites. Su *et al.*[43] prepared AgNPs immobilized within inorganic phyllosilicate clays in order to obtain nanohybrids exploiting an ion exchange between Ag^+ (provided by $AgNO_3$) and Na^+ from the clay, followed by *in situ* reduction of silver ions by methanol at 80°C. In this case the nanoparticles thus formed are free of polymeric surfactants and have a narrow size distribution with an average diameter around 30 nm (Figure 5).

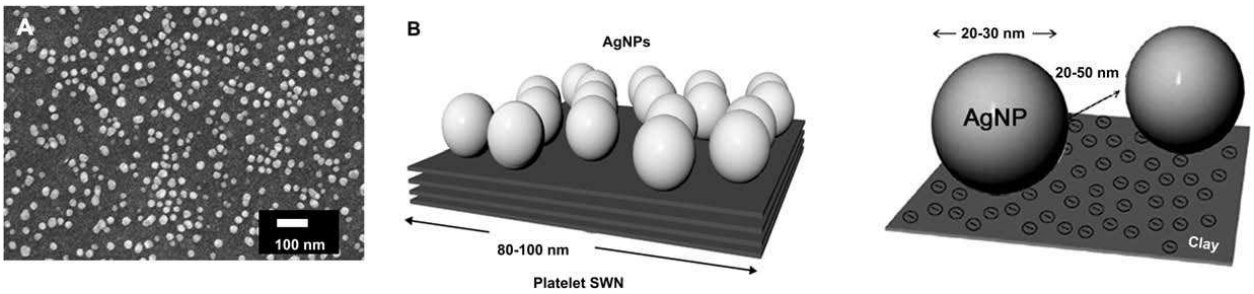

Figure 5. Silver nanoparticles dispersed on silicate clay. (A) The surface structure of the AgNP/Clay is characterized by Field-Emission SEM. (B) Representations of the nanocomposite structure. From Su *et al.* (2009), reproduced with permission.

Silver nanocomposites can be obtained in the form of bioceramics in order to endow osteoconductive materials with antimicrobial properties. Rameshbabu *et al.*[44] prepared silver-substituted hydroxyapatite nanocrystals by microwave processing.

Although the conventional chemical synthesis represents to date the most popular approach for the preparation of silver nanocomposites, other techniques are being explored which are based

on physical processes. A promising technique is the radiolytic method used for the generation of AgNPs in solution; with this technique, radiolytically generated species, solvated electrons and secondary radicals, exhibit strong reducing potentials towards metal ions. Krkljes *et al.*[45] reported the preparation of Ag-PVA nanocomposites by radiolytic procedure using steady state gamma irradiation.

Alternatively, ablation of a metal surface immersed in a liquid can produce nanoparticles of the metal in the liquid. In the laser ablation technique metal atoms and small metal clusters are ablated from a metal rod by laser irradiation; self-aggregation of the nanoparticles suspended in the liquid can be prevented by hindering direct contact of the nanoparticles by means of a surfactant. Mafunè *et al.*[46] performed the preparation of AgNPs by laser ablation against a silver plate in an aqueous solution of sodium dodecyl sulphate.

Photochemical methods can be used to prepare polymer-stabilized AgNPs[47]. Mallick *et al.*[48] prepared colloidal silver under UV photo irradiation of silver nitrate solution in the presence of methoxy poly(ethylene glycol) which acts as a reducing and stabilizing agent.

Further interesting routes to prepare silver nanocomposites are sonochemical treatments[49], potentiostatic and galvanostatic methods[50], vapour deposition[51], microwave irradiation[52], electron beam irradiation[53], synthesis templated by DNA[54], Langmuir-Blodgett-based techniques [55], ion implantation, sputtering, vapor-phase co-deposition, and vacuum co-condensation[56].

1.2.2 Characterization Techniques

The characterization of silver nanocomposites can be performed by means of different techniques; the most important ones are spectroscopic techniques (UV-Vis, infrared and X-ray photoelectron spectroscopy), X-ray diffraction and microscopic techniques (TEM, SEM, Dark-Field, AFM, NSOM).

In the chemical synthesis, colloidal solutions of AgNPs are obtained upon reduction of Ag^+ to the metal atom and consecutive coalescence of atoms yelding larger particles. The transition from atom to metal nanoparticle can be studied by pulse radiolysis techniques[57;58]. When a sufficient number of atoms coalesce, the particles start to display a typical property called “Surface Plasmon Resonance”, which is produced by a collective excitation of all the free electrons in the particles[59]. Under the influence of the electric field due to the incoming light, the movement of electrons leads to a dipole excitation across the particle sphere that makes the electrons oscillate (Figure 6, left).

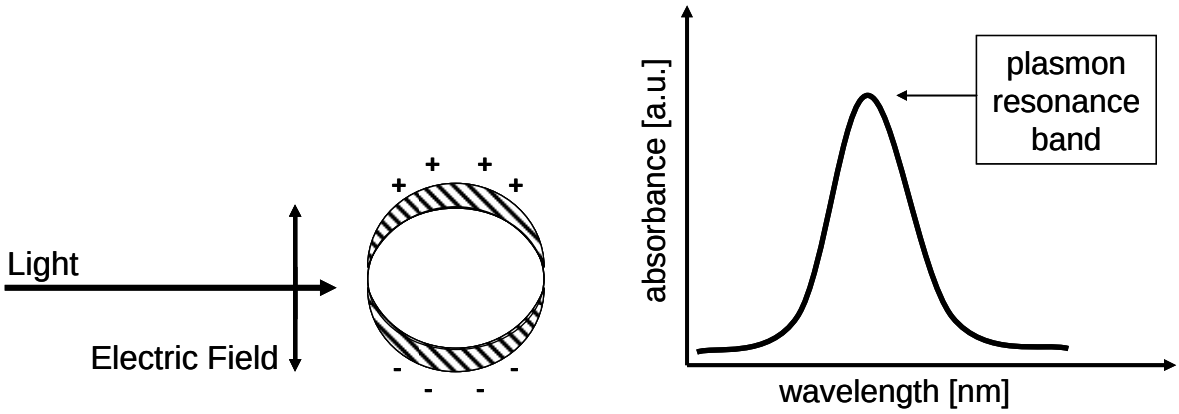

Figure 6. Left) Polarization of a spherical metal particle by the electrical field vector of the incoming light. Adapted from Henglein (1993). Right) A plasmon resonance band in the UV-Vis spectrum accounts for the presence of metallic nanoparticles.

The electron density within a surface layer (a few angstroms thick) oscillates, while the density in the interior of the particle remains constant. When the condition of resonance is reached, the UV-Vis spectrum displays an intense absorption band called "Surface Plasmon Resonance Band" (Figure 6, right). A symmetrical shape of the plasmon band suggests that the nanoparticles are well dispersed and spherical[10]. At variance, the aggregation of nanoparticles leads to a broader plasmon band, with a red-shifted maximum[60]. A systematic study on the formation of silver nanoparticles by absorption spectroscopy was tackled by Henglein[61] who reported the preparation of AgNPs from $AgClO_4$ solutions at a fixed concentration and studied the variations of the UV-Vis spectra as a function of the concentration of sodium citrate used as both reducing and capping agent. The UV-Vis spectra suggested that sodium citrate plays a drastic effect on the formation of AgNPs with different size; in fact according to its concentration it can determine the formation of well stabilized AgNPs or the coalescence of poorly stabilized polycrystallites.

Excess charge carriers influence the wavelength of the plasmon resonance band; a blue shift of the plasmon peak occurs upon electron donation to the particles, while a red shift occurs upon injection of positive holes into the particles. Furthermore, chemical modification on the surface of the particles, like interaction with organic molecules, strongly affects the plasmon absorption band.

Anions able to form complexes or insoluble salts with silver ions are strongly adsorbed on silver particles. Also the Fermi level floats upon chemisorption, depending whether the adsorbed molecule is nucleophilic or electrophilic. A surface atom carrying an adsorbed nucleophile molecule acquires a slightly positive charge ("preoxidation state"); the excess electron density is simultaneously transferred into the metal particle. Thus, the chemisorption of a nucleophile is

accompanied by a shift of the Fermi potential to a more negative value. AgNPs are highly sensitive to oxygen, resulting in the formation of partially oxidized AgNPs with chemisorbed Ag^+ on the surface. In the absorption spectra this partial oxidation leads to a red-shift of the surface plasmon resonance band, according to the following equation[62]:

$$\lambda = \lambda_0(1 + [Ag^+]/[Ag])^{1/2}$$

where λ_0 is the wavelength of the plasmon peak before oxidation, and λ after oxidation.

Lok *et al.*[63] reported that borohydride reduced (zeroth-valent) AgNPs in the presence of citrate exhibit a surface plasmon resonance peak at 375 nm, while subsequent exposure to oxygen led to a rapid shift of the absorption peak to 398 nm, with broadening of the band width and lowering of the maximum absorption. These changes in the absorption spectrum can be attributed to the partial oxidation of the nanoparticles with the formation of chemisorbed Ag^+ on their surface, indicating the sensitivity of AgNPs to oxygen. Further addition of borohydride induced a shift in the plasmon resonance band to the intensity and shape of non-oxidized zeroth-valent nanoparticles. It is important to notice that the presence of oxidized (or partially oxidized) atoms on the surface of the nanoparticle affects its biological properties, as discussed in chapter 3.4.
Infrared spectroscopy (IR) can provide information about the interaction (chemical bonding) between the nanoparticles and the matrix in a silver nanocomposite structure. Krkljes *et al.*[64] carried out IR analysis to point out the interaction between AgNPs and PVA chains *via* its OH groups. By means of Fourier Transform IR Dai *et al.*[2] characterized poly(acrylic acid)/polyethyleneimine-silver nanocomposites in order to evaluate the influence of silver reduction on the polymer matrix and Zhang *et al.*[65] verified the formation of coordination bonds between the amino/amide groups of a poly(amidoamine) derivative and AgNPs.
Transmission Electron Microscopy (TEM) is commonly used to investigate size, structure (crystallography, existence of twin planes, stacking faults…) and dimensional distribution of AgNPs. Wiley *et al.*[40;66] carried out TEM investigations to study a polymer-mediated polyol process that allows for the preparation of silver nanostructures with a number of different morphologies (*e.g.*, cubes, rods, wires, and spheres) as reported in Figure 7.

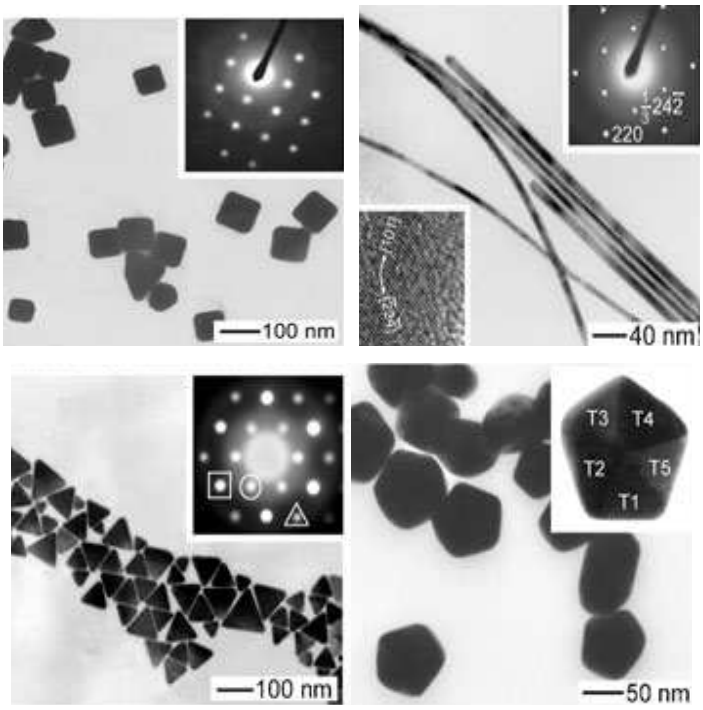

Figure 7. TEM characterization of AgNPs with different morphologies obtained by polyol synthesis. From Wiley *et al.* (2005), reproduced with permission.

Wang *et al.*[67] prepared polyelectrolyte multilayer films containing AgNPs and evaluated the distribution of the particles in the polymer matrix by means of cross-sectional TEM imaging. The pictures show spherical particles uniformly and randomly distributed throughout the film (Figure 8, left).

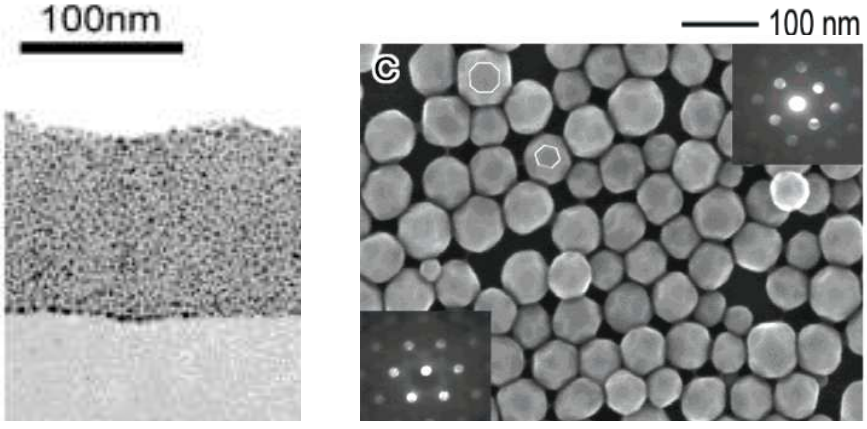

Figure 8. Left) Cross-sectional TEM image of a polyelectrolyte multilayer containing AgNPs. From Wang *et al.* (2002), reproduced with permission. Right) FE-SEM image of AgNPs obtained by polyol synthesis. The main image shows truncated cubes (indicated by an octagon) and truncated tetrahedrons (indicated by a hexagon), while the insets show the convergent beam electron diffraction patterns showing that these particles are single crystals. From Wiley *et al.* (2004), reproduced with permission.

Metal nanocomposites have been studied by means of Scanning Electron Microscopy (SEM), especially equipped with field-emission guns (FE-SEM) that allow avoiding the sputtering step of conventional SEM which could cover or affect the nanoparticles on the surface of the nanocomposite material[68;69]. Wiley *et al.*[70] carried out a polyol synthesis of AgNPs whose structure was analysed by FE-SEM: the images proved the formation of single-crystal, truncated cubes and tetrahedrons (Figure 8, right).

Among other techniques, Atomic Force Microscopy (AFM) is a useful means to characterize the morphology of nanocomposites materials containing a dispersion of nanoparticles[71;72]. Deshmukh *et al.*[73] explored by AFM the surface and bulk morphology of poly(methyl methacrylate) (PMMA) nanocomposite films containing AgNPs. Figure 9 (left) shows AFM image of the nanoparticles on the surface of the polymer film.

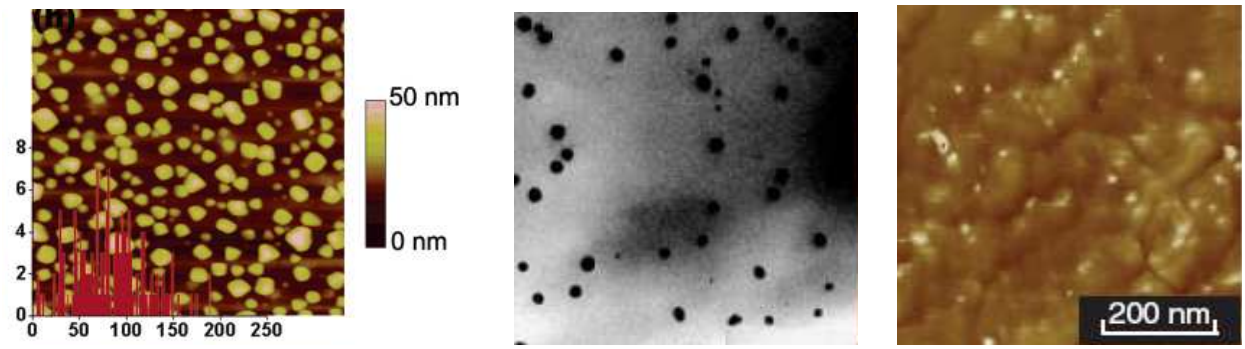

Figure 9. Left) AFM image and size distribution of silver nanoparticles dispersed in a PMMA film. The x-axis corresponds to the size of the protruding nanoparticles covered by the PMMA layer. From Deshmukh *et al.* (2007), reproduced with permission. Centre and Right) TEM image of a cross section and AFM (phase mode) image of the surface of poly(ethylene imine)-based films containing silver nanoparticles. From Ho *et al.* (2004), reproduced with permission.

Ho *et al.*[38]compared AFM and TEM techniques to characterize nanocomposite films based on poly(ethylene imine) and AgNPs. AFM images in the phase-contrast mode show the dispersion of nanoparticles that appear as bright spots on the surface of the film, while the corresponding TEM image of a cross-section of the film indicates the presence of non-aggregated nanoparticles with a size that ranges from 4 to 50 nm (Figure 9, centre and right).

The crystallographic structure of AgNPs formed within a matrix can be studied by means of XRD. Wang *et al.*[5] used such technique to carachterize Ag/PVP nanocomposite films: the XRD pattern revealed the presence of face-centred cubic (fcc) nanocrystals formed within the polymer matrix.

X-ray photoelectron spectroscopy (XPS) is a surface chemical analysis technique that can be used to analyze silver-nanocomposite materials. XPS was used by Zeng *et al.*[74] to characterize

polymer films (poly(styrene) and acrylonitrile–styrene copolymer) filled with silver nanoparticles: this technique pointed to the existence of charge transfer interaction between AgNPs and acrylonitrile segments, while no obvious interaction between silver and styrene segments was found. Stofik *et al.*[75]prepared silver-dendrimer nanocomposites for immunosensors application and confirmed with XPS the synthesis of AgNP. XPS studies on PVP-silver nanocomposite fibres showed the interaction between silver and the carbonyl oxygen; this strong Ag:O coordination can prevent AgNPs from aggregation within the polymer matrix[5].

Silver nanoparticles are extremely bright and can be directly observed using dark-field single nanoparticle optical microscopy and spectroscopy; with this technique Lee *et al.*[76] characterized AgNPs embedded in zebrafish embryos for studying their transport, biocompatibility, and toxicity in real time. Lu *et al.*[77] reported dark-field images of a high-density nanocomposite film obtained from poly (*N*-isopropylacrylamide) and AgNP.

Silver nanocomposites have also been characterized by means of Near-Field Scanning Optical Microscopy (NSOM), a microscopic technique that allows a surface inspection with high spatial, spectral and temporal resolution overcoming the far-field resolution limit by exploiting the properties of evanescent waves. Zhou *et al.*[78] studied the dispersion of AgNPs in polymer films containing azo groups by NSOM.

All the above mentioned techniques are the most widely used means of characterization for biomedical silver nanocomposites. Nevertheless, other techniques can provide valuable information regarding this new class of materials; to name a few, DSC[79], TGA[80], Dynamic Light Scattering[81;82] and Zeta Potential measurements[83] can also provide a deeper insight into some specific properties of the constructs, like thermodynamic properties and thermal stability, size, surface charge and diffusion.

1.3 BIOMEDICAL APPLICATIONS

1.3.1 General considerations

Nanoscale materials have emerged as novel bioactive agents thanks to their unique physical-chemical properties and their high surface area-to-volume ratio. A large interest in silver-based nanocomposites is due to silver biocidal properties[84;85]. In fact, silver has been extensively used to control infections since ancient times. For centauries it has been in use for the treatment of burns and chronic wounds. In the 1940s penicillin was introduced and the use of silver for the

treatment of bacterial infections diminished. In 1968 silver nitrate was combined with sulphonamide to obtain silver sulfadizine cream to treat burns[86]. Nowadays antibiotic-resistant bacterial strains have become a major issue in public health care and this is why silver-based nanocomposites in a variety of forms (*i.e.* wound dressings, coated medical devices, hydrogels) have made a tremendous comeback for anti-infective applications[87]. Silver-based medical products, ranging from topical ointments and bandages for wound healing to coated stents, have been proven to be effective in retarding and preventing bacterial infections[88].

Improvements in the development of novel silver nanoparticles-containing products are continuously sought. In particular, there is an increasing interest towards the exploitation of silver nanoparticles technology in the development of new bioactive biomaterials, aiming at combining the unique antibacterial properties of the metal at the nano-scale with the performance of the biomaterial[10;89-92]. Silver containing nanomaterials represent a promising strategy to combat infections related to indwelling medical devices like catheters, stents and bone prosthesis. These infections are the fifth leading-cause of hospital patients' death it the US[93].

Although silver is known and used primarily for its antibacterial properties, silver nanoparticles have been shown to exhibit also promising antiviral and antifungal properties. AgNPs exert cytoprotective activities towards HIV-infected T-cells by inhibiting the *in vitro* production of extracellular virions. It is hypothesized that the direct interaction between these nanoparticles and double-stranded DNA of HBV viral particles is responsible for their antiviral mechanism[94]; however, the effects of silver nanoparticles towards other kinds of viruses remain largely unexplored.

Although antifungal drug resistance does not seem to be as much of a problem as resistance to antibacterial agents in bacteria, one long-term concern is that the number of fundamentally different types of antifungal agents that are available for treatment remains extremely limited. There is an inevitable and urgent medical need for drugs with novel antifungal mechanisms. In the last years attention has been focused on the potential use of silver as an antifungal agent. Experimental results evidence that AgNPs exhibit potent antifungal effects on tested fungi, probably through destruction of membrane integrity[95-97].

1.3.2 Overview of *in vitro* results

This section overviews the most promising applications of silver nanocomposites as biocidal systems developed during the last few years. Silver-based materials are generally considered as good candidate for coating medical devices and many recent literature data deal with the preparation of nanocomposite-coatings based on polymers and silver nanoparticles. As it will be

discussed in chapter 3.4, the mechanism by which silver-based materials exert biocidal activity is only partially understood; this fact often leads to different interpretations of experimental results. For this reason, the results and discussions summarized in this paragraph in some cases may appear conflicting. For central venous catheter (CVCs) applications, Stevens *et al.*[98] reported the use of various hydrophilic polymer coatings loaded with silver nanoparticles in order to assess both the antimicrobial efficacy and the impact of silver on the coagulation of contacting blood. The roll-plate assay[99] showed that bacteria inhibition begins when silver ions released from the nanoparticles into the suspension exceeds 100 nM and no bacteria are found for Ag^+ concentrations higher than 10 µM. On the other hand, thrombin generation and platelet activation starts at Ag^+ concentrations higher than 100 µM. Interestingly, thrombin generation can occur also upon activation of blood platelets through collision (direct contact) with silver particles exposed on the surface, so it was suggested that the use of silver nanocomposite coatings for CVCs may enhance thrombus formation. Su *et al.*[100] successfully prepared AgNPs/Clay nanocomposites and by inductively coupled plasma mass spectrometry (ICP-MS) analysis showed that the immersion of the nanocomposite in water at 0.1 wt% after centrifugation causes a release of silver ions of only 139 ppb. A nanocomposite concentration of 0.05 wt% was enough for a complete inhibition of *S. aureus, S. pyogenes, P. aeruginosa* and *E. coli*. It must be noticed that the solution obtained from 0.5 wt% dispersion after centrifugation of the slurry was not effective for the inihition of *S. aureus*. This fact means that in this case AgNPs, and not the released Ag^+, appear to be involved in the antibacterial mechanism. In the case of multilayered nanocomposites, Dai *et al.*[2]demonstrated that their film based on the alternated deposition of poly(ethylene imine) and poly(acrylic acid) including AgNPs was effective in inhibiting *E. coli* growth. Remarkably, the effect was the same when the film contained silver ions or when it contained AgNPs; the latter case may be more desirable because it should minimize the amount of Ag^+ absorbed in the body. Grunlan *et al.*[101]prepared a multilayered film based on poly(acrylic acid) and poly(ethylene imine) containing silver ions and cetrimide (an organic quaternary ammonium molecule) as antimicrobial agents. The biocidal activity was studied by means of the Zone Of Inhibition (ZOI) test with *E. coli* and *S. aureus*. It was shown that such materials were effective in preventing bacteria growth and the antimicrobial efficacy of the silver containing films was further enhanced by the use of cetrimide. Choi *et al.*[102] tested nanocomposite capsules based on polyelectrolytes with AgNPs with a suspension of *E. coli*; optical density measurements at 260 nm, which are proportional to the number of bacteria, showed that the amount of bacteria decreased after only 1 min exposure to silver-embedded capsules. As a control, in the absence of silver the optical density of the *E. coli*

suspension remained almost unchanged. Ho *et al.*[38] reported the preparation of antimicrobial nanocomposite films based on poly(ethylene imine) and AgNPs which exploit both the release of silver ions and the direct contact between bacteria and nanoparticles (Figure 10).

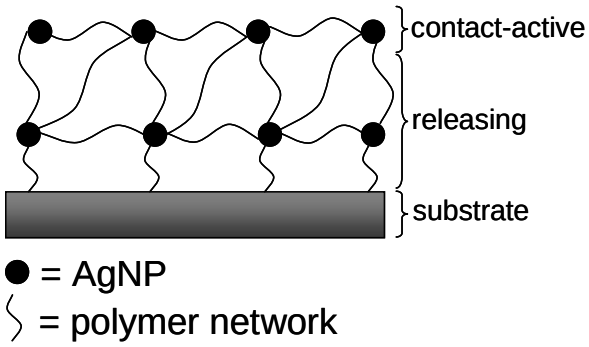

Fig 10. Representation of an antimicrobial nanocomposite coating that exploits both the release of silver ions and the direct contact of silver nanoparticles within a polymer matrix (adapted from Ho *et al.* 2004)

S. aureus was allowed to adhere to the film surface and then cultivated in agar to evaluate the viable cells. Results show that the film inhibits bacteria growth for 12 hours. When the amount of silver in the film reached the value of 10 $\mu g/cm^2$ no bacteria could grow even after two weeks, indicating a bactericidal effect of the nanocomposite material.

1.3.3 Effects of nanoparticles properties and role of the matrix

Many factors influence the biocidal activity associated with AgNPs-based constructs, which may complicate the understanding of the antibacterial mechanism, as discussed in chapter 3.4; for this reason it is not easy to evaluate one property at a time, which can lead to conflicting results in the literature. Moreover the biological effects of AgNPs are affected by the dispersing agent or matrix of each particular nanocomposite system.

In general, it can be stated that nanoparticles size, shape, surface properties, dispersion and stability are important issues for tailoring their biological performances. In particular, the effect of the particles dimensions has often been taken into account while characterizing the antibacterial activity: various researchers have documented that the size of AgNPs affects the biocidal effectiveness[103;104]. The antibacterial activity of AgNPs can be related to their size since the activity of smaller particles is higher due to the increase in surface area when compared on the basis of equivalent silver mass content. For such speculations it can be useful to evaluate the number of silver atoms in a nanoparticle (n) from the following relation[105]:

$$n = \frac{0.5 \cdot \pi \cdot \mathrm{N_A} \cdot \mathrm{dm}^3}{3 \cdot \mathrm{V_m}}$$

where dm is the particle diameter in nanometres, Na is Avogadro's number and V_m is the molar volume of silver (mL/mol). Considering the effect of AgNPs dimensions against *E. coli*, Lok *et al.*[106] showed that AgNPs with an average diameter of 9.2 nm were 9 times more active than particles with an average diameter of 62 nm. Morones *et al.*[107] reported that the bactericidal properties of the carbon-stabilized AgNPs are size dependent in four types of Gram-negative bacteria, since the only nanoparticles that displayed a direct interaction with bacteria preferentially had a diameter of 1–10 nm. At variance, Su *et al.*[108] prepared silver nanocomposites of different sizes (45.7 nm and 25.9 nm) within a silicate clay and found that the bacterial growth inhibition was not significantly dependent on the particle size but only on the silver amount (Figure 11).

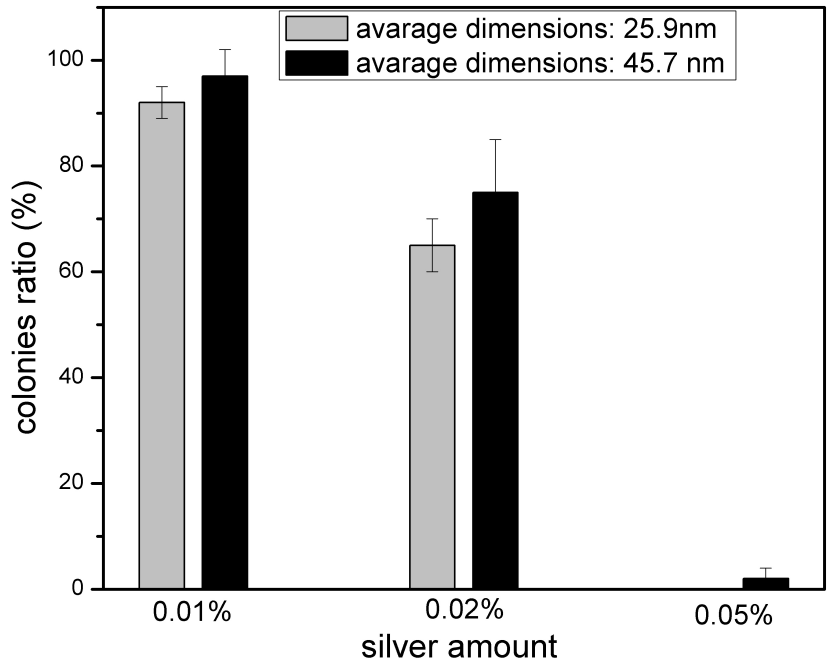

Figure 11. Antimicrobial study on AgNP/Clay nanocomposites: in this system the biocidal effect depends on the silver content and not on particles size (redrawn from Su *et al.* 2009)

The crystallographic structure and shape of the nanoparticles are considered as important properties affecting the antimicrobial behaviour. Recent works have demonstrated that the reactivity is favoured by high atom density facets such as {111}[107]. According to Pal *et al.*[109] truncated triangular nanoparticles display a higher antibacterial activity as compared to spherical nanoparticles and ionic silver.

Comparing the antibacterial activities of metallic and partially oxidized AgNPs, Lok *et al.*[110] indicated that only partially oxidized particles exhibited antibacterial activities and, since smaller AgNPs have a higher surface area-to-mass ratio, they provide higher relative concentration of chemisorbed silver ions.

The matrix where the nanoparticles are dispersed is of primary importance to determine the performance of the material; in fact, in the final nanocomposite constructs, stabilizers play a fundamental role to control the formation of nanoparticles as well as their dispersion stability. For example, in the case of polymer solutions, the concentration of the stabilizer operates as a controller of nucleation, affecting the size of the final nanoparticles as can be monitored by UV-Vis spectra and TEM observations. Polymeric dispersants or capping agents are generally used to stabilize AgNPs, but it must also be considered that they may deactivate the nanoparticles functions because the organic wrapping on the metal surface can limit or prevent its surface reactivity[111].

1.3.4 Antimicrobial mechanism

Three main strategies can be pursued to render materials antimicrobial[38], by choosing:

1. the anti-adhesiveness;
2. the biocide-release activity;
3. the activity by contact.

Silver-based systems can be developed both as biocide-releasing systems (Ag^{+}) and as contact-active materials. Although the toxic effects of silver on bacteria have been investigated for more than 60 years, the mechanism by which silver is able to kill bacteria is still only partially understood[107;112]. Several investigations have suggested possible mechanisms involving the interaction of silver ions with biological macromolecules.

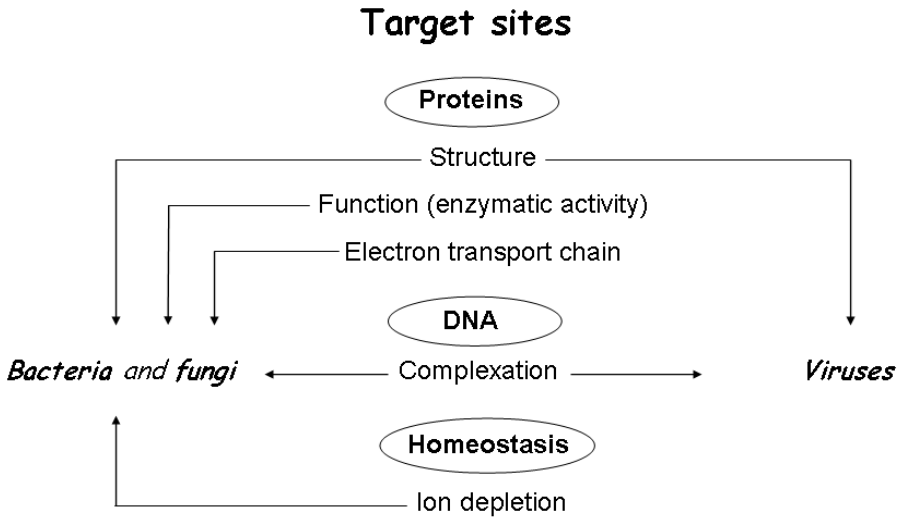

Figure 12: Interaction sites of silver ions on microorganisms

Most of the Ag^+ sensitive sites are likely to be proteins and their alterations will result in cell disruption due to structural and/or severe metabolic damage (Figure 12). Silver ions inhibit a number of enzymatic activities reacting with electron donor groups containing sulfur, oxygen, or nitrogen such as carboxylates, phosphates, hydroxyl, amines, imidazoles, indoles and especially sulfhydryl groups[113-116]. In the bacterial cell wall, free sulfhydryl groups are localized on transmembrane and outer-membrane proteins, including proteins of the electron transport chain, and they protrude in the extracellular portion of the membrane where they represent a very accessible interaction site for silver ions[107;117-120].

The Na^+-translocating NADH:ubiquinone oxydoreductase (NQR) has been recognized as one of the primary targets for Ag^+ ions. It is a component of the respiratory chain of various bacteria and it generates a redox-driven transmembrane electrochemical Na^+ potential. In two independent studies, submicromolar concentrations of Ag^+ ions were demonstrated to inhibit energy-dependent Na^+ transport in membrane vesicles of the NQR-possessing *Bacillus sp.* strain[121] and to inhibit purified NQR of *V. alginolyticus*[122]. Dibrov *et al.*[123] showed that low concentrations of Ag^+ (submicromolar) induce a massive proton leakage through the *Vibrio cholerae* membrane, which results into a complete alteration and elimination of transmembrane proton gradient, de-energization, followed by cell death.

A study performed on *E. coli* as a bacterial model pointed out that the bactericidal action of silver ions is correlated with the interaction with ribosomal subunit proteins and with the suppression of enzymes and proteins necessary for ATP production[124].

Ag^+ also forms complexes with the DNA bases, inducing DNA condensation. It is known that the replication of DNA molecules is effectively conducted only when DNA molecules are in a relaxed state. In a condensed form, DNA molecules lose their replicating abilities[107;125;126]. Feng *et al.*[127] have provided a morphological and structural study on the changes that occur on bacteria when treated with silver ions. They observed detachment of the cytoplasm membrane from the cell and the presence of dense electron granules around the cell wall and in the cytoplasm. As explained by Feng, these electron-dense granules, likely formed by the combination of silver and proteins, are prevented from permeating through the membrane, denying electron transport. Silver ions produce the formation of a low molecular weight region in the centre of the bacteria, which is considered a defense mechanism by which the bacteria conglomerates its DNA to protect it from toxic compounds when the bacteria senses a disturbance of the membrane (Figure 13).

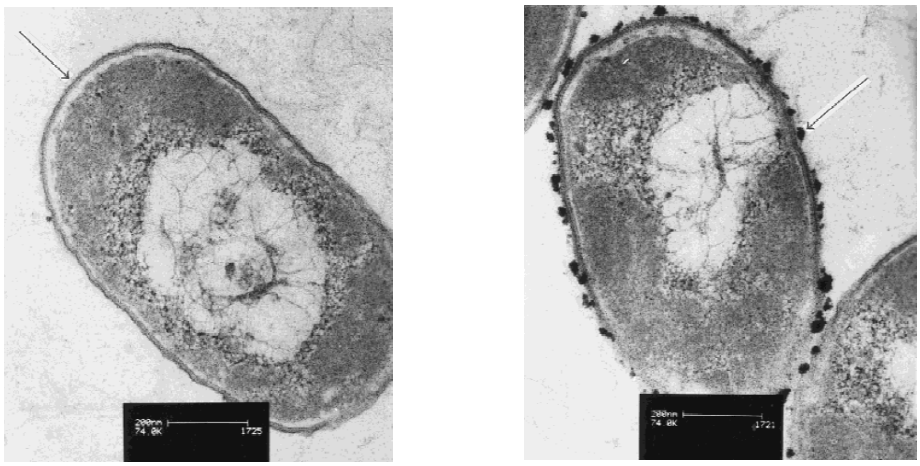

Figure 13: Internal structure of *E.coli* cells treated with silver ions. Left: Cytoplasm membrane detachment from cell wall (arrow). Right: Electron-dense granules around the cell wall (arrow). From Feng *et al.* (2000), reproduced with permission.

As to silver nanocomposite materials, it is still not clear whether the biocidal mechanism of the AgNPs involves only silver ions or it also follows different routes[128]. Various mechanisms have been suggested according to the morphological and structural changes of bacteria. Generally, silver is believed to interact with the bacterial membrane either by direct contact between the nanoparticle and the membrane causing a direct transfer (solvent free) of Ag^+ ions, or by means of silver ions released into the medium. A combination of the two mechanisms is also possible. Stevens *et al.*[129] suggested that when bacteria are in direct contact with silver nanoparticles in the medium they locally encounter high amounts of silver ions resulting in their death. In fact, the high surface-to-volume ratio of the nanoparticles accounts for a sustained local

supply of silver ions at the material-bacterium interface, preventing bacterial adhesion and biofilm formation (Figure 14). It must be also taken into account that if plasma proteins adsorb onto the biomaterial surface, the release of Ag^+ can be hampered as well as the direct contact between nanoparticles and bacteria can be prevented.

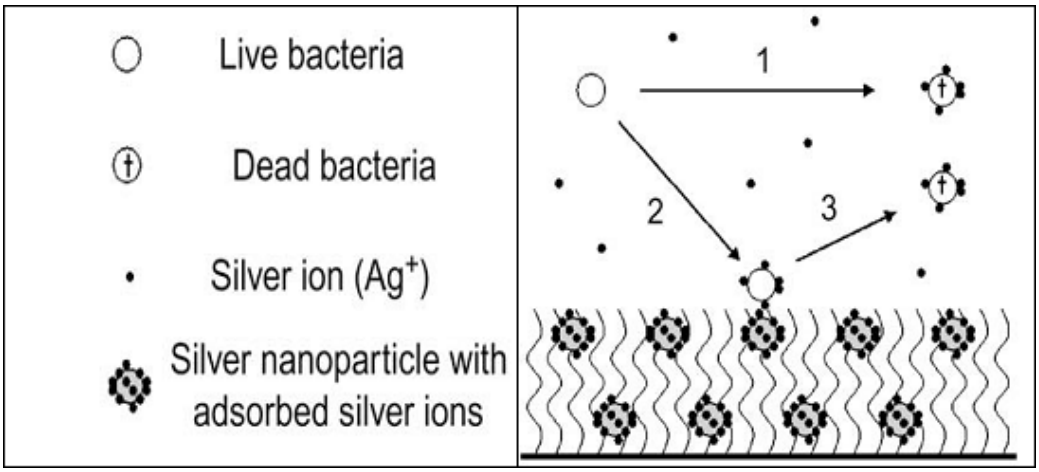

Figure 14. Schematic representation of the possible antimicrobial mechanisms by ions elution or by contact-dependent transfer of silver ions following collision with the silver nanoparticle-containing surface. From Stevens *et al.* (2009), reproduced with permission.

Catellano *et al.*[130] suggested that when metallic silver reacts with the moisture in the wounded skin it gets ionized and binds to bacterial membrane proteins, DNA and RNA, leading to bacteria death. Lok *et al.*[131] reported that the antibacterial activity of AgNPs is dependent on surface oxidation; in contrast with zeroth-valent nanoparticles, only partially oxidized AgNPs exhibit antibacterial activities suggesting that partially oxidized AgNPs may be carriers of chemisorbed Ag^+ in quantities that are sufficient to cause bacterial damage. A possible way of delivery of Ag^+ from oxidized AgNPs may involve a direct interaction with the bacterial membrane.

Su *et al.*[132] studied the antimicrobial mechanism of AgNPs/Silicate Clay nanocomposites; these constructs appear to exert their biocidal effect by means of a direct contact with the nanoparticles and not by means of the silver ions released, which indicates that in this system a simple contact with AgNPs is sufficient to trigger membrane leakage and cell death.

One of the main target sites of silver nanoparticles is the bacterial membrane where deep morphological changes are induced leading to a significant increase of permeability and to the alteration of transport mechanisms through the plasma membrane[133;134]. As reported by the authors[135], a colloidal system based on a lactose-modified chitosan and AgNPs, noticeably affects membrane potential and permeability. Morones *et al.*[107] have tested silver

nanoparticles on four types of Gram-negative bacteria: *E. coli, V. cholera, P. aeruginosa* and *S. typhus.* They observed silver nanoparticles attached to the cell membrane and in the cytoplasm of the bacteria (Figure 15). The mechanism by which the nanoparticles are able to penetrate into the bacteria is not totally understood, but the observation of silver nanoparticles on the cell surface and inside the bacteria is fundamental in the understanding of the bactericidal mechanism. In analogy with the mechanism suggested for silver ions, nanoparticles might tend to react with sulfur-containing proteins, as well as with phosphorus-containing compounds such as DNA, inducing irreversible cellular damages.

Proteomic data revealed that a short exposure of *E. coli* cells to antibacterial concentration of AgNPs resulted in an accumulation of envelope proteins precursors, indicative of the dissipation of proton motive force. Consistent with these proteomic findings, AgNPs were shown to destabilize the outer membrane, to collapse the plasma membrane potential and to deplete the levels of intracellular ATP[136].

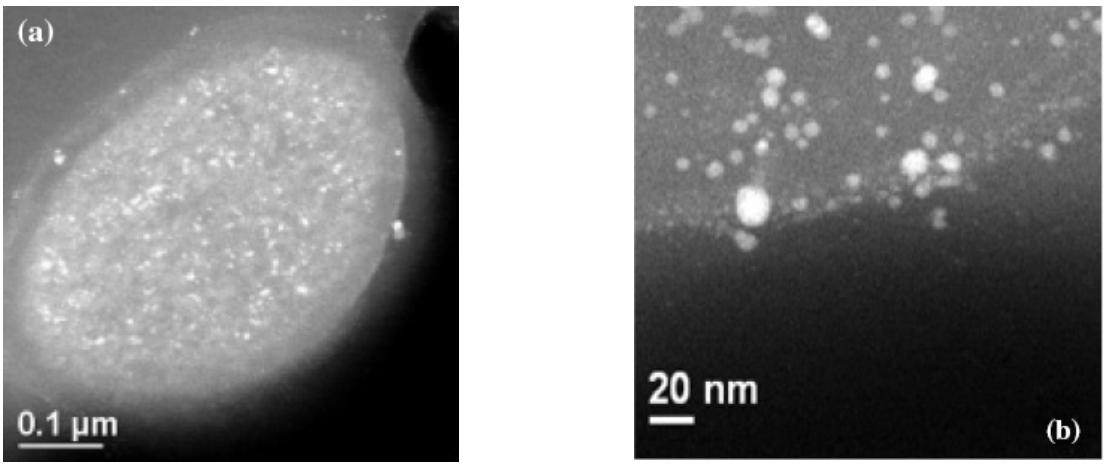

Figure 15: (a) Silver nanoparticles on the membrane and inside *E. coli* bacteria. (b) Magnification of *E. coli* membrane, where the presence of silver nanoparticles is clearly observed. From Morones *et al.* (2005), reproduced with permission.

As free-radicals increase is considered as one of the possible explanation of the antimicrobial mechanism[137;138], Su *et al.*[139]studied the burst of free radicals and reactive species of oxygen (ROS) in AgNPs/Clay-treated bacteria by measuring 2,7-dichlorofluorescin-diacetate (DCFH-DA) as intracellular-ROS indicator. Results show that 40.3% of the AgNPs/Clay-treated bacteria became DCF^{+}, indicating that ROS were generated and played a role in the killing mechanism. In addition it was observed that bacteria lost their mobility upon treatment with the nanocomposites, meaning that the motor function of the cytoskeleton is hampered with a consequent prevention of cytokinesis (Figure 16). Nanocrystalline silver-supported carbon[140]

showed kinetics of bacterial inactivation, in the presence of hydroxyl radical scavengers and superoxide anion radical inducer that suggest the contribution of the reactive oxygen species (ROS) to antibacterial effect. However, these ROS scavengers did not show any inhibition of bactericidal activity after approximately 1 hour, suggesting that generated ROS are responsible for *E. coli* inactivation only during the initial hour of the incubation time. The antibacterial process was found to be highly increased at higher temperature, which was ascribed to the enhanced ROS formation and Ag^+ elution.

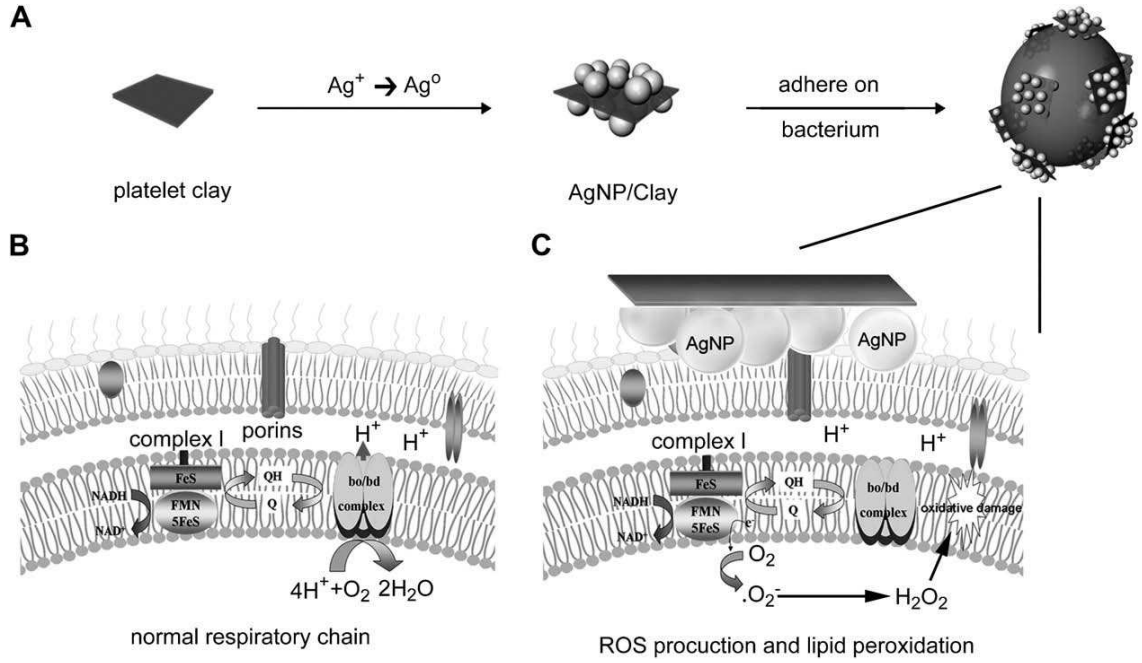

Figure 16. Possible mechanisms of AgNP/Clay-mediated cytotoxicity. (A) AgNPs on synthetic platelet clay show electrostatic attraction to bacteria and form AgNP clusters on the bacterial cell wall. (B) Electronic transport through the respiratory chain on plasma membrane of *E. coli* through complex I, ubiquinone oxidoreductase (Q) and cytochrome bo/bd ubiquinone oxidase (bo/bd complex). (C) AgNP/Clay on the cell wall interacts with transmembrane proteins and consequently interferes with the proton pool in the intermembrane space or the electronic flow through the respiratory chain. Accumulated electrons due to a disturbance of complex I are transferred to oxygen to form O_2 and H_2O_2, contributing to oxidative damage and membrane leakage in bacteria. From Su *et al.* (2009), reproduced with permission.

1.4 BIOLOGICAL HAZARDS OF SILVER NANOCOMPOSITES

Nano-sized materials are currently being used in medicine, biotechnology, energy and environmental technology. Given the wide variety and growing number of applications on the market, there is a lack of studies and information regarding the effects of nano-sized materials (silver nanoparticles included) on general human health and environment. At present silver-based products are widespread available on the market primarily as formulations for topical applications, both in the medical areas such as wound dressing and surgical instruments, coated or embedded with AgNPs, and in daily life where consumers have access to silver containing detergents and soaps, room sprays, water purificants, textiles, personal care products, handles and furniture for public places. Silver-based systems are also used in some food processing industry where pipelines are susceptible to biofilm formation. Besides, more recently AgNPs have been studied to be exploited for systemic applications and for the preparation of internal prosthesis and devices (*e.g.* bone cement, catheters). Hundreds of silver-based products are currently on the market, but there are not specific reporting requirements, risk assessments or official government indications for the commercialization of these kinds of products.

The widespread use of AgNPs and silver ion-based products is partially justified by the fact that till few years ago and even nowadays, many researchers associated to ionic silver a low toxicity in the human body and expected minimal risk with respect to clinical exposure by inhalation, ingestion, dermal application or through the urological or haematogenous routes. Silver is not known as a systemic toxic agent for humans, except at extreme doses. The most evident secondary effects derived by chronic ingestion or inhalation of silver preparations is the deposition of particles in the skin (argyria), eye (argyrosis) and other organs. These conditions are generally not considered life-threatening but simply cosmetically undesirable. Silver in form of ions is absorbed into the human body and enters the systemic circulation as a protein complex to be eliminated by the liver and kidneys with a metabolism modulated by induction and binding to metallothioneins. These protein complexes can mitigate the cellular toxicity of silver and contributes to tissue repair[141]. Literature does not report cases of people specifically harmed by the use or exposure AgNPs: this fact could be attributed to the lack of knowledge about what effects to expect. A recent work by Larese *et al*., demonstrated the absorption of silver nanoparticles through intact and damaged skin, detecting the presence of nanoparticles in the stratum corneum and the outermost surface of the epidermis[142].

In fact, in sharp contrast with the attention paid to new applications of silver nanocomposites, few studies provide insights into the possible interaction of AgNPs with the human body after

entering *via* different routes, and not only through skin. Systemic distribution and translocation, organ accumulation, degradation, possible adverse effects and toxicity in human tissues start to be considered and open major questions associated with the increased medical use of silver nanocomposites. An important and often disregarded aspect to be considered when studying the biological effect of silver nanocomposites is that nanoparticles show an impressive array of unusual physical-chemical properties that confer them higher and often unpredictable bioactivity when compared to the identical bulk materials. For instance, based upon size alone and not upon physical or chemical properties, nanomaterials have capabilities (normally attributed to micro-organisms like viruses) to penetrate circulatory system and to reach and to translocate in all living organs including the blood-brain barrier.

In the last 5 years most of the *in vitro* studies regarding the exposure of cell lines to silver nanoparticles have evidenced the presence of a potential cytotoxic mechanism that is strictly dependent on particle size and concentration. In spite of the limited number of cell lines tested, all experimental data agree that the mitochondria are the main intracellular target of silver nanoparticles. AgNPs mediate their toxicity through an oxidative stress with increase of ROS levels and following activation of the apoptotic mitochondrial pathway[143-147]. AgNPs induce mitochondrial membrane perturbation, generation of ROS, depletion of antioxidant GSH and reduction of mitochondrial function in BRL 3A rat liver cells[148], rat alveolar macrophages[149] and human THP-1 monocytic cells[150]. Furthermore, GSH depletion in human skin carcinoma and fibrosarcoma cell lines is associated to expression of apoptotic markers[151] and in human hepatoma cells HepG2 to the over expression of oxidative stress-related genes such us catalase and superoxide dismutase[152].

It is to note a report where four commercially available silver dressings were tested in terms of cytotoxicity towards keratinocyte HaCaT and fibroblast 142BR cells[153]; the results, as similarly observed by Burd *et al.*[154], showed that all tested dressings induce, albeit to a different degree, apoptotic cell death in a way dependent on the cell line and type of dressing investigated.

Although the molecular mechanism at the base of silver nanoparticles potential toxicity is yet to be completely elucidated, a work by Hsin *et al.*[155] shed partially light on it. The mitochondria-dependent apoptotic mechanisms identified in eukaryotic cells constitute an intrinsic and an extrinsic pathway characterized by the activation of pro-apoptotic proteins such as Bid, Bad, Bak and the inactivation of anti-apoptotic proteins as Bcl-2 e Bcl-Xl. Activation of Bad and Bak results in their traslocation and oligomerization on mitochondria membrane, to form ion channels allowing exit of cytochome C and other apoptotic factors.

By the experimental data so far collected by the researches, the prevailing hypothesis is that AgNPs interact with thiol groups of proteins and enzymes after passing through eukaryotic cell membrane. Most of those proteins can be involved in the antioxidant defense mechanism, like reduced glutathione, catalase, superoxide dismutase, that prevent tissue damage under normal conditions neutralizing ROS produced by the aerobic energy metabolism[156;157]. Over accumulation of ROS, an inflammatory response is induced and irreversible mitochondrial membrane damage and pemeabilization occurs, with following release of cytochrome C and of other apoptogenic factors[158]. Besides mitochondrial pathway activation, cell membrane destruction and lipoperoxidation can also take place and they represent another aspect of AgNPs toxicity (Figure 17).

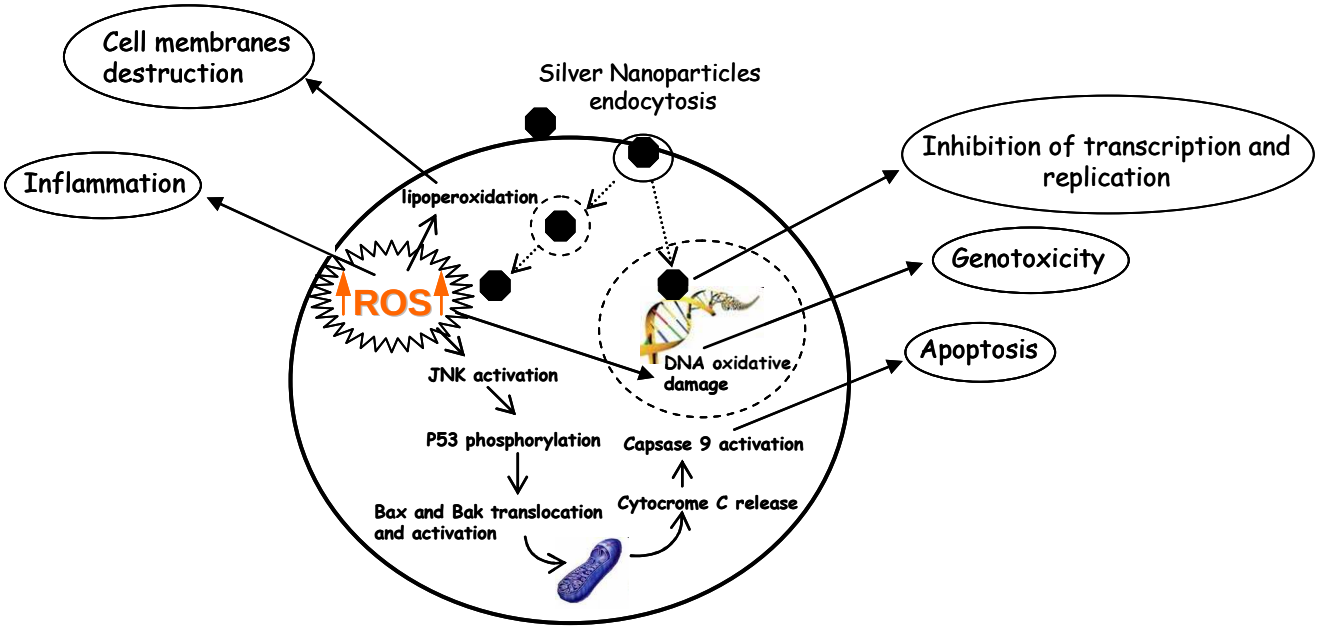

Figure 17. Cytotoxic effect of silver nanoparticles on eukaryotic cells

Silver nanoparticles can be internalized through the membrane by different mechanisms that include passive diffusion, receptor-mediated endocytosis and clathrin- or caveolae-mediated endocytosis[159-162].

The mechanism of action of AgNPs described above seems to be shared by silver ions[163], and supports the hypothesis that part of the toxic potentiality of silver nanoparticles is due to the Ag^{+} release from them.

The literature survey clearly shows that, over last years, the studies were mainly focused to asses the adverse biological affects of AgNPs by administering them at dose and concentrations that lead to cell death or irreversible cellular damage. These studies fail to consider concentrations of nanoparticles that may not result in cellular death but may cause sub-lethal cellular alterations

leading to serious consequences on human health. The most important examples are DNA damage and induction of inflammation processes. Mutation of DNA, induced by genotoxic materials, leads to carcinogenesis and has a deep impact on the biology of reproductive cells. As recently reviewed by Singh *et al.*[164], metal nanoparticles can generate DNA damage indirectly, by inducing oxidative stress and inflammation responses. ROS, whose increase is associated to an oxidative stress and subsequent redox imbalance, react with many biological macromolecules, including DNA, enzymes and lipids; in particular, they cause oxidative damage on DNA in the form of breaks of single and double-strands, purine, pyrimidine and deoxyribose modifications, abasic sites and DNA-DNA coupling[165]. At the same time, nanoparticles can gain direct access to the nucleus either though passive diffusion or transport across the nuclear pore complexes. Within this site they can trigger aggregation of nuclear proteins with subsequent inhibition of transcription, replication and cell proliferation[166-169].

Although there is a substantial experimental evidence on the genotoxic potential of many metal-based nanomaterials, the data accumulated on AgNPs point only very marginally on their genotoxicity.

An initial screen of nanomaterials toxicity must be always accomplished using *in vitro* studies, but they must be always supported by *in vivo* test, since the *in vitro-in vivo* gap is associated with the complexity of biological interactions in a higher order organism which are not reproducible by an *in vitro* system. *In vivo* tests require animal models to evaluate markers of inflammation, oxidant stress, and cell proliferation in portal-of-entry and selected remote organs and tissues, deposition, translocation of the materials and its degradation products, toxicokinetics and biopersistence studies, effects of multiple exposures and finally potential effects on the reproductive system, placenta, and fetus. In the field of silver nanocomposite materials the scarcity of toxicity data obtained on cellular models goes in parallel with the almost lack of exhaustive studies performed using *in vivo* models. In Zebrafish embryos, AgNPs in a concentration range between 250 and 0,25 μM caused toxic lethal and sub-lethal (morphological malformations) effects albeit in a size-dependent manner for certain concentrations and time ranges[170]. Silver nanoparticles administrated *via* intra-peritoneal injection in adult mice are able to traslocate to the circulatory system and reach the brain were they generated neurotoxicity by inducing free-radical oxidative stress, by altering gene expression and by producing apoptosis[171]. A study performed to compare the effects on liver caused on mice fed with nano- and micro-sized silver particles, revealed in both cases induction of liver inflammation[172]. Micro- and nano-silver particles implanted into rat's back muscle reveal a good biological effect

on days 7 and 14 but an inflammation process at day 30, more serious in AgNPs-treated rats than in the micro-silver treated ones[173].

All the studies are acute toxicity tests and no information was obtained from more informative chronic tests.

An increasing number of papers take into consideration the development and characterization of materials based on silver nanocomposites and their interaction with eukaryotic systems. As examples, Fu *et al.*[174] describe the realization of antibacterial multilayer films containing AgNPs via layer-by-layer assembly of heparin and chitosan, lacking of toxic effects on osteoblasts. Nanocomposite materials based on acrylic resins and Ag NPs stimulate fibroblast and osteoblast aggregation and growth without displaying any toxic effect[175;176], and stainless steel orthopaedic materials already commonly used in the biomedical field, when coated with silver, efficiently sustain the growth of osteoblasts and do not show genotoxicity[177].

However, besides the potential toxicity of silver when topically or systematically administrated, a general concern must be also considered on the hazardous effects of nanoparticles accumulation in the environment. As the scientific literature often points out, there is a great lack of knowledge about AgNPs impact on human health but even less is what we know about its environmental pathways and its environmental effects. At present, silver is classified by EPA (US Environmental Protection Agency) as an environmental hazard because in some circumstances it is toxic, persistent, and bio-accumulative. Nanotechnology is not well researched or regulated, so the environmental impact and risks of silver nanoparticles is not known.

Although the scientific community is in agreement to retain that the paucity of data renders it premature to formulate any definite risk assessment about silver-based materials, an increasing public debate is emerging, and very contradictory opinions and experimental evidences about the potential impact of these nanomaterials on health are often presented[178;179]. A central point is that silver nanocomposites should not be considered as a uniform group of materials. The toxicity of nanocomposite materials may be influenced by particle concentration, size distribution, agglomeration state, shape, chemical and physical nature of the matrix, physical status of the composite and finally site and time of exposure. The ultimate and main goal in the field of silver nanotechnology remains still the development and choice of products with a superior profile of functionality (like for instance high infection control) associated to reduced host cell cytotoxicity and a moderate environmental risk to fully exploit the potential benefits and limit the unnecessary risks of this technology.

In general, the rapid proliferation of many different engineered nanomaterials presents at the moment a dilemma to regulators regarding hazard identification. The International Life Sciences Institute Research Foundation/Risk Science Institute[180] convened an expert working group to develop a screening strategy for the hazard identification of engineered nanomaterials. Based on the evaluation of the limited data currently available, the report presents only a broad data gathering strategy applicable to this very early stage in the development of a risk assessment process for nanomaterials. Oral, dermal and inhalation routes of exposure must be considered recognizing that, depending on use patterns, exposure to nanomaterials may occur by any of these routes. In particular, three key elements of the toxicity screening strategy have been identified: 1) physicochemical characteristics, 2) *in vitro* assays (cellular and non-cellular), 3) in vivo assays. It is common opinion that in the next future every new nanomaterial entering the market will need to be screened for toxicity and biopersistence, using low-cost, fast-throughput but scientifically rigorous and standardized tests.

1.5 POLYSACCHARIDES AS BIOMATERIALS

Polysaccharides constitute an important class of biological materials. They display well documented biocompatibility and biodegradability, which are the basic characteristics for polymers used as biomaterials[181]. Besides, polysaccharides are involved in cell embedding and signalling including tissue addressing and transport mechanisms.

Polysaccharides in biomaterials are often used in order to manipulate surface properties such as wettability, adhesion, and biocompatibility. On a general point of view, polysaccharides are rich in –OH functional groups allowing good solvation in aqueous medium and possible chemical modifications. Due to their stereoregularity, and to the presence of –OH groups, H-bond networks are formed which stabilize intra and inter-polymeric chain interactions; they cause the characteristic semi-rigid behaviour of polysaccharides in well defined thermodynamic conditions. Polysaccharides can be either neutral polymers (such as cellulose, amylose, and galactomannans) or charged ones; carboxylic or sulfate groups are present in hyaluronan and alginate or carrageenan respectively; amino groups are naturally present in the only natural cationic polysaccharide, *i.e.* chitosan. The polyelectrolyte character favours the dissolution in aqueous solutions, depending on the pH.

Polysaccharides are usually obtained by biosynthesis in plants (*e.g.* algae) and animals. Polysaccharides can also be synthetized by microorganisms such as bacterial hyaluronan, dextran, gellan or xanthan. The large amount of polysaccharides with different chemical structures and physical properties constitutes a source of materials for many applications especially in the domain of biomaterials for tissue engineering, drug vehicle and viscosupplementation. Few polysaccharides reach the level of consideration as good basis for biomedical applications: among these, alginate and chitosan will be considered for the aim of the present thesis.

1.5.1 Chitosan and Derivatives

Chitosan is a partially deacetylated derivative of chitin, the second most abundant natural biopolymer on earth, which is the main component of the exoskeleton of marine crustaceans and cell walls of fungi. Chitosan is a linear polysaccharide consisting of β(1-4) linked D-glucosamine residues ($GlcNH_2$) with a variable number of randomly located N-acetylglucosamine groups (GlcNAc) (Figure 18).

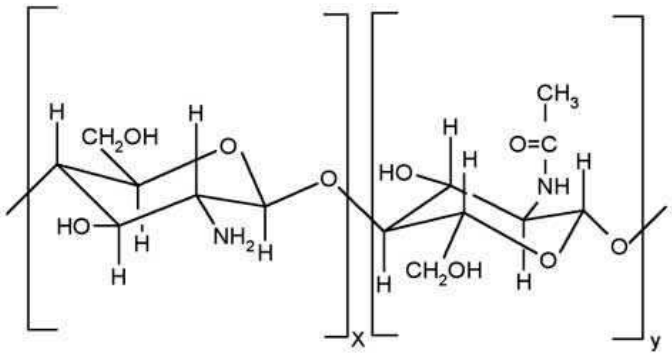

Figure 18. Structure of chitin and chitosan. Chitin is composed predominantly of GlcNAc units (y). Chitosan is composed predominantly of $GlcNH_2$ units (x)[182].

Chitosan is very abundant, and its production is low cost. Nowadays chitosan is receiving a great deal of interest for medical and pharmaceutical applications[183]. Chitosan is well known for being biocompatible allowing its use in different medical applications such as topical ocular application[184], implantation[185] or injection[186]. Moreover, chitosan is considered as biodegradable because it is metabolized by several human enzymes, especially lysozyme[187]. In addition, it has been demonstrated that chitosan acts as a penetration enhancer by opening epithelial tight-junctions[188]. Chitosan was also reported to promote wound-healing[189;190] and to display bacteriostatic effects[191].

One of the most interesting feature of chitosan as biomaterial is connected with the presence of amino groups located on the glucosamine units. Chemical derivatization based on the reactivity of the glucosamine residues leads to strong modification of the physico-chemical and biological properties of the polycation. Derivatization examples include acylation[192;193], alkylation[194] and carboxymethylation[195]. Starting from these assumptions, our group has modified highly deacetylated chitosan by grafting lactose moieties on the free amino groups of the polymer to obtain, by reductive amination, the corresponding lactitol derivative. This low charged, highly hydrophilic chitosan derivative was named “Chitlac” (Figure 19). This glycopolymer exhibited the ability to induce chondrocyte aggregation leading to the formation of nodules of high dimensions (up to 0.5–1 mm) within 12–24 hours; it also stimulates the biosynthesis of typical markers of articular cartilage, such as type II collagen and glycosaminoglycan[196].

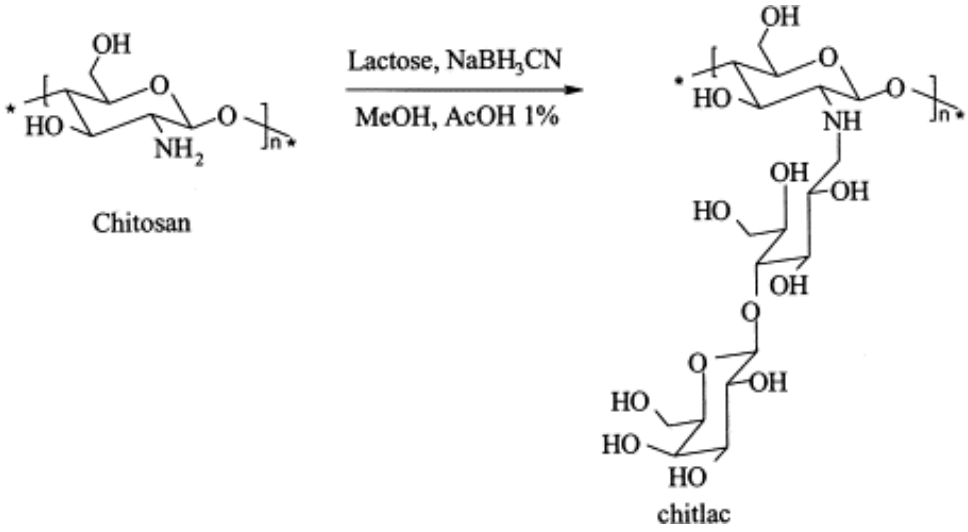

Figure 19: Synthesis of Chitlac via *N*-alkylation of chitosan with lactose[197].

These findings seem promising in connection to a possible application of Chitlac in protocols of tissue engineering applied to the regeneration of bone and articular cartilage. The localization of Chitlac at the plasma membrane of isolated chondrocytes and its permanence at the same site also after nodule formation indicate that the process is mediated by a specific binding of Chitlac to cells, most likely through its β-galactose residues[198]. Further experiments demonstrated the involvement of Galectin-1 as a molecular bridge between Chitlac and chondrocyte cell surfaces[199]. Galectin-1 is a member of the S-type galactoside-binding animal lectins [200;201]. The discovery that Galectin-1 binds with high affinity to polylactosamine-containing ligands (such as laminin) and the co-localization of Galectin-1 with laminin in extracellular matrix suggested that its major function could be to promote cell adhesion to glycoconjugates[202-204].

In general, the polysaccharide biofunctiontality can be enhanced by modifications on different levels of complexity, from relatively simple changes in the hydrophilicity of the material to the functionalization with charged groups, peptides or proteins. The incorporation of bioactive peptide motifs such as Arginine-Glycine-Aspartic acid (RGD), which is recognized by the cell transmembrane integrin receptors, is perhaps the most commonly adopted strategy to enhance functionality[205]; in fact, integrins are heterodimeric cell surface receptors that mediate adhesion between cells and the extracellular matrix by binding to ligands with an exposed RGD sequence. These receptors also stimulate intracellular signalling and gene expression involved in cell growth, migration, and survival. In the studies discussed in Paper 3[206], Chitlac was modified with RGD peptide in order to promote cell attachment and proliferation. For anchoring the bioactive peptide onto the Chitlac chain, the biopolymer was treated with the RGD peptide in

the presence of 1-[3-(Dimethylamino)propyl]-3-ethylcarbodiimide methiodide (EDC) and N-hydroxysuccimide (NHS) as coupling agents.

1.5.2 Alginate

Alginate was first described in 1881, by the British chemist E.E.E. Standford[207]. It is synthesized in large quantities by marine brown algae (*Phaeophyceae*)[208], and it can also be synthesized by bacteria belonging to the genera *Azotobacter* and *Pseudomonas*[209;210]. Alginate is an unbranched polysaccharide consisting of the two sugar residues 1-4 linked β-D-mannuronic acid (M) and α-L-guluronic acid (G) (Figure 20 a). The monomers are arranged in a pattern of blocks along the chain, with homopolymeric regions (M and G-blocks) interspersed with regions of alternating structure (MG-blocks)[211-213]. A strong correlation between structural features and functional properties has been found in alginate. The intrinsic flexibility of alginate in solution increases in order MG > MM > GG[214], but the viscosity depends mainly on the molecular size[215]. By contrast, the selectivity for binding of cations and the gel forming properties varies strongly with the composition[214] and sequence[212;213]. It has been reported that divalent cations like Ca^{2+}, Sr^{2+} and Ba^{2+} bind preferentially to G-blocks in a highly cooperative manner[216]. It is this selective binding to alginate which accounts for its gel forming properties (Figure 20 b).

In fact this complexation with ions has been described by the “egg-box” model in which each divalent ion interacts with two adjacent G-residues as well as with two G-residues in an opposing chain, giving rise to the junction zone in the gel network [217] (Figure 20 c).

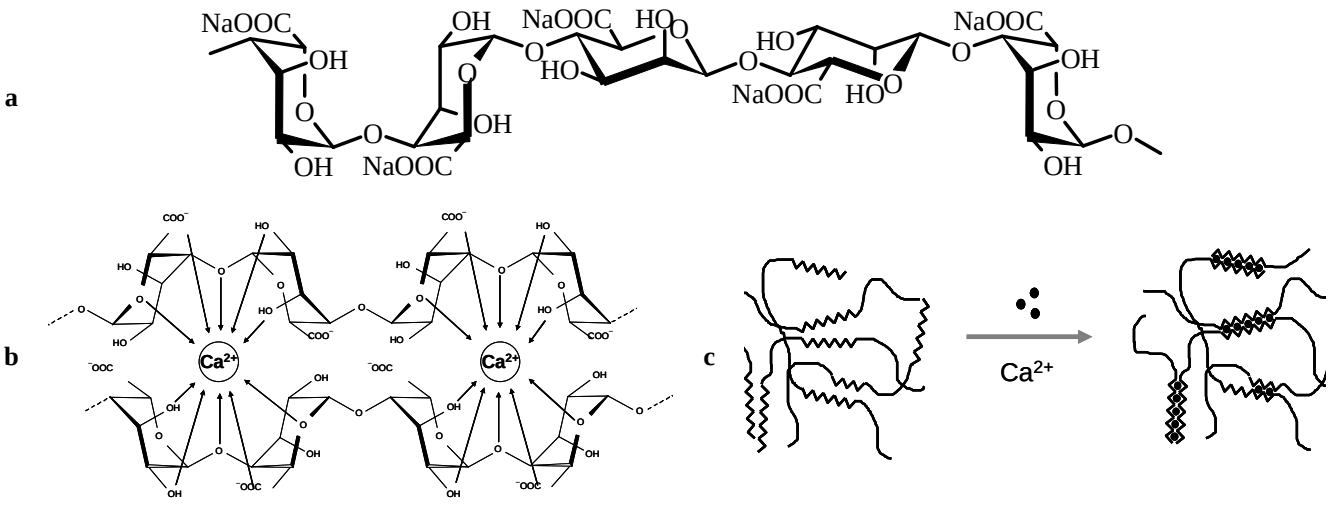

Figure 20: a) Chemical structure of alginate; b) Probable Ca-binding site in a GG-sequence and c) ionic cross-linking of two homopolymeric blocks of G-residues in the egg-box model[217]. Adapted from Strand[218].

Recently, it has been suggested by Donati *et al*.[219] that G-blocks are not the only sequences involved in junction formation. Based on experiments with polyalternating alginate, mannuronan and alginate rich in G-blocks, it could be hypothesized that junction zones in the gel network could occur even between MG/MG-blocks and between GG/MG-blocks.

Alginate from brown algae is the basis for numerous applications in biotechnology and biomedicine, due to its water-binding, viscosity and gel-forming properties[220]. At present, alginate gels are being employed in several areas of drug delivery and tissue engineering[221]. Alginate represents an attractive material for the preparation of "biohybrid organs" and "micro-bioreactors" because its hydrated three-dimensional (3D) network allows cells to survive and be protected by immunosystem[222]. Three-dimensional matrixes are broadly used in tissue engineering, in particular for stem cell culturing, as they have high specific surface area and support high cell density growth. Moreover, this kind of matrices allows control over permeability and mechanical strength. The 3D structure of matrices has the potential to provide cells with a biomimetic environment that aims to resemble the *in vivo* conditions[223]. Alginate encapsulation system, exploiting the ability to form cross-linked matrixes involving the use of divalent cations, includes the paramount benefit to be a flexible technology allowing variations in polymer concentration, composition, bead size and cell seeding density. Alginate-based systems have been widely tested for islet encapsulation and have been shown to provide immuno-isolation after the system transplantation, thus prolonging the survival of encapsulated islets[224-228].

1.6 METHACRYLIC THERMOSETS AS BIOMATERIALS FOR ORTHOPAEDIC AND DENTAL APPLICATIONS

Methacrylic thermosets are largely employed as biomaterials for different applications like bone cements, screw fixation, filler for cavities and skull defects and also vertebrae stabilization in osteoporotic patients. They are also used as dental cements, bonding substances that are placed in the mouth as a viscous liquid and set to a hard mass[229].

The structure of polymethylmethacrylate (PMMA) incorporates methyl and methacrylate groups on alternate carbon atoms as shown in Figure 21 (left).

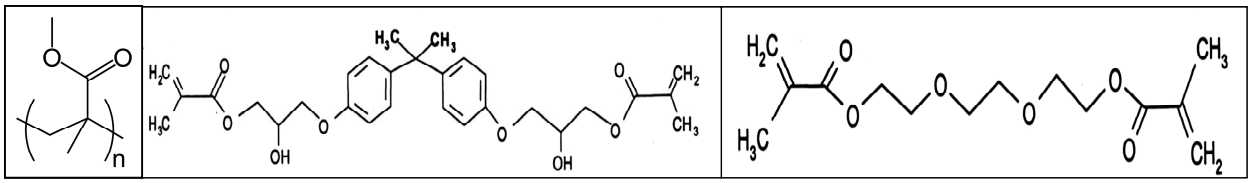

Figure 21. Chemical structure of PMMA (left), BisGMA (centre) and TEGDMA (right)

PMMA has been extensively used as bone cement since the late 1950s[230]. In bone surgery, bone cements based on PMMA are particularly used for their capacity to be moulded into fixed-design implants or to be polymerized at the time of surgery for tailor-made implant applications like as filler material in total-hip insertion[231]. Cement injections help to fix bone screws in weak bone and can significantly increase the strength of vertebral bodies or femoral necks even if applied without a metallic implant. PMMA is currently used for anchoring cemented arthroplasties to the continuous bones; in this application, the main functions of the cement are to transfer the body weight and service loads from the prosthesis to the bone and increase the load-carrying capacity of the prosthesis-bone system. The first use of polymethyl methacrylate (PMMA) as a dental device was for the fabrication of complete denture bases[232].

In the literature there are some conflicting results about the effects of PMMA on bone tissue. In several studies, fibrous layer formation around PMMA has been observed due to exothermal polymerisation reaction or toxic effect of leachable residual monomers; on the other hand, some authors have observed direct bone contacts with PMMA after 15 days to more than 17 years after implantation of cemented hip prosthesis[233]. Vallittu *et al*. have shown that glass or carbon fibre reinforced PMMA composite have relatively good biocompatibility *in vitro* [234]. However, experimental results on animal models by Heikkilä *et al*. revealed disturbed bone formation at the surface of PMMA implants loaded with bioactive glass or hydroxyapatite particles[235]. Moreover, PMMA displays shrinkage during polymerization and can cause a stiffness mismatch between the cement and the contiguous bone.

Efforts at improving the properties of PMMA-based cements have explored different directions. One involves the preparation of composite materials were PMMA is the matrix in which are dispersed small quantities of reinforcements like carbon nanotubes[236], graphite, aramid, bone particles[237;238], polyethylene, polyethylene terephthalate, titanium[239], ultrahigh molecular weight polyethylene or PMMA fibres[240].

Alternatively, various methacrylate-based thermosets have been developed in order to overcome PMMA limitations and tailor-make the material to match the requirements of the specific application. Among these, 2,2-bis[4-(2-hydroxy-3-methacryloxyprop-1-oxy)phenyl]propane (BisGMA) has received particular attention (Figure 21, centre); it is an aromatic dimethacrylate

used in photocurable pit and fissure sealants and in composite restorative dental materials. BisGMA can be formed by the reaction of bisphenol A with glycidyl methacrylate, it is extremely viscous due to intermolecular hydrogen bonding between the hydroxyl groups. Today, dental cements usually contain high-viscosity BisGMA as the main component mixed with a low-viscosity dimethacrylate, namely triethyleneglycol dimethacrylate (TEGDMA) (Figure 21, right). Since BisGMA has five times the molecular weight of methylmethacrylate, the density of methacrylate double-bond groups of BisGMA is approximately two-fifth as high in these monomers, which results in reduced polymerization shrinkage. The use of dimethacrylates also results in extensive cross-linking, which increases the strength and rigidity of the polymer and reduces degradation by heat and solvents compared to methylmethacrylate[241]. Moreover BisGMA/TEGDMA dental cements display high strength, high fracture toughness, low oral solubility and high micromechanical bonding to prepared enamel, dentin alloys and ceramic surfaces.

Methacrylate monomers polymerize by the addition mechanism initiated by free radicals. The main system used for the polymerization initiation of BisGMA is light curing. The blue light (λ = 450 nm) is absorbed by a diketone (*e.g.* camphorquinone, radical initiator), which, in the presence of an organic amine (*e.g.* dimethylaminoethyl methacrylate, coinitiator), starts polymerization reaction. Exposure time of 20 to 40 seconds is needed to start the polymerization[242].

Thermosets based on light-induced reticulation of BisGMA and TEGDMA have found a large use in the biomedical field, in particular, in dentistry. BisGMA-based biomaterials were originally developed for dental composites more than 25 years ago and are nowadays used in most of the commercial products[243]. A number of brands of BisGMA-based dental cements (*e.g.* Variolink® II from Ivoclar Vivadent, Orthocomp from Orthovita-Malvern) are available in the market for the cementation of crowns, bridges, inlays and veneers[244]. The fillers generally used for this application are silica, glass particles and colloidal silica.

BisGMA/TEGDMA materials are also prone to be reinforced with fibers, for example, glass fibers, rendering them particularly interesting for load bearing conditions such as in dental[245;246], orthopaedic and craniofacial applications[247].

1.7 INFECTION RISKS IN ORTHOPAEDIC IMPLANTS

During last 15 years the advent of modern standards in the control of sterility within the operating room environment and the use of adequate protocols of peri-operative antibiotic prophylaxis have decreased the incidence of infections associated with orthopaedic implants.

Nevertheless, the event of infection still represents one of the most serious and devastating complications which may involve prosthetic devices. It can lead to complex revision procedures and even to the failure of the implant and the need for its complete removal. In orthopaedics, given the enormous number of surgical procedures involving invasive implant materials, infections have a huge impact in terms of morbidity, mortality, and medical costs. For example, in the US alone, total hip and knee arthroplasties currently account for over half a million interventions each year. In view of this enormous population of patients with orthopaedic implants, even a currently low risk of infection, estimated to be in the range of 0.5–5% for total joint replacements, has to be considered very relevant for its serious consequences.

The chemotherapy treatment with antimicrobial agents is not always effective on infections that are already established. Often prosthesis removal and replacement, represent the only salvage option to definitively eradicate severe infections. These drastic interventions bear serious implications in terms of attendant patient trauma, prolonged hospitalization as well as in terms of health and social costs, since it has been estimated that the treatment of each single episode of infected arthroplasty costs more than 50000 $.

In the strategy for the prevention of infections, much has been done to improve the operating standards, minimize the possibility of contamination during surgery, reduce the establishment of infection by peri-operative antibiotic prophylaxis, and confine pathogenic strains by patient isolation; along these directions little advancements in terms of decreased infection rates are being expected in return of this type of efforts.

During the last years increasing attention has been focused on the epidemiology and the pathogenesis of the infections, especially associated to implant materials, in order to increase knowledge and control over this phenomenon. Many efforts have been directed to investigate which are the most important etiologic agents involved, the pathogenetic mechanisms leading to microbial adhesion, colonization of implant surfaces, and evasion of the host defenses, the most crucial virulence factors and the nature and properties of microbial biofilms. The pathogenesis of peri-implant infections differs from that of other post-surgical infections for a series of phenomena that are strictly related to the presence of biomaterials because the interstitial milieu surrounding prosthetic implants represents a region of local immune depression susceptible to

microbial colonization, and favorable to the instauration of infections. Bacteria are initially passively adsorbed on the biomaterial surfaces, but the establishment of prosthesis-associated infections relies also on specific active interactions of the bacteria with biomaterial surfaces. For instance, several microbial species possess adhesins, receptorial proteins which mediate cell anchorage and fixation to host extracellular matrix proteins (such as collagen, fibrinogen, fibronectin, and elastin) adsorbed on biomaterials. In addition, bacteria elaborate a complex polysaccharidic glycocalix, forming adherent biofilms on implant surfaces which increase their protection from the host defense and enhance resistance to antibiotic treatments.

The diagnosis of orthopaedic implant-related infections is a difficoult task since, while early post-operative prosthetic joint infections are often characterized by acute onset of symptoms and signs of infections, late post-operative prosthetic joint infections (which generally occur after the first 3 months following surgery) show more subtle signs of inflammation, chronic persistent post-operative pain and/or early loosening of the implant. The vast majority of implant-related infections is due to *S. aureus* and *S. epidermidis* (Gram+ bacteria), but also other strains are involved with the frequency reported in Figure 22.

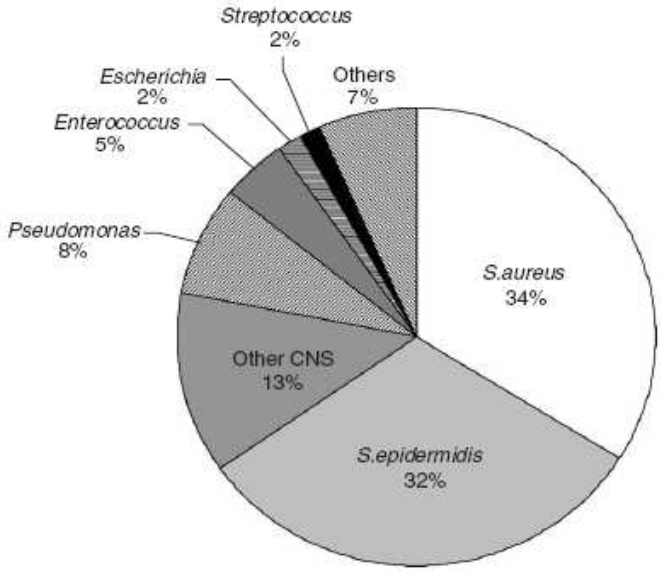

Figure 22. Frequency of main pathogenic species among orthopaedic clinical isolates of implant-associated infections.

The progressive alarming appearance of antibiotic resistant strains (*e.g. S. aureus* strains) is a main issue requiring primary clinical attention. Moreover, bacteria forming biofilms on prosthetic surfaces are particularly resistant to antimicrobials and tend to survive to aggressive chemotherapy even in the absence of specific antibiotic resistance factors.

Material chemical properties and superficial topography of implant materials can influence early microbial adhesion and the chances of successful colonization of the prosthesis; in fact a

modification of the chemistry or the micro/nanotopology of the outer layer of the device represents the most convenient way to interfere with the early phases of microbial adhesion. Many attempts of superficial chemical modifications include the coating of the device with surfactants, proteins such as albumin, hydrophilic negatively charged polysaccharides like hyaluronic acid and heparin, with the scope to generate adhesion resistant or even bacteria repellent surfaces. Even if for *in vitro* simplified conditions some of these surfaces result effective, up to now little evidence has been produced of a significant reduction in implant susceptibility to infection under *in vivo* conditions deriving from this type of approach. A more incisive approach considers the use of bioactive materials and coatings endowed with intrinsic large spectrum anti-microbial properties; in this way, a sustained release of disinfectants, drugs or antibiotics, can reach critical concentrations directly at the interface of the implant. In the list of the bioactive material surfaces, there are coatings able to release metals like copper[248] and silver ions[249], or silver sulfadiazine[250], disinfectants such as chlorhexidine[251] or other bactericidal chemicals such as nitric oxide and various antibiotics (*e.g.* gentamicin, vancomycin…)[252;253]. Active substances can also be incorporated into bulk materials and cavity filling materials, either by simple impregnation or by covalent bonding; for instance, antibiotic loaded cements are nowadays frequently applied in orthopaedics, especially in association with the replacement of infected prostheses for the high risk of recidive.

On the other hand, toxicological issues related to systemic metal accumulation or local cytotoxicity could limit the broad use of certain anti-microbial chemicals other than antibiotics, supporting their utilization only in special circumstances at high infection risk such as in percutaneous implants or catheters. In fact, for bone implants, cytotoxicity can be a very crucial issue, interfering with optimal osteointegration when not even leading to bone resorption phenomena and aseptic mobilization.

Overall, it is hard to expect that a single strategy among all these just mentioned could represent the ideal solution in the fight against infections. More plausibly, depending on the type of implant, the anatomic site of implantation, and the circumstances of the intervention (*e.g.* revision with risk of recidive), a number of new valid options should be made available to the surgeons. The appropriate choice when not even combination of these expedients will contribute both to decrease the chances of implant colonization, and to increase the effectiveness of traditional chemotherapy, contributing to further lowering the risks of implant failure. The development of anti-infective surfaces is just at a very early stage and, in a near future, efforts and investments in this direction are expected to multiply[254].

2. AIMS

The overall scope of these studies has been to develop a nanocomposite coating for a polymer-based bone prosthesis, with particular focus on its interaction with bacteria and eukaryotic cells.

The specific aims were to:

1. define preparation protocols of antibacterial metal nanoparticles stabilized by biocompatible polysaccharides;

2. develop nanocomposite materials based on silver nanoparticles that could exert antibacterial activity without showing cytotoxic effects;

3. devise a technique to graft the nanocomposite coating to the substrate material of the prosthesis (methacrylic thermoset);

4. evaluate the biological response of the final construct.

3. SUMMARY OF PAPERS

PAPER 1:

Polyol Synthesis of Silver Nanoparticles: Mechanism of Reduction by Alditol Bearing Polysaccharides

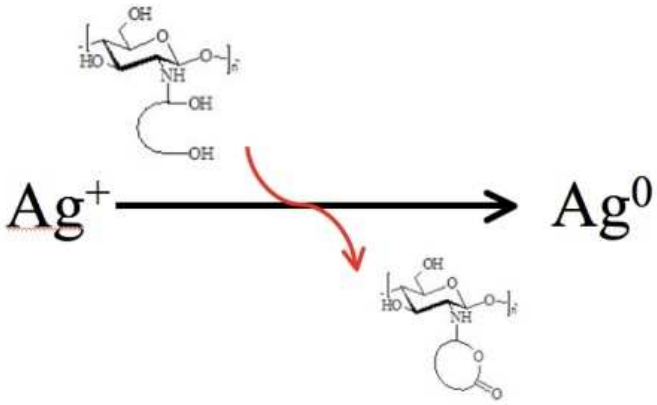

This work tackles the preparation of silver nanoparticles by means of alditol bearing polysaccharides derived from natural resources (chitosan), without the addition of exogenous reducing agent. In fact, the alditol itself is used to induce the metal reduction thanks to the Fetizon reaction. For the first time, alditols, *i.e.* completely reduced sugars, are shown to be able to reduce silver ions in mild conditions. The mechanism of the reaction has been proved using different derivatives of chitosan which showed that when the primary hydroxyl group of the alditol moiety is involved in glycosidic bonds, silver ion reduction does not take place. Thanks to the multivalent arrangement of the alditol on the polysaccharide backbone, a very efficient reduction takes place and round shaped silver nanoparticles (Ø ~ 5 nm) are formed. This systems proved to give rise to a notable Surface Enhanced Raman Scattering effect (SERS) and, depending on the experimental conditions, to lead to the formation of hydrogels.

The possibility of using alditols to reduce silver ions in mild conditions and their arrangement on a polysaccharide backbone to form silver nanoparticles represents the main novelty of this paper.

PAPER 2:

Non-Cytotoxic Silver Nanoparticle – Polysaccharide Nanocomposites with Antimicrobial Activity

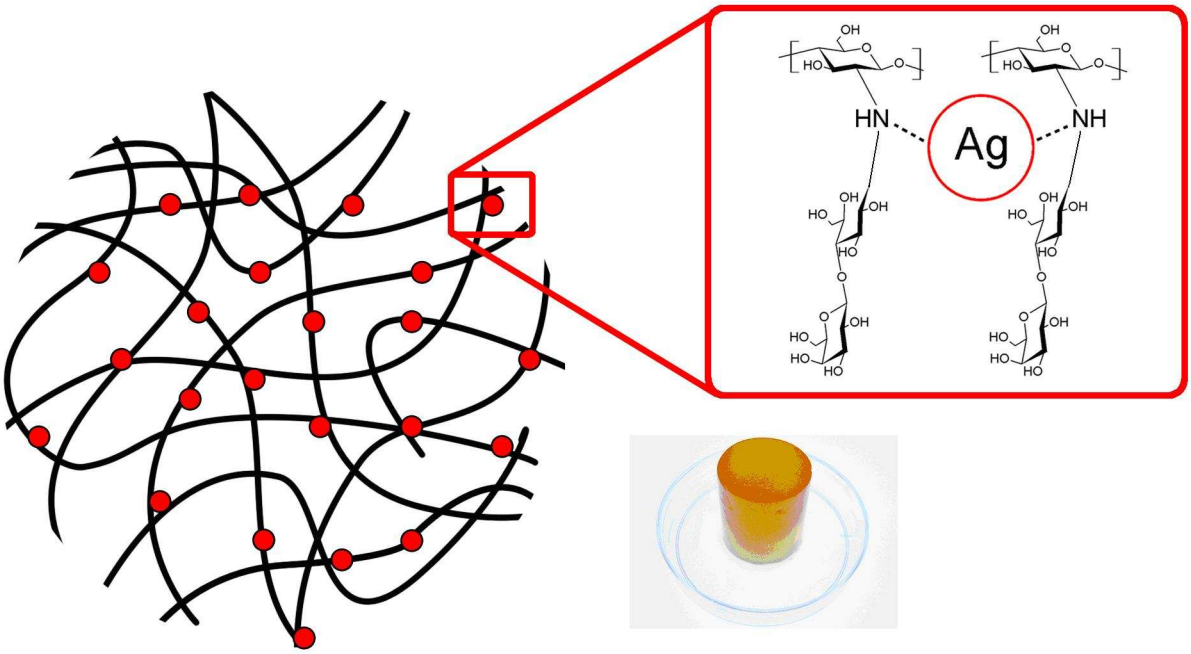

This paper describes the preparation of a nanocomposite system based on bioactive polysaccharides and antimicrobial silver nanoparticles. The use of a lactose-modified chitosan ("Chitlac") as dispersing agent allows for a more effective formation and stabilization of the nanoparticles, with respect to unmodified chitosan. Moreover, the miscibility of Chitlac-silver nanoparticles (Chitlac-nAg) with the polysaccharide alginate was exploited to obtain homogeneous hydrogels that do not exert any cytotoxic effect on eukaryotic cells while displaying considerable antimicrobial activity. This is attributed to the fact that the nanoparticles, immobilized in the gel matrix, can exert their antimicrobial activity by simple contact with the bacterial membrane, while they can not be uptaken and internalized by eukaryotic cells. This novel approach could provide new tools to design engineered materials exploiting, to different purposes, the cell-stimulating activity provided by the saccharidic component and the properties of silver at the nanoscale level.

PAPER 3:

Surface Modification and Polysaccharide Deposition on BisGMA/TEGDMA Thermoset

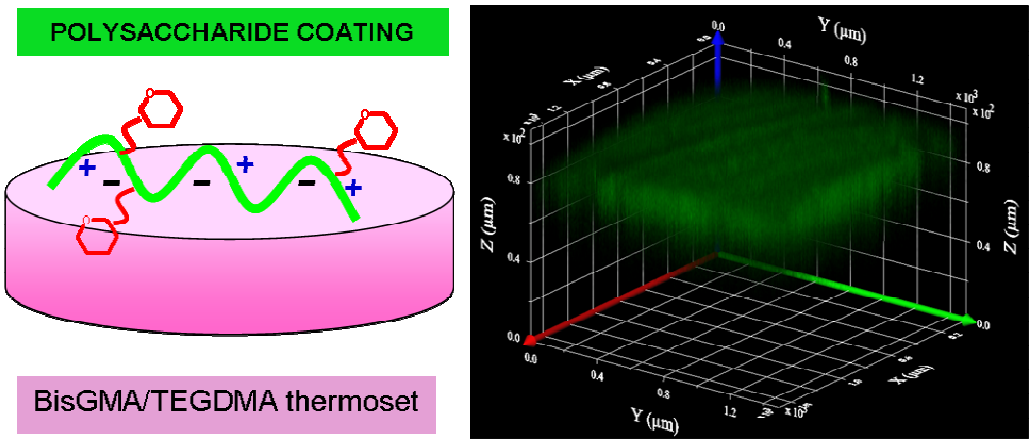

This work describes the preparation of BisGMA/TEGDMA thermoset whose surface has been functionalized by deposition of a bioactive polysaccharide coating (Chitlac) in order to stimulate cell proliferation. The coating was characterized by means of AFM, Confocal Laser Scanning Microscopy (CLSM) and SEM and its friction properties were evaluated. Biological tests *in vitro* revealed that the presence of Chitlac decorated with an RGD-peptide led to a significant enhancement of cell proliferation with respect to the unmodified BisGMA/TEGDMA resin. The performance of the coated BisGMA/TEGDMA resin became comparable with that of clinically used roughened titanium. The approach presented in this work efficiently combines aspects like proper mechanical performances and cell-directed biochemical signaling to upgrade these largely used thermosets. This approach could lead to new materials capable to meet the complex requirements of biomechanical and biological properties expected for a “third generation” biomaterial.

PAPER 4:

Silver-Polysaccharide Nanocomposite Antimicrobial Coatings for Methacrylic Thermosets

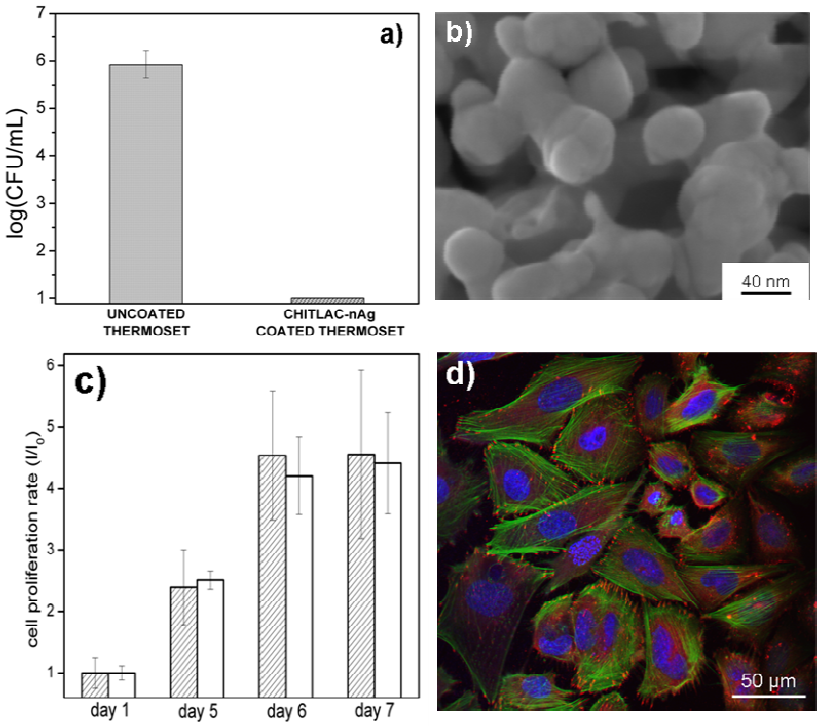

This paper describes the preparation of an antimicrobial non-cytotoxic coating for methacrylic thermosets based on Chitlac and silver nanoparticles. The coating was characterized by means of UV-Visible spectrophotometry, TEM and SEM, while its antimicrobial properties were evaluated with both Gram+ and Gram- strains. Cell proliferation on the coating was studied with osteoblasts-like cell lines, primary human fibroblasts and adipose-derived stem cells by means of Alamar Blue assays, SEM and Confocal Laser Scanning Microscopy (CLSM).

This nanocomposite coating is effective in killing bacteria without exerting any significant cytotoxic effect towards tested cells, which are able to firmly attach and proliferate on the surface of the coating. Such biocompatible antimicrobial polymeric films containing silver nanoparticles have good potentials for surface modification of medical devices, especially for prosthetic applications in orthopedics and dentistry.

PAPER 5:

Cytotoxicity Evaluation of Hydrogels Embedding Gold Nanoparticles

(In preparation)

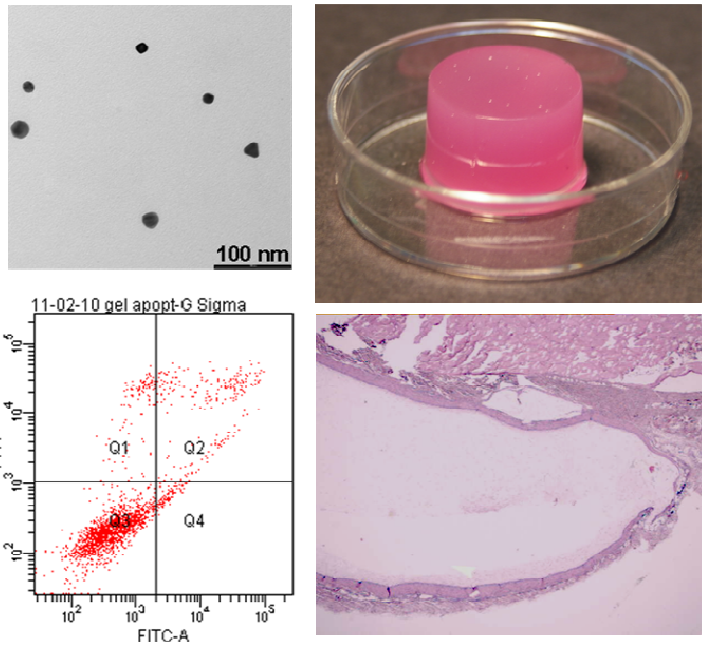

This paper describes the preparation of a nanocomposite hydrogel based on alginate and Chitlac embedding gold nanoparticles. The use of Chitlac allows for the preparation of a homogeneous colloidal solution where gold nanoparticles are better stabilized with respect to chitosan. In line with the case of Chitlac-nAg, also this gold-based colloidal solution displayed antimicrobial activity. Despite the miscibility with alginate that allowed obtaining semi-solid structures (AC-nAu), *in vitro* cytotoxicity assays pointed out a gold-related toxicity towards eukaryotic cells which are induced into apoptosis, at variance with silver-based hydrogels (AC-nAg). *In vivo* tests in a rat model showed a good biocompatibility of both AC-nAg and AC-nAu materials, but in the latter case it was noticed the formation of a thicker fibrous capsule surrounding the implant, stemming from its lower biocompatibility. This finding opens up for debate about gold-related toxicity and the use of this noble metal for biomedical applications.

PAPER 6:

Silver Nanocomposites and their Biomedical Applications

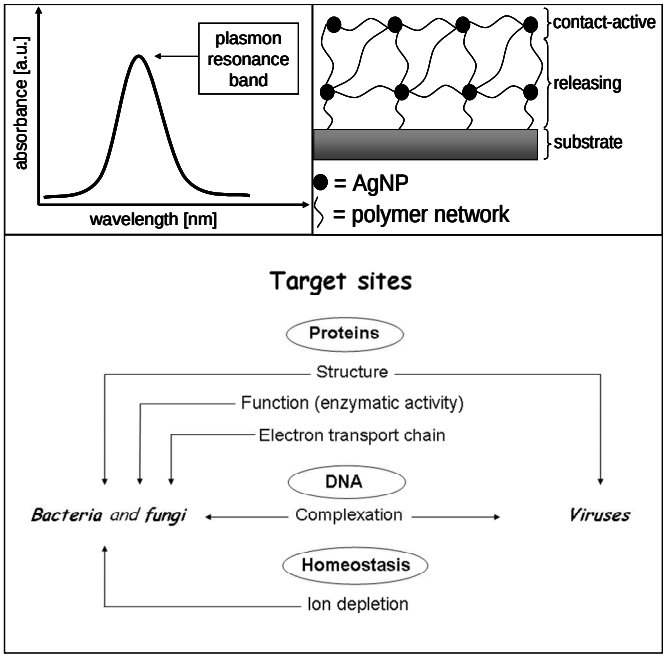

This paper represents a chapter of the book entitled “Nanocomposites for the Life Sciences” (*Wiley-VCH* 2010) and overviews the state-of-the-art of silver nanocomposites for the most promising pathways in the biomedical field.

It starts with an introduction about the new class of materials referred to as “silver nanocomposites” and the discussion of the main routes of preparation of silver nanoparticles and final composite constructs. Subsequently it reports the main results and applications over the last few years, with a particular attention to the antimicrobial field. In fact, as the largest efforts aim at exploiting the antimicrobial properties of silver, this paper sums up results and hypotheses about the details of the antimicrobial mechanism, which is today only partially understood. Moreover it specifically considers the use of silver nanocomposites for applications related to wound healing, inflammations and biological sensing. The work on silver nanocomposites also tackles the issue of possible biological hazards, which are rarely taken into account and often represent a matter of controversy in terms of contradictory results. Finally, this review suggests possible upcoming biomedical applications of this class of materials.

Part of this work has been adapted in the Introduction section of this thesis.

4. GENERAL DISCUSSION

This work aimed at realizing a nanocomposite coating for the development of a polymer-based bone prosthesis. Overall, the objective to prepare a coating endowed with *i*) antimicrobial activity and *ii*) good biocompatibility was fulfilled. Moreover, this research contributed to shed light on a complex interdisciplinary topic that regards the preparation of nanocomposite materials and their interaction with the biological world. In fact, as discussed in the Introduction, to date little is known about exact mechanisms that involve nano-scale materials and prokaryotic or eukaryotic microorganisms; the existence of contradictory results in the literature indicates the extreme complexity of these aspects and the numerous variables that may influence the results of each study (Paper 6). This is why this thesis aims at improving the knowledge in the field, being aware that some issues can be tackled only by hypotheses or suggestions, since much has to be done to completely elucidate exact mechanisms and gain a deeper understanding over these nano-biotechnolgical techniques.

Choice of the polysaccharides in the preparation of nanoparticles

For the preparation of metal nanoparticles we took advantage of the "wet chemical synthesis" in the presence of a stabilizing agent because this *in situ* approach allowed the formation of homogeneous nanoparticles dispersed within the polymer solution. For both silver and gold nanoparticles, the choice of Chitlac as stabilizing agent was due to two main reasons:

1. the functional groups of Chitlac can interact with metal species (coordination interactions);
2. Chitlac is biocompatible and stimulates cell proliferation, thus being an excellent candidate for biomaterial applications.

Moreover, thanks to the presence of the lactitol side chain, Chitlac overcomes the chemical and biological limitations of unmodified chitosan (solubility at physiological pH, miscibility with anionic polysaccharides, cell signalling). The colloidal solutions obtained in the presence of Chitlac are highly homogeneous in terms of nanoparticle dimensions and degree of aggregation, and their stability is maintained over long time scale (years) as discussed in Paper 2. Chitlac is also endowed with the functionality to reduce silver ions without requiring additional exogenous reactants (Paper 1).

The miscibility of Chitlac with the anionic polysaccharide alginate was particularly useful in our attempt to prepare semi-solid matrixes entrapping the nanoparticles: in fact Chitlac-based colloidal solutions were used to obtain soluble binary mixtures with alginate, which eventually

were gelified exploiting the properties of the latter polyelectrolyte. The final constructs were highly hydrated three-dimensional gels containing well dispersed nanoparticles (Paper 2 and 5).

Preparation of the coating

The technique adopted to coat the methacrylic thermosets was based on polyelectrolyte physisorption driven by electrostatic forces, in analogy to the procedure used for the so called "layer by layer deposition" (Paper 6). In particular, we have proposed a novel strategy for the coating of a BisGMA/TEGDMA thermoset material based on a chemical modification that exposes negative charges (carboxylate groups) on its surface (Paper 3). The formation of a thick polysaccharide layer on the thermoset was accomplished by deposition of Chitlac, for the large number of positive charges on Chitlac and the amount of negative groups on the methacrylate surface ensured cooperative interactions. The stability of this layer was explored by scratch tests that indicate a gel-like mechanical behaviour of the coating firmly grafted on the substrate.

The same preparation technique was successfully applied also in the case of Chitlac-nAg (Paper 4); in this case the silver nanocomposite layer attached on the thermoset surface was able to exert considerable antimicrobial effects without being harmful to eukaryotic cells. Stability tests in water demonstrated that electrostatic forces suffice to prevent the dissolution of the nanocomposite layer, at least over a short time scale.

Antibacterial mechanism of silver nanoparticles

An important aspect in the characterization of metal-based antimicrobial systems regarded the study of the mechanisms involved in bacteria inactivation induced by the nanoparticles. As discussed in the Introduction section, in the literature the exact antibacterial mechanism has not been reported yet, despite the wide use of silver for many applications; the most popular explanation is that the main molecular targets in bacteria are the thiol groups (-SH) of the membrane proteins exposed to the extracellular portion of the membrane, although it is still not clear whether the active species is metallic or ionic silver. In our cytofluorimetry studies we demonstrated that the potent bactericidal activity of Chitlac-nAg is associated with bacteria membrane depolarization and permeabilization, thus confirming that the nanoparticles induce damages at bacteria membrane level (Paper 2). It was also important to prove that bacteria inactivation persists when the nanoparticles are entrapped in the polymer matrix (Paper 2 and 4), which suggests that nanoparticles can exert their antimicrobial activity by simple contact with the bacteria.

The contact mechanism proposed was confirmed also in the case of the nanocomposite layer deposited on the methacrylic thermoset, where silver nanoparticles are embedded in the Chitlac matrix attached onto the resin surface; also in this case, bacteria are killed upon direct contact with the silver-containing material, while the metal release is negligible and does not cause any biological effect (Paper 4).

Cytotoxicity issues

The issue of possible adverse effects and toxicity of nanoparticles toward eukaryotic cells was a central point in the development of our nanocomposite biomaterials.

Although in the literature a widely accepted consensus on the detailed molecular mechanism of nanoparticles toxicity is still missing, it is possible to state that a lack of physical barriers to nanoparticle diffusion into cells determines their generalized availability, with the risk of a massive uptake by cells, which eventually leads to their death. In this work we have verified that nanoparticles in the colloidal solution state exerted cytotoxicity effects (Paper 2, Paper 5); at variance, the grafting of silver nanoparticles in the hydrogel (Paper 2) or coating (Paper 4) structures ruled out any risk of toxicity while keeping the antimicrobial properties unaltered. This was ascribed to the fact that, while in bacteria the main molecular targets of silver are thiol groups of proteins exposed to the extracellular portion of the membrane, eukaryotic cells do not have exterior proteins with thiol groups; thus, silver ions or nanoparticles must first permeate through cell membranes to react with thiol groups of intracellular proteins and enzymes, which can happen only upon nanoparticles internalization. In light of this explanation, our strategy of incorporating silver nanoparticles on the surface of the polysaccharide matrix was effective to overcome cytotoxicity issues.

Preliminary evaluation of gold nanocomposites

The study of gold nanoparticles was preliminary tackled because this metal is also widely employed for biomedical applications and its use in the antimicrobial field has been proposed (Paper 5). We managed to prepare homogeneous and stable colloidal solutions of gold nanoparticles formed in Chitlac; the antimicrobial activity was proved both in solution and in the form of hydrogels obtained in association with alginate (AC-nAu). Nevertheless, these nanocomposite hydrogels displayed cytotoxic effects towards eukaryotic cells exerted due to apoptosis mechanisms, at variance with silver-based gels. Additional work is needed to further elucidate the cause of this biological effect.

5. CONCLUDING REMARKS

In spite of extensive research over the recent years in the field of antimicrobial biomaterials based on metal nanocomposites, further studies on the antibacterial mechanism and on possible cytotoxicity towards eukaryotic cells are needed in order to develop new materials that can exploit the peculiar properties of noble metals at the nano-scale without representing a threat for human health. The present work aimed at realizing a coating for a new generation bone prosthesis, whose surface should be able to prevent infections without being harmful to cells of the tissues surrounding the implant.

In this respect, we have shown that natural polysaccharides can be successfully employed to prepare homogeneous nanocomposite systems which, depending on their physical status (colloidal solution, hydrogel, coating) and on the nature of the nanoparticles (silver or gold), can be used to realize biocompatible materials for antimicrobial applications. Since the most important results were obtained in the case of silver nanoparticles, the main part of the work was based on this metal, while the studies on gold nanoparticles can be considered a preliminary investigation.

In particular, it was demonstrated that:

- the polysaccharide Chitlac can be efficiently used as a reducing agent for silver ions as well as a stabilizer of the nanoparticles. This “green synthesis” is based on a particular mechanism (Fetizon reaction) that brings to the preparation of colloidal solutions for biological and optical applications;

- silver nanoparticles prepared in Chitlac solutions display remarkable antibacterial activity due to the interaction between metal and bacteria membranes; such colloidal solution is toxic also for eukaryotic cells, which suggests the need to prevent the cellular internalization of nanoparticles;

- the miscibility of Chitlac-silver colloidal solution with the polysaccharide Alginate led to the preparation of homogeneous hydrogels (AC-nAg) that entrap the nanoparticles and inactivate bacteria upon direct contact with the nanocomposite material;

- AC-nAg hydrogels are able to exert a broad spectrum antibacterial activity without being harmful to mammalian cells both *in vitro* and *in vivo*;

- methacrylic thermosets (BisGMA/TEGDMA), which represent the substrate material of the prosthesis (when reinforced with glass fibres), can be coated with Chitlac-based systems by a deposition technique that exploits electrostatic forces between the polyelectrolyte and the activated thermoset surface, leading to cell proliferation rates comparable to clinically used titanium;

- this deposition technique can also bring to the preparation of a nanocomposite coating where silver nanoparticles are grafted within the Chitlac matrix; such material endows the thermoset surface with potent antimicrobial properties while, at the same time, allowing for adhesion and proliferation of eukaryotic cells;

- the techniques devised follow a non-demanding chemical approach based on reliable and reproducible procedures.

6. BIBLIOGRAPHY

[1] P. N. Prasad, *Nanophotonics* Wiley Interscience, 2004, pp. 278-279.

[2] J. H. Dai and M. L. Bruening, "Catalytic nanoparticles formed by reduction of metal ions in multilayered polyelectrolyte films," *Nano Lett.*, vol. 2, no. 5, pp. 497-501, 2002.

[3] A. Henglein, "Physicochemical properties of small metal particles in solution: "microelectrode" reactions, chemisorption, composite metal particles, and the atom-to-metal transition," *J. Phys. Chem.*, vol. 97, no. 21, pp. 5457-5471, May1993.

[4] C. N. Lok, C. M. Ho, R. Chen, Q. Y. He, W. Y. Yu, H. Sun, P. Tam, J. F. Chiu, and C. M. Che, "Silver nanoparticles: partial oxidation and antibacterial activities," *Journal of Biological Inorganic Chemistry*, vol. 12, no. 4, pp. 527-534, May2007.

[5] Y. Z. Wang, Y. X. Li, S. T. Yang, G. L. Zhang, D. M. An, C. Wang, Q. B. Yang, X. S. Chen, X. B. Jing, and Y. Wei, "A convenient route to polyvinyl pyrrolidone/silver nanocomposite by electrospinning," *Nanotechnology*, vol. 17, no. 13, pp. 3304-3307, 2006.

[6] H. L. Su, C. C. Chou, D. J. Hung, S. H. Lin, I. C. Pao, J. H. Lin, F. L. Huang, R. X. Dong, and J. J. Lin, "The disruption of bacterial membrane integrity through ROS generation induced by nanohybrids of silver and clay," *Biomaterials*, vol. 30, no. 30, pp. 5979-5987, Aug.2009.

[7] K. Mallick, M. J. Witcomb, and M. S. Scurrell, "Polymer stabilized silver nanoparticles: A photochemical synthesis route," *J. Mater. Sci.*, vol. 39, no. 14, pp. 4459-4463, July2004.

[8] A. Henglein, "Physicochemical properties of small metal particles in solution: "microelectrode" reactions, chemisorption, composite metal particles, and the atom-to-metal transition," *J. Phys. Chem.*, vol. 97, no. 21, pp. 5457-5471, May1993.

[9] K. Esumi, A. Suzuki, N. Aihara, K. Usui, and K. Torigoe, "Preparation of Gold Colloids with UV Irradiation Using Dendrimers as Stabilizer," *Langmuir*, vol. 14, no. 12, pp. 3157-3159, June1998.

[10] P. L. Kuo and W. F. Chen, "Formation of silver nanoparticles under structured amino groups in pseudo-dendritic poly(allylamine) derivatives," *J. Phys. Chem. B*, vol. 107, no. 41, pp. 11267-11272, 2003.

[11] J. C. Grunlan, J. K. Choi, and A. Lin, "Antimicrobial Behavior of Polyelectrolyte Multilayer Films Containing Cetrimide and Silver," *Biomacromolecules*, vol. 6, no. 2, pp. 1149-1153, Mar.2005.

[12] A. Henglein, "Physicochemical properties of small metal particles in solution: "microelectrode" reactions, chemisorption, composite metal particles, and the atom-to-metal transition," *J. Phys. Chem.*, vol. 97, no. 21, pp. 5457-5471, May1993.

[13] D. S. dos Santos, P. J. G. Goulet, N. P. W. Pieczonka, O. N. Oliveira, and R. F. Aroca, "Gold nanoparticle embedded, self-sustained chitosan films as substrates for surface-enhanced Raman scattering," *Langmuir*, vol. 20, no. 23, pp. 10273-10277, 2004.

[14] H. Huang, Q. Yuan, and X. Yang, "Preparation and characterization of metal-chitosan nanocomposites," *Colloid Surface B*, vol. 39, no. 1-2, pp. 31-37, Nov.2004.

[15] Y. Yi, Y. Wang, and H. Liu, "Preparation of new crosslinked chitosan with crown ether and their adsorption for silver ion for antibacterial activities," *Carbohyd. Polym.*, vol. 53, no. 4, pp. 425-430, Sept.2003.

[16] H. Yu, X. Xu, X. Chen, T. Lu, P. Zhang, and X. Jing, "Preparation and Antibacterial Effects of PVA-PVP Hydrogels Containing Silver Nanoparticles," *J Appl Polym Sci*, vol. 103, pp. 125-133, 2006.

[17] H. Huang and X. Yang, "Synthesis of polysaccharide-stabilized gold and silver nanoparticles: a green method," *Carbohyd Res*, vol. 339, no. 15, pp. 2627-2631, Oct.2004.

[18] J. Fu, J. Ji, D. Fan, and J. Shen, "Construction of antibacterial multilayer films containing nanosilver via layer-by-layer assembly of heparin and chitosan-silver ions complex," *J. Biomed. Mater. Res. A*, vol. 79, no. 3, pp. 665-674, Dec.2006.

[19] I. Sondi, D. V. Goia, and E. Matijevic, "Preparation of highly concentrated stable dispersions of uniform silver nanoparticles," *J. Colloid Interf. Sci.*, vol. 260, no. 1, pp. 75-81, Apr.2003.

[20] H. Huang, Q. Yuan, and X. Yang, "Morphology study of gold-chitosan nanocomposites," *J. Colloid Interf. Sci.*, vol. 282, no. 1, pp. 26-31, Feb.2005.

[21] A. Bonifacio, L. van der Sneppen, C. Gooijer, and G. van der Zwan, "Citrate-reduced silver hydrosol modified with ω-mercaptoalkanoic acids self-assembled monolayers as a substrate for surface-enhanced resonance raman scattering. A study with cytochrome c," *Langmuir*, vol. 20, no. 14, pp. 5858-5864, July2004.

[22] Z. S. Pillai and P. V. Kamat, "What Factors Control the Size and Shape of Silver Nanoparticles in the Citrate Ion Reduction Method?," *J. Phys. Chem. B*, vol. 108, no. 3, pp. 945-951, Dec.2003.

[23] Z. S. Pillai and P. V. Kamat, "What Factors Control the Size and Shape of Silver Nanoparticles in the Citrate Ion Reduction Method?," *J. Phys. Chem. B*, vol. 108, no. 3, pp. 945-951, Dec.2003.

[24] Z. Liu, X. Wang, H. Wu, and C. Li, "Silver nanocomposite layer-by-layer films based on assembled polyelectrolyte/dendrimer," *J. Colloid Interf. Sci.*, vol. 287, no. 2, pp. 604-611, July2005.

[25] Y. Sun, B. Mayers, T. Herricks, and Y. Xia, "Polyol Synthesis of Uniform Silver Nanowires: A Plausible Growth Mechanism and the Supporting Evidence," *Nano Lett.*, vol. 3, pp. 955-960, 2003.

[26] B. Wiley, T. Herricks, Y. Sun, and Y. Xia, "Polyol synthesis of silver nanoparticles: use of chloride and oxygen to promote the formation of single-crystal, truncated cubes and tetrahedrons," *Nano Lett.*, vol. 4, no. 9, pp. 1733-1739, Sept.2004.

[27] Y. Yin, Y. Lu, Y. Sun, and Y. Xia, "Silver nanowires can be directly coated with amorphous silica to generate well-controlled coaxial nanocables of silver/silica," *Nano Lett.*, vol. 2, no. 4, pp. 427-430, Apr.2002.

[28] H. Huang and X. Yang, "Synthesis of polysaccharide-stabilized gold and silver nanoparticles: a green method," *Carbohyd Res*, vol. 339, no. 15, pp. 2627-2631, Oct.2004.

[29] A. Panacek, L. Kvitek, R. Prucek, M. Kolar, R. Vecerova, N. Pizurova, V. K. Sharma, T. Nevecna, and R. Zboril, "Silver Colloid Nanoparticles: Synthesis, Characterization, and Their Antibacterial Activity," *J. Phys. Chem. B*, vol. 110, no. 33, pp. 16248-16253, Aug.2006.

[30] I. Donati, A. Travan, C. Pelillo, T. Scarpa, A. Coslovi, A. Bonifacio, V. Sergo, and S. Paoletti, "Polyol Synthesis of Silver Nanoparticles: Mechanism of Reduction by Alditol Bearing Polysaccharides," *Biomacromolecules*, vol. 10, no. 2, pp. 210-213, Feb.2009.

[31] A. Travan, C. Pelillo, I. Donati, E. Marsich, M. Benincasa, T. Scarpa, S. Semeraro, G. Turco, R. Gennaro, and S. Paoletti, "Non-cytotoxic Silver Nanoparticle-Polysaccharide Nanocomposites with Antimicrobial Activity," *Biomacromolecules*, vol. 10, no. 6, p. 1429, Apr.2009.

[32] J. Fu, J. Ji, D. Fan, and J. Shen, "Construction of antibacterial multilayer films containing nanosilver via layer-by-layer assembly of heparin and chitosan-silver ions complex," *J. Biomed. Mater. Res. A*, vol. 79, no. 3, pp. 665-674, Dec.2006.

[33] I. Sondi, D. V. Goia, and E. Matijevic, "Preparation of highly concentrated stable dispersions of uniform silver nanoparticles," *J. Colloid Interf. Sci.*, vol. 260, no. 1, pp. 75-81, Apr.2003.

[34] K. Esumi, A. Suzuki, N. Aihara, K. Usui, and K. Torigoe, "Preparation of Gold Colloids with UV Irradiation Using Dendrimers as Stabilizer," *Langmuir*, vol. 14, no. 12, pp. 3157-3159, June1998.

[35] H. Huang, Q. Yuan, and X. Yang, "Preparation and characterization of metal-chitosan nanocomposites," *Colloid Surface B*, vol. 39, no. 1-2, pp. 31-37, Nov.2004.

[36] J. C. Grunlan, J. K. Choi, and A. Lin, "Antimicrobial Behavior of Polyelectrolyte Multilayer Films Containing Cetrimide and Silver," *Biomacromolecules*, vol. 6, no. 2, pp. 1149-1153, Mar.2005.

[37] W. S. Choi, H. Y. Koo, J. H. Park, and D. Y. Kim, "Synthesis of Two Types of Nanoparticles in Polyelectrolyte Capsule Nanoreactors and Their Dual Functionality," *J. Am. Chem. Soc.*, vol. 127, no. 46, pp. 16136-16142, Nov.2005.

[38] C. H. Ho, J. Tobis, C. Sprich, R. Thomann, and J. C. Tiller, "Nanoseparated Plymeric Network with Multiple Antimicrobial Properties," *Adv. Mater.*, vol. 16, no. 12, pp. 957-961, 2004.

[39] B. Wiley, T. Herricks, Y. Sun, and Y. Xia, "Polyol synthesis of silver nanoparticles: use of chloride and oxygen to promote the formation of single-crystal, truncated cubes and tetrahedrons," *Nano Lett.*, vol. 4, no. 9, pp. 1733-1739, Sept.2004.

[40] B. Wiley, Y. Sun, B. Mayers, and Y. Xia, "Shape-controlled synthesis of metal nanostructures: the case of silver," *Chem. -Eur. J.*, vol. 11, no. 2, pp. 454-463, 2005.

[41] L. Balogh, D. R. Swanson, D. A. Tomalia, G. L. Hagnauer, and A. T. McManus, "Dendrimer-Silver Complexes and Nanocomposites as Antimicrobial Agents," *Nano Lett.*, vol. 1, no. 1, pp. 18-21, Jan.2001.

[42] C. N. Lok, C. M. Ho, R. Chen, Q. Y. He, W. Y. Yu, H. Sun, P. Tam, J. F. Chiu, and C. M. Che, "Silver nanoparticles: partial oxidation and antibacterial activities," *Journal of Biological Inorganic Chemistry*, vol. 12, no. 4, pp. 527-534, May2007.

[43] H. L. Su, C. C. Chou, D. J. Hung, S. H. Lin, I. C. Pao, J. H. Lin, F. L. Huang, R. X. Dong, and J. J. Lin, "The disruption of bacterial membrane integrity through ROS generation induced by nanohybrids of silver and clay," *Biomaterials*, vol. 30, no. 30, pp. 5979-5987, Aug.2009.

[44] N. Rameshbabu, T. S. Sampath Kumar, T. G. Prabhakar, V. S. Sastry, K. V. Murty, and R. K. Prasad, "Antibacterial nanosized silver substituted hydroxyapatite: Synthesis and characterization," *J Biomed. Mater. Res. A*, vol. 80, no. 3, pp. 581-591, Mar.2007.

[45] A. N. Krkljes, M. T. Marinovic-Cincovic, Z. M. Kacarevic-Popovic, and J. M. Nedeljkovic, "Radiolytic synthesis and characterization of Ag-PVA nanocomposites," *Eur. Polym. J.*, vol. 43, no. 6, pp. 2171-2176, June2007.

[46] F. Mafune, J. y. Kohno, Y. Takeda, T. Kondow, and H. Sawabe, "Formation and Size Control of Silver Nanoparticles by Laser Ablation in Aqueous Solution," *The Journal of Physical Chemistry B*, vol. 104, no. 39, pp. 9111-9117, Sept.2000.

[47] S. Kundu, M. Mandal, S. K. Ghosh, and T. Pal, "Photochemical deposition of SERS active silver nanoparticles on silica gel and their application as catalysts for the reduction of aromatic nitro compounds," *J. Colloid Interf. Sci.*, vol. 272, no. 1, pp. 134-144, Apr.2004.

[48] K. Mallick, M. J. Witcomb, and M. S. Scurrell, "Polymer stabilized silver nanoparticles: A photochemical synthesis route," *J. Mater. Sci.*, vol. 39, no. 14, pp. 4459-4463, July2004.

[49] J. Zhu, S. Liu, O. Palchik, Y. Koltypin, and A. Gedanken, "Shape-Controlled Synthesis of Silver Nanoparticles by Pulse Sonoelectrochemical Methods," *Langmuir*, vol. 16, no. 16, pp. 6396-6399, July2000.

[50] M. Starowicz, B. Stypula, and J. Banas, "Electrochemical synthesis of silver nanoparticles," *Electrochem. Commun.*, vol. 8, no. 2, pp. 227-230, Feb.2006.

[51] X. M. Yan, J. Ni, M. Robbins, H. J. Park, W. Zhao, and J. M. White, "Silver Nanoparticles Synthesized by Vapor Deposition onto an Ice Matrix," *J. Nanopart. Res.*, vol. 4, no. 6, pp. 525-533, Dec.2002.

[52] H. Yin, T. Yamamoto, Y. Wada, and S. Yanagida, "Large-scale and size-controlled synthesis of silver nanoparticles under microwave irradiation," *Mater. Chem. Phys.*, vol. 83, no. 1, pp. 66-70, Jan.2004.

[53] K. Li and F. S. Zhang, "A novel approach for preparing silver nanoparticles under electron beam irradiation," *J. Nanopart. Res.*, Jan.2009.

[54] E. Braun, Y. Eichen, U. Sivan, and G. Ben-Yoseph, "DNA-templated assembly and electrode attachment of a conducting silver wire," *Nature*, vol. 391, no. 6669, pp. 775-778, Feb.1998.

[55] Y. Lu, G. L. Liu, and L. P. Lee, "High-Density Silver Nanoparticle Film with Temperature-Controllable Interparticle Spacing for a Tunable Surface Enhanced Raman Scattering Substrate," *Nano Lett.*, vol. 5, no. 1, pp. 5-9, Jan.2005.

[56] R. D. Deshmukh and R. J. Composto, "Surface Segregation and Formation of Silver Nanoparticles Created In situ in Poly(methyl Methacrylate) Films," *Chem. Mater.*, vol. 19, no. 4, pp. 745-754, Jan.2007.

[57] A. Henglein, "Physicochemical properties of small metal particles in solution: "microelectrode" reactions, chemisorption, composite metal particles, and the atom-to-metal transition," *J. Phys. Chem.*, vol. 97, no. 21, pp. 5457-5471, May1993.

[58] Z. S. Pillai and P. V. Kamat, "What Factors Control the Size and Shape of Silver Nanoparticles in the Citrate Ion Reduction Method?," *J. Phys. Chem. B*, vol. 108, no. 3, pp. 945-951, Dec.2003.

[59] A. Henglein, "Physicochemical properties of small metal particles in solution: "microelectrode" reactions, chemisorption, composite metal particles, and the atom-to-metal transition," *J. Phys. Chem.*, vol. 97, no. 21, pp. 5457-5471, May1993.

[60] A. Henglein, "Colloidal Silver Nanoparticles: Photochemical Preparation and Interaction with O2, CCl4, and Some Metal Ions," *Chem. Mater.*, vol. 10, no. 1, pp. 444-450, Jan.1998.

[61] A. Henglein and M. Giersig, "Formation of Colloidal Silver Nanoparticles: Capping Action of Citrate," *J. Phys. Chem. B*, vol. 103, no. 44, pp. 9533-9539, Nov.1999.

[62] A. Henglein, "Colloidal Silver Nanoparticles: Photochemical Preparation and Interaction with O2, CCl4, and Some Metal Ions," *Chem. Mater.*, vol. 10, no. 1, pp. 444-450, Jan.1998.

[63] C. N. Lok, C. M. Ho, R. Chen, Q. Y. He, W. Y. Yu, H. Sun, P. Tam, J. F. Chiu, and C. M. Che, "Silver nanoparticles: partial oxidation and antibacterial activities," *Journal of Biological Inorganic Chemistry*, vol. 12, no. 4, pp. 527-534, May2007.

[64] A. N. Krkljes, M. T. Marinovic-Cincovic, Z. M. Kacarevic-Popovic, and J. M. Nedeljkovic, "Radiolytic synthesis and characterization of Ag-PVA nanocomposites," *Eur. Polym. J.*, vol. 43, no. 6, pp. 2171-2176, June2007.

[65] Y. Zhang, H. Peng, W. Huang, Y. Zhou, and D. Yan, "Facile preparation and characterization of highly antimicrobial colloid Ag or Au nanoparticles," *J. Colloid Interf. Sci.*, vol. 325, no. 2, pp. 371-376, Sept.2008.

[66] B. Wiley, Y. Sun, and Y. Xia, "Synthesis of Silver Nanostructures with Controlled Shapes and Properties," *Accounts Chem. Res.*, vol. 40, no. 10, pp. 1067-1076, July2007.

[67] T. C. Wang, M. F. Rubner, and R. E. Cohen, "Polyelectrolyte Multilayer Nanoreactors for Preparing Silver Nanoparticle Composites: Controlling Metal Concentration and Nanoparticle Size," *Langmuir*, vol. 18, no. 8, pp. 3370-3375, Apr.2002.

[68] D. M. Dotzauer, J. Dai, L. Sun, and M. L. Bruening, "Catalytic Membranes Prepared Using Layer-by-Layer Adsorption of Polyelectrolyte/Metal Nanoparticle Films in Porous Supports," *Nano Lett.*, vol. 6, no. 10, pp. 2268-2272, Oct.2006.

[69] W. S. Choi, H. Y. Koo, J. H. Park, and D. Y. Kim, "Synthesis of Two Types of Nanoparticles in Polyelectrolyte Capsule Nanoreactors and Their Dual Functionality," *J. Am. Chem. Soc.*, vol. 127, no. 46, pp. 16136-16142, Nov.2005.

[70] B. Wiley, T. Herricks, Y. Sun, and Y. Xia, "Polyol synthesis of silver nanoparticles: use of chloride and oxygen to promote the formation of single-crystal, truncated cubes and tetrahedrons," *Nano Lett.*, vol. 4, no. 9, pp. 1733-1739, Sept.2004.

[71] N. Malikova, I. Pastoriza-Santos, M. Schierhorn, N. A. Kotov, and L. M. Liz-Marzan, "Layer-by-Layer Assembled Mixed Spherical and Planar Gold Nanoparticles: Control of Interparticle Interactions," *Langmuir*, vol. 18, no. 9, pp. 3694-3697, Apr.2002.

[72] A. Csaki, F. Garwe, A. Steinbruck, G. Maubach, G. Festag, A. Weise, I. Riemann, K. Konig, and W. Fritzsche, "A Parallel Approach for Subwavelength Molecular Surgery Using Gene-Specific Positioned Metal Nanoparticles as Laser Light Antennas," *Nano Lett.*, vol. 7, no. 2, pp. 247-253, Feb.2007.

[73] R. D. Deshmukh and R. J. Composto, "Surface Segregation and Formation of Silver Nanoparticles Created In situ in Poly(methyl Methacrylate) Films," *Chem. Mater.*, vol. 19, no. 4, pp. 745-754, Jan.2007.

[74] R. Zeng, M. Z. Rong, M. Q. Zhang, H. C. Liang, and H. M. Zeng, "Laser ablation of polymer-based silver nanocomposites," *Appl. Surf. Sci.*, vol. 187, no. 3-4, pp. 239-247, Feb.2002.

[75] M. Stofik, Z. Stryhal, and J. Maly, "Dendrimer-encapsulated silver nanoparticles as a novel electrochemical label for sensitive immunosensors," *Biosens. Bioelectron.*, vol. 24, no. 7, pp. 1918-1923, Mar.2009.

[76] K. J. Lee, P. D. Nallathamby, L. M. Browning, C. J. Osgood, and X. H. N. Xu, "In Vivo Imaging of Transport and Biocompatibility of Single Silver Nanoparticles in Early Development of Zebrafish Embryos," *ACS Nano*, vol. 1, no. 2, pp. 133-143, Sept.2007.

[77] Y. Lu, G. L. Liu, and L. P. Lee, "High-Density Silver Nanoparticle Film with Temperature-Controllable Interparticle Spacing for a Tunable Surface Enhanced Raman Scattering Substrate," *Nano Lett.*, vol. 5, no. 1, pp. 5-9, Jan.2005.

[78] J. Zhou, J. Yang, Y. Sun, D. Zhang, J. Shen, Q. Zhang, and K. Wang, "Effect of silver nanoparticles on photo-induced reorientation of azo groups in polymer films," *Thin Solid Films*, vol. 515, no. 18, pp. 7242-7246, June2007.

[79] A. N. Krkljes, M. T. Marinovic-Cincovic, Z. M. Kacarevic-Popovic, and J. M. Nedeljkovic, "Radiolytic synthesis and characterization of Ag-PVA nanocomposites," *Eur. Polym. J.*, vol. 43, no. 6, pp. 2171-2176, June2007.

[80] P. S. K. Murthy, Y. Murali Mohan, K. Varaprasad, B. Sreedhar, and K. Mohana Raju, "First successful design of semi-IPN hydrogel-silver nanocomposites: A facile approach for antibacterial application," *Journal of Colloid and Interface Science*, vol. 318, no. 2, pp. 217-224, Feb.2008.

[81] T. Huang, P. D. Nallathamby, D. Gillet, and X. H. N. Xu, "Design and Synthesis of Single-Nanoparticle Optical Biosensors for Imaging and Characterization of Single Receptor Molecules on Single Living Cells," *Anal. Chem.*, vol. 79, no. 20, pp. 7708-7718, Sept.2007.

[82] W. Lesniak, A. U. Bielinska, K. Sun, K. W. Janczak, X. Shi, J. R. Baker, and L. P. Balogh, "Silver/Dendrimer Nanocomposites as Biomarkers: Fabrication, Characterization, in Vitro Toxicity, and Intracellular Detection," *Nano Lett.*, vol. 5, no. 11, pp. 2123-2130, Nov.2005.

[83] W. Lesniak, A. U. Bielinska, K. Sun, K. W. Janczak, X. Shi, J. R. Baker, and L. P. Balogh, "Silver/Dendrimer Nanocomposites as Biomarkers: Fabrication, Characterization, in Vitro Toxicity, and Intracellular Detection," *Nano Lett.*, vol. 5, no. 11, pp. 2123-2130, Nov.2005.

[84] M. Rai, A. Yadav, and A. Gade, "Silver nanoparticles as a new generation of antimicrobials," *Biotechnology Advances*, vol. 27, no. 1, pp. 76-83, Jan.2001.

[85] L. Grishchenko, S. Medvedeva, G. Aleksandrova, L. Feoktistova, A. Sapozhnikov, B. Sukhov, and B. Trofimov, "Redox reactions of arabinogalactan with silver ions and formation of nanocomposites," *Russ. J. Gen. Chem.*, vol. 76, no. 7, pp. 1111-1116, July2006.

[86] M. Rai, A. Yadav, and A. Gade, "Silver nanoparticles as a new generation of antimicrobials," *Biotechnology Advances*, vol. 27, no. 1, pp. 76-83, Jan.2001.

[87] A. Travan, C. Pelillo, I. Donati, E. Marsich, M. Benincasa, T. Scarpa, S. Semeraro, G. Turco, R. Gennaro, and S. Paoletti, "Non-cytotoxic Silver Nanoparticle-Polysaccharide Nanocomposites with Antimicrobial Activity," *Biomacromolecules*, vol. 10, no. 6, p. 1429, Apr.2009.

[88] J. P. Chen, "Late angiographic stent thrombosis (LAST): the cloud behind the drug-eluting stent silver lining?," *J. Invasive. Cardiol.*, vol. 19, no. 9, pp. 395-400, Sept.2007.

[89] L. Balogh, D. R. Swanson, D. A. Tomalia, G. L. Hagnauer, and A. T. McManus, "Dendrimer-Silver Complexes and Nanocomposites as Antimicrobial Agents," *Nano Lett.*, vol. 1, no. 1, pp. 18-21, Jan.2001.

[90] J. Fu, J. Ji, D. Fan, and J. Shen, "Construction of antibacterial multilayer films containing nanosilver via layer-by-layer assembly of heparin and chitosan-silver ions complex," *J. Biomed. Mater. Res. A*, vol. 79, no. 3, pp. 665-674, Dec.2006.

[91] H. Huang, Q. Yuan, and X. Yang, "Preparation and characterization of metal-chitosan nanocomposites," *Colloid Surface B*, vol. 39, no. 1-2, pp. 31-37, Nov.2004.

[92] P. Sanpui, A. Murugadoss, P. V. D. Prasad, S. S. Ghosh, and A. Chattopadhyay, "The antibacterial properties of a novel chitosan-Ag-nanoparticle composite," *Int. J. Food Microbiol.*, vol. 124, no. 2, pp. 142-146, May2008.

[93] K. N. J. Stevens, O. Crespo-Biel, E. E. M. van den Bosch, A. A. Dias, M. L. W. Knetsch, Y. B. J. Aldenhoff, F. H. van der Veen, J. G. Maessen, E. E. Stobberingh, and L. H. Koole, "The relationship between the antimicrobial effect of catheter coatings containing silver nanoparticles and the coagulation of contacting blood," *Biomaterials*, vol. 30, no. 22, pp. 3682-3690, Aug.2009.

[94] L. Lu, R. W. Sun, R. Chen, C. K. Hui, C. M. Ho, J. M. Luk, G. K. Lau, and C. M. Che, "Silver nanoparticles inhibit hepatitis B virus replication," *Antivir. Ther.*, vol. 13, no. 2, pp. 253-262, 2008.

[95] K. J. Kim, W. S. Sung, B. K. Suh, S. K. Moon, J. S. Choi, J. G. Kim, and D. G. Lee, "Antifungal activity and mode of action of silver nano-particles on Candida albicans," *Biometals*, vol. 22, no. 2, pp. 235-242, Apr.2009.

[96] L. Esteban-Tejeda, F. Malpartida, A. Esteban-Cubillo, C. Pecharroman, and J. S. Moya, "The antibacterial and antifungal activity of a soda-lime glass containing silver nanoparticles," *Nanotechnology.*, vol. 20, no. 8, p. 85103, Feb.2009.

[97] M. B. Gajbhiye, J. G. Kesharwani, A. P. Ingle, A. K. Gade, and M. K. Rai, "Fungus-mediated synthesis of silver nanoparticles and their activity against pathogenic fungi in combination with fluconazole," *Nanomedicine.*, July2009.

[98] K. N. J. Stevens, O. Crespo-Biel, E. E. M. van den Bosch, A. A. Dias, M. L. W. Knetsch, Y. B. J. Aldenhoff, F. H. van der Veen, J. G. Maessen, E. E. Stobberingh, and L. H. Koole, "The relationship between the antimicrobial effect of catheter coatings containing silver nanoparticles and the coagulation of contacting blood," *Biomaterials*, vol. 30, no. 22, pp. 3682-3690, Aug.2009.

[99] D. G. Maki, C. E. Weise, and H. W. Sarafin, "A semiquantitative culture method for identifying intravenous-catheter-related infection," *N Engl J Med*, vol. 296, no. 23, pp. 1305-1309, June1977.

[100] H. L. Su, C. C. Chou, D. J. Hung, S. H. Lin, I. C. Pao, J. H. Lin, F. L. Huang, R. X. Dong, and J. J. Lin, "The disruption of bacterial membrane integrity through ROS generation induced by nanohybrids of silver and clay," *Biomaterials*, vol. 30, no. 30, pp. 5979-5987, Aug.2009.

[101] J. C. Grunlan, J. K. Choi, and A. Lin, "Antimicrobial Behavior of Polyelectrolyte Multilayer Films Containing Cetrimide and Silver," *Biomacromolecules*, vol. 6, no. 2, pp. 1149-1153, Mar.2005.

[102] W. S. Choi, H. Y. Koo, J. H. Park, and D. Y. Kim, "Synthesis of Two Types of Nanoparticles in Polyelectrolyte Capsule Nanoreactors and Their Dual Functionality," *J. Am. Chem. Soc.*, vol. 127, no. 46, pp. 16136-16142, Nov.2005.

[103] Y. Zhang, H. Peng, W. Huang, Y. Zhou, and D. Yan, "Facile preparation and characterization of highly antimicrobial colloid Ag or Au nanoparticles," *J. Colloid Interf. Sci.*, vol. 325, no. 2, pp. 371-376, Sept.2008.

[104] I. Sondi and B. Salopek-Sondi, "Silver nanoparticles as antimicrobial agent: a case study on *E. coli* as a model for Gram-negative bacteria," *J Colloid Interface Sci*, vol. 275, no. 1, pp. 177-182, July2004.

[105] A. Henglein and M. Giersig, "Formation of Colloidal Silver Nanoparticles: Capping Action of Citrate," *J. Phys. Chem. B*, vol. 103, no. 44, pp. 9533-9539, Nov.1999.

[106] C. N. Lok, C. M. Ho, R. Chen, Q. Y. He, W. Y. Yu, H. Sun, P. Tam, J. F. Chiu, and C. M. Che, "Silver nanoparticles: partial oxidation and antibacterial activities," *Journal of Biological Inorganic Chemistry*, vol. 12, no. 4, pp. 527-534, May2007.

[107] J. R. Morones, J. L. Elechiguerra, A. Camacho, K. Holt, J. B. Kouri, J. T. Ramirez, and M. J. Yacaman, "The bactericidal effect of silver nanoparticles," *Nanotechnology*, vol. 16, no. 10, pp. 2346-2353, 2005.

[108] H. L. Su, C. C. Chou, D. J. Hung, S. H. Lin, I. C. Pao, J. H. Lin, F. L. Huang, R. X. Dong, and J. J. Lin, "The disruption of bacterial membrane integrity through ROS generation induced by nanohybrids of silver and clay," *Biomaterials*, vol. 30, no. 30, pp. 5979-5987, Aug.2009.

[109] S. Pal, Y. K. Tak, and J. M. Song, "Does the Antibacterial Activity of Silver Nanoparticles Depend on the Shape of the Nanoparticle? A Study of the Gram-Negative Bacterium Escherichia coli," *Appl. Environ. Microbiol.*, vol. 73, no. 6, pp. 1712-1720, Mar.2007.

[110] C. N. Lok, C. M. Ho, R. Chen, Q. Y. He, W. Y. Yu, H. Sun, P. Tam, J. F. Chiu, and C. M. Che, "Silver nanoparticles: partial oxidation and antibacterial activities," *Journal of Biological Inorganic Chemistry*, vol. 12, no. 4, pp. 527-534, May2007.

[111] H. L. Su, C. C. Chou, D. J. Hung, S. H. Lin, I. C. Pao, J. H. Lin, F. L. Huang, R. X. Dong, and J. J. Lin, "The disruption of bacterial membrane integrity through ROS generation induced by nanohybrids of silver and clay," *Biomaterials*, vol. 30, no. 30, pp. 5979-5987, Aug.2009.

[112] M. Rai, A. Yadav, and A. Gade, "Silver nanoparticles as a new generation of antimicrobials," *Biotechnology Advances*, vol. 27, no. 1, pp. 76-83, Jan.2001.

[113] P. D. Bragg and D. J. Rainnie, "The effect of silver ions on the respiratory chain of Escherichia coli," *Can. J Microbiol.*, vol. 20, no. 6, pp. 883-889, June1974.

[114] Q. L. Feng, J. Wu, G. Q. Chen, F. Z. Cui, T. N. Kim, and J. O. Kim, "A mechanistic study of the antibacterial effect of silver ions on Escherichia coli and Staphylococcus aureus," *J Biomed. Mater. Res*, vol. 52, no. 4, pp. 662-668, Dec.2000.

[115] J. R. Furr, A. D. Russell, T. D. Turner, and A. Andrews, "Antibacterial activity of Actisorb Plus, Actisorb and silver nitrate," *J Hosp. Infect.*, vol. 27, no. 3, pp. 201-208, July1994.

[116] A. Gupta, K. Matsui, J. F. Lo, and S. Silver, "Molecular basis for resistance to silver cations in Salmonella," *Nat Med*, vol. 5, no. 2, pp. 183-188, Feb.1999.

[117] J. L. Clement and P. S. Jarrett, "Antibacterial silver," *Met. Based. Drugs*, vol. 1, no. 5-6, pp. 467-482, 1994.

[118] J. Elechiguerra, J. Burt, J. Morones, A. Camacho-Bragado, X. Gao, H. Lara, and M. Yacaman, "Interaction of silver nanoparticles with HIV-1," *J. Nanobiotechnology*, vol. 3, no. 1, p. 6, 2005.

[119] Q. L. Feng, J. Wu, G. Q. Chen, F. Z. Cui, T. N. Kim, and J. O. Kim, "A mechanistic study of the antibacterial effect of silver ions on Escherichia coli and Staphylococcus aureus," *J Biomed. Mater. Res*, vol. 52, no. 4, pp. 662-668, Dec.2000.

[120] A. Nel, "Air Pollution-Related Illness: Effects of Particles," *Science*, vol. 308, no. 5723, pp. 804-806, May2005.

[121] A. L. Semeykina and V. P. Skulachev, "Submicromolar Ag^{+} increases passive Na^{+} permeability and inhibits the respiration-supported formation of Na+ gradient in Bacillus FTU vesicles," *FEBS Lett*, vol. 269, no. 1, pp. 69-72, Aug.1990.

[122] M. Hayashi, T. Miyoshi, M. Sato, and T. Unemoto, "Properties of respiratory chain-linked Na(+)-independent NADH-quinone reductase in a marine Vibrio alginolyticus," *Biochim. Biophys. Acta*, vol. 1099, no. 2, pp. 145-151, Feb.1992.

[123] P. Dibrov, J. Dzioba, K. K. Gosink, and C. C. Hase, "Chemiosmotic mechanism of antimicrobial activity of Ag(+) in Vibrio cholerae," *Antimicrob. Agents Chemother.*, vol. 46, no. 8, pp. 2668-2670, Aug.2002.

[124] M. Yamanaka, K. Hara, and J. Kudo, "Bactericidal actions of a silver ion solution on Escherichia coli, studied by energy-filtering transmission electron microscopy and proteomic analysis," *Appl. Environ. Microbiol.*, vol. 71, no. 11, pp. 7589-7593, Nov.2005.

[125] Q. L. Feng, J. Wu, G. Q. Chen, F. Z. Cui, T. N. Kim, and J. O. Kim, "A mechanistic study of the antibacterial effect of silver ions on Escherichia coli and Staphylococcus aureus," *J Biomed. Mater. Res*, vol. 52, no. 4, pp. 662-668, Dec.2000.

[126] M. Rai, A. Yadav, and A. Gade, "Silver nanoparticles as a new generation of antimicrobials," *Biotechnology Advances*, vol. 27, no. 1, pp. 76-83, Jan.2001.

[127] Q. L. Feng, J. Wu, G. Q. Chen, F. Z. Cui, T. N. Kim, and J. O. Kim, "A mechanistic study of the antibacterial effect of silver ions on Escherichia coli and Staphylococcus aureus," *J Biomed. Mater. Res*, vol. 52, no. 4, pp. 662-668, Dec.2000.

[128] H. L. Su, C. C. Chou, D. J. Hung, S. H. Lin, I. C. Pao, J. H. Lin, F. L. Huang, R. X. Dong, and J. J. Lin, "The disruption of bacterial membrane integrity through ROS generation induced by nanohybrids of silver and clay," *Biomaterials*, vol. 30, no. 30, pp. 5979-5987, Aug.2009.

[129] K. N. J. Stevens, O. Crespo-Biel, E. E. M. van den Bosch, A. A. Dias, M. L. W. Knetsch, Y. B. J. Aldenhoff, F. H. van der Veen, J. G. Maessen, E. E. Stobberingh, and L. H. Koole, "The relationship between the antimicrobial effect of catheter coatings containing silver nanoparticles and the coagulation of contacting blood," *Biomaterials*, vol. 30, no. 22, pp. 3682-3690, Aug.2009.

[130] J. J. Castellano, S. M. Shafii, F. Ko, G. Donate, T. E. Wright, R. J. Mannari, W. G. Payne, D. J. Smith, and M. C. Robson, "Comparative evaluation of silver-containing antimicrobial dressings and drugs," *Int Wound. J*, vol. 4, no. 2, pp. 114-122, June2007.

[131] C. N. Lok, C. M. Ho, R. Chen, Q. Y. He, W. Y. Yu, H. Sun, P. Tam, J. F. Chiu, and C. M. Che, "Silver nanoparticles: partial oxidation and antibacterial activities," *Journal of Biological Inorganic Chemistry*, vol. 12, no. 4, pp. 527-534, May2007.

[132] H. L. Su, C. C. Chou, D. J. Hung, S. H. Lin, I. C. Pao, J. H. Lin, F. L. Huang, R. X. Dong, and J. J. Lin, "The disruption of bacterial membrane integrity through ROS generation induced by nanohybrids of silver and clay," *Biomaterials*, vol. 30, no. 30, pp. 5979-5987, Aug.2009.

[133] A. Travan, C. Pelillo, I. Donati, E. Marsich, M. Benincasa, T. Scarpa, S. Semeraro, G. Turco, R. Gennaro, and S. Paoletti, "Non-cytotoxic Silver Nanoparticle-Polysaccharide Nanocomposites with Antimicrobial Activity," *Biomacromolecules*, vol. 10, no. 6, p. 1429, Apr.2009.

[134] I. Sondi and B. Salopek-Sondi, "Silver nanoparticles as antimicrobial agent: a case study on E. coli as aámodel for Gram-negative bacteria," *Journal of Colloid and Interface Science*, vol. 275, no. 1, pp. 177-182, July2004.

[135] A. Travan, C. Pelillo, I. Donati, E. Marsich, M. Benincasa, T. Scarpa, S. Semeraro, G. Turco, R. Gennaro, and S. Paoletti, "Non-cytotoxic Silver Nanoparticle-Polysaccharide Nanocomposites with Antimicrobial Activity," *Biomacromolecules*, vol. 10, no. 6, p. 1429, Apr.2009.

[136] C. N. Lok, C. M. Ho, R. Chen, Q. Y. He, W. Y. Yu, H. Sun, P. K. H. Tam, J. F. Chiu, and C. M. Che, "Proteomic Analysis of the Mode of Antibacterial Action of Silver Nanoparticles," *J. Proteome Res.*, vol. 5, no. 4, pp. 916-924, Apr.2006.

[137] J. S. Kim, E. Kuk, K. N. Yu, J. H. Kim, S. J. Park, H. J. Lee, S. H. Kim, Y. K. Park, Y. H. Park, C. Y. Hwang, Y. K. Kim, Y. S. Lee, D. H. Jeong, and M. H. Cho, "Antimicrobial effects of silver nanoparticles," *Nanomed. Nanotechnol. Biol. Med.*, vol. 3, no. 1, pp. 95-101, Mar.2007.

[138] O. Choi and Z. Hu, "Size dependent and reactive oxygen species related nanosilver toxicity to nitrifying bacteria," *Environ Sci Technol*, vol. 42, no. 12, pp. 4583-4588, June2008.

[139] H. L. Su, C. C. Chou, D. J. Hung, S. H. Lin, I. C. Pao, J. H. Lin, F. L. Huang, R. X. Dong, and J. J. Lin, "The disruption of bacterial membrane integrity through ROS generation induced by nanohybrids of silver and clay," *Biomaterials*, vol. 30, no. 30, pp. 5979-5987, Aug.2009.

[140] S. Pal, Y. K. Tak, J. Joardar, W. Kim, J. E. Lee, M. S. Han, and J. M. Song, "Nanocrystalline silver supported on activated carbon matrix from hydrosol: antibacterial mechanism under prolonged incubation conditions," *J Nanosci. Nanotechnol.*, vol. 9, no. 3, pp. 2092-2103, Mar.2009.

[141] A. B. Lansdown, "Silver in health care: antimicrobial effects and safety in use," *Curr Probl. Dermatol.*, vol. 33, pp. 17-34, 2006.

[142] F. F. Larese, F. D'Agostin, M. Crosera, G. Adami, N. Renzi, M. Bovenzi, and G. Maina, "Human skin penetration of silver nanoparticles through intact and damaged skin," *Toxicology*, vol. 255, no. 1-2, pp. 33-37, Jan.2009.

[143] H. D. Um, J. M. Orenstein, and S. M. Wahl, "Fas mediates apoptosis in human monocytes by a reactive oxygen intermediate dependent pathway," *J Immunol*, vol. 156, no. 9, pp. 3469-3477, May1996.

[144] A. K. Talley, S. Dewhurst, S. W. Perry, S. C. Dollard, S. Gummuluru, S. M. Fine, D. New, L. G. Epstein, H. E. Gendelman, and H. A. Gelbard, "Tumor necrosis factor alpha-induced apoptosis in human neuronal cells: protection by the antioxidant N-acetylcysteine and the genes bcl-2 and crmA," *Mol. Cell Biol*, vol. 15, no. 5, pp. 2359-2366, May1995.

[145] N. Zamzami, P. Marchetti, M. Castedo, D. Decaudin, A. Macho, T. Hirsch, S. A. Susin, P. X. Petit, B. Mignotte, and G. Kroemer, "Sequential reduction of mitochondrial transmembrane potential and generation of reactive oxygen species in early programmed cell death," *J Exp. Med*, vol. 182, no. 2, pp. 367-377, Aug.1995.

[146] M. T. Lin and M. F. Beal, "Mitochondrial dysfunction and oxidative stress in neurodegenerative diseases," *Nature*, vol. 443, no. 7113, pp. 787-795, Oct.2006.

[147] M. Ott, V. Gogvadze, S. Orrenius, and B. Zhivotovsky, "Mitochondria, oxidative stress and cell death," *Apoptosis.*, vol. 12, no. 5, pp. 913-922, May2007.

[148] S. M. Hussain, K. L. Hess, J. M. Gearhart, K. T. Geiss, and J. J. Schlager, "In vitro toxicity of nanoparticles in BRL 3A rat liver cells," *Toxicol. In Vitro*, vol. 19, no. 7, pp. 975-983, Oct.2005.

[149] C. Carlson, S. M. Hussain, A. M. Schrand, L. K. Braydich-Stolle, K. L. Hess, R. L. Jones, and J. J. Schlager, "Unique cellular interaction of silver nanoparticles: size-dependent generation of reactive oxygen species," *J Phys. Chem. B*, vol. 112, no. 43, pp. 13608-13619, Oct.2008.

[150] R. Foldbjerg, P. Olesen, M. Hougaard, D. A. Dang, H. J. Hoffmann, and H. Autrup, "PVP-coated silver nanoparticles and silver ions induce reactive oxygen species, apoptosis and necrosis in THP-1 monocytes," *Toxicol. Lett.*, July2009.

[151] S. Arora, J. Jain, J. M. Rajwade, and K. M. Paknikar, "Cellular responses induced by silver nanoparticles: In vitro studies," *Toxicol. Lett*, vol. 179, no. 2, pp. 93-100, June2008.

[152] S. Kim, J. E. Choi, J. Choi, K. H. Chung, K. Park, J. Yi, and D. Y. Ryu, "Oxidative stress-dependent toxicity of silver nanoparticles in human hepatoma cells," *Toxicol. In Vitro*, vol. 23, no. 6, pp. 1076-1084, Sept.2009.

[153] P. D. Van Den, S. K. De, D. Lens, and P. Sollie, "Differential cell death programmes induced by silver dressings in vitro," *Eur J Dermatol.*, vol. 18, no. 4, pp. 416-421, July2008.

[154] A. Burd, C. H. Kwok, S. C. Hung, H. S. Chan, H. Gu, W. K. Lam, and L. Huang, "A comparative study of the cytotoxicity of silver-based dressings in monolayer cell, tissue explant, and animal models," *Wound. Repair Regen.*, vol. 15, no. 1, pp. 94-104, Jan.2007.

[155] Y. H. Hsin, C. F. Chen, S. Huang, T. S. Shih, P. S. Lai, and P. J. Chueh, "The apoptotic effect of nanosilver is mediated by a ROS- and JNK-dependent mechanism involving

the mitochondrial pathway in NIH3T3 cells," *Toxicol. Lett*, vol. 179, no. 3, pp. 130-139, July2008.

[156] V. B. Djordjevic, "Free radicals in cell biology," *Int Rev Cytol.*, vol. 237, pp. 57-89, 2004.

[157] M. Gilca, I. Stoian, V. Atanasiu, and B. Virgolici, "The oxidative hypothesis of senescence," *J Postgrad. Med*, vol. 53, no. 3, pp. 207-213, July2007.

[158] H. U. Simon, A. Haj-Yehia, and F. Levi-Schaffer, "Role of reactive oxygen species (ROS) in apoptosis induction," *Apoptosis.*, vol. 5, no. 5, pp. 415-418, Nov.2000.

[159] M. Ahamed, M. Karns, M. Goodson, J. Rowe, S. M. Hussain, J. J. Schlager, and Y. Hong, "DNA damage response to different surface chemistry of silver nanoparticles in mammalian cells," *Toxicol. Appl. Pharmacol.*, vol. 233, no. 3, pp. 404-410, Dec.2008.

[160] C. Carlson, S. M. Hussain, A. M. Schrand, L. K. Braydich-Stolle, K. L. Hess, R. L. Jones, and J. J. Schlager, "Unique cellular interaction of silver nanoparticles: size-dependent generation of reactive oxygen species," *J Phys. Chem. B*, vol. 112, no. 43, pp. 13608-13619, Oct.2008.

[161] K. Cha, H. W. Hong, Y. G. Choi, M. J. Lee, J. H. Park, H. K. Chae, G. Ryu, and H. Myung, "Comparison of acute responses of mice livers to short-term exposure to nano-sized or micro-sized silver particles," *Biotechnol. Lett*, vol. 30, no. 11, pp. 1893-1899, Nov.2008.

[162] S. Kim, J. E. Choi, J. Choi, K. H. Chung, K. Park, J. Yi, and D. Y. Ryu, "Oxidative stress-dependent toxicity of silver nanoparticles in human hepatoma cells," *Toxicol. In Vitro*, vol. 23, no. 6, pp. 1076-1084, Sept.2009.

[163] N. Lubick, "Nanosilver toxicity: ions, nanoparticles--or both?," *Environ Sci Technol*, vol. 42, no. 23, p. 8617, Dec.2008.

[164] N. Singh, B. Manshian, G. J. S. Jenkins, S. M. Griffiths, P. M. Williams, T. G. G. Maffeis, C. J. Wright, and S. H. Doak, "NanoGenotoxicology: The DNA damaging potential of engineered nanomaterials," *Biomaterials*, vol. 30, no. 23-24, pp. 3891-3914, Aug.2009.

[165] T. Paz-Elizur, Z. Sevilya, Y. Leitner-Dagan, D. Elinger, L. C. Roisman, and Z. Livneh, "DNA repair of oxidative DNA damage in human carcinogenesis: potential application for cancer risk assessment and prevention," *Cancer Lett*, vol. 266, no. 1, pp. 60-72, July2008.

[166] M. Chen and M. A. von, "Formation of nucleoplasmic protein aggregates impairs nuclear function in response to SiO2 nanoparticles," *Exp. Cell Res*, vol. 305, no. 1, pp. 51-62, Apr.2005.

[167] M. Geiser, B. Rothen-Rutishauser, N. Kapp, S. Schurch, W. Kreyling, H. Schulz, M. Semmler, H. Im, V, J. Heyder, and P. Gehr, "Ultrafine particles cross cellular membranes by nonphagocytic mechanisms in lungs and in cultured cells," *Environ. Health Perspect.*, vol. 113, no. 11, pp. 1555-1560, Nov.2005.

[168] I. Nabiev, S. Mitchell, A. Davies, Y. Williams, D. Kelleher, R. Moore, Y. K. Gun'ko, S. Byrne, Y. P. Rakovich, J. F. Donegan, A. Sukhanova, J. Conroy, D. Cottell, N. Gaponik, A. Rogach, and Y. Volkov, "Nonfunctionalized nanocrystals can exploit a cell's active transport machinery delivering them to specific nuclear and cytoplasmic compartments," *Nano Lett*, vol. 7, no. 11, pp. 3452-3461, Nov.2007.

[169] W. Yang, C. Shen, Q. Ji, H. An, J. Wang, Q. Liu, and Z. Zhang, "Food storage material silver nanoparticles interfere with DNA replication fidelity and bind with DNA," *Nanotechnology.*, vol. 20, no. 8, p. 85102, Feb.2009.

[170] O. Bar-Ilan, R. M. Albrecht, V. E. Fako, and D. Y. Furgeson, "Toxicity assessments of multisized gold and silver nanoparticles in zebrafish embryos," *Small*, vol. 5, no. 16, pp. 1897-1910, Aug.2009.

[171] M. F. Rahman, J. Wang, T. A. Patterson, U. T. Saini, B. L. Robinson, G. D. Newport, R. C. Murdock, J. J. Schlager, S. M. Hussain, and S. F. Ali, "Expression of genes related to oxidative stress in the mouse brain after exposure to silver-25 nanoparticles," *Toxicol. Lett*, vol. 187, no. 1, pp. 15-21, May2009.

[172] K. Cha, H. W. Hong, Y. G. Choi, M. J. Lee, J. H. Park, H. K. Chae, G. Ryu, and H. Myung, "Comparison of acute responses of mice livers to short-term exposure to nano-sized or micro-sized silver particles," *Biotechnol. Lett*, vol. 30, no. 11, pp. 1893-1899, Nov.2008.

[173] D. Chen, T. Xi, and J. Bai, "Biological effects induced by nanosilver particles: in vivo study," *Biomed. Mater.*, vol. 2, no. 3, p. S126-S128, Sept.2007.

[174] J. Fu, J. Ji, D. Fan, and J. Shen, "Construction of antibacterial multilayer films containing nanosilver via layer-by-layer assembly of heparin and chitosan-silver ions complex," *J. Biomed. Mater. Res. A*, vol. 79, no. 3, pp. 665-674, Dec.2006.

[175] V. Alt, T. Bechert, P. Steinrucke, M. Wagener, P. Seidel, E. Dingeldein, E. Domann, and R. Schnettler, "An in vitro assessment of the antibacterial properties and cytotoxicity of nanoparticulate silver bone cement," *Biomaterials*, vol. 25, no. 18, pp. 4383-4391, Aug.2004.

[176] H. C. Wen, Y. N. Lin, S. R. Jian, S. C. Tseng, M. X. Weng, Y. P. Liu, P. T. Lee, P. Y. Chen, R. Q. Hsu, W. F. Wu, and C. P. Chou, "Observation of Growth of Human Fibroblasts on Silver Nanoparticles," *J. Phys. Conf. Ser.*, vol. 61, pp. 445-449, 2007.

[177] M. Bosetti, A. Masse, E. Tobin, and M. Cannas, "Silver coated materials for external fixation devices: in vitro biocompatibility and genotoxicity," *Biomaterials*, vol. 23, no. 3, pp. 887-892, Feb.2002.

[178] V. L. Colvin, "The potential environmental impact of engineered nanomaterials," *Nat Biotech*, vol. 21, no. 10, pp. 1166-1170, Oct.2003.

[179] P. H. Hoet, A. Nemmar, and B. Nemery, "Health impact of nanomaterials?," *Nat. Biotechnol.*, vol. 22, no. 1, p. 19, Jan.2004.

[180] G. Oberdorster, A. Maynard, K. Donaldson, V. Castranova, J. Fitzpatrick, K. Ausman, J. Carter, B. Karn, W. Kreyling, D. Lai, S. Olin, N. Monteiro-Riviere, D. Warheit, and H. Yang, "Principles for characterizing the potential human health effects from

exposure to nanomaterials: elements of a screening strategy," *Part Fibre. Toxicol.*, vol. 2, p. 8, Oct.2005.

[181] D. B. Aaron and L. K. Kristi, "Polysaccharide-modified synthetic polymeric biomaterials," *Peptide Science*, vol. 94, no. 1, pp. 128-140, 2010.

[182] J. Retuert, S. Fuentes, G. Gonzales, and R. Benavente, "Thermal effect on the microhardness of chitosan films," *Bol. Soc. Chil. Quim.*, vol. 45, no. 2 2000.

[183] C. H. Yang, K. S. Huang, and J. Y. Chang, "Manufacturing monodisperse chitosan microparticles containing ampicillin using a microchannel chip," *Biomedical Microdevices*, vol. 9, no. 2, pp. 253-259, Apr.2007.

[184] O. Felt, P. Furrer, J. M. Mayer, B. Plazonnet, P. Buri, and R. Gurny, "Topical use of chitosan in ophthalmology: tolerance assessment and evaluation of precorneal retention," *Int. J. Pharm.*, vol. 180, no. 2, pp. 185-193, Apr.1999.

[185] S. Patashnik, L. Rabinovich, and G. Golomb, "Preparation and evaluation of chitosan microspheres containing bisphosphonates," *J. Drug Target*, vol. 4, no. 6, pp. 371-380, 1997.

[186] J. Song, C. H. Suh, Y. B. Park, S. H. Lee, N. C. Yoo, J. D. Lee, K. H. Kim, and S. K. Lee, "A phase I/IIa study on intra-articular injection of holmium-166-chitosan complex for the treatment of knee synovitis of rheumatoid arthritis," *Eur. J. Nucl. Med.*, vol. 28, no. 4, pp. 489-497, Apr.2001.

[187] R. A. Muzzarelli, "Human enzymatic activities related to the therapeutic administration of chitin derivatives," *Cell Mol. Life Sci.*, vol. 53, no. 2, pp. 131-140, Feb.1997.

[188] A. F. Kotze, H. L. Luessen, A. G. de Boer, J. C. Verhoef, and H. E. Junginger, "Chitosan for enhanced intestinal permeability: prospects for derivatives soluble in neutral and basic environments," *Eur. J. Pharm. Sci.*, vol. 7, no. 2, pp. 145-151, Jan.1999.

[189] B. Biagini, R. A. Muzzarelli, R. Giardino, and C. Castaldini, "Biological materials for wound healing," in *Advances in chitin and chitosan*, Elsevier ed. C. J. Brine, P. A. Sandford, and J. P. Zikakis, Eds. 1992, pp. 16-24.

[190] H. Ueno, T. Mori, and T. Fujinaga, "Topical formulations and wound healing applications of chitosan," *Adv. Drug Deliv. Rev.*, vol. 52, no. 2, pp. 105-115, Nov.2001.

[191] O. Felt, A. Carrel, P. Baehni, P. Buri, and R. Gurny, "Chitosan as tear substitute: a wetting agent endowed with antimicrobial efficacy," *J. Ocul. Pharmacol. Ther.*, vol. 16, no. 3, pp. 261-270, June2000.

[192] N. Kubota, N. Tatsumoto, T. Sano, and K. Toya, "A simple preparation of half N-acetylated chitosan highly soluble in water and aqueous organic solvents," *Carbohydr Res.*, vol. 324, no. 4, pp. 268-274, Mar.2000.

[193] P. Sorlier, A. Denuziere, C. Viton, and A. Domard, "Relation between the degree of acetylation and the electrostatic properties of chitin and chitosan," *Biomacromolecules*, vol. 2, no. 3, pp. 765-772, 2001.

[194] T. C. Yang, C. C. Chou, and C. F. Li, "Antibacterial activity of N-alkylated disaccharide chitosan derivatives," *Int. J. Food Microbiol.*, vol. 97, no. 3, pp. 237-245, Jan.2005.

[195] R. A. Muzzarelli, F. Tanfani, M. Emanuelli, D. P. Pace, E. Chiurazzi, and M. Piani, "Sulfated N-(carboxymethyl)chitosans: novel blood anticoagulants," *Carbohydr Res.*, vol. 126, no. 2, pp. 225-231, Mar.1984.

[196] I. Donati, S. Stredanska, G. Silvestrini, A. Vetere, P. Marcon, E. Marsich, P. Mozetic, A. Gamini, S. Paoletti, and F. Vittur, "The aggregation of pig articular chondrocyte and synthesis of extracellular matrix by a lactose-modified chitosan," *Biomaterials*, vol. 26, no. 9, pp. 987-998, Mar.2005.

[197] I. Donati, S. Stredanska, G. Silvestrini, A. Vetere, P. Marcon, E. Marsich, P. Mozetic, A. Gamini, S. Paoletti, and F. Vittur, "The aggregation of pig articular chondrocyte and synthesis of extracellular matrix by a lactose-modified chitosan," *Biomaterials*, vol. 26, no. 9, pp. 987-998, Mar.2005.

[198] I. Donati, S. Stredanska, G. Silvestrini, A. Vetere, P. Marcon, E. Marsich, P. Mozetic, A. Gamini, S. Paoletti, and F. Vittur, "The aggregation of pig articular chondrocyte and synthesis of extracellular matrix by a lactose-modified chitosan," *Biomaterials*, vol. 26, no. 9, pp. 987-998, Mar.2005.

[199] P. Marcon, E. Marsich, A. Vetere, P. Mozetic, C. Campa, I. Donati, F. Vittur, A. Gamini, and S. Paoletti, "The role of Galectin-1 in the interaction between chondrocytes and a lactose-modified chitosan," *Biomaterials*, vol. 26, no. 24, pp. 4975-4984, Aug.2005.

[200] S. H. Barondes, V. Castronovo, D. N. Cooper, R. D. Cummings, K. Drickamer, T. Feizi, M. A. Gitt, J. Hirabayashi, C. Hughes, K. Kasai, and ., "Galectins: a family of animal beta-galactoside-binding lectins," *Cell*, vol. 76, no. 4, pp. 597-598, Feb.1994.

[201] D. N. Cooper and S. H. Barondes, "God must love galectins; he made so many of them," *Glycobiology*, vol. 9, no. 10, pp. 979-984, Oct.1999.

[202] R. Ramkumar and S. K. Podder, "Elucidation of the mechanism of interaction of sheep spleen galectin-1 with splenocytes and its role in cell-matrix adhesion," *J. Mol. Recognit.*, vol. 13, no. 5, pp. 299-309, Sept.2000.

[203] F. A. van den Brule, C. Buicu, M. Baldet, M. E. Sobel, D. N. Cooper, P. Marschal, and V. Castronovo, "Galectin-1 modulates human melanoma cell adhesion to laminin," *Biochem. Biophys. Res. Commun.*, vol. 209, no. 2, pp. 760-767, Apr.1995.

[204] K. Wasano and Y. Hirakawa, "Recombinant galectin-1 recognizes mucin and epithelial cell surface glycocalyces of gastrointestinal tract," *J. Histochem. Cytochem.*, vol. 45, no. 2, pp. 275-283, Feb.1997.

[205] C. Bokel and N. H. Brown, "Integrins in development: moving on, responding to, and sticking to the extracellular matrix," *Dev. Cell*, vol. 3, no. 3, pp. 311-321, Sept.2002.

[206] A. Travan, I. Donati, E. Marsich, F. Bellomo, S. Achanta, M. Toppazzini, S. Semeraro, T. Scarpa, V. Spreafico, and S. Paoletti, "Surface Modification and Polysaccharide Deposition on BisGMA/TEGDMA Thermoset," *Biomacromolecules*, Feb.2010.

[207] S. A. Guelcher and J. O. Hollinger, *An Introduction to Biomaterials* Taylor & Francis, 2006.

[208] A. Haug, B. Larsen, and O. Smidsrød, "Uronic acid sequence in alginate from different sources," *Carbohydr. Res.*, pp. 217-225, 1974.

[209] P. A. j. Gorin and J. F. T. Spencer, "Exocellular alginic acid fron Azotobacter vinelandii," *Can. J. Chem.*, vol. 44, p. 993, 1966.

[210] J. R. Govan, J. A. Fyfe, and T. R. Jarman, "Isolation of alginate-producing mutants of Pseudomonas fluorescens, Pseudomonas putida and Pseudomonas mendocina," *J. Gen. Microbiol.*, vol. 125, no. 1, pp. 217-220, July1981.

[211] A. Haug, B. Larsen, and O. Smidsrød, "Studies on the sequence of uronic acid residues in alginic acid," *Acta Chem Scand*, vol. 21, pp. 691-704, 1967.

[212] O. Smidsrød, A. Haug, and B. Lian, "Properties of Poly(1,4-hexuronates) in the gel state," *Acta Chem Scand*, vol. 26, pp. 71-78, 1972.

[213] O. Smidsrød, "Molecular basis for some physical properties of alginate in the gel state," *Fraday Discuss Chem*, vol. 57, pp. 263-274, 1974.

[214] O. Smidsrød, R. Glover, and S. Whittington, "The relative extension of alginates having different chemical composition," *Carbohydrate Research*, vol. 27, pp. 107-118, 1973.

[215] A. Martinses, G. Skjåk-Bræk, O. Smidsrød, F. Zanetti, and S. Paoletti, "Comparison for different methods for determination of molecular weight and molecular weight distribution of alginates," *Carbohydr. Polym.*, vol. 15, pp. 171-193, 1991.

[216] R. Kohn and B. Larsen, "Preparation of water-soluble polyuronic acids and their calcium salts, and the determination of calcium ion activity in relation to the degree of polymerization," *Acta Chem Scand*, vol. 26, no. 6, pp. 2455-2468, 1972.

[217] G. T. Grant, E. R. Morris, D. A. Rees, P. J. C. Smith, and D. Thom, "Biological interactions between polysaccharides and divalent cations: the egg box model," *Anonymouspp*, pp. 195-198, 1973.

[218] B. Strand, G. Skjåk-Bræk, and O. Gaserod, "Microcapsule formulation and formation," in *Fundamentals of cell immobilization biotechnology*, Nedovic and R. Willaert eds ed 2004, pp. 165-183.

[219] I. Donati, S. Holtan, Y. A. Mørch, M. Borgogna, M. Dentini, and G. Skjåk-Bræk, "New hypothesis on the role of alternating sequences in calcium-alginate gels," *Biomacromolecules*, vol. 6, no. 2, pp. 1031-1040, Mar.2005.

[220] O. Smidsrød and K. I. Draget, "Chemistry and physical properties of alginates," *Carbohydr. Eur.*, vol. 14, pp. 6-12, 1996.

[221] N. Wang, G. Adams, L. Buttery, F. H. Falcone, and S. Stolnik, "Alginate encapsulation technology supports embryonic stem cells differentiation into insulin-producing cells," *J. Biotechnol.*, vol. 144, no. 4, pp. 304-312, Dec.2009.

[222] U. Zimmermann, F. Thurmer, A. Jork, M. Weber, S. Mimietz, M. Hillgartner, F. Brunnenmeier, H. Zimmermann, I. Westphal, G. Fuhr, U. Noth, A. Haase, A. Steinert, and C. Hendrich, "A novel class of amitogenic alginate microcapsules for long-term immunoisolated transplantation," *Ann. N. Y. Acad. Sci.*, vol. 944, pp. 199-215, Nov.2001.

[223] A. Ouyang, R. Ng, and S. T. Yang, "Long-term culturing of undifferentiated embryonic stem cells in conditioned media and three-dimensional fibrous matrices without extracellular matrix coating," *Stem Cells*, vol. 25, no. 2, pp. 447-454, Feb.2007.

[224] W. Cui, G. Barr, K. M. Faucher, X. L. Sun, S. A. Safley, C. J. Weber, and E. L. Chaikof, "A membrane-mimetic barrier for islet encapsulation," *Transplant. Proc.*, vol. 36, no. 4, pp. 1206-1208, May2004.

[225] A. Omer, V. Duvivier-Kali, J. Fernandes, V. Tchipashvili, C. K. Colton, and G. C. Weir, "Long-term normoglycemia in rats receiving transplants with encapsulated islets," *Transplantation*, vol. 79, no. 1, pp. 52-58, Jan.2005.

[226] J. Wijsman, P. Atkison, R. Mazaheri, B. Garcia, T. Paul, J. Vose, G. O'Shea, and C. Stiller, "Histological and immunopathological analysis of recovered encapsulated allogeneic islets from transplanted diabetic BB/W rats," *Transplantation*, vol. 54, no. 4, pp. 588-592, Oct.1992.

[227] F. Lim and A. M. Sun, "Microencapsulated islets as bioartificial endocrine pancreas," *Science*, vol. 210, no. 4472, pp. 908-910, Nov.1980.

[228] P. Soon-Shiong, E. Feldman, R. Nelson, R. Heintz, Q. Yao, Z. Yao, T. Zheng, N. Merideth, G. Skjak-Braek, T. Espevik, and ., "Long-term reversal of diabetes by the injection of immunoprotected islets," *Proc. Natl Acad. Sci U. S. A*, vol. 90, no. 12, pp. 5843-5847, June1993.

[229] J. Lehtinen, T. Laurila, L. V. J. Lassila, P. K. Vallittu, J. Räty, and R. Hernberg, "Optical characterization of bisphenol-A-glycidyldimethacrylate-triethyleneglycoldimethacrylate (BisGMA/TEGDMA) monomers and copolymer," *Dental Materials*, vol. 24, no. 10, pp. 1324-1328, Oct.2008.

[230] J. CHARNLEY, "Surgery of the hip-joint: present and future developments," *Br Med J*, vol. 1, no. 5176, pp. 821-826, Mar.1960.

[231] J. C. J. Webb and R. F. Spencer, "The role of polymethylmethacrylate bone cement in modern orthopaedic surgery," *J Bone Joint Surg Br*, vol. 89-B, no. 7, pp. 851-857, July2007.

[232] P. F. Heini and U. Berlemann, "Bone substitutes in vertebroplasty," *Eur Spine J*, vol. 10 Suppl 2, p. S205-S213, Oct.2001.

[233] L. Linder and H. A. Hansson, "Ultrastructural aspects of the interface between bone and cement in man. Report of three cases," *J Bone Joint Surg Br*, vol. 65, no. 5, pp. 646-649, Nov.1983.

[234] P. K. Vallittu and K. Ekstrand, "In vitro cytotoxicity of fibre-polymethyl methacrylate composite used in dentures," *J Oral Rehabil.*, vol. 26, no. 8, pp. 666-671, Aug.1999.

[235] J. T. Heikkila, H. J. Aho, A. Yli-Urpo, R. P. Happonen, and A. J. Aho, "Bone formation in rabbit cancellous bone defects filled with bioactive glass granules," *Acta Orthop. Scand.*, vol. 66, no. 5, pp. 463-467, Oct.1995.

[236] B. Marrs, R. Andrews, T. Rantell, and D. Pienkowski, "Augmentation of acrylic bone cement with multiwall carbon nanotubes," *J Biomed. Mater Res A*, vol. 77, no. 2, pp. 269-276, May2006.

[237] Y. S. Kim, Y. H. Kang, J. K. Kim, and J. B. Park, "Effect of bone mineral particles on the porosity of bone cement," *Biomed. Mater Eng*, vol. 4, no. 1, pp. 37-46, 1994.

[238] B. Marrs, R. Andrews, T. Rantell, and D. Pienkowski, "Augmentation of acrylic bone cement with multiwall carbon nanotubes," *J Biomed. Mater Res A*, vol. 77, no. 2, pp. 269-276, May2006.

[239] L. D. Topoleski, P. Ducheyne, and J. M. Cuckler, "The fracture toughness of titanium-fiber-reinforced bone cement," *J Biomed. Mater. Res.*, vol. 26, no. 12, pp. 1599-1617, Dec.1992.

[240] D. D. Wright, E. P. Lautenschlager, and J. L. Gilbert, "Bending and fracture toughness of woven self-reinforced composite poly(methyl methacrylate)," *J. Biomed. Mater. Res.*, vol. 36, no. 4, pp. 441-453, Sept.1997.

[241] A. Peutzfeldt, "Resin composites in dentistry: the monomer systems," *Eur J Oral Sci*, vol. 105, no. 2, pp. 97-116, Apr.1997.

[242] G. J. Pomrink, M. P. DiCicco, T. D. Clineff, and E. M. Erbe, "Evaluation of the reaction kinetics of CORTOSSTM, a thermoset cortical bone void filler," *Biomaterials*, vol. 24, no. 6, pp. 1023-1031, Mar.2003.

[243] J. L. Ferracane, "Current trends in dental composites," *Crit Rev Oral Biol Med*, vol. 6, no. 4, pp. 302-318, 1995.

[244] S. M. P. Belkoff, J. M. M. Mathis, E. M. P. Erbe, and D. C. M. Fenton, "Biomechanical Evaluation of a New Bone Cement for Use in Vertebroplasty. [Miscellaneous Article]," *Spine*, vol. 25, no. 9, pp. 1061-1064, May2000.

[245] P. K. Vallittu, "Flexural properties of acrylic resin polymers reinforced with unidirectional and woven glass fibres," *J. Prosthet. Dent.*, vol. 81, pp. 318-326, 1998.

[246] P. K. Vallittu and C. Sevelius, "Resin-bonded, glass fiber-reinforced composite fixed partial dentures: a clinical study," *J Prosthet. Dent*, vol. 84, no. 4, pp. 413-418, Oct.2000.

[247] D. S. Zhao, N. Moritz, P. Laurila, R. Mattila, L. V. J. Lassila, N. Strandberg, T. MΣntylΣ, P. K. Vallittu, and H. T. Aro, "Development of a multi-component fiber-reinforced composite implant for load-sharing conditions," *Med. Eng. Phys.*, vol. 31, no. 4, pp. 461-469, May2009.

[248] G. Borkow and J. Gabbay, "Putting copper into action: copper-impregnated products with potent biocidal activities," *FASEB J.*, pp. 04-2029fje, Sept.2004.

[249] R. O. Darouiche, "Anti-infective efficacy of silver-coated medical prostheses," *Clin Infect. Dis*, vol. 29, no. 6, pp. 1371-1377, Dec.1999.

[250] J. E. Lee, J. C. Park, K. H. Lee, S. H. Oh, and H. Suh, "Laminin modified infection-preventing collagen membrane containing silver sulfadiazine-hyaluronan microparticles," *Artif. Organs*, vol. 26, no. 6, pp. 521-528, June2002.

[251] K. Jaeger, S. Zenz, B. J++ttner, H. Ruschulte, E. Kuse, J. Heine, S. Piepenbrock, A. Ganser, and M. Karthaus, "Reduction of catheter-related infections in neutropenic patients: a prospective controlled randomized trial using a chlorhexidine and silver sulfadiazine-impregnated central venous catheter," *Ann. Hematol.*, vol. 84, no. 4, pp. 258-262, Apr.2005.

[252] B. J. Nablo, H. L. Prichard, R. D. Butler, B. Klitzman, and M. H. Schoenfisch, "Inhibition of implant-associated infections via nitric oxide release," *Biomaterials*, vol. 26, no. 34, pp. 6984-6990, Dec.2005.

[253] G. Donelli and I. Francolini, "Efficacy of antiadhesive, antibiotic and antiseptic coatings in preventing catheter-related infections: review," *J Chemother.*, vol. 13, no. 6, pp. 595-606, Dec.2001.

[254] D. Campoccia, L. Montanaro, and C. R. Arciola, "The significance of infection related to orthopedic devices and issues of antibiotic resistance," *Biomaterials*, vol. 27, no. 11, pp. 2331-2339, Apr.2006.

Paper 1

Communication

Polyol Synthesis of Silver Nanoparticles: Mechanism of Reduction by Alditol Bearing Polysaccharides

Ivan Donati, Andrea Travan, Chiara Pelillo, Tommaso Scarpa, Anna Coslovi, Alois Bonifacio, Valter Sergo, and Sergio Paoletti

Biomacromolecules, **2009**, 10 (2), 210-213• DOI: 10.1021/bm801253c • Publication Date (Web): 13 January 2009

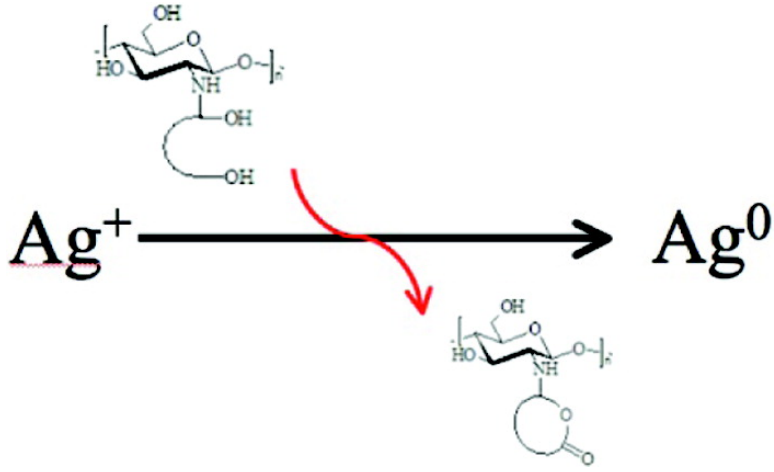

More About This Article

Additional resources and features associated with this article are available within the HTML version:

- Supporting Information
- Access to high resolution figures
- Links to articles and content related to this article
- Copyright permission to reproduce figures and/or text from this article

View the Full Text HTML

Biomacromolecules is published by the American Chemical Society. 1155 Sixteenth Street N.W., Washington, DC 20036

Communications

Polyol Synthesis of Silver Nanoparticles: Mechanism of Reduction by Alditol Bearing Polysaccharides

Ivan Donati,*,† Andrea Travan,† Chiara Pelillo,† Tommaso Scarpa,† Anna Coslovi,† Alois Bonifacio,‡ Valter Sergo,‡ and Sergio Paoletti†

Departments of Life Sciences and Materials Engineering and Natural Resources, University of Trieste, 34127 Trieste, Italy

Received October 31, 2008; Revised Manuscript Received December 9, 2008

Alditol bearing chitosans have shown the ability to reduce silver ions in mild conditions and without addition of exogenous reducing agents. The ion reduction induces the formation of a lactone moiety on the polysaccharide (Fetizon reaction) without causing C−C bond cleavage on the polyol. The close and multivalent arrangement of the endogenous reducing agent (alditols) on the polysaccharide backbone resulted in the formation of silver nanoparticles (∅ < 10 nm), which induced a considerable SERS effect and led to hydrogel formation.

Introduction

Stable and well dispersed nanoparticles can be obtained by adding the metal precursor (like metal salts) to a polymer solution followed by reduction with an exogenous reducing agent. Stabilizers (like polymers) play an important role in controlling the formation and dispersion stability[1] of nanoparticles, while avoiding their aggregation. In particular, polymers containing amino groups like chitosan[2] and poly(ethyleneimine)[3] efficiently coordinate metal ions, enabling the formation of particles of small dimensions. In addition, exogenous reducing agents are used such as ascorbic acid,[4,5] sodium borohydride,[6] sodium citrate,[7] polyols, hydroxyalkyl radicals, and aldehyde groups of reducing sugars.[8,9] In particular, in the case of polyols, the silver-reduction mechanism typically involves heat treatment and could lead to C−C bond cleavage.[10−14]

Lactit-1-yl chitosan (Chitlac) is an engineered polysaccharide characterized by multifunctional properties modulating its chemical and biological features. In fact, the presence of the lactitol side chains on the polysaccharide backbone endows such a weak polycation with a very high solubility over a wide pH range and with the ability to efficiently disperse silver nanoparticles formed from $AgNO_3$ by the addition of an exogenous reducing agent (i.e., ascorbic acid). This particular aspect points to the possibility of using Chitlac in the preparation of antibacterial and noncytotoxic films and hydrogels for biomaterial applications.[15] Moreover, the presence of a large number of galactose moieties arranged on the polymer side chain triggers chondrocytes adhesion and proliferation by the interaction with S-type lectins: this galectin-mediated cell stimulation enhances production of type-II collagen and GAGs production.[16−18] Because of the presence of the lactitol side chain, Chitlac overcomes the chemical and biological limitations of the parent polysaccharide, chitosan.

In the present contribution, Chitlac was used as both dispersing and reducing agent for silver nanoparticles. In particular, the alditol group linked on the chitosan backbone is shown, for the first time, to be able to reduce silver ions in mild conditions following the Fetizon oxidation mechanism.

Experimental Section

Materials. Chitosan was purchased from Aldrich Chemical Co. (U.S.A.) and purified as reported elsewhere.[16] The residual degree of acetylation was 11.3 (±0.3)%, as assessed by ^{1}H NMR. The molecular weight of the sample was 650000, as estimated from viscosity measurements. Silver nitrate, ascorbic acid, and 4-(2-hydroxyethyl)-1-piperazineethanesulfonic acid (HEPES) were purchased from Sigma Chemical Co (St. Louis, MO). All other chemicals were of analytical grade.

Synthesis of *S*accharide Derivatives of Chitosan. Chitosan (300 mg) was dissolved in 21 mL of a 1:1 mixture of methanol and 1% acetic acid (pH 4.5); 12 mL of the same methanol/acetic acid mixture containing a saccharide (2.5 equiv) and sodium cyanoborohydride (6 equiv) were then added. The solution was stirred at room temperature, diluted with water, and dialyzed against deionized water. The polymer solution was filtered through 0.45 μm Millipore filters and freeze-dried. The composition of the modified chitosans is reported in Table 1 of the Supporting Information.

Oxidation of Glucitol by the Tollens Assay. Sodium hydroxide (2 M, 2 mL) is poured into a silver nitrate solution (5%, 2 mL). Ammonium hydroxide solution (10%) is then added until the precipitate is completely dissolved. A few drops of this solution are then dropwise added to a solution containing glucitol (1%). The formation of a silver mirror is immediate.

Chitlac-Silver Nanoparticles (Chitlac-nAg) Preparation. *Preparation without Ascorbic Acid.* Silver nanoparticles were obtained by reducing silver ions in Chitlac solutions according to the following procedures: freeze-dried Chitlac was dissolved in deionized water to obtain solutions with different concentrations (2 g/L and 4 g/L). Chitlac solutions were mixed with $AgNO_3$ solutions to achieve final concentrations of 1, 5, 10, and 14 mM. The solution was vigorously stirred at 25 °C and its color immediately turned to dark-orange.

* To whom correspondence should be addressed. Tel.: +39 040 558 3682. Fax: +39 040 558 3691. E-mail: idonati@units.it.
† Department of Life Sciences.
‡ Department of Materials Engineering and Natural Resources.

10.1021/bm801253c CCC: $40.75
Published on Web 01/13/2009

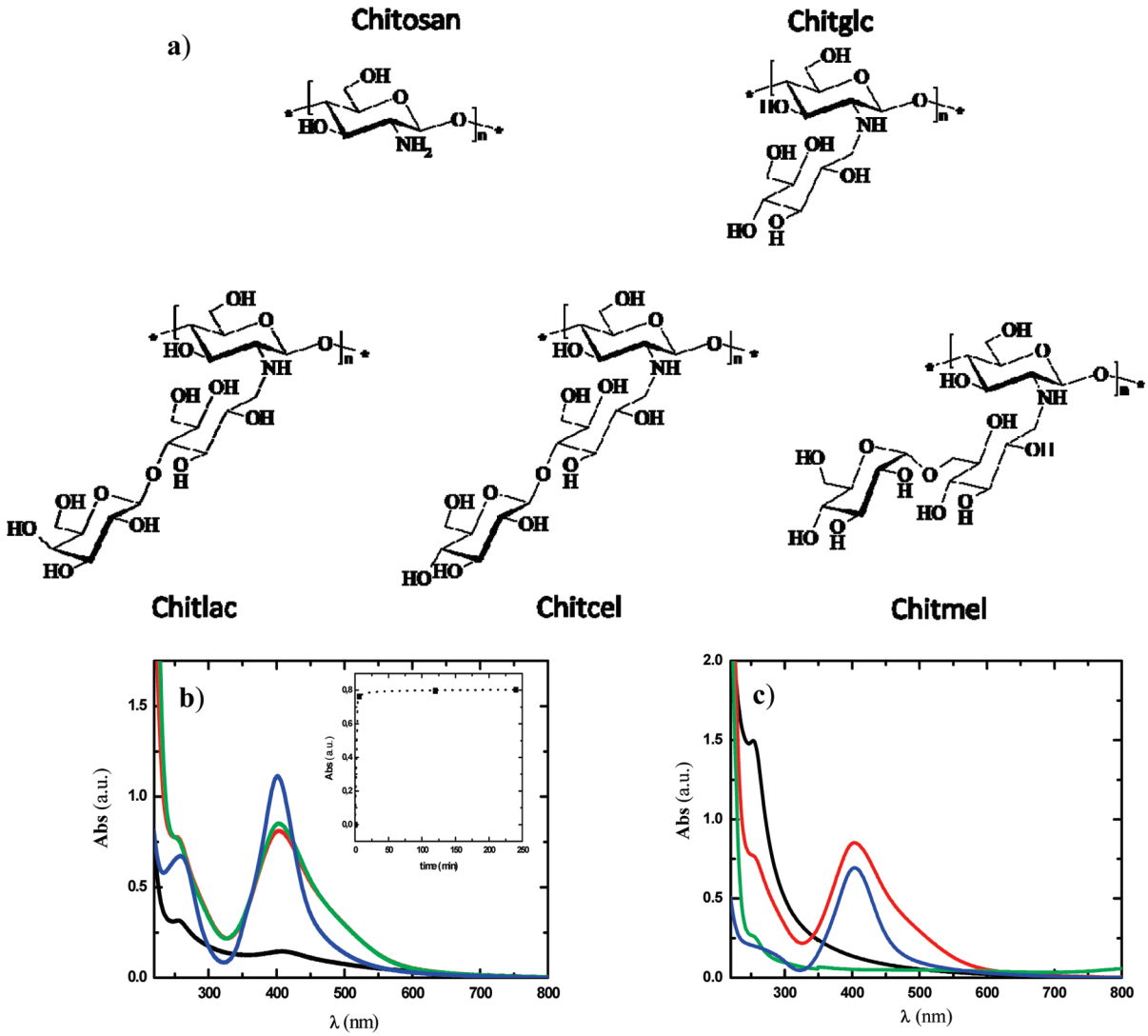

Figure 1. (a) Schematic representation of chitosan and of the alditol containing structure of Chitlac, Chitcel, Chitglc, and Chitmel. (b) UV−vis spectra of Chitlac (2 g/L in deionized water) in the presence of 1 mM (black), 5 mM (red) and 10 mM (green) $AgNO_3$. For comparison, the UV−vis spectrum obtained from a 2 g/L Chitlac solution in the presence of 1 mM $AgNO_3$ and 0.5 mM ascorbic acid (blue) is also reported. Inset: evolution with time of the surface plasmon resonance peak at 403nm. (c) UV−vis spectra of 2 g/L solutions of chitosan (black), Chitlac (red), Chitmel (green), and Chitglc (blue) treated with $AgNO_3$ (10 mM).

Preparation with Ascorbic Acid. Silver nanoparticles were obtained by reducing silver ions with ascorbic acid in Chitlac solutions according to the following procedures: freeze-dried Chitlac was dissolved in deionized water in order to obtain solutions with different concentrations (2 g/L and 4 g/L). Chitlac solutions were mixed with $AgNO_3$ solutions to achieve final concentrations of 0.5 and 1 mM; then ascorbic acid ($C_6H_8O_6$) solutions were added to final concentrations of 0.25 and 0.5 mM, respectively. The solution was vigorously stirred at 25 °C and its color immediately turned to dark-orange.

Chitlac-Silver Nanoparticle (Chitlac-nAg) Hydrogels. Chitlac (4 g/L) was dissolved in HEPES buffer (10 mM) at pH 7 and mixed with $AgNO_3$ (final concentration, 14 mM). The solution was stirred vigorously and incubated at room temperature. Hydrogel formation was noted few hours after mixing of the components.

UV−vis Spectroscopy. UV−visible spectroscopy measurements were performed with a Cary 400 spectrophotometer (data interval: 0.5 nm; scan speed: 300 nm/min). All sample solutions were diluted 1:10.

Transmission Electron Microscopy (TEM). TEM images were taken by means of a PHILIPS EM 208 microscope; the solutions were deposited onto Nickel grids coated with a carbon film and dried overnight.

Raman Spectroscopy. Raman spectra were collected using an *inVia* Raman system (Renishaw plc, Wotton-under-Edge, U.K.). The laser (514.5 nm argon-ion laser, LaserPhysics, West Jordan UT, U.S.A.) was focused on the sample by a 20× objective (0.4 NA). Laser power at the sample was 3 mW; to minimize laser-induced photodegradation of the sample, the laser power density was lowered by defocusing the beam by 10%. The exposure time was 5 accumulations of 10 s for each spectrum, for a total exposure time of 50 s per spectrum.

Scheme 1. Fetizon Oxidation in the Case of Chitlac, Chitcel, and Chitglc

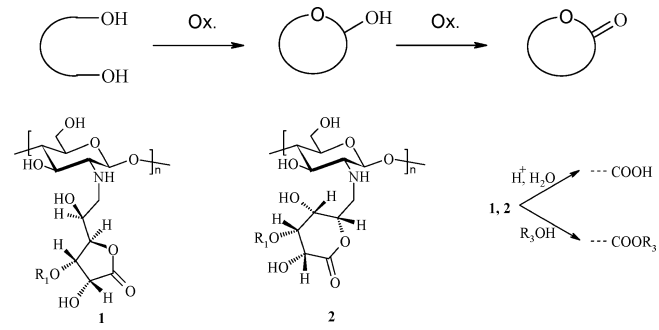

NMR. NMR spectra were recorded in D_2O with a 270 MHz Jeol instrument using 3-(trimethylsilyl) propanesulfonate as internal standard.

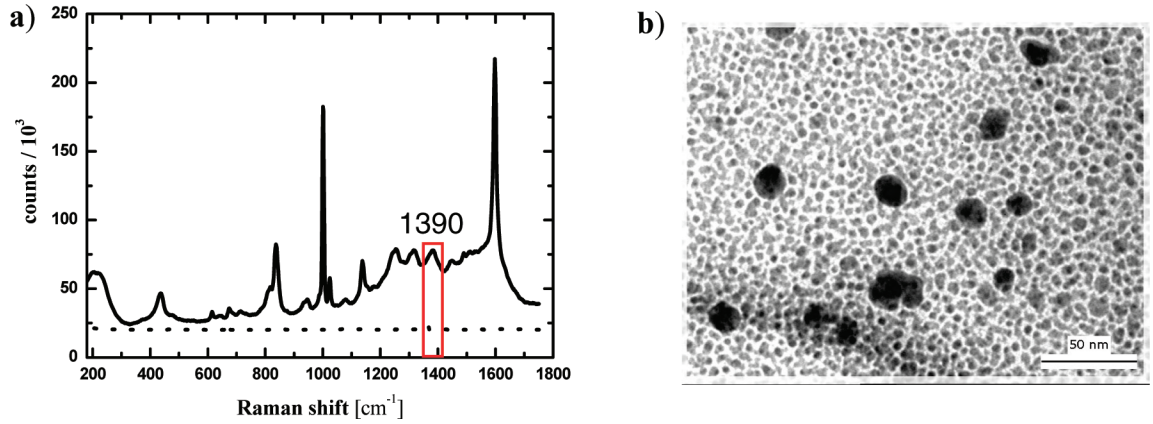

Figure 2. (a) Raman-SERS spectra of Chitlac (····, 50 g/L) and Chitlac treated with 14 mM $AgNO_3$ (—, 4 g/L). (b) TEM micrograph of silver nanoparticles in Chitlac (4 g/L, $AgNO_3$ 14 mM).

^{1}H NMR spectra of the modified chitosans were recorded at 90 °C, while ^{13}C NMR spectra of ascorbic acid, glucitol, and silver-oxidized glucitol were recorded at 25 °C.

FT-IR. Infrared spectra of silver-treated Chitlac in KBr were recorded with a FT-IR Perkin-Elmer 2000 System spectrometer.

Mechanical Spectroscopy. Dynamic viscoelastic characterization was carried out on a Stress-Tech general-purpose rheometer (Reologica instruments AB, 22363 Lund, Sweden). The experiments were performed at 25 °C with a serrated plate−plate (d = 40 mm) measuring geometry with a gap of 1.00 mm. Frequency sweeps were performed at a constant strain (0.001) in the frequency range 0.01−5 Hz. The sample was sealed with a low-density silicon oil to avoid adverse effects associated with evaporation of the solvent.

Results and Discussion

In the present paper, we focus on the possibility of exploiting the glucitol-component of the side chain of Chitlac, that is, the open-chain polyol part, as Ag^+ reducing agent for the formation of silver nanoparticles. In this sense, Chitlac could be granted of an additional functionality, that is, the ability to "auto-reduce" the metal ions without requiring additional exogenous reactants. This idea springs from the observation of the reducing properties of alditols toward silver ions. As such, alditols do not conform to the classic definition of "reducing sugars" and are not expected to give rise to a positive Tollens assay. In fact, Ag^+ belongs to a group of oxidizing agents that are unable to oxidize alcoholic groups under mild conditions (i.e., room temperature). However, according to the Fetizon oxidation mechanism, diol-containing molecules could be efficiently oxidized by silver ions, provided that five- or six-membered rings are formed.[19] To prove the applicability of the above-reported oxidation mechanism, glucitol was treated under the Tollens conditions with silver ions, instantaneously leading to the formation of a silver mirror and to a complex mixture of oxidation products of glucitol (see Supporting Information). The peak at ~173 ppm in the ^{13}C NMR of the oxidized mixture likely stems from the presence of a lactone group much like in another lactone-containing oxidized sugar derivative, namely ascorbic acid. As such, these results seem to point (for the first time to the best of the authors' knowledge) to the ability of alditols to reduce silver ions by means of the Fetizon oxidation mechanism.

Prompted by these results, the silver-reducing ability of the glucitol moiety entrapped in the side chain of the lactit-1-yl chitosan was assessed (Figure 1b). Upon addition of silver ions to the polysaccharide solution, a sharp and intense surface plasmon resonance peak, arising from the formation of metallic nanoparticles, is displayed without requiring exogenous reducing agents. The shape of the surface plasmon resonance peak at 403 nm suggests a narrow size distribution of the silver nanoparticles obtained through this approach.[3,20] The presence and the close arrangement of the Ag^+-coordinating amino group and of the reducing component (glucitol) in a polyvalent assembly account for a strong enhancement of reactivity, as nonpolymer-linked glucitol is ineffective at the same alditol molar concentrations. Moreover, they produce a very fast kinetics of the reduction (Figure 1b inset), as the maximum intensity of the surface plasmon resonance was reached a few minutes after the addition of silver ions to the polymer solution. Finally, the polymer component also allowed the stabilization of the silver nanoparticles toward coalescence, maintaining them stable over several months.

To gain a more detailed insight into the mechanism of silver ion reduction, different oligosaccharide derivatives of chitosan have been prepared, all being characterized by the presence of a glucitol in the side chain (Figure 1a). Chitlac, Chitcel, and Chitglc were all able to efficiently reduce silver ions in aqueous solution in mild conditions without the addition of exogenous reducing agents (Figure 1c), as revealed by the presence of a surface plasmon resonance band at 403 nm. In all cases, the formation of silver nanoparticles is traced back to an oxidation process involving the glucitol moiety in the modified polysaccharide. In fact, neither native chitosan nor other nonglucitol-containing polyols like dextran (data not reported) were able to lead to a plasmon resonance band once treated with silver nitrate.

The first step of the Fetizon oxidation mechanism is the oxidation of a primary alcohol to an aldehyde group. This is followed by the formation of a cyclic hemiacetal, which is further oxidized to lactone. These requirements are met by the chitosan samples modified with glucose, lactose, and cellobiose where the Ag^+ treatment can lead to the formation of a lactone intermediate involving the C6 and C2 (six-membered ring) or C3 (five-membered ring) of the glucitol moiety (Scheme 1). As a negative control, in melibiose-modified chitosan (Chitmel) the primary alcohol at C6 is not available for the oxidation by silver ions: no reduction was observed (Figure 1c). Because chitosan and all its oligosaccharide derivatives tested have been prepared as hydrochloride salts, a direct effect of the counterion (chloride) in the formation of the nanoparticles[21,22] can be ruled out. Moreover, it is important to underline that the present mechanism, at variance with previous reports on the use of

polyols for silver ion reduction, requires mild conditions and does not cause C−C bond cleavage.

The lactone group formed after treatment of Chitlac, Chitcel, and Chitglc with silver ions is surrounded by water molecules and by several hydroxyl groups from the modified polysaccharide itself. It follows that the lactone groups can undergo (i) hydrolysis or (ii) *trans*-esterification reactions. The former case is likely to occur when the treatment with silver ions is performed under slightly acidic media. This hypothesis was corroborated by the appearance of a IR peak at around 1384 cm^{-1} and of a SERS peak around 1390 cm^{-1} (Figure 2a), which can be assigned to the vibrational frequency of the carboxylic moiety upon $AgNO_3$ treatment of Chitlac in deionized water. The peak at 1390 cm^{-1} is considered to be characteristic of carboxylic acids adsorbed on silver and corresponds to the symmetric stretching mode of a carboxylate.[23,24]

In the *trans*-esterification reaction the lactone group can react with hydroxyl groups located on different polysaccharide chains leading to a chemically cross-linked network. Hence, the silver-induced oxidation of the polysaccharide results in a chemical hydrogel. In the case of Chitlac, the gel formation process upon treatment with silver ions at pH 7 is very effective and a semisolid system (albeit a weak one) is achieved even with a relatively low concentration of polysaccharide (4 g/L), as qualitatively confirmed by shear rheology (see Supporting Information). Although further analysis is required to characterize the kinetics of gel formation and dissolution, it can be anticipated that a complete degradation of the ester bonds in water environment spans over 1 week. This latter aspect points to a possible and very appealing application of branched chitosans for the preparation of silver containing antibacterial hydrogels with programmed erosion for topical use.

Overall, the Chitlac molecule represents a polyvalent system containing both a coordinating group and the reducing agent in spatial proximity for the production of silver nanoparticles. From these considerations, it can be foreseen that nanoparticles of very small dimensions and in close contact with the polysaccharide chain are obtained. Transmission electron microscopy confirmed the presence of well dispersed nanoparticles with an average diameter smaller than 10 nm, together with few larger particles (∼ 30 nm) (Figure 2b). Such close arrangement of electron dense metal particles allows obtaining a very strong SERS effect (Figure 2a) when the Raman spectrum of this polymer is recorded. In fact, the intensity of the signals arising from the polysaccharide is enormously enhanced when these small silver nanoparticles are present. Given the biological significance of Chitlac and its ability of interacting with different carbohydrate-binding proteins, the SERS effect becomes particularly appealing in designing novel and specific biosensors.

Conclusion

In the present manuscript, we propose a new mechanism for the formation of stable silver nanoparticles based on the presence of alditols in an engineered polysaccharide; this integrated system displays multivalent properties that can be exploited in biological and optical applications. The reduction of silver ions is achieved through the Fetizon oxidation mechanism that, for the first time, is shown to work on alditols. An insight on the detail of the mechanism proposed and on the complete characterization of the different products will be tackled in a future work.

Supporting Information Available. A complete description of materials and methods. This material is available free of charge via the Internet at http://pubs.acs.org.

References and Notes

(1) Huang, H.; Yuan, Q.; Yang, X. *Colloids Surf., B* **2004**, *39* (1−2), 31–37.
(2) Yi, Y.; Wang, Y.; Liu, H. *Carbohydr. Polym.* **2003**, *53* (4), 425–430.
(3) Kuo, P. L.; Chen, W. F. *J. Phys. Chem. B* **2003**, *107* (41), 11267–11272.
(4) Fu, J.; Ji, J.; Fan, D.; Shen, J. *J. Biomed. Mater. Res. A* **2006**, *79* (3), 665–674.
(5) Sondi, I.; Goia, D. V.; Matijevic, E. *J. Colloid Interface Sci.* **2003**, *260* (1), 75–81.
(6) Huang, H.; Yuan, Q.; Yang, X. *J. Colloid Interface Sci.* **2005**, *282* (1), 26–31.
(7) Bonifacio, A.; van der Sneppen, L.; Gooijer, C.; van der Zwan, G. *Langmuir* **2004**, *20* (14), 5858–5864.
(8) Wiley, B.; Herricks, T.; Sun, Y.; Xia, Y. *Nano Lett.* **2004**, *4* (9), 1733–1739.
(9) Yin, Y.; Lu, Y.; Sun, Y.; Xia, Y. *Nano Lett.* **2002**, *2* (4), 427–430.
(10) Sun, Y.; Xia, Y. *Science* **2002**, *298* (5601), 2176–2179.
(11) Sun, Y.; Xia, Y. *Adv. Mater.* **2002**, *14* (11), 833–837.
(12) Sun, Y.; Yin, Y.; Mayers, B. T.; Herricks, T.; Xia, Y. *Chem. Mater.* **2002**, *14* (11), 4736–4745.
(13) Wiley, B.; Sun, Y.; Mayers, B.; Xia, Y. *Chem.—Eur. J.* **2005**, *11* (2), 454–463.
(14) Fiével, F.; Lagier, J. P.; Figlarz, M. *MRS Bull.* **1989**, *14*, 29–40.
(15) Travan, A.; Donati, I.; Marsich, E.; Pelillo, C.; Benincasa, M.; Scarpa, T.; Semeraro, S.; Turco, G.; Gennaro, R.; Paoletti, S. *Biomaterials*, **2008**, submitted for publication.
(16) Donati, I.; Stredanska, S.; Silvestrini, G.; Vetere, A.; Marcon, P.; Marsich, E.; Mozetic, P.; Gamini, A.; Paoletti, S.; Vittur, F. *Biomaterials* **2005**, *26* (9), 987–998.
(17) Marcon, P.; Marsich, E.; Vetere, A.; Mozetic, P.; Campa, C.; Donati, I.; Vittur, F.; Gamini, A.; Paoletti, S. *Biomaterials* **2005**, *26* (24), 4975–4984.
(18) Marsich, E.; Borgogna, M.; Donati, I.; Mozetic, P.; Strand, B. L.; Salvador, S. G.; Vittur, F.; Paoletti, S. *J. Biomed. Mater. Res. A* **2008**, *84*, 364−376.
(19) Fetizon, M.; Golfier, M.; Louis, J. M. *Tetrahedron* **1975**, *31* (2), 171–176.
(20) Henglein, A. *J. Phys. Chem.* **1993**, *97* (21), 5457–5471.
(21) Wiley, B.; Herricks, T.; Sun, Y.; Xia, Y. *Nano Lett.* **2004**, *4* (9), 1733–1739.
(22) Yin, Y.; Lu, Y.; Sun, Y.; Xia, Y. *Nano Lett.* **2002**, *2* (4), 427–430.
(23) Moskovits, M.; Suh, J. S. *J. Am. Chem. Soc.* **1985**, *107* (24), 6826–6829.
(24) Cotton, T. M. In *Spectroscopy of Surfaces*; Clark, R. J. H., Hester, R. E., Eds.; Wiley: New York, 1988.

BM801253C

Paper 2

Non-cytotoxic Silver Nanoparticle-Polysaccharide Nanocomposites with Antimicrobial Activity

Andrea Travan,* Chiara Pelillo, Ivan Donati, Eleonora Marsich, Monica Benincasa, Tommaso Scarpa, Sabrina Semeraro, Gianluca Turco, Renato Gennaro, and Sergio Paoletti

Department of Life Sciences, University of Trieste, Via Giorgieri 1, Trieste I-34127, Italy

Received January 9, 2009; Revised Manuscript Received April 7, 2009

In this work we study (i) the formation and stabilization of silver nanoparticles in a bioactive chitosan-derived polysaccharide solution, (ii) the antimicrobial properties, either in solution or in 3D hydrogel structures, obtained by mixtures with the polysaccharide alginate, and (iii) the cytotoxicity of the latter nanocomposite materials on different eukaryotic cell lines. Antimicrobial results show that these nanocomposite systems display a very effective bactericidal activity toward both Gram+ and Gram− bacteria. However, the hydrogel does not show any cytotoxic effect toward three different eukaryotic cell lines. This is due to the fact that the nanoparticles, immobilized in the gel matrix, can exert their antimicrobial activity by simple contact with the bacterial membrane, while they can not be uptaken and internalized by eukaryotic cells. This novel finding could advantageously contribute to responding to the growing concerns on the toxicity of nanoparticles and facilitate the use of silver−biopolymer composites in the preparation of biomaterials.

1. Introduction

Since ancient times, silver has been extensively used to control infections. At present, silver as an antimicrobial agent is gaining increasing appeal for medical applications because antibiotic-resistant bacterial strains have become a major issue in public health care.[1−3] Silver-based medical products, ranging from topical ointments and bandages for wound healing to coated stents, have been proven to be effective in retarding and preventing bacterial infections.[4] Improvements in the development of novel silver nanoparticles-containing products are continuously sought. In particular, there is an increasing interest toward the exploitation of silver nanoparticles technology in the development of bioactive biomaterials, aiming at combining the relevant antibacterial properties of the metal with the peculiar performance of the biomaterial.[5−9]

However, a widely accepted consensus on the detailed molecular mechanism of silver nanoparticles toxicity is still missing. It is possible to state that a lack of physical barriers to nanoparticle diffusion into cells determines their generalized (bio)availability, with the risk of a massive uptake by eukaryotic cells, which eventually leads to their death.[10] A critical survey of the present nanotechnology literature suggests that the drive toward new formulations often overwhelms the interest for a better assessment of the cytotoxicity of the nanoparticles. In fact, the issue of possible adverse effects and toxicity of nanoparticles for the human body is progressively recognized as central by a still limited, albeit increasing, number of studies.[11] So far, water-based biomaterials able to successfully combine antibacterial properties of silver nanoparticles with demonstrated absence of cytotoxicity have not yet been reported in the literature. At the nanometric level, a crucial issue about silver nanoparticles is their tendency to aggregate, thus losing the peculiar properties associated with the nanoscale. Consequently, the preparation and stabilization of metal nanoparticles represent to date an open challenge. To this scope, polyelectrolytes in small concentration, such as polyphosphate, polyacrylate, poly(vinyl-sulfate), poly(ethylene-imine),[12−14] poly(allylamine),[8] and chitosan,[7,15,16] have been used with variable results to stabilize the nanoparticles preventing the growth of aggregates, in addition to the more widely used poly(vinylpyrrolidone),[17] a neutral polymer. The stabilization of metal nanoparticles is explained by the electronic interaction of the polymer functional groups with the metal particles. In fact, their (albeit minor) nucleophilic character is sufficient to bind the metal particles by donating electrons.[14] Protective polymers can coordinate metal ions before reduction, forming a polymer−metal ion complex; such a complex can then be reduced under mild conditions, resulting in a smaller size and a narrower size distribution than those obtained without protective polymers.[18] Once the reduction occurred, the stabilizing effect of these macromolecules is attributable to the fact that either the particles are attached to the much larger protecting polymers or the protecting molecules cover or encapsulate the metal particles.[8] To find applications in the biomaterials field, both the stabilizing and the reducing agents must not represent a biological hazard.[19]

Chitosan, a natural saccharidic polybase composed of β-(1→4)-linked glucosamine residues interspersed with residual *N*-acetylglucosamine moieties, has been previously used to prepare and stabilize metal nanoparticles.[7,15,16] However, the limitations of such polysaccharide are connected with its pH-dependent solubility (limited to low pH only, as a polycation), immiscibility with other oppositely charged polyelectrolytes and lack of cell-specific molecular signals. To overcome these problems, we decided to use a lactose-substituted chitosan, 1-deoxylactit-1-yl chitosan, short-named "Chitlac". Chitlac is a highly branched polymer devoid of pH limitations as to aqueous solubility; it is both biocompatible and bioactive, owing to the terminal galactose unit on the side chain.[20] In addition, at neutral pH the moderately cationic Chitlac can give rise to soluble binary mixtures with alginate, an anionic polysaccharide composed of (1→4)-linked α-L-guluronic acid and β-D-mannuronic acid

* To whom correspondence should be addressed. Tel.: +39 040 558 3682. Fax: +39 040 558 3691. E-mail: atravan@units.it.

10.1021/bm900039x CCC: $40.75
Published on Web 04/30/2009

residues. These mixtures were shown to be able to form stable hydrogels in cell-friendly conditions.[21,22]

The aim of this work is (i) to characterize the formation and stabilization of silver nanoparticles in Chitlac solutions, (ii) to assess the antimicrobial properties, either in solution or in 3D hydrogel structures, obtained by mixtures with the polysaccharide alginate, and (iii) to evaluate the cytotoxicity of the latter nanocomposite materials on different eukaryotic cell lines.

2. Materials and Methods

2.1. Materials. Chitlac (1-deoxylactit-1-yl chitosan, CAS registry number 85941-43-1) sample was prepared according to the procedure reported elsewhere[23] starting from a highly deacetylated chitosan (residual acetylation degree = 11.3%, Aldrich Chemical Co. (U.S.A.)). The molecular weight of Chitlac was estimated to be approximately 1.5×10^6. Alginate ($M_w \sim 130000$, $F_G = 0.65$, $F_{GG} = 0.53$) was provided by FMC Biopolymers. Silver nitrate, ascorbic acid, lead citrate, uranyl acetate, 4-(2-hydroxyethyl)-1-piperazine-ethanesulfonic acid, $CaCO_3$ (mean particle size 3 μm), glucono-D-lactone (GDL), and LDH (lactate dehydrogenase)-based TOX-7 kit (Sigma-Aldrich) were purchased from Sigma Chemical Co (St. Louis, MO). Mueller Hinton (MH) was from Difco Microbiology (Sparks, MD).

2.2. Chitlac−Silver Nanoparticles (Chitlac-nAg) Preparation. Silver nanoparticles were obtained by reducing silver ions with ascorbic acid in Chitlac solutions according to the following procedures: freeze-dried Chitlac was dissolved in deionized water to obtain solutions with different concentrations (1, 2, and 4 g/L). Chitlac solutions were mixed with $AgNO_3$ solutions to achieve final $AgNO_3$ concentrations of 0.5 and 1 mM; then ascorbic acid ($C_6H_8O_6$) solutions were added at final concentrations of 0.25 and 0.5 mM, respectively. For antibacterial tests 20% Mueller−Hinton broth was added to Chitlac-nAg solutions.

2.3. Hydrogels Preparation. *2.3.1. AC-Gel.* For the preparation of alginate−Chitlac hydrogels (AC-Gel), an in situ calcium release approach was used. Briefly, a Chitlac solution was added to an alginate solution (final concentrations: alginate 15 g/L, Chitlac 2 g/L, NaCl 0.15 M, HEPES buffer 0.01 M, pH 7.4) and the mixture was blended with an inactivated form of Ca^{2+} ($CaCO_3$, 15 mM) followed by the addition of the slowly hydrolyzing D-glucono-δ-lactone (GDL; $[GDL]/[Ca^{2+}] = 2$). Aliquots of this gelling solution were poured into well tissue culture plates. Finally, the gels were washed with $CaCl_2$ solution 5 mM to remove residual GDL. For antibacterial tests, 20% Mueller−Hinton broth was added to both Chitlac and alginate solutions.

2.3.2. AC-nAg-Gel. Alginate−Chitlac hydrogels containing silver nanoparticles were prepared according to the procedure of the AC-Gels using Chitlac-nAg instead of Chitlac solutions. For antibacterial tests, 20% Mueller−Hinton broth was added to both Chitlac and alginate solutions.

2.4. UV−Vis Spectroscopy. UV−visible spectroscopy measurements were performed with a Cary 400 spectrophotometer (data interval, 0.5 nm; scan speed, 300 nm/min). All samples solutions were diluted 1:10.

2.5. Transmission Electron Microscopy (TEM). TEM images were taken by means of a PHILIPS EM 208 Microscope; the solutions were deposited onto Nickel grids coated with a carbon film and dried overnight. In the samples in which the polymer was stained, a mixed solution of lead citrate (5 g/L) and uranyl acetate (5 g/L) was added 1:1 to the Chitlac−silver nanoparticles (nAg) solutions.

2.6. Bacterial Killing Kinetics Assays. The killing kinetics assays were performed using cultures of *E. coli* (ATCC 25922), *S. epidermidis* (clinical isolate), *S. aureus* (ATCC 25923), and *P. aeruginosa* (ATCC 27853) diluted in 20% Mueller−Hinton broth to give 1×10^6 CFU/mL (CFU = colony forming units) in the presence or absence of Chitlac-nAg. The bacterial suspensions were then incubated in a shaking water bath at 37 °C. At the indicated times, samples were removed, serially diluted with buffered saline solution, plated in duplicate on Mueller−Hinton agar, and incubated for 24 h to allow colony counts. Data are the mean of at least four independent determinations with comparable results.

2.7. Growth Inhibition Assays in Solid Medium. The growth inhibition in solid medium was evaluated after smearing, with sterile cotton swabs, of bacterial suspensions at final concentrations of 10^6 and 10^5 CFU/mL on Petri dishes prepared as described above (hydrogel preparation). After overnight incubation at 37 °C, the presence of visible colonies was evaluated. Growth controls were carried out on Mueller−Hinton agar plates and AC gels in the presence of Mueller−Hinton medium.

2.8. Evaluation of Bacterial Membrane Alteration by Flow Cytometric Assays. Flow cytometric assays were used to evaluate the transmembrane potential and the membrane permeabilization of bacterial cells treated with the system Chitlac-nAg. For these analyses, midlogarithmic phase bacterial cultures were diluted in 20% MH broth to 1×10^6 CFU/mL. Aliquots of the bacterial suspension were then incubated with or without (controls) the system Chitlac-nAg for 10 or 30 min at 37 °C. At the end of the incubation time, the bacterial suspensions were incubated in the dark for 4 min at 37 °C with bis-(1,3-dibutylbarbituric acid)-trimethine oxonol ($DiBAC_4(3)$; Molecular Probes Inc., Eugene, OR) at a final concentration of 1 μM to evaluate alterations in the transmembrane potential. The fluorescence intensity was detected with a Cytomics FC 500 instrument (Beckman-Coulter, Inc., Fullerton, CA) equipped with an argon laser (488 nm, 5 mW) and using a photomultiplier tube fluorescence detector for green (525 nm) filtered light. The detectors were set on logarithmic amplification. Optical and electronic noise were eliminated by setting an electronic gating threshold on forward scattering detector, while the flow rate was kept at a data rate below 200 events/second to avoid cell coincidence. For each sample, at least 10000 events were acquired and stored as list mode files. Membrane permeabilization following treatment with the system Chitlac-nAg was determined by means of a flow cytometer, measuring the propidium iodide (PI; Sigma-Aldrich) uptake by bacterial cells. For the analyses, bacterial suspensions of 1×10^6 cells/mL were incubated in 20% MH broth with the system Chitlac-nAg at 37 °C for different times. A filtered solution of propidium iodide was then added to the bacterial suspensions at a final concentration of 10 μg/mL, and the cells were analyzed in the flow cytometer after 4 min incubation at 37 °C. The fluorescence intensity was detected as reported above using a detector for red light (610 nm). All the experiments with the fluorescent probes were conducted in triplicate and the analysis of data was performed with the WinMDI software (Dr. J. Trotter, Scripps Research Institute, La Jolla, CA, U.S.A.).

2.9. LDH Cytotoxicity Assay. In vitro cytotoxicity of AC-nAg-Gels was evaluated by using the lactate dehydrogenase assay (LDH assay, TOX-7, Sigma) on the mouse fibroblast-like (NIH-3T3), human hepatocarcinoma (HepG2), and human osteosarcoma (MG63) cell lines, respectively. Cylindrical gel samples, with a length of 5 mm and a diameter of 4 mm, were used and the tests were performed by direct contact with the gel or with liquid extract of the gel material. For a direct contact test, 70000 cells were plated on 24-well plates and, after complete adhesion, culture medium was changed with 250 μL of fresh medium. Tested materials (in quadruplicate) were directly deposited on the cell layer. After 24 and 72 h, medium was collected and the LDH assay was performed according to the manufacture's protocol. In an extraction test, samples were incubated in extraction medium (Dulbecco's modified Eagle's medium, inactivated fetal bovine serum 10%, penicillin 100 U/mL, streptomycin 100 μg/mL, and L-glutamine 2 mM) for 24 h at 37 °C and 5% pCO_2. The surface/volume ratio of the samples and the medium was 1.25 cm^2/mL. After incubation, extraction media were added on cells seeded on 24-well plates (70000 cells/well). The LDH assays were performed after 24 and 72 h as described above. Each material test was performed in quadruplicate. Evaluation of cytotoxicity was calculated according to the formula: % LDH released = $[(A - B)/(C - B)] \times 100\%$, with A = LDH activity in the culture medium of gel-treated or extraction medium-treated cells; B = LDH activity of culture medium from untreated cells; and C = LDH activity after total cell lysis).

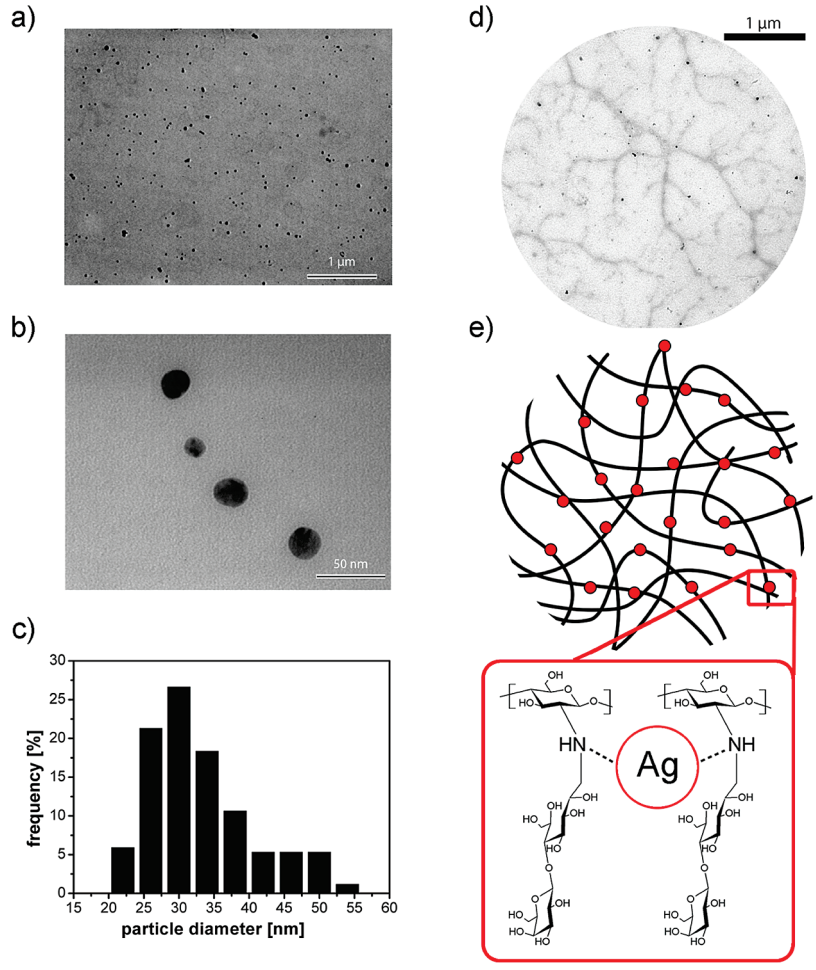

Figure 1. (a,b) TEM images of silver nanoparticles dispersed in Chitlac at different magnifications (Chitlac 4 g/L, $AgNO_3$ 1 mM, $C_6H_8O_6$ 0.5 mM); (c) silver nanoparticles size distribution histogram based on the TEM image in Figure 1a; the mean particle size is 33.6 ± 7.6 nm; (d) TEM image of silver nanoparticles formed on the polymeric chains of Chitlac (Chitlac 2 g/L, $AgNO_3$ 1 mM, $C_6H_8O_6$ 0.5 mM). Chitlac chains have been stained with a mixed solution of lead citrate (5 g/L) and uranyl acetate (5 g/L); (e) schematic representation of the polymeric chains of Chitlac providing the nitrogen atoms for the coordination and stabilization of silver nanoparticles.

2.10. Preparation of Microspheres and ICP-MS Analysis. Calcium microspheres from AC-nAg mixtures (final concentrations: alginate 15 g/L, Chitlac 2 g/L nAg, NaCl 0.15 M, HEPES 0.01 M, pH 7.4) were obtained by dripping the polymer blend into a gelling solution (0.05 M $CaCl_2$). The droplet size was controlled by use of a high-voltage electrostatic bead generator (7 kV, 10 mL/h, steel needle with 0.7 mm outer diameter, 1 cm distance from the needle to the gelling solution). The gel beads obtained were stirred for 30 min in the gelling solution prior to use.

To evaluate the amount of silver released from the AC-nAg gel, the microspheres were vigorously stirred for 5 weeks in a saline solution (NaCl 0.015 M) with a volume ratio microspheres/solution of 4; after incubation, supernatants from the microsphere suspensions were analyzed by ICP-MS (inductively coupled plasma mass spectrometry).

2.11. MTT Assay. Cytotoxicity of AC-nAg gel microspheres external solutions was evaluated by the MTT (3-(4,5-dimethylthiazol-2-yl)-2,5-diphenyltetrazolium bromide) reduction assay using mouse fibroblast (NIH-3T3), human hepatocarcinoma (HepG2), and human osteosarcoma (MG63) cell lines, respectively. Cells (5000 cells/well) were seeded into 96-well plates and allowed to adhere for 16 h. Extracts from the microspheres were then added to cell cultures for 72 h at 37 °C in the presence of DMEM culture medium and 10% fetal bovine serum. Cell cultures treated with 1% (v/v) Triton-X 100 in complete DMEM medium or with a solution of 0.015 M NaCl supplemented with DMEM culture medium and fetal bovine serum were used, respectively, as positive and negative controls. Finally, MTT (5 mg/mL in PBS) was added to the medium in each well to obtain a final concentration of 0.5 mg/mL, and the cell cultures were incubated for a further 4 h. Cell viability was determined by measuring the cellular reduction of MTT to the crystalline formazan product, which was dissolved by addition of 100 μL of DMSO. The formazan concentration was determined spectrophotometrically at 570 nm.

3. Results and Discussion

Chitlac nanocomposites containing silver were prepared by chemical reduction of corresponding metal ions to zeroth-valent metal nanoparticles; the reduction was performed using ascorbic acid, a nontoxic reagent which can form metallic silver according to the following stoichiometry:[6]

$$2Ag^+ + C_6H_8O_6 \rightleftarrows 2Ag^0 + C_6H_6O_6 + 2H^+$$

The formation of nanoparticles, their shape, distribution and dimensions have been evaluated by means of transmission electron microscopy (TEM) imaging and analyses. Figure 1a,b shows the nanoparticles dispersed in Chitlac at two different magnifications; they are mostly round-shaped and well-dispersed. TEM images have been analyzed to evaluate the dimensional distribution, as the size affects the antimicrobial properties of the nanoparticles.[24] The histogram shows a narrow distribution of the silver nanoparticles dispersed in Chitlac with a maximum frequency at around 30 nm (Figure 1c) and a mean

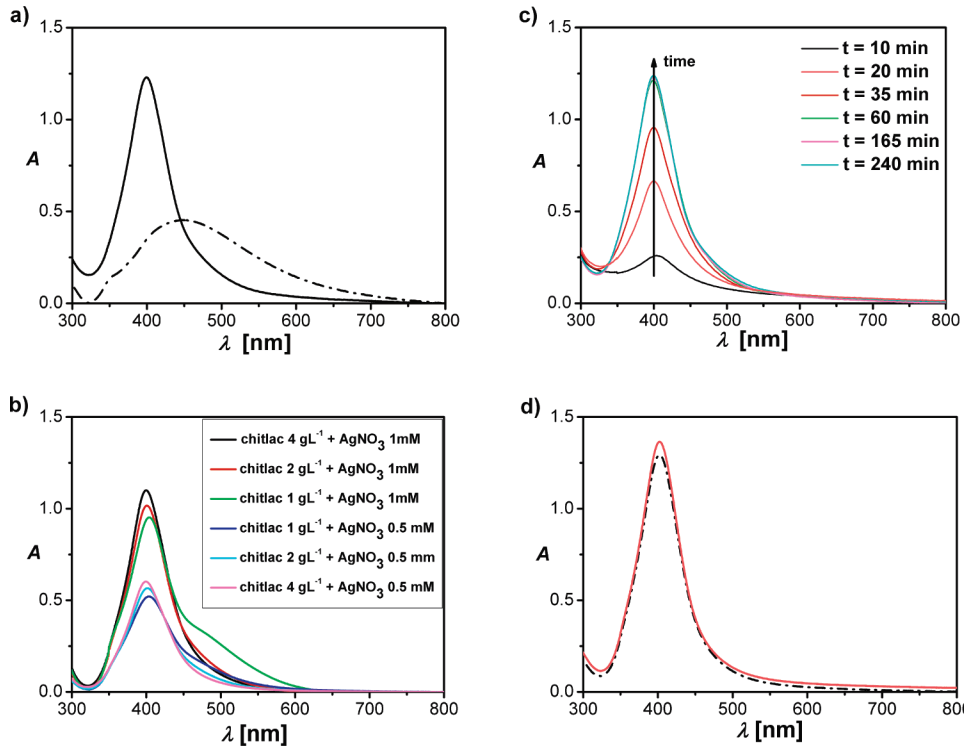

Figure 2. (a) UV−vis spectra of silver nanoparticles formed in chitosan (dashed line) and Chitlac (solid line) solutions under the same conditions (polymer concentrations 2 g/L; $AgNO_3$ 1 mM; $C_6H_8O_6$ 0.5 mM). (b) Effect of polymer and $AgNO_3$ concentrations on UV−vis spectra of silver nanoparticles. In each sample, the $AgNO_3/C_6H_8O_6$ concentration ratio is 2, according to the reaction stoichiometry. (c) Time dependence of UV−vis spectra variations of Chitlac 2 g/L + $AgNO_3$ 1 mM after the addition of ascorbic acid. d) UV−vis spectra of silver nanoparticles in Chitlac after 1 day (black dashed line) and after 90 days (orange solid line).

diameter of 33.6 ± 7.6 nm. TEM analyses were conducted also to visualize the polymeric chains using staining agents (i.e., Pb^{2+}, UO_2^{2+}). As revealed by Figure 1d, Chitlac chains ("gray threads") efficiently coordinate the silver nanoparticles ("black dots"), thus hampering their large scale collapsing (Figure 1e); the image shows a vein-like structure formed by different polysaccharide chains, which likely associate as a consequence of the drying process during sample preparation for TEM analysis.

The formation of silver nanoparticles was verified also by means of UV−vis absorption spectroscopy (Figure 2a), where an intense band centered at about 400 nm was clearly detected. This band, identified as a "surface plasmon resonance band", is due to a collective excitation of the free electrons in the nanoparticles. The shape of the plasmon band is almost symmetrical, suggesting that the nanoparticles are well dispersed and spherical. At variance, the aggregation of nanoparticles would lead to a broader plasmon band, with a red-shifted maximum.

The effect of concentration in solution of both polymer and silver nitrate was explored (Figure 2b). The changes in UV−vis absorption indicate that the size and dispersion of silver nanoparticles were affected by both the concentration of Chitlac (which operates as a controller of nucleation as well as a stabilizer) and of $AgNO_3$. The highest plasmon peaks were recorded for Chitlac at 2 and 4 g/L in the presence of $AgNO_3$ 1 mM and $C_6H_8O_6$ 0.5 mM. The kinetics of the reduction process was monitored for 4 h immediately after the addition of ascorbic acid (Figure 2c). It can be seen that the intensity of the plasmon resonance peak increases with time; for reaction times exceeding 4 h no significant increase in the absorption peak was found. As previously noted, long-term stability of silver nanoparticles in solution is an important goal to be reached. In fact, agglomeration of particles may occur upon aging of solutions which initially contained isolated particles. Figure 2d shows that the presence of Chitlac allows the stabilization of silver nanoparticles in solution up to several months, thus preventing colloidal instability. In view of this result, it can be safely stated that Chitlac acts as an efficient stabilizing ligand for silver ions and silver nanoparticles thanks to the presence of amino groups. Esumi[18] demonstrated that metal nanoparticles can be protected by the exterior amino groups of dendrimers which act as stabilizers. When $AgNO_3$ is mixed with Chitlac solutions, Ag^+ ions probably give rise to a localized binding to Chitlac macromolecules via amino groups chelation persisting also with the formed silver nanoparticles.

The hydrophilic side-chains also play a fundamental role in the stabilization by embedding the silver nanoparticles bound in the proximity of the polymer backbone and isolating them from the surrounding species (Figure 1e). In fact, it is known that chitosan, which shares with Chitlac the same backbone chemical structure, is able to stabilize silver nanoparticles according to the same mechanism proposed above. However, a comparison of the UV−vis spectra arising from the reduction of silver ions in the presence of Chitlac or chitosan points to a marked difference in behavior of the two polysaccharides under the same experimental conditions (Figure 2a). In fact, a broader, less intense and nonsymmetrical peak was detected for chitosan, suggesting the formation of more aggregated nanoparticles. The better performance of Chitlac must be traced back to the presence of the highly hydrophilic and bulky lactitol groups decorating the modified polysaccharide; they provide silver nanoparticles with coordination (amino groups) and protection (steric hindrance), thus preventing their aggregation.

In order to study the antimicrobial activity of Chitlac-nAg, killing kinetics assays were performed with *S. epidermidis*, *E.*

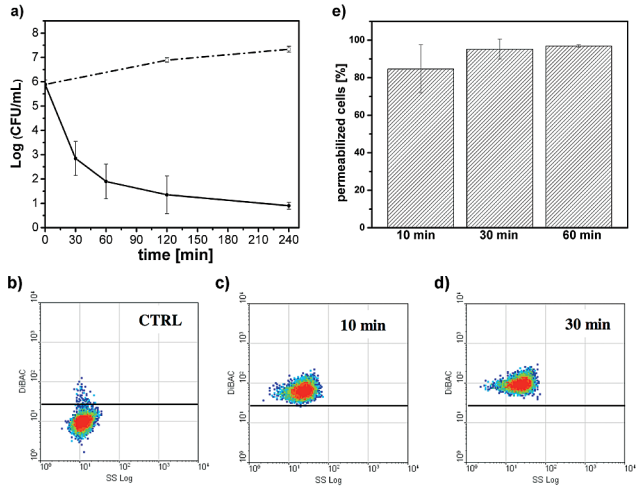

	Depolarized Cells [%]	MFI
Control 10 min	2.5±0.8	8.2±1.8
Chitlac-nAg 10 min	97.5±3.9	57.1±6.0
Control 30 min	8.8±5.0	11.0±3.8
Chitlac-nAg 30 min	99.6±0.4	81.7±13.3

Figure 3. (a) Killing kinetics of Chitlac-nAg (solid line) against *S. epidermidis*. The dashed line indicates control runs in the absence of Chitlac-nAg. Results are mean values (±SD) of at least four independent determinations; (b−d) Dual-parameter dot plot of the side scatter intensity versus DiBAC4(3) fluorescence relative to *S. epidermidis* after incubation with Chitlac-nAg; (b) CTRL = control at 10 min, (c) Chitlac-nAg treated sample after 10 min, (d) Chitlac-nAg treated sample after 30 min. The table reports the percentage of depolarized cells and the corresponding mean fluorescence intensity (MFI) values in nontreated and Chitlac-nAg treated samples; (e) effect of Chitlac-nAg on the membrane integrity of *S. epidermidis*. Bacteria were incubated for 10, 30, and 60 min with Chitlac-nAg in 20% MH broth. The percentage of PI-fluorescent cells after treatment is shown. Background values obtained with untreated samples (<5% of permeabilized cells) were subtracted to each nAg-treated sample. Results are the mean (±SD) of 3 independent experiments.

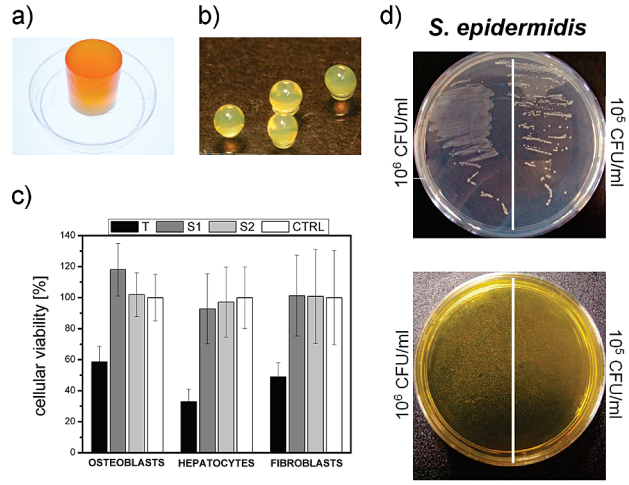

Figure 4. (a) Mixed alginate−Chitlac cylindrical hydrogel containing silver nanoparticles (AC-nAg gel). (b) AC-nAg microspheres. (c) Cytotoxicity analysis (MTT assay) on mouse fibroblast (NIH-3T3), human hepatocarcinoma (HepG2), and human osteosarcoma (MG63) cell lines of AC-nAg gel microspheres external solutions (S1 and S2, external solutions not diluted and 1:10 diluted, respectively; T, cytotoxicity positive control, cells treated with Triton 1%; CTRL, cytotoxicity negative control, cells treated with 0.015 M NaCl solution). (d) Growth of *S. epidermidis* on 20% Mueller−Hinton AC gel (upper Petri dish) and on 20% Mueller−Hinton AC-nAg gel (lower Petri dish).

coli, *S. aureus*, and *P. aeruginosa* to determine the amount of viable cells after treatment with Chitlac-nAg solutions. Bacteria were incubated with Chitlac-nAg for different times and then plated on Mueller−Hinton agar to allow counting of colony forming units (CFU). Overall, the Chitlac-nAg system showed a remarkable bactericidal effect against all four bacterial strains with a very fast killing kinetics: as representative data, Figure 3a reports the results for the *S. epidermidis* strain. The number of viable cells drastically decreased (a drop of 3 log units in CFU/mL) after only 30 min of incubation with the Chitlac-nAg system and, after 2 h of treatment, a complete inactivation of bacterial cells was found.

To study the mechanism by which the system Chitlac-nAg inactivates bacterial cells, the effect on membrane potential was evaluated by flow cytometry. Cell membrane depolarization was assessed by addition of DiBAC4(3), a fluorescent probe able to selectively enter and fluorescently label the cells whose membrane potential has collapsed, resulting in an increase of the mean fluorescence intensity (MFI). The fluorescence intensity of *S. epidermidis* was shifted toward higher channel numbers with respect to untreated cells after only 10 min of incubation with the system Chitlac-nAg, revealing a remarkable depolarization of the cell population (97.5 ± 3.9% of fluorescent cells vs 2.5 ± 0.8% of the control; Figure 3b−d).

The depolarization effect shown by the use of the DiBAC4(3) probe suggests that the system Chitlac-nAg interacts with the bacterial membranes. To evaluate the membrane damage caused by the system Chitlac-nAg, untreated and treated bacterial cells were labeled with the fluorescent probe propidium iodide (PI), which is excluded from cells with an intact plasma membrane and thus used as a marker of membrane integrity. A remarkable permeabilizing effect was observed after treatment of *S. epidermidis*; when the cells were incubated with Chitlac-nAg for 10 min, the percentage of PI-positive cells was of 80% versus <5% of the control. The membrane damage is even more evident after 30 and 60 min of treatment (>90% PI-positive cells; Figure 3e). Similar results of antibacterial activity were obtained with all the bacterial strains tested.

LDH tests carried out on the system Chitlac-nAg in solution pointed out a cytotoxic effect on mouse fibroblast (NIH-3T3), human hepatocarcinoma (HepG2), and human osteosarcoma (MG63) cell lines leading to cell death after 24 h (data not shown). This observation prompted us to focus our attention toward the preparation of Chitlac-based 3D structures entrapping the silver nanoparticles. If successful, such hydrogels could possibly be used in the preparation of bioactive biomaterials. To this end, the gel forming properties of alginate were exploited allowing the production of a highly hydrated system in a mixture with Chitlac-nAg. The rationale of this approach is that the 3D system could prevent nanoparticles from being available for eukaryotic cellular uptake but, at the same time, preserve its antimicrobial activity allowing the direct interaction of the nanoparticles with the proteins localized on the bacterial surface. In fact, in bacteria the thiol groups (-SH) of membrane proteins, exposed to the extracellular portion of the membrane, are the main molecular targets of the silver antibacterial activity.[25−29] At variance, eukaryotic cells do not have exterior thiol groups, thus silver ions or nanoparticles must first permeate through cell membranes to react with -SH groups of intracellular proteins and enzymes, such as inner membrane mitochondrial proteins and the enzymes of the antioxidant defense mechanism.[30−36] The use of alginate allows casting of different gel shapes (cylinders, slabs, microcapsules, etc.), which makes it possible to tailor-make different semisolid systems for various applications. The advantage of the presence of Chitlac over chitosan

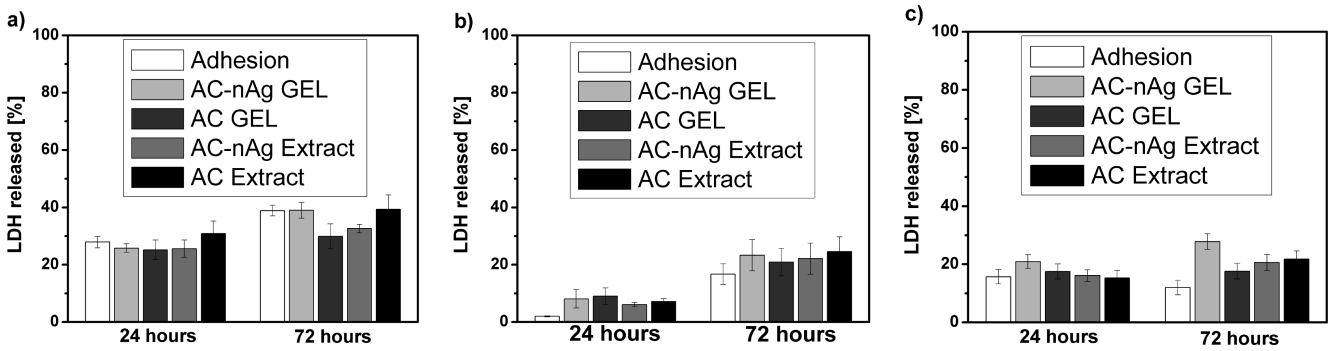

Figure 5. Effect of AC-nAg gels on LDH leakage from (a) mouse fibroblast (NIH-3T3), (b) human hepatocarcinoma (HepG2), and (c) human osteosarcoma (MG63) cell lines. The cytotoxicity test was performed both with the extract from gel material (AC-nAg extract) and with the gel material itself by direct contact with cell layer (AC-nAg GEL). Control cells cultured in adhesion in complete DMEM medium and cells treated with AC gels lacking silver nanoparticles (AC GEL and AC extract) were run in parallel to AC-nAg gels treated groups. The percentage of LDH release was calculated by dividing the amount of activity in the medium by the total activity (medium and cell lysate) after subtraction of the control. The data are expressed as mean ± SD of four independent experiments.

in the preparation of three-dimensional gels is connected with the ability of the former to allow complete miscibility between the two oppositely charged biopolymers, as already pointed out,[21] at variance with the latter polycation. This process can thus be efficiently exploited to entrap silver nanoparticles stabilized by polycations within a homogeneous gel construct avoiding coacervation. The final nanocomposite structure arising from the treatment of the binary mixture of alginate and Chitlac-nAg with calcium was a yellow-orange yet transparent hydrogel. (Figure 4a). It is important to underline that neither nanoparticles aggregation nor polymer phase separation was observed during and after gel formation. Homogeneous highly swollen microspheres (Ø = 500 μm) were obtained[37] (Figure 4b), which ensure a high surface/volume ratio. The amount of silver released by AC-nAg gel microspheres[0] was evaluated from two independent measurements. The microspheres were kept under vigorous stirring for 5 weeks in saline solution with a microspheres/solution volume-ratio of 4; the external solution was eventually analyzed by ICP-MS to evaluate the amount of silver released by the microspheres. The concentration of silver released was 58 μg/L, which corresponds to 2.6% of the total silver amount inside the microspheres, pointing out that a very low amount of silver had been released from the gel. The MTT tests showed that such low concentration of silver released from the microspheres was not cytotoxic for three different cell lines: fibroblasts (NIH-3T3), osteoblasts (MG63), and hepatocytes (HepG2; Figure 4c).

The possibility of obtaining three-dimensional highly hydrated structures results particularly appealing for tissue engineering applications in which an ideal candidate biomaterial must associate antibacterial properties with lack of cytotoxicity. To assess the extent of bacterial growth on semisolid system, two different concentrations of the four bacterial strains (10^6 and 10^5 CFU/mL, respectively) were smeared on the surface of nanocomposite AC-nAg gel. Both agar and alginate−Chitlac gels (AC gels) were used as controls. After overnight incubation, bacterial colonies were clearly visible on control plates, while they were completely absent on the silver nanoparticles-containing gels. Figure 4d shows the case of *S. epidermidis*; similar results were obtained with all the strains tested (data not reported).

We evaluated the cytotoxicity of the nanocomposite system also in the form of gel (AC-nAg). As reported in Figure 5, AC-nAg gels did not exert any cytotoxic effect on the cell lines used. In fact, there was no significant difference in the release of lactate dehydrogenase between the AC-nAg treated cells and control groups after 24 and 72 h.

The combination of these results shows that the AC-nAg hydrogels, besides providing for an efficient stabilization of the silver nanoparticles against aggregation, are able to display antibacterial activity without being harmful to mammalian cells. In the AC-nAg gels, nanoparticles coordinated to Chitlac are firmly grafted and immobilized in the gel matrix and therefore do not diffuse into the surrounding environment, as demonstrated by the ICP-MS analysis.

4. Conclusions

In this work we have successfully obtained new nanocomposite systems based on polysaccharides and silver nanoparticles. The role of the branched polysaccharide Chitlac is fundamental in the formation and stabilization of well-dispersed silver nanoparticles having a mean diameter of about 35 nm. Reproducibility of size distribution together with a demonstrated stability of the nanoparticles over time have been successfully achieved. Moreover, the use of a nondemanding chemical approach adds a considerable appeal to the results obtained. The simultaneous presence, in the final system, of a sugar-based bioactive polymer for cell stimulation[22] and of silver nanoparticles for antibacterial activity represents a major achievement of the present work. This novel approach arises at the crossover of nanotechnology and glycobiology. It might pave the way (i) to facilitate the use of silver nanoparticle-biopolymer composites in the preparation of bioactive biomaterials and (ii) to provide new tools to design engineered materials exploiting, to different purposes, the bioactivity provided by the carbohydrate component and the properties of silver at the nanoscale level.

Acknowledgment. The authors would like to acknowledge Prof. G. Adami for the ICP-MS measurements. This study was supported by grants from the Italian Ministry for University and Research (PRIN 2007), the Friuli Venezia Giulia Region (LR 26/2005, art. 23 for the R3A2 network), and the EU-FP6 Project "NEWBONE" (Contract Number 026279-2).

References and Notes

(1) Chastre, J. *Clin. Microbiol. Infect.* **2008**, *14* (Suppl 3), 3–14.
(2) Slama, T. G. *Crit. Care* **2008**, *12* (Suppl 4), S4.
(3) Goldmann, D. A.; Weinstein, R. A.; Wenzel, R. P.; Tablan, O. C.; Duma, R. J.; Gaynes, R. P.; Schlosser, J.; Martone, W. J. *JAMA, J. Am. Med. Assoc.* **1996**, *275* (3), 234–240.
(4) Chen, J. P. *J. Invasive Cardiol.* **2007**, *19* (9), 395–400.
(5) Balogh, L.; Swanson, D. R.; Tomalia, D. A.; Hagnauer, G. L.; McManus, A. T. *Nano Lett.* **2001**, *1* (1), 18–21.

(6) Fu, J.; Ji, J.; Fan, D.; Shen, J. *J. Biomed. Mater. Res., Part A* **2006**, *79* (3), 665–674.
(7) Huang, H.; Yuan, Q.; Yang, X. *Colloids Surf., B* **2004**, *39* (1−2), 31–37.
(8) Kuo, P. L.; Chen, W. F. *J. Phys. Chem. B* **2003**, *107* (41), 11267–11272.
(9) Sanpui, P.; Murugadoss, A.; Prasad, P. V. D.; Ghosh, S. S.; Chattopadhyay, A. *Int. J. Food Microbiol.* **2008**, *124* (2), 142–146.
(10) Geiser, M.; Rothen-Rutishauser, B.; Kapp, N.; Schurch, S.; Kreyling, W.; Schulz, H.; Semmler, M.; Im, H., V.; Heyder, J.; Gehr, P. *Environ. Health Perspect.* **2005**, *113* (11), 1555–1560.
(11) Chen, X.; Schluesener, H. J. *Toxicol. Lett.* **2008**, *176* (1), 1–12.
(12) Dai, J. H.; Bruening, M. L. *Nano Lett.* **2002**, *2* (5), 497–501.
(13) Grunlan, J. C.; Choi, J. K.; Lin, A. *Biomacromolecules* **2005**, *6* (2), 1149–1153.
(14) Henglein, A. *J. Phys. Chem.* **1993**, *97* (21), 5457–5471.
(15) dos Santos, D. S.; Goulet, P. J. G.; Pieczonka, N. P. W.; Oliveira, O. N.; Aroca, R. F. *Langmuir* **2004**, *20* (23), 10273–10277.
(16) Yi, Y.; Wang, Y.; Liu, H. *Carbohydr. Polym.* **2003**, *53* (4), 425–430.
(17) Yu, H.; Xu, X.; Chen, X.; Lu, T.; Zhang, P.; Jing, X. *J. Appl. Polym. Sci.* **2006**, *103*, 125−133.
(18) Esumi, K.; Suzuki, A.; Aihara, N.; Usui, K.; Torigoe, K. *Langmuir* **1998**, *14* (12), 3157–3159.
(19) Huang, H.; Yang, X. *Carbohydr. Res.* **2004**, *339* (15), 2627–2631.
(20) Donati, I.; Stredanska, S.; Silvestrini, G.; Vetere, A.; Marcon, P.; Marsich, E.; Mozetic, P.; Gamini, A.; Paoletti, S.; Vittur, F. *Biomaterials* **2005**, *26* (9), 987–998.
(21) Donati, I.; Haug, I. J.; Scarpa, T.; Borgogna, M.; Draget, K. I.; Skjåk-Bræk, G.; Paoletti, S. *Biomacromolecules* **2007**, *8* (3), 957–962.
(22) Marsich, E.; Borgogna, M.; Donati, I.; Mozetic, P.; Strand, B. L.; Salvador, S. G.; Vittur, F.; Paoletti, S. *J. Biomed. Mater. Res., Part A* **2007**, *84* (2), 364−376.
(23) Yalpani, M.; Hall, L. D. *Macromolecules* **1984**, *17* (3), 272–281.
(24) Panacek, A.; Kvitek, L.; Prucek, R.; Kolar, M.; Vecerova, R.; Pizurova, N.; Sharma, V. K.; Nevecna, T.; Zboril, R. *J. Phys. Chem. B* **2006**, *110* (33), 16248–16253.
(25) Clement, J. L.; Jarrett, P. S. *Met. Based Drugs* **1994**, *1* (5−6), 467–482.
(26) Feng, Q. L.; Wu, J.; Chen, G. Q.; Cui, F. Z.; Kim, T. N.; Kim, J. O. *J Biomed. Mater. Res.* **2000**, *52* (4), 662–668.
(27) Elechiguerra, J.; Burt, J.; Morones, J.; Camacho-Bragado, A.; Gao, X.; Lara, H.; Yacaman, M. *J. Nanobiotechnol.* **2005**, *3* (1), 6.
(28) Morones, J. R.; Elechiguerra, J. L.; Camacho, A.; Holt, K.; Kouri, J. B.; Ramirez, J. T.; Yacaman, M. J. *Nanotechnology* **2005**, *16* (10), 2346–2353.
(29) Nel, A. *Science* **2005**, *308* (5723), 804–806.
(30) Braydich-Stolle, L.; Hussain, S.; Schlager, J. J.; Hofmann, M. C. *Toxicol. Sci.* **2005**, *88* (2), 412–419.
(31) Hussain, S. M.; Hess, K. L.; Gearhart, J. M.; Geiss, K. T.; Schlager, J. J. *Toxicol. In Vitro* **2005**, *19* (7), 975–983.
(32) Hussain, S. M.; Javorina, A. K.; Schrand, A. M.; Duhart, H. M.; Ali, S. F.; Schlager, J. J. *Toxicol. Sci.* **2006**, *92* (2), 456–463.
(33) Kone, B. C.; Kaleta, M.; Gullans, S. R. *J. Membr. Biol.* **1988**, *102* (1), 11–19.
(34) Oberdorster, G.; Maynard, A.; Donaldson, K.; Castranova, V.; Fitzpatrick, J.; Ausman, K.; Carter, J.; Karn, B.; Kreyling, W.; Lai, D.; Olin, S.; Monteiro-Riviere, N.; Warheit, D.; Yang, H.; ILSI Research Foundation, A. r. f. t. *Part. Fibre Toxicol.* **2005**, *2* (1), 8.
(35) Donaldson, K.; Tran, C. L. *Inhalation Toxicol.* **2002**, *14* (1), 5–27.
(36) Donaldson, K.; Stone, V.; Tran, C. L.; Kreyling, W.; Borm, P. J. *Occup. Environ. Med.* **2004**, *61*, 727–728.
(37) Strand, B. L.; Gåserød, O.; Kulseng, B.; Espevik, T.; Skjåk-Bræk, G. *J. Microencapsulation* **2002**, *19* (5), 615–630.

BM900039X

Paper 3

Surface Modification and Polysaccharide Deposition on BisGMA/TEGDMA Thermoset

Andrea Travan,*,† Ivan Donati,† Eleonora Marsich,† Francesca Bellomo,† Satish Achanta,‡ Mila Toppazzini,† Sabrina Semeraro,† Tommaso Scarpa,† Vittorio Spreafico,§ and Sergio Paoletti†

Department of Life Sciences, University of Trieste, Via Licio Giorgieri 1, 34127 - Trieste, Italy, Falex Tribology, Wingepark 23B, Rotselaar, B3110 Belgium, and APE Research, Area Science Park, Basovizza, 34012 Trieste, Italy

Received October 6, 2009; Revised Manuscript Received February 4, 2010

Bisphenol A glycidylmethacrylate (BisGMA)/triethyleneglycol dimethacrylate (TEGDMA) thermosets and composites are well-known examples of biomaterials for dental applications that are receiving growing interest for orthopedic applications. While mechanical bulk properties are guaranteed by the presence of reinforcing fibers, in vitro and in vivo performances of these materials are ultimately driven by their ability to establish proper interactions between their surface and the surrounding tissues. Hence, the development of novel chemical processes enabling the introduction of bioactive molecules on the surface of these methacrylate-based thermosets is of particular interest. In the present work, we have devised a chemical strategy to expose carboxylic groups on the surface of the BisGMA/TEGDMA thermoset. The presence of negative charges was confirmed by Fourier transform infrared-attenuated total reflectance and by UV−vis spectrophotometry. Bulk mechanical properties and surface morphology of the thermoset were only slightly affected upon chemical functionalization. The activated material was further refined by the deposition of a lactose-modified chitosan (chitlac) driven by strong electrostatic interactions. The presence of the bioactive polysaccharide was confirmed by fluorescence spectroscopy and by confocal laser scanning microscopy measurements. Scratch tests were performed to evaluate the mechanical behavior of the coating. Finally, in vitro tests revealed that the presence of chitlac led to a slight enhancement of cell proliferation with respect to the unmodified BisGMA/TEGDMA thermoset. This effect was more pronounced when chitlac decorated with an arginine-glycine-aspartic acid (RGD) peptide was used in the preparation of the coating. In the latter case, the in vitro performance of the coated BisGMA/TEGDMA thermoset became comparable with that of clinically used roughened titanium.

1. Introduction

The reconstruction of large bone defects represents an extraordinary challenge for biomaterial design and manufacturing as it requires a balanced combination of biochemical, biophysical, and material science concepts. In particular, an ideal biomaterial should be able to merge an advanced technological approach (like design of the implant by aid of computer tomography and rapid prototyping) with an appropriate biochemical focus on its interaction with the surrounding tissues.

Metallic implants, such as titanium compression plates and femoral nails, have been largely used for fixing different bone fractures. Apart from the numerous advantages, such materials do present limitations with respect to formability and compatibility with advanced imaging techniques (e.g., MRI).[1,2] In addition, the mismatch in mechanical properties between the metallic implant and the surrounding tissue causes the so-called "stress shielding" effect leading ultimately to periprosthetic bone loss.[3]

Thermosets based on the light-induced reticulation of BisGMA and TEGDMA have found a large use in the biomedical field, in particular, in dentistry. BisGMA-based biomaterials were originally developed for dental composites more than 25 years ago and are nowadays used in most of the commercial products.[4] These thermoset materials are prone to be reinforced with fibers, for example, glass fibers (FRC, fibers reinforced composite), rendering them particularly interesting for load-bearing conditions such as in dental[5,6] and orthopedic applications.[7–10]

Apart from the considerations on the bulk properties of the materials (mostly due to the fiber component), it is important to stress the fundamental role played by the material surface in triggering the interaction with the surrounding tissues.[11] Processes like protein adsorption and cell adhesion, which are fundamental steps in the biological integration of the implant, are promoted or prevented depending on electric charge, hydrophilicity/hydrophobicity, and the presence of specific signals on the surface of the material. As an example, BisGMA composite materials coated with bioactive glass have been proposed in the reconstruction of critical size calvarial bone defects[12] and in frontal bone defect repair.[13] In both cases, the bioactive FRC-implant promoted the healing of critical size bone defects and it has shown the potential to become a feasible alternative to bone grafts.

Among the different biomolecules used to decorate the surface of biomaterials, polysaccharides possess unique properties. They compose the natural highly hydrated structure embedding cells, known as "extracellular matrix" (ECM). Polysaccharides provide for the biomechanical performances of the ECM, enabling both biological recognition and proper viscoelastic responses to stresses. These biomolecules have raised notable interest in the

* To whom correspondence should be addressed. Tel.: +39 040 558 3681. Fax: +39 040 558 3692. E-mail: atravan@units.it; andrea.travan@iol.it.
† University of Trieste.
‡ Falex Tribology.
§ APE Research.

10.1021/bm9011419

field of biomaterials as their physical−chemical characteristics, as well as the chemical composition, influence their interaction with biological systems.

Several reports have focused on the ability of positively charged polyelectrolytes to stimulate cell adhesion. Chitosan is a polycation derived from the deacetylation of chitin, and its cationic nature increases upon decreasing the residual degree of acetylation. Different authors have argued for a direct correlation between the presence of amino groups on the polymer chain and the proliferation of keratinocytes, fibroblasts,[14] gliosarcoma cells,[15] and primary chicken dorsal root ganglion neurons.[16] Finally, multilayer coatings based on a combination of chitosan and hyaluronate or chondroitin sulfate have shown to boost cell proliferation, providing, at the same time, for their protection.[17] A lactose-modified chitosan (chitlac) has been recently reported[18,19] to have biological properties toward articular chondrocytes, stimulating cell growth and chondro-specific glycosaminoglycans and collagen production in tissue-engineered biomaterials.

Aside from the use of natural polysaccharides, another common strategy for improving cell/biomaterial interactions resides in the functionalization of the material surface with biomimetic peptides such as arginine-glycine-aspartic acid (RGD) and laminin adhesion peptides.

RGD is the well-known integrin recognition site embedded within many cell attachment proteins, including fibronectin, vibronectin, and fibrinogen.[20–25] Numerous studies have shown that the RGD peptide promotes increased binding of cells (including mesenchymal stem cells) to many types of biomaterials and that this activity is modulated by the pattern distribution of the signal.[26,27] RGD containing peptides are often covalently coupled to bioactive polysaccharides. Hyaluronan, dextran, chitosan, and alginate have largely been used as backbone structures to be decorated with this peptide.[28–34] As an example, chitosan-based scaffolds modified with RGD showed an increase in ROS cell attachment onto the substrate with respect to the unmodified material.[31] In addition, polyelectrolyte complexes, obtained from the combination of oppositely charged polysaccharides containing the RGD motif, promoted the attachment of immortalized rat chondrocytes as well as primary cultures and displayed an enhanced healing rate of rabbit joint cartilage defect.[28] In particular, alginate represents a very interesting example of modulation of biological properties upon addition of cell signals. In fact, this otherwise nonbioadhesive polysaccharide resulted to regulate myoblast proliferation and differentiation once the RGD motif was inserted in its backbone.[35]

The present work reports a novel strategy for the coating of a BisGMA/TEGDMA thermoset material based on a chemical modification that exposes carboxylic groups on its surface. The formation of a polysaccharide layer on the thermoset was then accomplished by means of a polycation, that is, chitlac. Due to this feature, electrostatic interactions will take place between the negatively charged surface of the treated BisGMA/TEGDMA thermoset and the cationic polysaccharide. The large number of positive charges on chitlac (due to its large molar mass) and the almost unlimited size (on a molecular scale) of the negative methacrylate surface ensure highly cooperative interactions with a very high energy stabilization. The ensuing polyelectrolyte complex (PEC) can be visualized as an ionomer. This is the rationale behind the hypothesis of the formation of a strongly adherent bioactive polymer coating. Moreover, the production of repelling anionic groups over several surface layers very likely produces an overall loosening of the thermoset surface compactness allowing for some polycation penetration, adding the contribution of entanglement to the attractive interactions of the PECs.

2. Materials and Methods

Chitlac (lactose-modified chitosan, CAS registry number 85941−43−1) was prepared according to the procedure reported elsewhere[18] starting from a highly deacetylated chitosan (residual acetylation degree approximately 11%). The (viscosity average) relative molar mass of chitosan was estimated to be approximately 7×10^5. The composition of chitlac was determined by means of ^{1}H NMR and resulted to be glucosamine residue = 24%; *N*-acetylglucosamine = 11%; and 2-(lactit-1-yl)-glucosamine = 65%. The relative molar mass of chitlac was estimated to be approximately 1.5×10^6. Bisphenol A glycidylmethacrylate (Bis-GMA), triethyleneglycol dimethacrylate (TEGDMA), 2-[*N*-morpholino]ethanesulfonic acid (MES), 1-ethyl-3-[3-(dimethylamino)propyl] carbodiimide (EDC), *N*-hydroxy-succinimide (NHS), 7-amino-1,3-naphtalene disulfonic acid (7-ANA), and fluorescein isothiocianate (FITC) were purchased from Aldrich. Camphorquinone (CQ) and 2-dimethylamino ethylmethacrylate (DMAEMA) were purchased from Fluka. E-glass fibres were from Ahlström (Karhula, Finland). Alamar blue was purchased from Biosource™ (Invitrogen). Titanium disks (Ti6Al4V) with roughened surface (R_a = 3 μm) were kindly provided by Medacta Int. (Lugano, Switzerland).

2.1. Preparation of the BisGMA/TEGDMA Thermosets (TS and fTS). BisGMA (70% w/w) and TEGDMA (30% w/w) were mixed under vigorous stirring at 37 °C. CQ (0.7% w/w) and DMAEMA (0.7% w/w) were added and the solution was protected from light and degassed for 12 h in vacuum oven at 40 °C. The solution was poured in Teflon mold (∅ =14 mm, h = 2.5 mm) and the wells were covered with a PET film. The polymerization was light initiated with a hand cure light device (Optilux 501, λ: 400−505 nm, light power: 850 mW/cm^2) for 20 s. The postcuring was performed with a Photopol IR/UV Plus oven (Dentalfarm, Italy) equipped with eight lamps and two spots operating in the wavelength range 320−550 nm following the procedure: 20 min in light oven (eight lamps), 20 min in light oven (eight lamps) on a rotating plate, 60 min in light oven (eight lamps) under vacuum, and 7 min in light oven (eight lamps plus two spots). The thermosets were then sandpaper polished (granulometry: 1200). This sample is indicated as TS in Table 1 (Supporting Information). For ultraflat samples (fTS, Table 1, Supporting Information), quartz molds (∅ = 14 mm, h = 2.5 mm) were employed without final polishing. In the case of fiber containing composites (BarTS), thermoset bars (20 mm length × 2 mm width × 2 mm thickness) were reinforced by adding 50% (w/w) of longitudinally oriented E-glass fibers in the mold.

2.2. Synthesis of Glycine-Arginine-Glycine-Aspartic Acid-Serine (GRGDS) Peptide. Solid phase peptide synthesis was performed by using Fmoc-chemistry on Liberty Microwave Peptide Synthesizer (CEM Corporation, Matthews, NC) with a computer-assisted operation system at a 0.12 mmol scale (500 mg of PEG-PS resin, 0.24 meq/g). Couplings were carried out with HCTU as an activator. GRGDS peptide was cleaved from the thermoset and deprotected using a mixture consisting of trifluoroacetic acid, water, and triisopropylsilane (95:2.5:2.5, by volume). The crude peptide was precipitated by the addition of *tert*-butylmethyl ether, washed several times with the same ether and its mass was confirmed by ESI-MS spectrometer Bruker Esquire 4000 (Bruker Daltonics, Billerica, MA). No further purification of the peptide was necessary.

2.3. GRGDS Functionalized Chitlac (RGD Chitlac). Chitlac (0.26 mmol; expressed as average repeating unit) was dissolved in 20 mL of 25 mM MES buffer (pH 6.5). The peptide GRGDS (0.14 mmol) was dissolved in 1 mL of buffer and activated with 0.35 mmol of EDC and 0.07 mmol of NHS. The solution containing chitlac was then added and the mixture was stirred overnight at room temperature. The polymer was dialyzed (cutoff molecular weight of the membrane: approximately 10000) against deionized water until the conductivity was below 2 μS

at 4 °C. The polymer was filtered through 0.45 μm Millipore filters and freeze-dried.

To determine the degree of substitution, 2 mg of functionalized polymer were dissolved in 2 mL of 6 M HCl and stirred at 110 °C for 20 h under reflux. After evaporation of the hydrochloric acid, the residue was redissolved in 500 μL of capillary electrophoresis running buffer (100 mM borate buffer pH 8.95). The obtained solution was then filtered and the degree of substitution was evaluated by the quantification of Arginine derived from the peptide degradation. Quantitative analysis was performed by capillary electrophoresis (CE-UV conditions: buffer borate 100 mM, pH 8.95; 15 kV; fused silica capillary total length 64 cm, effective length 56 cm, internal diameter 50 μm; wavelength 195 nm). The degree of polymer functionalization was equal to 0.45% with respect to the average repeating unit, corresponding to 2% of primary amines.

2.4. Hydrolysis of the Methacrylate Esters on the Surface of the BisGMA/TEGDMA Thermosets. TS, fTS, and BarTS (Table 1, Supporting Information) were treated with 12 M HCl at 80 °C for different times. Eventually, a treatment for 7 h was selected for all the specimens used in the present work. The thermosets were removed and rinsed with deionized water (2 × 50 mL), NaOH (0.1 M, 50 mL), and water again (50 mL). The thermosets were finally air-dried overnight. The sample thus obtained is indicated as HCl-TS, HCl-fTS, and HCl-BarTS in Table 1 (Supporting Information).

2.5. ATR-FTIR Analysis of Acid-Treated Thermosets. FT-IR was performed on TS and HCl-TS (Table 1, Supporting Information) with a Bruker HYPERION 3000 instrument equipped with a Mercury−Cadmium-Telluride detector MCT D316 working in ATR mode.

2.6. Indirect Quantification of the Carboxylic Groups Density on the Surface of the BisGMA/TEGDMA Thermosets. HCl-TS was immersed in MES buffer (1 mL, pH 5.5) containing 7-ANA (2×10^{-4} M). EDC (20 mg) and NHS (10 mg) were added and the reaction mixture was gently stirred for 24 h prior to the analysis. The residual concentration of 7-ANA in the supernatant was evaluated at 350 nm by means of UV−vis spectroscopy (Cary 4E) through a calibration curve.

2.7. Coating of the Thermoset Surface with a Positively Charged Polysaccharide (Chitlac or RGD chitlac). HCl-TS was immersed in 1 mL of polycation (chitlac or RGD chitlac) dissolved in water (2 mg/mL or 4 mg/mL), and the system was gently stirred for 24 h. The thermosets were rinsed extensively with water and air-dried. The samples obtained have been indicated as chitlac-TS and RGD chitlac-TS (Table 1, Supporting Information) when chitlac and RGD-chitlac were used for the coating, respectively. For confocal laser scanning microscopy (CLSM) experiments and for fluorimetric determinations, a fluorescein-labeled chitlac, prepared as previously reported, was used.[18,36] In the case of HCl-fTS, 4 mL of chitlac solution (4 mg/mL) were used.

2.8. Atomic Force Microscopy. Surface morphology studies were conducted on TS and chitlac-TS samples by means of an atomic force microscope (AFM) using a Perception (Assing, Rome, IT) instrument in contact mode. Silicon cantilevers with a nominal resonance frequency of 100 kHz, force constant of 5 N/m, and tip radius of <10 nm (Veeco, Santa Barbara, CA) were used. For the tip, proportional (pGain) and integral (iGain) feedback parameters were optimized. The feedback parameters were adjusted to provide maximum possible feedback performance while avoiding ringing due to feedback instability. Image processing of the 10 × 10 μm area was done using the software Gwyddion (Czech Metrology Institute, Brno, Czech Republic). A second-order polynomial plane correction was carried out to reduce waviness due to scanner bow and variations of the film thickness, and a line-wise leveling was performed to reduce a possible line-by-line repetition error. AFM analyses were performed also on fTS and chitlac-fTS thermosets prepared according to the procedure reported in section 2.1. Images were taken in noncontact mode with an A100 APE Research AFM. XY scanner mounted a closed loop scanner with capacitive sensors that ensure subnanometric resolution, with a 1 × 1 μm scan range. Mikromasch NSC15 probes (tip radius < 10 nm) were employed and the same tip was for both images. Tip oscillation amplitude was used in the range of a few tens of nanometers. RMS values obtained by Gwyddion software are calculated on original data without any tip deconvolution.

2.9. Spectrofluorimetry. The fluorescence of fluorescein-labeled chitlac was measured with a Perkin-Elmer LS50B spectrofluorimeter ($T = 25$ °C). A calibration curve was performed prior to quantitative analyses ($R^2 = 0.98$). A 498 nm excitation wavelength was used and the emission spectrum was recorded in the range 460−600 nm. Both the excitation and the emission bandwidths were set to 4.5 nm.

2.10. Confocal Laser Scanning Microscopy (CLSM). Fluorescein-labeled chitlac was used for the visualization of the coating on the thermoset samples by means of CLSM. The wet specimen was placed on a coverslip and mounted on the stage of an inverted microscope LEICA TCS SP2 associated with a confocal argon-ion laser scanning microscope. Confocal data have been processed by means of Image Pro Plus 6.2 software extended with the 3D Constructor package. Laser excitation light was provided at 488 nm and fluorescent emissions were collected in the wavelength range between 510 and 580 nm. For image acquisition, an exposure time of 0.8 s was adopted with a binning of 2 × 2 on the charge-coupled device camera, yielding a pixel size of 1.46 μm. The lens magnification was 10×.

2.11. Scratch Test on Chitlac-Coated Thermosets. The scratch tests were performed in a ball-on-flat contact configuration using a microrange surface tester (MUST Falex Tribology NV, Belgium).[37] The measuring element of this device is a 25 by 50 mm cantilever with a given tangential (k_t) and normal stiffness (k_n).

In this study, a 2 mm Ø ruby ball was used as the scratch probe. A compressive normal load of 25−100 mN was applied during the test. The scratch speed was kept constant at 0.5 mm/s, while the scratch length was 1 mm. All the tests were carried out in ambient air at 20 ± 2 °C and 45 ± 3% Relative Humidity. For the scratch tests a sensitive steel cantilever with normal stiffness of 800 N/m and tangential stiffness of 1400 N/m was used. During scratch tests, friction force between the ball and the surface is measured as a function of time. From this data, the coefficient of friction is determined by dividing the same with the applied normal load. Two square samples were tested and compared, namely, sTS (square thermoset) and chitlac-sTS (Table 1, Supporting Information). A surface microtester, equipped with a cantilever, was used. The deflections of this cantilever are detected with a set of optical sensors (FOS) placed in the normal and the tangential direction of the cantilever, which transmits and receive light. On deflection of the cantilever, either in the tangential or normal direction, the intensities of the received light change, leading to subsequent changes in the voltage. These differential voltages are converted to forces using the prerecorded sensor calibration files in the instrument. Before testing, the counterbody is glued at one end of this cantilever and the coated sample is placed on a moveable table. During a scratch test, the cantilever is loaded on the sample and by measuring the cantilever deflection, dz, the magnitude of the applied normal force is controlled. After reaching the destination load, the sample containing table moves causing some tangential deflection on the cantilever due to friction. By recording the deflections in tangential direction, the friction force or shear force between the material couple is calculated.

2.12. Three Points Bending Tests. Mechanical tests were performed on fiber reinforced bars (BarTS) and HCl-BarTS samples by means of a universal mechanical testing machine (Galdabini Sun 500, Galdabini, Varese, Italy). Three points bending tests were performed according to the ISO10477 standard. The probe speed was maintained constant to 5 mm/min. The force−deformation profile was recorded and the flexural modulus (E_f) and strength (σ_f) were calculated. For each measurement, results from 10 samples were averaged.

2.13. Biological Tests on Chitlac and RGD Chitlac-Coated Thermosets. TS, chitlac-TS, HCl-TS, and RGD chitlac-TS (Table 1, Supporting Information) were prepared and sterilized by exposure to a UV lamp for 1 h. Approximately 20000 cells (Osteosarcoma MG-63,

ATCC number: CRL-1427) suspended in 50 μL of culture medium (Dulbecco's modified Eagle's medium added of inactivated fetal bovine serum (10%), penicillin (100 units/mL), streptomycin (100 μg/mL), and L-glutamine (2 mM)) were added in the center of the materials and incubated for 4 h at 37 °C and 5% pCO_2. A total of 0.85 mL of culture medium was added and the thermoset samples were further incubated for 18 h under the same conditions. 0.1 mL of Alamar blue solution was then added and the cells were incubated for an additional 6 h. Media was removed from each sample and its fluorescence was measured at the excitation wavelength of 530 nm and at the emission wavelength of 590 nm. The thermoset samples were washed with PBS (2×1 mL), 0.9 mL of fresh culture medium was added, and the incubation was protracted for 16 h before the alamar blue assay was repeated. Alamar blue test was performed for four consecutive days. Six replicates were used for each coating, two cell-free coated thermosets were used as blanks, and the average signal was subtracted to the signal of the samples.

2.14. Scanning Electron Microscopy Analysis. The samples were analyzed using a scanning electron microscope (XL 30 ESEM FEG) after sputter-coating with gold.

3. Results and Discussion

3.1. Chemical Modification on the Surface of BisGMA/TEGDMA Thermoset Samples. To expose carboxylate moieties on the surface of the samples, BisGMA/TEGDMA thermosets were treated with HCl (12 M) at 80 °C (HCl-TS), followed by neutralization (Table 1, Supporting Information). An indirect quantitative evaluation of the carboxylate moieties formed on the surface was obtained by reacting the treated thermosets with 7-ANA and measuring the residual dye in the supernatant. Figure 1a reports the UV−vis spectrum of the solution containing 7-ANA after the exposure to the acid-treated thermoset samples in the presence of the coupling reagents EDC/NHS. For comparison, the UV−vis spectrum of the amino containing dye was recorded in the presence of untreated sample. The reduction of the amount of dye in solution observed in the former case stems from its anchoring to the acid-treated thermosets via an amide linkage. This allowed the quantitative determination of the carboxylic groups exposed which resulted to depend on the time exposure to the acid solution (Figure 1b). In particular, after 7 h the concentration of carboxylate moieties was found to be $\sim 5.5 \times 10^{-2}$ μmol/cm^2. This number corresponds to about 300 COO^- groups/nm^2, which can be explained invoking the penetration of the hydrolyzing H^+ ions down to several molecular layers of the thermoset surface. In view of these results, 7 h of exposure to hydrochloric acid were considered sufficient for introducing enough carboxylate moieties without compromising the integrity of the material. It should be mentioned that longer treatments, namely, 12 h, caused the formation of small milky-white droplets in the bulk of the thermoset.

A direct evidence of the presence of carboxylic groups on the surface of the sample was obtained from the comparison of the first derivative of the ATR-FTIR spectrum of the HCl-TS and of the TS samples (Supporting Information). A newly formed peak at ~ 1620 cm^{-1} was detected in the case of HCl-TS, which can be safely attributed to the stretching mode of the carboxylate anion on the surface of the thermoset.

These results show that the treatment with hydrochloric acid is an efficient and simple approach for the chemical functionalization of these thermoset materials.

The harshness of the acid treatment used might cast doubt about its suitability for biomaterials design. If fact, the hydrolytic effect of the acid exerted on the surface might ultimately result in a loss of mechanical properties for the whole specimen hampering its potential applications in the orthopedic field. In the latter, the mechanical properties of the implant should meet those of the bone tissue. For this reason, it was decided to focus on fiber reinforced composites, as the sole thermoset does not perform adequately well from the mechanical point of view.

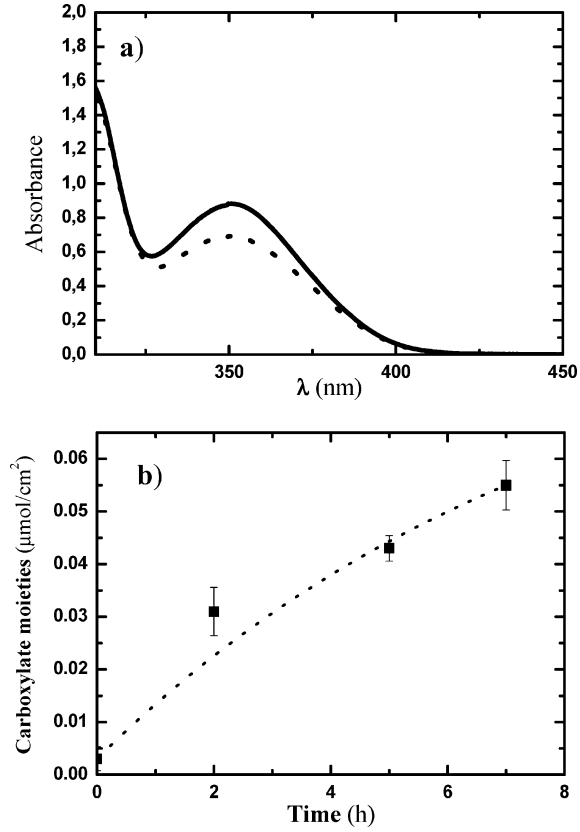

Figure 1. (a) UV−vis spectrum of a 7-ANA solution upon exposure to TS (straight line) and HCl-TS (12 M HCl, 80 °C, 7 h; dotted line) samples. (b) Dependence of the amount of carboxylic moieties in the thermoset samples on the time exposure to HCl (12 M, 80 °C). Values are reported as mean ± sd ($n = 3$). Line is drawn to guide the eye. See Table 1 (Supporting Information) for legend.

To evaluate the bulk mechanical properties of the BarTS and HCl-BarTS (Table 1, Supporting Information), three-points bending tests were performed according to the ISO 10447 standard. The flexural modulus (E_f) of the BarTS and of the HCl-BarTS samples were 31.2 ± 1.2 and 25.9 ± 1.6 GPa, respectively (relative decrease 17%). Similarly, the flexural strength (σ_f) was 790 ± 29 MPa for the untreated sample (BarsTS) and 650 ± 82 MPa for the acid-treated sample (HCl-BarTS; relative decrease 18%). These results show that the treatment with hydrochloric acid only slightly affects both the flexural modulus (E_f) and the flexural strength (σ_f).

The effect of acid treatment on the morphology of the surface of the TS and HCl-TS samples was preliminary assessed by means of scanning electron microscopy (SEM). Figure 2 shows that no considerable topography modification was noticed upon acid treatment allowing to conclude that the treatment so far described does not significantly affect the BisGMA/TEGDMA thermoset.

3.2. Coating with Bioactive Polysaccharides. The second step considered in the present work was the coating of the modified thermosets with a bioactive polysaccharide. To this end, chitlac was selected both for its biological activity and for the presence of positively charged amino groups.[18,19,38,39] To

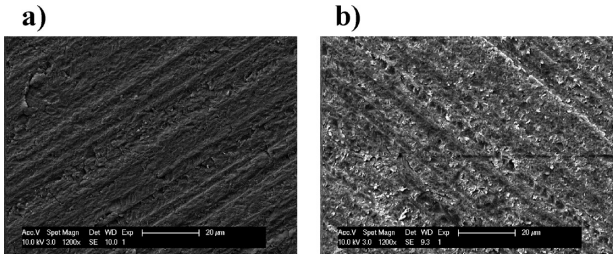

Figure 2. Scanning electron microscopy of TS (a) and HCl-TS (b) samples. Magnification = 1200×. See Table 1 (Supporting Information) for legend.

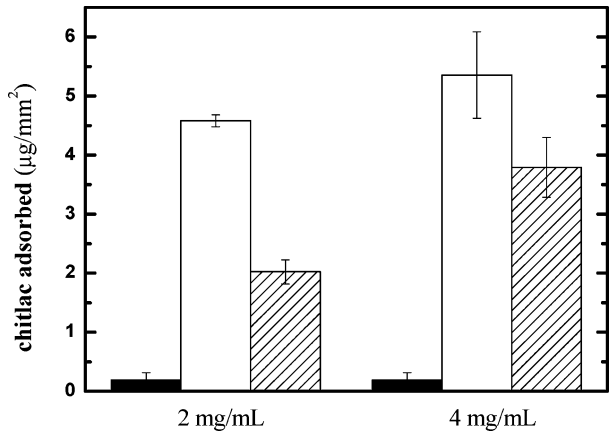

Figure 3. Amount of chitlac adsorbed on HCl-TS sample upon exposure to a solution of polysaccharide at a concentration of 2 or 4 mg/mL, respectively. Open and striped bars correspond to dried and wet HCl-TS, respectively. The control is represented by TS sample (full bars). Values are reported as mean ± s.d. ($n = 3$). See Table 1 (Supporting Information) for legend.

evaluate quantitatively the amount of chitlac deposited on the surface of the thermosets, a fluorescent tag, namely, fluorescein isothiocyanate, was chemically linked to the polycation. The very low degree of tag grafting (maximum 1 amino group is modified over 2000 available) did not modify the overall properties of chitlac (solubility, hydrophobic character, charge), allowing, at the same time, the monitoring of the deposition of the polymer on the acid-treated thermosets. Dried or wet HCl-TS samples were put into contact with a solution containing the fluorescein-labeled polycation at different concentrations, namely, 2 and 4 g/L. The decrease of the fluorescent signal in the supernatant, quantified by means of spectrofluorimetry, was assessed after 24 h (Figure 3). The coated samples obtained were indicated as chitlac-TS (Table 1, Supporting Information). In all cases, the wet HCl-TS samples showed a lower chitlac adsorption when compared to the dried ones. In particular, when a 2 mg/mL chitlac solution was used for the coating of the dry HCl-TS, a surface concentration of the polysaccharide of approximately 4.5 μg/mm^2 was reached. At variance, a 2 μg/mm^2 surface concentration of chitlac was noted when wet HCl-TS sample was used. The use of a 4 mg/mL concentration led to an increase of adsorbed bioactive polysaccharide with respect to the 2 mg/mL solution. In fact, in this latter case a surface concentration of 5.25 and 3.75 μg/mm^2 was obtained for the chitlac-TS when starting from dried and wet HCl-TS, respectively. It should be noted that TS samples (nonfunctionalized thermosets) adsorbed only a very low amount of chitlac (~0.2 μg/mm^2) compared to the functionalized ones. The stability of the coating of the chitlac-TS sample (Table 1, Supporting Information) was assessed upon treatment with a solution of sodium chloride (0.5 M) to shield electrostatic interactions. No release of the fluorescent polysaccharide was detected in the supernatant after 24 h (data not shown). At variance, the TS sample (i.e., nonfunctionalized thermoset) released even the low amount of chitlac deposited as proof of a weak interaction with the surface.

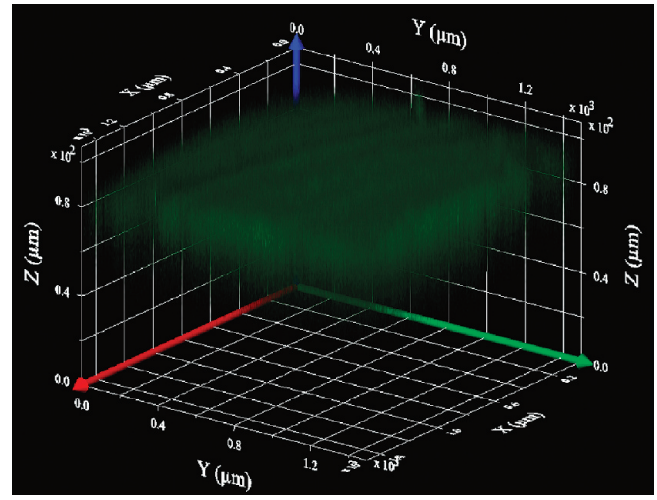

Figure 4. Chitlac-TS (Table 1, Supporting Information) prepared with fluorescein-labeled chitlac: 3D reconstruction of the coating layer covering the underlying thermoset. Magnification lens: 10×.

The use of fluoresceine-labeled polysaccharide in the chitlac-TS sample allowed the visualization of the coating on the surface of the sample by means of confocal laser scanning microscopy (CLSM). This technique has been used by different researchers to quantitatively determine the thickness of biofilms[40,41] and polymers coatings.[42,43] The coating was laser-scanned throughout its entire height and its three-dimensional reconstruction, reported in Figure 4, allowed estimating a layer of thickness 80−100 μm, resulting in a hydrated polysaccharide "cushion".

The morphology of the surface of the uncoated and coated thermosets was assessed by means of atomic force microscopy (AFM; Figure 5): in the case of the TS sample, polishing causes deep scratches to appear on the surface (Figure 5a), which are partially filled once the thermoset is coated with the cationic polysaccharide (Figure 5b). In fact, the morphological parameters, obtained from AFM analysis, reveal that the chitlac-TS sample displays, with respect to the TS sample, a lower maximum peak height (h_{max}) as well as a lower average roughness (R_a); similarly, the surface area excess (Sdr) parameter shows that the overall surface area is reduced upon coating of the TS samples with chitlac (Table 2, Supporting Information).

An insight at the nanometer scale on the morphology of the polysaccharide on the surface of the BisGMA/TEGDMA thermosets was obtained by means of AFM measurements on ultraflat disks (fTS and chitlac-fTS). They both are completely devoid of scratches introduced by the polishing which might give rise to artifacts in the interpretation of the result; they can thus be used to highlight the specific morphological features of the polysaccharide coating. At the nanometer scale, the AFM image of the fTS sample displays round-shaped thermoset particles (<10 nm) homogeneously arranged on the surface of the material and a root-mean square roughness (R_{rms}) of 1.2 nm (Figure 5c, Table 2, Supporting Information). At variance, in the case of chitlac-fTS (Figure 5d, Table 2, Supporting Information), R_{rms} increased to 3.6 nm and the surface is characterized by grainy particles with a diameter of about 20 nm, which is attributed to the coiled polysaccharide chain after air drying and represents the roughness of the outer layer of

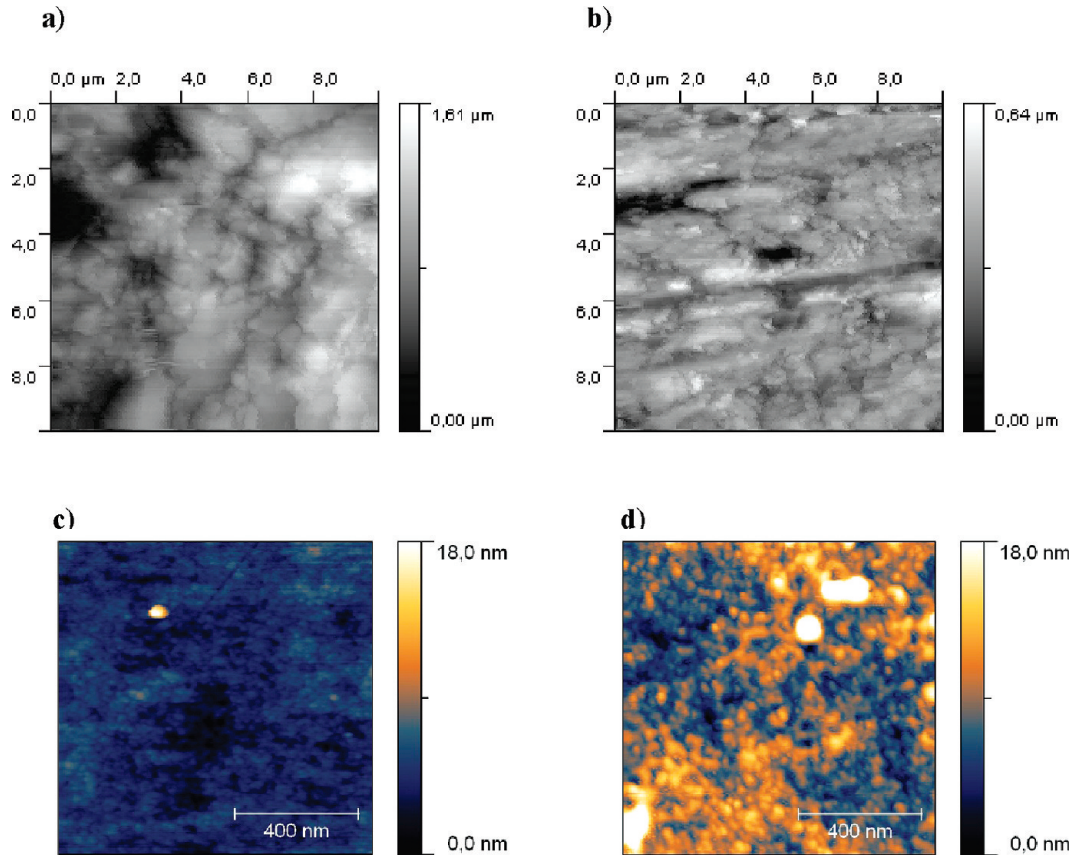

Figure 5. Atomic force Microscopy of TS (a), chitlac-TS (b), fTS (c), and chitlac-fTS (d) samples. Scanned area of 10 × 10 μm for (a) and (b) and of 1 × 1 μm for (c) and (d). See Table 1 (Supporting Information) for legend.

the polysaccharide cushion. This is the typical morphology found when using biopolymers in the layer-by-layer (LbL) technique[44] and, in particular, a grainy morphology has been reported for chitosan on gold surfaces[45] and in a LbL structure with hyaluronan.[46]

Scratch tests were performed on thermosets coated with chitlac (chitlac-sTS sample, Table 1, Supporting Information), using the acid-treated thermoset samples as control (HCl-sTS). The scratch tests are commonly used in determining mechanical integrity of coatings based on both organic and inorganic formulations.[47,48] This technique is widely used for quantifying various properties of coatings and thin films, such as critical load bearing, adhesion strength, coating durability, and failure mechanisms,[49] although the performance of the coating in physiological conditions cannot be directly inferred from these measurements. In this study of gel-like chitlac coatings, low load sensitive scratch tests would help detect the overall response of this coating under combined compression and shear forces. A schematic illustration of the setup and of the test is reported in Figure 6.

A plot of coefficient of friction against the sliding distance for the two tested materials is shown in Figure 7a,b. The four curves are the results of scratch tests at different normal loads measured on different locations of the sample. The coefficient of friction recorded on HCl-fTS sample seems to vary with the sliding distance. This variation could be due to the surface roughness or waviness of the surface. In general, the coefficient of friction seems to drop with the increasing compressive force or contact pressure.

The coefficient of friction recorded on the chitlac-sTS sample exhibited a chaotic stick−slip behavior. The stick−slip is commonly observed when the static friction between the contacts is high and when surface slides at low speeds.[50] This event is analogous to pushing a mass with a weak spring, which has to be first loaded until the block overcomes the friction force and then relaxes as the mass stops and the sequence repeats. This stick−slip phenomenon exists even at atomic scale as explained using the so-called Tomlinson model.[51] In the present case, the coefficient of friction is not high and it is believed that the origin of stick−slip is due to the structure of the polysaccharide coating which might resemble a gel on this observation scale. During sliding, the ball may plow the network structure of the gel, and once excess material is formed on the sliding front, the ball stops. As the specimen continues to move, the cantilever spring loads until sufficient energy is gathered and finally moves again creating a drop in friction (slip). This action repeats causing this chaotic stick−slip pattern in the signal.

The same stick−slip behavior was noticed in multiple pass scratch test performed at contact load of 75 mN. In all, 20 repeated scratches were performed on the same location. For clarity, four scratch curves recorded at regular intervals are shown in Figure 7c,d. The magnitude of stick−slip (noise level) in this measurement seems lower than Figure 7b, which could be attributed to possible irregularities of the chitlac coating.

An interesting feature was noticed in the evolution of the normal load during the multipass scratch test (Figure 8). On the HCl-sTS sample, the normal load during 20 scratches is shown by the jigsaw pattern. Every test starts at 75 mN and normal force drops as the test progresses. This average drop of 13.7 mN in normal force corresponds to 17 μm inclination over 1000 μm length or 1° slope which causes relaxation of the cantilever. The evolution of normal force for the chitlac-sTS surface is completely different and shows no fixed pattern. Moreover there was always some shoot-up of the force from

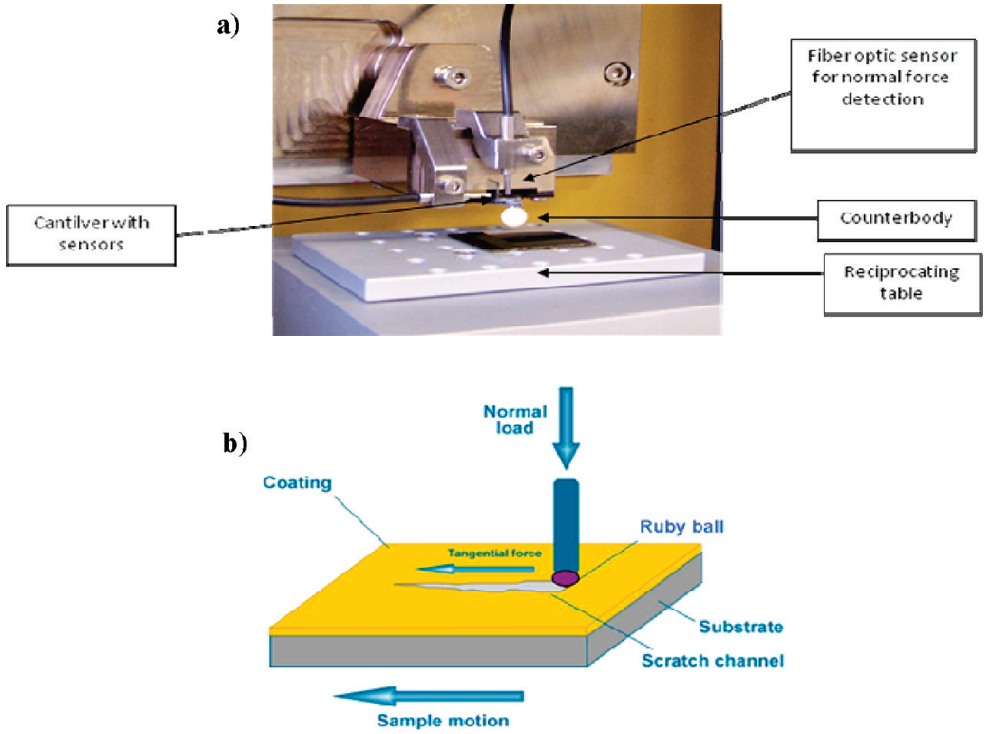

Figure 6. (a) Microrange surface tester and its components; (b) schematic illustration of the test.

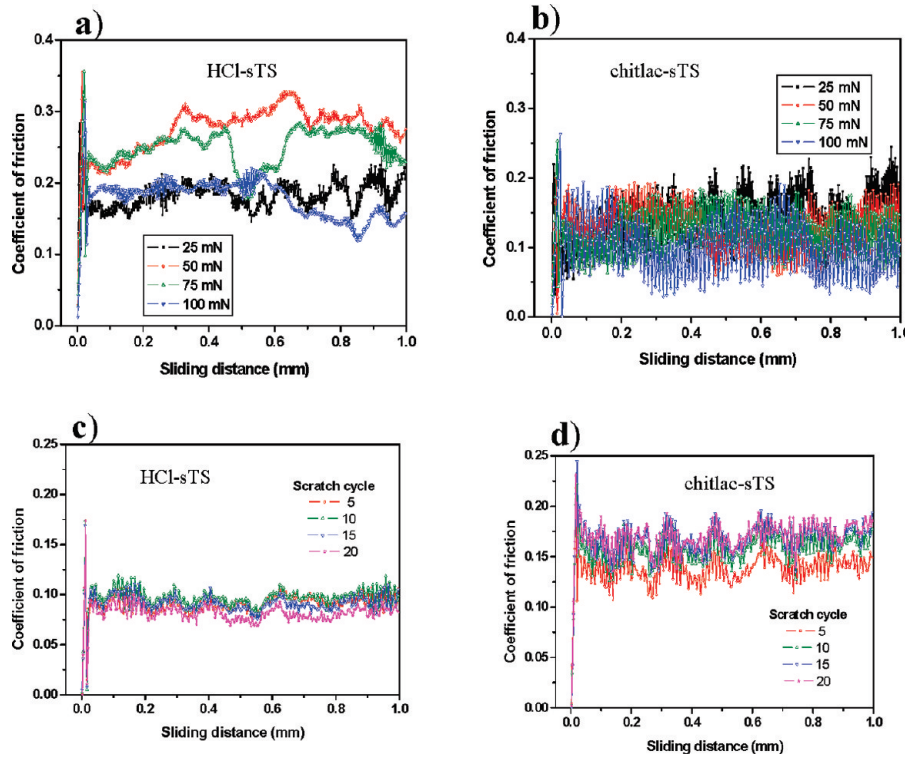

Figure 7. (a, b) Evolution of coefficient of friction with sliding distance during scratch test against 2 mm Ø ruby ball on HCl-sTS (a) and chitlac-sTS (b). (c,d) Evolution of coefficient of friction with sliding distance during constant load multipass scratch test against 2 mm Ø ruby ball on HCl-sTS (c) and chitlac-sTS (d). See Table 1 (Supporting Information) for legend.

the set point normal load indicating some sort of a resistance from the surface. This aspect is illustrated in Table 3 (Supporting Information) where a deviation from set point loads for both HCl-sTS and chitlac-sTS are recorded. In the case of uncoated thermosets, the error in normal load was within ±1.2%, whereas on chitlac there was always a higher load up to +34% of the set point. This overshoot is physically equivalent to deflecting the cantilever more than the minimum. It is hypothesized that the network structure of the polysaccharide layer responds under compression, which causes some mismatch in the piezo-displacement of the instrument. It is interesting to note that this overshoot is not the same for all the scratch cycles, which may be due to changes in the coating thickness during every scratch. This unusual effect will be investigated further through some systematic studies on the structural strength, mechanical properties like elastic modulus, creep, and so on, of the chitlac coating.

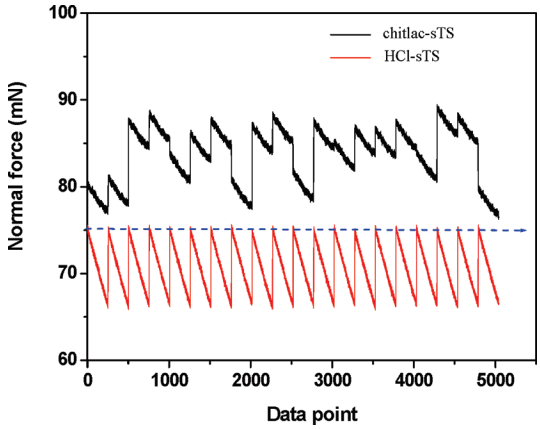

Figure 8. Fluctuations in the normal load during multiple scratch test on HCl-sTS and chitlac-sTS. See Table 1 (Supporting Information) for legend.

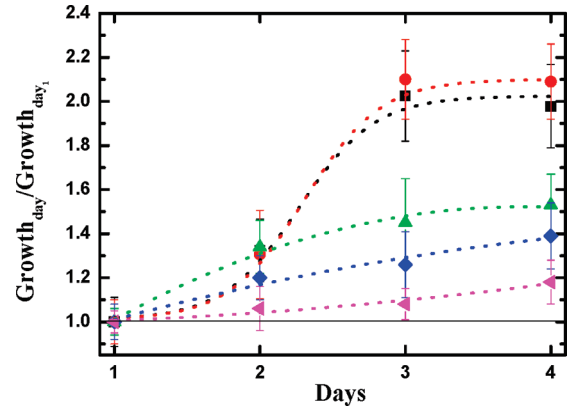

Figure 9. Relative MG63 cell growth (with respect to day 1) on TS (blue diamonds), HCl-TS (purple triangles), chitlac-TS (green triangles), RGD chitlac-TS (red circles), and titanium (control, black squares) samples (Table 1, Supporting Information). The dotted lines are drawn to guide the eye. The straight black line represents the limit of no cell proliferation.

At any event, one should always take into account that the chitlac layer can be depicted as a highly concentrated hyperentangled solution of the cationic polysaccharide.

In this respect, it is tempting to correlate the present observations with an unusual rheological behavior of chitlac reported by Yalpani et al.[52] who observed a low shear Newtonian behavior, a medium shear viscosity increase (dilatancy), and a high shear viscosity drop (pseudoplasticity) of the polysaccharide; at the transition point between the dilatant and the pseudoplastic regimes, a semiconcentrated chitlac solution (2%) exhibits unique oscillatory behavior under steady shear.

3.3. Biological Tests. The final aim of the surface modification deals with the possibility of introducing, on the outer layer of a TS sample, a biopolymer that would promote and facilitate biological events like cell adhesion and proliferation. In fact, when such synthetic thermosets are considered for orthopedic applications, the bioactive coating interacts with the surrounding tissue (bone), facilitating biological integration and interlocking. The proper and guided interface−tissue interaction is the key issue for the design of a successful biomaterial.

A standard cell proliferation test (Alamar blue essay) was conducted on coated thermosets to detect and highlight the effect of the different bioactive molecules added on the surface. The results were normalized with respect to day 1 to obtain a relative cell proliferation rate which allows a direct comparison between the different coatings. Standard titanium disks, with a roughened surface (Titanium, Table 1, Supporting Information), were used as control.

From the graph reported in Figure 9, it can be seen that the exposure of carboxylic moieties (HCl-TS sample) reduces cell proliferation with respect to untreated thermosets. This is attributed to the modification of the physical properties of the surface, such as charge density or wettability, which can alter the mechanism of cellular adhesion and spreading and, consequently, the subsequent processes of cell growth and proliferation.[53] This is also in line with the general consideration that negative charges hamper cell adhesion and proliferation.[54–56]

The presence of chitlac coating stimulates cell proliferation with respect to the acid-treated (polyanionic) sample, reaching a result similar to that of the untreated thermoset. Very likely this could be attributed to the slightly positive charge on the surface of the material given by the presence of the polysaccharide. However, coating with chitlac is not sufficient to bring the observed cell growth rate to the level exhibited by the standard material considered, that is, roughened titanium.

The strategy presented in this work for the modification of the surface of the BisGMA/TEGDMA thermoset aims especially at using polysaccharides whose bioactivity can be further modified and modulated by anchoring additional specific biological signals to boost and facilitate tissue formation and integration.

In this perspective, chitlac was decorated with the cell adhesion sequence arginine-glycine-aspartic acid (RGD) via coupling reaction with EDC/NHS. The ligand-coupled polymer was prepared with a low degree of substitution (approximately 2% of the residual primary amines) so that the polysaccharide still contains enough positive charges to bind with the thermoset surface by means of electrostatic interactions (RGD chitlac-TS). The degree of substitution is in line with the RGD-modified alginate reported by Mooney and co-workers.[57] The amount and distribution of RGD peptides are important parameters influencing cell adhesion, which shows a sigmoid increase indicating that there is a critical density for cell response. Moreover, several aspects are correlated to the attachment of cells, namely, the different cell lines, the sequence of the RGD peptide, the peptide distribution at the surface, and the polysaccharide composition.[58]

As can be seen in Figure 9, RGD ligands upregulate the proliferation rate of MG63 cells with respect to uncoated and chitlac-coated thermoset samples. In this case, the cell growth rate is fully comparable with that displayed by titanium alloy used as control.

In view of these results, it can be concluded that the physical−chemical characteristics of the polysaccharide, together with the presence of biological signals arranged on a polymeric backbone, likely allows the RGD peptide to extend over the layer of adsorbed serum proteins and to interact with integrin molecules of the osteoblast membrane.

4. Conclusions

The present work tackled the problem of the coating of a BisGMA/TEGDMA thermoset with bioactive polysaccharides. In the first step, the functionalization of the thermoset has been achieved through an acid treatment that enables the introduction of carboxylate moieties on its surface. It is noteworthy that the acid treatment does not significantly affect the bulk mechanical properties of the construct. The introduction of such versatile chemical groups opens up for several chemical and physical−chemical routes, allowing further modifications of the thermoset surface.

In the present work, we have exploited electrostatic interactions to coat the BisGMA/TEGDMA surface with a bioactive derivative of chitosan (chitlac). This approach led to a well-anchored deposition of a soft, hydrophilic positively charged layer on the thermoset surface, showing physical−chemical properties that are likely not far from those of the hydrated extracellular matrix. The biological properties of the biopolymer on the thermoset surface can be further enhanced by chemical incorporation on the polysaccharide backbone of bioactive signals (e.g., RGD-peptides). In principle, this system could be used also for the creation of a polyelectrolyte multilayer coating through a layer-by-layer approach.[59,60] In both cases, the bioactivity of the BisGMA/TEGDMA thermoset can be finely tuned to meet the requirements for cell adhesion and tissue integration of the BisGMA/TEGDMA implant. In this sense, the results on cell proliferation reported, although preliminary, are quite promising as they clearly show that the in vitro biological performances of the methacrylate based thermosets can be boosted to reach or even to overcome those of the standard material used in orthopedic applications, that is, roughened titanium. Factors like optimal spacing between the biological signals and their clustering are expected to bring about a further gain in performance as to biological responsiveness of the coated material.

The approach presented in this work efficiently combines aspects like proper mechanical performances and cell-directed biochemical signaling to upgrade the largely used BisGMA based thermosets. This could lead to new materials which can meet the complex requirements of biomechanical and biological properties expected for a "third generation" biomaterial.

Finally, the demonstrated feasibility of a chemical activation for the introduction of functional groups on the thermoset surface can be a key point to extend the present work well beyond the limit of methacrylate-based thermosets and toward more challenging materials like PET, PU, and PLLA.

Acknowledgment. This study was supported by the EU-FP6 Project "NEWBONE" (Contract Number 026279-2). The authors thank Philippe Lambert (Medacta Intl.) for providing the titanium samples, Dr. Lisa Vaccari for valuable help with the FTIR-ATR measurements, and Marta Giazzon (CSEM) for SEM analysis.

Supporting Information Available. Main features and characterizations of the samples used (Table 1), morphological parameters obtained by AFM analyses (Table 2), and scratch test values (Table 3), as mentioned in the manuscript. In addition, the FTIR-ATR data, a schematic representation of the EDC/NHS reaction mechanism, and the chemical structure of chitlac are presented. This material is available free of charge via the Internet at http://pubs.acs.org.

References and Notes

(1) Langford, R. J.; Frame, J. W. *Int. J. Oral Surg.* **2002**, *31*, 511–518.
(2) Langford, R. J.; Frame, J. W. *J. Cranio-Maxill. Surg.* **2002**, *30*, 103–107.
(3) Bhandari, M.; Bajammal, S.; Guyatt, G. H.; Griffith, L.; Busse, J. W.; Schunemann, H.; et al. *J. Bone Joint Surg. Am.* **2005**, *87*, 293–301.
(4) Ferracane, J. L. *Crit. Rev. Oral Biol. Med.* **1995**, *6*, 302–318.
(5) Vallittu, P. K. *J. Prosthet. Dent.* **1998**, *81*, 318–326.
(6) Vallittu, P. K.; Sevelius, C. *J. Prosthet. Dent.* **2000**, *84*, 413–418.
(7) Zhao, D. S.; Moritz, N.; Laurilla, P.; Mattila, R.; Lassila, L. V. J.; Strandberg, N.; Mäntylä, T.; Vallittu, P. K.; Aro, H. T. *Med. Eng. Phys.* **2009**, *31*, 461–469.
(8) Tezvergil, A.; Lassila, L. V.; Vallittu, P. K. *J. Dent.* **2005**, *33*, 509–516.
(9) Tezvergil, A.; Lassila, L. V.; Vallittu, P. K. *Dent. Mater.* **2003**, *19*, 471–477.
(10) Galhano, G. A.; Valandro, L. F.; de Melo, R. M.; Scotti, R.; Bottino, M. A. *J. Endodont.* **2005**, *31*, 209–211.
(11) Chua, P. H.; Neoh, K. G.; Kang, E. T.; Wang, W. *Biomaterials* **2008**, *29*, 1412–1421.
(12) Tuusa, S. M.; Peltola, M. J.; Tirri, T.; Puska, M. A.; Roytta, M.; Aho, H.; Sandholm, J.; Lassila, L. V.; Vallittu, P. K. *J. Biomed. Mater. Res., Part B* **2008**, *84*, 510–519.
(13) Tuusa, S. M.; Peltola, M. J.; Tirri, T.; Lassila, L. V.; Vallittu, P. K. *J. Biomed. Mater. Res., Part B* **2007**, *82*, 149–155.
(14) Chatelet, C.; Damour, O.; Domard, A. *Biomaterials* **2001**, *22*, 261–268.
(15) Haipeng, G.; Yinghui, Z.; Jianchun, L.; Yandao, G.; Nanming, Z.; Xiufang, Z. *J. Biomed. Mater. Res.* **2000**, *52*, 285–295.
(16) Freier, T.; Koh, H. S.; Kazazian, K.; Shoichet, M. S. *Biomaterials* **2005**, *26*, 5872–5878.
(17) Denuziere, A.; Ferrier, D.; Damour, O.; Domard, A. *Biomaterials* **1998**, *19*, 1275–1285.
(18) Donati, I.; Stredanska, S.; Silvestrini, G.; Vetere, A.; Marcon, P.; Marsich, E.; Mozetic, P.; Gamini, A.; Paoletti, S.; Vittur, F. *Biomaterials* **2005**, *26*, 987–998.
(19) Marcon, P.; Marsich, E.; Vetere, A.; Mozetic, P.; Campa, C.; Donati, I.; Vittur, F.; Gamini, A.; Paoletti, S. *Biomaterials* **2005**, *26*, 4975–4984.
(20) Abelda, S. M.; Buck, C. A. *FASEB J.* **1990**, *4*, 2868–2881.
(21) Humphries, J. D.; Byron, A.; Humphries, M. J. *J. Cell Sci.* **2006**, *119*, 3901–3903.
(22) Humphries, M. J. *J. Cell Sci.* **1990**, *97*, 585–592.
(23) Hynes, R. O. *Cell* **1992**, *69*, 11–25.
(24) Hynes, R. O. *Cell* **1987**, *48*, 549–554.
(25) Ruoslahti, E.; Pierschbacher, M. D. *Science* **1987**, *238*, 491–497.
(26) Massia, S. P.; Hubbell, J. A. *J. Cell Biol.* **1991**, *114*, 1089–1100.
(27) Comisar, W. A.; Kazmers, N. H.; Mooney, D. J.; Linderman, J. J. *Biomaterials* **2007**, *28*, 4409–4417.
(28) Hsu, S. H.; Whu, S. W.; Hsieh, S. C.; Tsai, C. L.; Chen, D. C.; Tan, T. S. *Artif. Organs* **2004**, *28*, 693–703.
(29) Massia, S. P.; Stark, J. *J. Biomed. Mater. Res.* **2001**, *56*, 390–399.
(30) Picart, C.; Elkaim, R.; Richert, L.; Audoin, F.; Arntz, Y.; Da Silva Cardoso, M.; Schaaf, P.; Voegel, J.-C.; Frisch, B. *Adv. Funct. Mater.* **2005**, *15*, 83–94.
(31) Ho, M. H.; Wang, D. M.; Hsieh, H. J.; Liu, H. C.; Hsien, T. Y.; Lai, J. Y.; Hou, L. T. *Biomaterials* **2005**, *26*, 3197–3206.
(32) Kirsebom, H.; Aguilar, M. R.; San Roman, J.; Fernandez, M.; Prieto, M. A.; Bondar, B. *J. Bioact. Compat. Polym.* **2007**, *22*, 621–636.
(33) Yu, J.; Gu, Y.; Du, K. T.; Mihardja, S.; Sievers, R. E.; Lee, R. J. *Biomaterials* **2009**, *30*, 751–756.
(34) Shu, X. Z.; Ghosh, K.; Liu, Y.; Palumbo, F. S.; Luo, Y.; Clark, R. A.; Prestwich, G. D. *J Biomed. Mater. Res., Part A* **2004**, *68*, 365–375.
(35) Rowley, J. A.; Mooney, D. J. *J. Biomed. Mater. Res.* **2002**, *60*, 217–223.
(36) Donati, I.; Borgogna, M.; Turello, E.; Cesàro, A.; Paoletti, S. *Biomacromolecules* **2007**, *8*, 1471–1479.
(37) Achanta, S.; Drees, D. *J. ASTM Int.* **2007**, *9*, 15–19.
(38) Marsich, E.; Borgogna, M.; Donati, I.; Mozetic, P.; Strand, B. L.; Salvador, S. G.; Vittur, F.; Paoletti, S. *J. Biomed. Mater. Res., Part A* **2008**, *84*, 364–376.
(39) Travan, A.; Pelillo, C.; Donati, I.; Marsich, E.; Benincasa, M.; Scarpa, T.; Semeraro, S.; Turco, G.; Gennaro, R.; Paoletti, S. *Biomacromolecules* **2009**, *10*, 1429.
(40) Paramonova, E.; de Jong, E. D.; Krom, B. P.; van der Mei, H. C.; Busscher, H. J.; Sharma, P. K. *Appl. Environ. Microb.* **2007**, *73*, 7023–7028.
(41) Wagner, M.; Ivleva, N. P.; Haisch, C.; Niessner, R.; Horn, H. *Water Res.* **2009**, *43*, 63–76.
(42) Depypere, F.; Van Oostveldt, P.; Pieters, J. G.; Dewettinck, K. *Eur. J. Pharm. Biopharm.* **2009**, *73*, 179–186.
(43) Strand, B. L.; Morch, Y. A.; Espevik, T.; Skjak-Braek, G. *Biotechnol. Bioeng.* **2003**, *82*, 386–394.
(44) Johnston, A. P.; Read, E. S.; Caruso, F. *Nano Lett.* **2005**, *5*, 953–956.
(45) Xu, S.; Dong, M.; Liu, X.; Howard, K. A.; Kjems, J.; Besenbacher, F. *Biophys. J.* **2007**, *93*, 952–959.
(46) Manna, U.; Bharani, S.; Patil, S. *Biomacromolecules* **2009**, *10*, 2632–2639.
(47) Tang, W.; Weng, X.; Deng, L.; Xu, K.; Lu, J. *Surf. Coat. Technol.* **2007**, *201*, 5664–5666.
(48) Roche, S.; Pavan, S.; Loubet, J. L.; Barbeau, P.; Magny, B. *Prog. Org. Coat.* **2003**, *47*, 37–48.
(49) Huang, L.; Lu, J.; Xu, K. *Thin Solid Films* **2004**, *466*, 175–182.

(50) Persson, B. N. J.; Contact mechanics, friction and adhesion with application to quasicrystals. In *Fundamentals of friction and wear on the nanoscale*; Gnecco, E., Meyer, E., Eds.; Springer: New York, 2007.
(51) Zhang, T.; Wang, H.; Hu, Y. *Tribol. Lett.* **2003**, *14*, 1573.
(52) Yalpani, M.; Hall, L. D.; Tung, M. A.; Brooks, D. E. *Nature* **1983**, *302*, 812–814.
(53) Roach, P.; Eglin, D.; Rohde, K.; Perry, C. *J. Mater. Sci.: Mater. Med.* **2007**, *18*, 1263–1277.
(54) McLean, K. M.; Johnson, G.; Chatelier, R. C.; Beumer, G. J.; Steele, J. G.; Griesser, H. J. *Colloids Surf., B* **2000**, *18*, 221–234.
(55) Massia, S. P.; Stark, J.; Letbetter, D. S. *Biomaterials* **2000**, *21*, 2253–2261.
(56) Yoshioka, T.; Tsuru, K.; Hayakawa, S.; Osaka, A. *Biomaterials* **2003**, *24*, 2889–2894.
(57) Kong, H. J.; Boontheekul, T.; Mooney, D. J. *Proc. Natl. Acad. Sci. U.S.A.* **2006**, *103*, 18534–18539.
(58) Hersel, U.; Dahmen, C.; Kessler, H. *Biomaterials* **2003**, *24*, 4385–4415.
(59) Fu, J.; Ji, J.; Fan, D.; Shen, J. *J. Biomed. Mater. Res., Part A* **2006**, *79*, 665–674.
(60) Meng, S.; Liu, Z.; Shen, L.; Guo, Z.; Chou, L. L.; Zhong, W.; Du, Q.; Ge, J. *Biomaterials* **2009**, *30*, 2276–2283.

BM9011419

Paper 4

Silver-Polysaccharide Nanocomposite Antimicrobial Coatings for Methacrylic Thermosets

Andrea Travan[1]*, Eleonora Marsich[1], Ivan Donati[1], Monica Benincasa[1], Marta Giazzon[2], Laura Felisari[3], Sergio Paoletti[1]

[1] Department of Life Sciences, University of Trieste, Via Licio Giorgieri 1, 34127 - Trieste, Italy

[2] Centre Suisse d' Electronique et Microtechnique (CSEM),

Rue Jaquet-Droz 1, CH-2002 Neuchâtel, Switzerland

[3] Consorzio per la fisica, Strada Costiera 11, Trieste, Italy and

TASC National Laboratories, Area Science Park, Basovizza, 34149 Trieste, Italy

*Address for correspondence:

Andrea Travan

Department of Life Sciences, University of Trieste

Via Giorgieri 1, Trieste, 34100, Italy

Telephone number: +39 (0) 40 5583682

E-mail: atravan@units.it; andrea.travan@iol.it

(Submitted to *European Cells and Materials* on 26th February 2010)

Abstract

Bisphenol A glycidylmethacrylate (BisGMA)/triethyleneglycol dimethacrylate (TEGDMA) thermosets are receiving a growing interest as biomaterials for dental and orthopaedic applications; for both these fields, bacterial adhesion to the surface of the implant represents a major issue for the outcome of the surgical procedure. Moreover, the biological behavior of these materials is influenced by their ability to establish proper interactions between their surface and eukaryotic cells of the surrounding tissues which accounts for a good implant integration. The aim of this work was to develop an antimicrobial non-cytotoxic coating for methacrylic thermosets by means of a nanocomposite material based on a lactose-modified chitosan and ancitbacterial silver nanoparticles. The coating was characterized by UV-Visible spectrophotometry, optical microscopy, transmission electron microscopy (TEM) and scanning electron microscopy (SEM). *In vitro* tests were employed for a biological characterization of the material: antimicrobial efficacy tests were carried out with both Gram+ and Gram- strains. Osteoblasts-like cell lines, primary human fibroblasts and adipose-derived stem cells were used for LDH cytotoxicity assays and Alamar Blue cell proliferation assays. Cell morphology and distribution analyses were evaluated by SEM and Confocal Laser Scanning Microscopy (CLSM). The results showed that the nanocomposite coating is effective in killing both bacteria strains and that this material does not exert any significant cytotoxic effect towards tested cells, which are able to firmly attach and proliferate on the surface of the coating. Such biocompatible antimicrobial polymeric films containing silver nanoparticles may have good potentials for surface modification of medical devices, especially for prosthetic applications in orthopaedics and dentistry.

Keywords: Biomaterials, Silver nanoparticles, Polysaccharides, Methacrylic thermosets, Antimicrobial activity, Cytotoxicity, Stem cells.

Introduction

In the field of biomaterials, the issue of infections associated with the material surface is of overriding relevance. When the microbial adhesion to surfaces is followed by bacterial growth and colonization, the outcome is the formation of a compact biofilm matrix which protects the underlying bacteria from the action of antibiotics and host defense mechanisms. In the case of biomedical devices, such as prosthetic implants, this phenomenon can result in serious infection leading to the failure of the implant (Sambhy *et al.*, 2006). Nowadays there is an increasing demand for antimicrobial materials that do not allow microbes to adhere and proliferate on material surfaces (Ho *et al.*, 2004). Many efforts have been made to design a coating that can prevent or eradicate occurring infections (Grunlan *et al.*, 2005). For biomaterials applications, antimicrobial coatings need to combine antibacterial efficacy and low toxicity to eukaryotic cells.

Different strategies have been used to endow coatings with antimicrobial properties (Ho et al., 2004;Sambhy et al., 2006): a) addition of anti-adhesive components (Ignatova *et al.*, 2005), b) controlled release of biocides (Kohnen *et al.*, 2003) and c) use of contact-active systems (Lee *et al.*, 2004), where the antimicrobial agent is incorporated within the matrix and is not supposed to be released. The advantage of using a contact-active material is that microorganisms can be killed upon direct contact without releasing compounds that might be toxic not only to bacteria but also to mammalian cells. Among contact-active agents, silver-based coatings are of great interest. In fact, silver, in form of nanoparticles (Panacek et al., 2006;Travan et al., 2009), ions (Balogh et al., 2001;Rhim et al., 2006) and salts (Sambhy *et al.*, 2006), is widely used as antimicrobial agent for different applications like wound-healing devices (Ip et al., 2006;Tian et al., 2007), chatheters (Hachem *et al.*, 2003), dental materials {Hernandez-Sierra, 2008 584 /id}, and stents (Multanen *et al.*, 2000) due to its ability to kill a broad spectrum of bacteria (Grunlan et al., 2005;Rhim et al., 2006). Although the antibacterial mechanism is not totally understood (Morones *et al.*, 2005), the main molecular targets of the silver antibacterial activity are supposed to be the thiol groups (-SH) of proteins exposed to the extracellular portion of the bacterial membrane (Elechiguerra et al.,

2005;Feng et al., 2000;Furr et al., 1994;Gupta et al., 1999;Morones et al., 2005); conversely, eukaryotic cells lack these exterior binding sites, so the nanoparticles are supposed to interact with them only upon metal internalization. The issue of possible adverse effects and toxicity of nanoparticles for eukaryotic cells is now recognized as central by an increasing number of studies; these indicate that the lack of physical barriers to nanoparticle diffusion into cells represents a risk of uptake by eukaryotic cells, which can lead to their death (Chen and Schluesener, 2008;Geiser et al., 2005;Hussain et al., 2005) in a dose-dependent manner (Lee *et al.*, 2007).

Silver nanoparticles are usually prepared in the presence of a stabilizing agent in order to avoid their aggregation, which could lead to the loss of the high antimicrobial activity associated with the nanoscale (Huang and Yang, 2004;Kuo and Chen, 2003); typically, polyelectrolyte solutions can be used to control the formation and the long-term stability of nanoparticles (dos Santos et al., 2004;Dotzauer et al., 2006). Silver nanoparticles formed and stabilized in a lactose-modified chitosan (1-deoxylactit-1-yl chitosan, shortly named “Chitlac”) were previously employed as antimicrobial agents effective towards both Gram+ and Gram- bacteria (Travan *et al.*, 2009). Convenient and effective ways of preparing and embodying silver nanoparticles in polymeric materials are continuously sought (Wang *et al.*, 2006). A widely employed strategy is based on the dehydration of the polymer solution containing nanoparticles, to obtain a nanocomposite material where the nanoparticles are embedded in the polymer matrix (Fu et al., 2006;Huang et al., 2004;Rhim et al., 2006). Since the nanocomposite is supposed to get in contact with both bacteria and eukaryotic cells, the choice of the polymer is crucial in order to obtain a biocompatible antimicrobial system.

Currently, the biocompatibility of nanoparticles-based systems is quite often not well-characterized (Lee et al., 2007;Chen and Schluesener, 2008). It would be desirable to firmly incorporate silver nanoparticles into a biocompatible polymeric film so that the nanoparticles can directly interact with the bacterial membrane without being uptaken by eukaryotic cells. Moreover the preparation of homogeneous coatings containing nanoparticles is an ongoing challenge; a crucial feature is to

prepare stabilized nanoparticles before film construction (Dai and Bruening, 2002). Recently the application of silver-binding membranes has been suggested to further reduce the silver toxicity towards eukaryotic cells minimizing the metal absorption (Yu *et al.*, 2006). The film construction can be made by means of different techniques like dehydration (Rhim *et al.*, 2006) or alternating adsorption of oppositely charged polyelectrolytes (Dotzauer et al., 2006;Grunlan et al., 2005). After choosing the proper materials for the nanocomposite film, an effective technique must be used to graft firmly the coating onto the substrate material. One approach (the "layer by layer" technique) is to obtain a polymeric film by dipping the substrate material with a charged surface in a polyelectrolyte solution of opposite charge in order to exploit electrostatic bonds (Grunlan *et al.*, 2005). This is a simple procedure that can be adapted to almost any type of surface and regardless the shape of the solid (Fu *et al.*, 2006). As a result, since nanoparticles are stabilized within the polyelectrolyte solution, this approach allows obtaining a nanocomposite film electrostatically bound to the substrate material.

For this study, the substrate material is a thermoset based on Bisphenol A glycidylmethacrylate (BisGMA) and triethyleneglycol dimethacrylate (TEGDMA). Such polymeric material finds wide application as biomaterial for dental applications (Ballo *et al.*, 2008;Lehtinen *et al.*, 2008) and is being studied for prosthetic purposes (Ballo et al., 2007;Ballo et al., 2009); in fact Fiber Reinforced Composites (FRC) based on BisGMA/TEGDMA are promising alternatives for metallic implants since FRC can be tailored to closely match the mechanical properties of bone. Moreover diagnostic imaging of FRC implants with suspected mechanical loosening or infection might be easier if compared to metallic implants (Zhao *et al.*, 2009). In any case it would be desirable to render the surface antimicrobial by means of a biocompatible coating. In this work we report the preparation of a coating for a BisGMA/TEGDMA thermoset material by means of a physisorption of a nanocomposite system based on Chitlac and silver nanoparticles (Travan *et al.*, 2009) (hereafter "Chitlac-nAg"). Biological tests are performed in order to assay the interaction of the coating with both bacteria and eukaryotic cells.

Materials and methods

Materials

Chitlac (lactose-modified chitosan, CAS registry number 85941-43-1) was prepared according to the procedure reported elsewhere (Donati *et al.*, 2005) starting from a highly deacetylated chitosan (residual acetylation degree approx. 11 %): briefly, 300 mg of chitosan were dissolved in 21 mL of a 1:1 mixture of methanol and 1 % acetic acid (pH 4.5); 12 mL of the same methanol/acetic acid mixture containing 1.6 g of lactose and 660 mg of sodium cyanoborohydride were then added. The solution was stirred for 24 h at room temperature and after dilution with water (30 mL), exhaustively dialysed against deionized water. The polymer solution was filtered through 0.45 mm Millipore filters and freeze-dried. The composition of Chitlac was determined by means of ^{1}H-NMR and resulted to be: Glucosamine residue = 24%; N-Acetylglucosamine = 11 %; 2-(lactit-1-yl)-glucosamine = 65 %. The molecular weight of Chitlac was estimated to be approximately 1.5 x 10^{6}. Bisphenol A glycidylmethacrylate (Bis-GMA), triethyleneglycol dimethacrylate (TEGDMA) and Triton x-100 were purchased from Aldrich. Camphorquinone (CQ) and 2-dimethylamino ethylmethacrylate (DMAEMA) were purchased from Fluka. Alamar blue was purchased from Biosource^{TM} (Invitrogen). Polyurethane films containing 0.25% zinc dibuthyldithiocarbamate (ZDBC) (8 mm discs) were from Hatano Research Institute / Food and Drug Safety Center Reference Material Office (JAPAN). Plastic sheets (8 mm discs) were from Wako Pure Chemical Industries, Ltd., Cat.No.160-08893). Basic fuchsine was from “Società Italiana Chimici”, cod.11260.

Preparation of the BisGMA/TEGDMA thermosets (“uncoated samples”)

BisGMA (70% w/w) and TEGDMA (30% w/w) were mixed under vigorous stirring at 37 °C. CQ (0.7% w/w) and DMAEMA (0.7% w/w) were added and the solution was protected from light and degassed for 12 hours in vacuum oven at 40 °C. The solution was poured in Teflon mould (∅ =14

mm, h = 2.5 mm) and the wells were covered with a PET film. The polymerization was light initiated with a hand cure light device (Optilux 501, λ: 400-505 nm, light power: 850 mW/cm^2) for 20 seconds. The post-curing was performed with a Photopol IR/UV Plus oven (Dentalfarm, Italy) equipped with 8 lamps and 2 spots operating in the wavelength range 320-550 nm following the procedure: 20 minutes in light oven (8 lamps), 20 minutes in light oven (8 lamps) on a rotating plate, 60 minutes in light oven (8 lamps) under vacuum, 7 minutes in light oven (8 lamps plus 2 spots). The thermosets were then sandpaper polished (granulometry: 1200).

Preparation of the colloidal solution Chitlac-silver nanoparticles (Chitlac-nAg)

Silver nanoparticles were obtained by reducing silver ions with ascorbic acid in Chitlac solutions according to the following procedures (Travan *et al.*, 2009): Chitlac was dissolved in deionized water at the concentration of 4 g/L. Chitlac solution was mixed with $AgNO_3$ solution to a final $AgNO_3$ concentrations of 1 mM. Ascorbic acid ($C_6H_8O_6$) solution was added at final concentration of 0.5 mM. After 4 hours, a yellow-orange stable colloidal solution was obtained.

BisGMA/TEGDMA thermosets surface activation

In order to expose on the surface of the material COO^- functional groups by hydrolysis of the methacrylate esters, the samples where immersed in HCl 12 M at 80 °C for 7 h. The thermosets were then removed, rinsed with deionized water (2 x 50 mL), with NaOH 0.1 M (50 mL) and with water again (50 mL) and finally air dried overnight (Travan et al., 2010).

Coating of the thermoset surface with Chitlac-nAg

The activated samples where immersed for 24 hours in wells containing Chitlac-nAg and subsequently rinsed in deionized water for 60 min under agitation. The absorption of Chitlac-nAg was followed by UV-Vis spectroscopy (dilution 1:10, Spectrophotometer Cary 400) . The samples were dried under hood overnight and sterilized by means of UV light.

Antimicrobial efficacy test

The antimicrobial efficacy was evaluated by means of a slightly modified protocol of the Japanese Industrial Standard method (JIS Z 2801:2000). Mid-log phase culture in Mueller Hinton (MH) broth of *S. aureus* ATCC25923 and *P. aeruginosa* ATCC27853 were centrifuged at 1000 x *g* for 5 min and resuspended in Phosphate Buffered Saline (PBS) at the final concentration of $1\div5 \times 10^8$ CFU/mL. 10 μL of each bacterial suspension were deposed on Chitlac-nAg coated and uncoated disks samples, and covered with UV sterilized plastic sheets (14 x 14 mm) (from Wako Pure Chemical Industries, Ltd., Cat.No.160-08893). The "sandwich" was incubated for 3 h at 37°C at saturation humidity. At the end of incubation, the samples were immersed in 2 mL of high salt solution (10 mM Na-phosphate, 400 mM NaCl and 10 mM $MgCl_2$) and vigorously vortexed for 30 seconds to allow the detachment of bacteria from the support. After proper serial dilutions in PBS, the bacterial suspensions were plated on MH agar and incubated overnight at 37 °C to allow the viable colony counts. The values reported are the mean ± standard deviation of three independent experiments with comparable results.

Cell cultures

Primary human skin fibroblasts, human adipose-derived stem cells (ADSCs) and human osteosarcoma cell-lines (MG63 cell line, ATCC number: CRL-1427 and Saos-2 cell line, ATCC number: HTB-85^{TM}) were used for the *in vitro* experiments. MG63 cells and fibroblasts were cultured in Dulbecco's Modified Eagle's medium (Sigma), 10 % heat-inactivated fetal bovine serum (Sigma), 100 U/mL penicillin, 100 μg/mL streptomycin and 2 mM L-glutamine in a humidified atmosphere of 5 % CO_2 at 37 °C. Saos-2 cells were grown in McCoy's 5A medium (Sigma) supplemented with 15 % heat-inactivated fetal bovine serum (Sigma), 20 U/mL penicillin and 20 μg/mL streptomycin at 37°C in a humidified 5 % CO_2, 95 % air. Human adipose-derived stem cells (ADSC) were purchased from Invitrogen (STEMPro® cells). ADSCs were expanded in MesenPRO

Basal RS Medium (Invitrogen) supplemented with 10 % MesenPRO RS™ Growth Supplement and 2 mM L-glutamine at 37°C in a humidified 5 % CO_2, 95 % air.

Cell Proliferation Assay (Alamar Blue)

Coated and uncoated thermosets were prepared and sterilized by exposure to a UV lamp. Approximately 20000 fibroblasts and osteoblast-like cells or 7500 ADSCs suspended in 50 µL of culture medium were dropped in the center of the sample surface and incubated for 4 hours at 37 °C and 5 % pCO_2. After incubation, 0.85 mL of culture medium were added and the thermoset samples were further incubated for 18 h under the same conditions. 0.1 mL of Alamar Blue solution was then added and cells were incubated for additional 6 hours. Then the medium was removed from each sample and its fluorescence was measured (excitation wavelength = 530 nm, emission wavelength = 590 nm). The thermoset samples were then washed with PBS (2 x 1 mL), added of 0.9 mL of fresh culture medium and the incubation protracted before the Alamar Blue assay repeated. Six replicates were used for each coating and two cell-free coated thermosets were used as blank and the average signal was subtracted to the signal of the samples.

Cytotoxicity (LDH) assay

In vitro cytotoxicity of the samples was evaluated by using the lactate dehydrogenase assay (LDH assay, TOX-7, Sigma). Each cylindrical sample (∅ = 14 mm; h = 2.5 mm) was cut into 4 equal parts used for direct contact test with the cells or for the extraction test. For the direct contact test, 50000 cells/well were plated on 24-well plates and, after complete adhesion, culture medium was replaced with 500 µL of fresh medium. Tested materials (in quadruplicate) were directly deposited on the cell layer. After 24 and 72 hours, medium was collected and the LDH assay was performed according to the manufacture's protocol. As a positive control material, polyurethane films containing 0.25% zinc dibuthyldithiocarbamate (ZDBC) (8 mm discs) were used. As negative control material, plastic sheet (8 mm discs) were used.

For the extraction test, each sample (in quadruplicate) was incubated in cell culture medium (1 mL) for 24 h at 37 °C and 5 % pCO_2. After incubation, the extraction media were added on cells seeded on 24-well plates (50000 cells/well). As positive control, Triton 1% was used.

The LDH assays were performed after 24 and 72 hours as described above. Each material test was performed in quadruplicate. Evaluation of cytotoxicity was calculated according to the formula: % LDH released = [(A - B)/(C - B)] × 100, with A = LDH activity in the culture medium of material-treated or extraction medium-treated cells, B = LDH activity of culture medium from untreated cells and C = LDH activity after total cell lysis.

Optical microscopy

The sample was included in epoxy resin (Electron Microscopy Sciences, DER 332) and transversally cut by means of a Leica Ultracut UCT Ultramicrotome in order to obtain slices with a thickness between 80 and 120 nm. The slices were dyed to allow the visualization of the polysaccharide layer: a fuchsine stock solution (1 % basic fuchsine dissolved in 50 % water-ethanol solution) was diluted to the concentration of 5 % in water and incubated with the samples for 5 min at 50-60 °C. Finally the samples were air dried and observed by means of an Optical Microscope Leitz Dialux 20 EB equipped with the recording system Leica DC300 (Leica Microsystems S.p.A.).

Transmission Electron Microscopy (TEM)

The microtomed samples were deposited onto Nickel grids coated with a carbon film. TEM images were recorded by means of a PHILIPS EM 208 Microscope operating at 100 kV equipped with the recording system Olympus Soft Imaging Solutions GmbH (Software: iTEM; TEM Camera: Morada 4008 x 2672 pixel max).

Scanning Electron Microscopy (SEM)

Sputtered samples: gold-sputtered samples were analyzed by means of a Environmental Scanning Electron Microscope (ESEM) Philips XL30 ESEM equipped with a Field Emission Gun (FEG): FE-SEM. In the case of cells cultured on the surface, the samples were prepared according to the following procedure: after removal of the culture medium, samples were rinsed with Phosphate Buffered Saline (PBS), and cells were fixed in 1.5 % glutaraldehyde, sodium cacodylate 0.1 M, pH 7.4 for 1 hour. After cell fixation the samples were rinsed with sodium cacodylate 0.1 M (pH 7.4) for 12 hours, dehydrated in ethanol solutions of increasing concentrations (20, 30, 40, 50, 60, 70, 80, 90, and 100 %) for 5 min at each concentration and then dried under hood.

Non-sputtered samples: non-sputtered samples were observed by means of a FE-SEM ZEISS SUPRA operating at 15.00 kV and equipped with an Energy Dispersive X-Rays (EDX) spectrometer.

Inductively Coupled Plasma - Atomic Emission Spectrometry (ICP-AES)

The quantitative analysis of the silver released from the coating was performed by means of ICP-AES Spectroflame Modula E optical plasma interface (OPI) instrument (Spectro^{TM}, Germany). The following samples were analyzed: 1) Chitlac-nAg (colloidal solution), 2) supernatant solution (1 mL) after incubation with the activated thermoset for 24 hours, 3) rinsing solution after washing the dried coated sample with deionized water (1 mL) for 1 hour under agitation**.** The metal concentrations were evaluated after centrifugation and filtration with a 0.42 µm membrane (Millipore, USA) using calibration curves obtained by dilution of Silver ICP/DCP standard solution 10,000 µg/mL in HNO_3 (Sigma Aldrich). The emission wavelength used was 328.068 nm, the limit of detection 0.03 mg/L. Calibration curves obtained by means of 5 standard solutions had correlation coefficients higher than 0.998.

Confocal Laser Scanning Microscopy (CLSM)

The cells were fixed with paraformaldehyde 4% in PBS, rinsed with PBS, incubated in glycine 0.1 M in PBS, rinsed again in PBS and incubated in blocking buffer solution (Saponine 0.05 % w/v, BSA 0.2% w/v in PBS). Subsequently, cells were treated with DAPI for nucleus visualization, phalloidin alexafluor 488 for actin filaments staining and with anti-human vinculin (mouse) and sheep anti-mouse CY3 for vinculin immunostaining. The samples were then rinsed in sequence with blocking buffer, PBS and distilled water, and finally cover-slipped with a mounting medium (Mowiol). The samples were analyzed by means of a confocal laser microscopy LEICA DM 6000 B.

Results and Discussion

In the field of biomaterials, thermosets based on light-initiated reticulation of BisGMA and TEGDMA are being widely employed due to their good mechanical properties and biocompatibility (Tezvergil et al., 2005;Vakiparta et al., 2006). Since such materials do not display any biochemical feature that prevents bacteria adhesion and the formation of biofilms, modifications of their surface properties are of primary importance. To this end, a surface of these thermosets has been activated according to the procedure reported elsewhere (Travan et al., 2010). Briefly, the material was immersed in HCl and subsequently rinsed in NaOH to expose negative charges (COO^- groups) on the surface; then, the activated thermoset was immersed in a polysaccharide-silver nanoparticles colloidal solution (Chitlac-nAg) in order to promote the grafting of the nanocomposite coating on the thermoset substrate by exploiting electrostatic interactions between the carboxylate moieties and the positive chains of the polysaccharide.

The deposition process was indirectly monitored by recording the variations of the UV-Vis spectra of the supernatant colloidal solution in contact with the activated thermoset. In fact, the Chitlac-nAg solution is characterized by an absorption peak at about 400 nm (plasmon resonance absorption band) (Donati *et al.*, 2009) and thus a decrease in the plasmon peak intensity over time accounts for

a deposition process of the metallic nanoparticles from the solution onto the substrate; Figure 1a shows that the peak intensity decreases considerably after 24 hours, which indicates a time-dependent adsorption of Chitlac-nAg on the activated thermoset. Moreover, a 6 nm blue-shift of the plasmon peak was observed pointing to a smaller size of the particles remaining in solution, which means that larger nanoparticles tend to be incorporated in the coating somewhat more easily than smaller ones. A non-activated thermoset was used as a control and in this case no change in the absorption peak was noticed (data not shown).

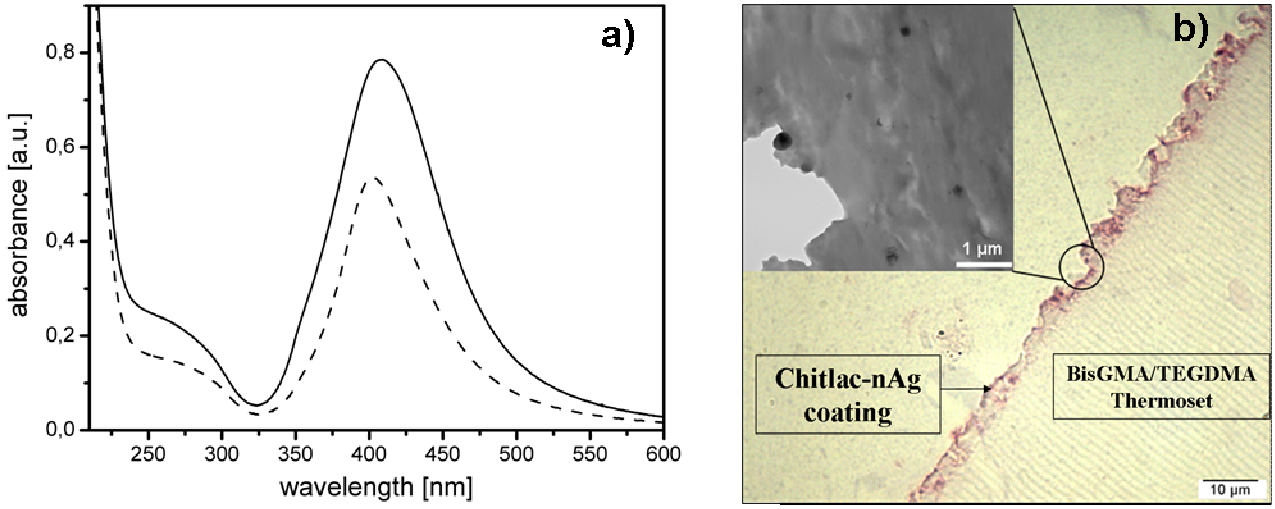

Figure 1. a) UV-Vis spectra of Chitlac-nAg freshly prepared (solid line) and after incubation with the activated thermoset for 24 h (dotted line). b) Optical image of the cross section of the nanocomposite coating. Inset: TEM image of the coating at higher magnifications showing the presence of electron-dense domains.

The concentration of total silver in the colloidal suspension was monitored by ICP-AES during each step of the coating preparation in order to quantitatively estimate the deposition of the nanoparticles on the substrate; after incubation with the activated thermoset for 24 hours, the silver amount in the supernatant solution decreased by about 85 %, thus confirming the silver deposition on the substrate. The dried coated sample was then rinsed in 1 mL of deionized water for 1 hour under

constant stirring and the silver concentration measured in the rinsing solution; the silver release was below the detection limit (< 0.01 ppm), showing that the nanocomposite film formed on the acrylic thermoset has a good stability in water, at least for short times.

A further characterization of the nanocomposite coating was carried out by direct imaging the cross section of Chitlac-nAg coated samples. The optical image in Figure 1b points to the presence of a Chitlac-nAg layer about 10÷15 μm thick, grafted onto the underlying thermoset substrate. TEM images of the cross section of the coating confirmed the presence of electron-dense domains buried inside, or protruding from, the surface of the polysaccharide matrix, which can be safely attributed to silver-nanoparticles clusters (Figure 1b, inset).

The location of silver nanoparticles both on the surface and inside the coating could be particularly beneficial for long-term *in vivo* applications, since this thick antimicrobial and biodegradable layer is expected to be slowly remodeled and adsorbed from the surrounding tissues, acting like a reservoir of the biocidal agent.

Since the coating is supposed to exert its antimicrobial activity mainly by means of a direct contact between silver nanoparticles and bacteria membranes (Stevens *et al.*, 2009), examination of the distribution and organization of the nanoparticles emerging from the outer nanocomposite layer has been undertaken. To this end, FE-SEM was employed to explore the surface of the coating: Figure 2 collects top-views of the Chitlac-nAg layer at various magnifications. In Figure 2a it is possible to notice the presence of white spots spread all over the surface; these zones are polysaccharide domains particularly enriched with round-shaped silver nanoparticles kept together by the polymer matrix and appear like clusters of nanoparticles and Chitlac. The clusters are homogeneously dispersed over the sample surface and display irregular shapes. The average size is about 1 μm, but, occasionaly, both larger (up to 5 μm) and smaller clusters (hundreds of nanometers) can be found. The chemical composition of the clusters was analyzed by means of EDX measurements that confirmed the presence of silver (Figure 2a, inset). Figure 2b shows a single cluster, Figure 2c is a magnification of the nanoparticles entrapped within the polymer matrix. The smoothness of the

nanoparticles indicates that a Chitlac film seems to wrap the particles around. Figure 2d shows smaller clusters of isolated particles embedded in the polysaccharide layer and protruding through its surface.

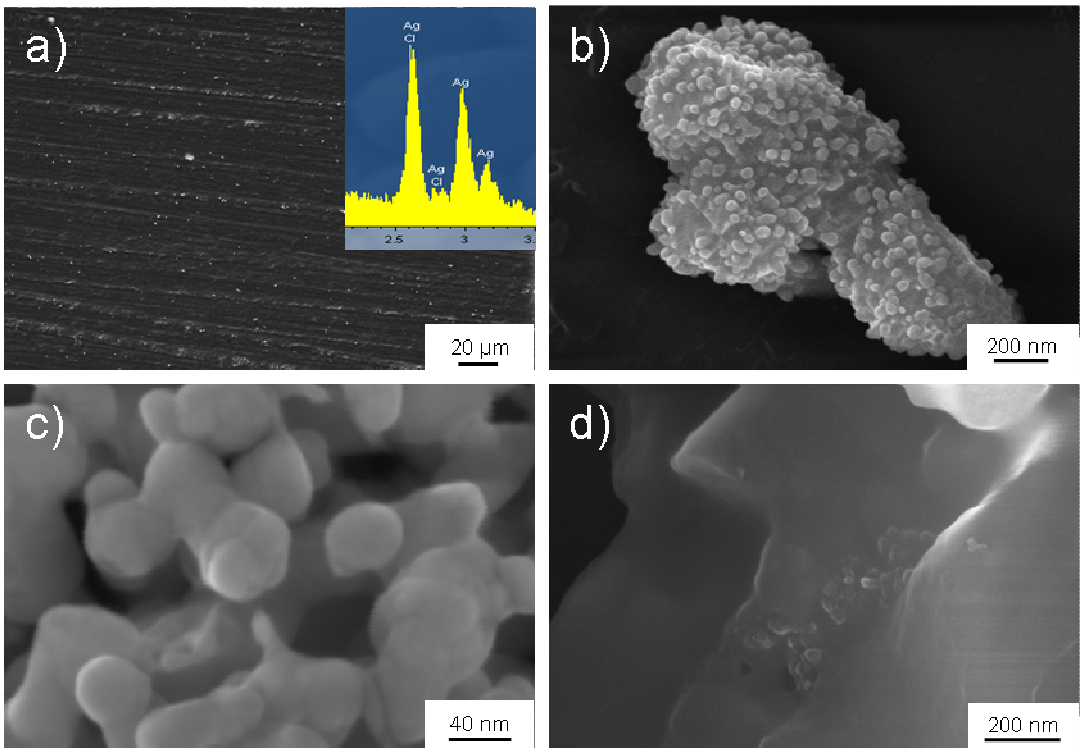

Figure 2. FE-SEM images of the nanocomposite coating (top views) at various magnifications. a) Surface distribution of Chitlac-nAg clusters and EDX spectrum showing the presence of silver on the surface (inset). b) Single cluster. c) Silver nanoparticles entrapped in the polymer matrix. d) Smaller clusters of nanoparticles on the surface layer.

These FE-SEM images confirmed the presence of silver nanoparticles, attached to the polysaccharide matrix, able to directly interact with bacteria when they come into contact with the biomaterial surface.

Antibacterial efficacy tests were carried out with two different bacteria strains, namely S. *aureus* (Gram+) and *P. aeruginosa* (Gram-); each bacterial strain was smeared on the surface of the Chitlac-nAg coated thermoset while the uncoated thermoset was used as control. After 3 hours of incubation, the bacteria were detached from the samples and the number of Colony Forming Units

(CFU)/mL was evaluated. Figure 3 indicates that both bacteria strains were effectively inactivated by the nanocomposite coating, with a drop of almost 6 orders of magnitude in the CFU/mL, while the uncoated thermoset does not display any remarkable antibacterial activity.

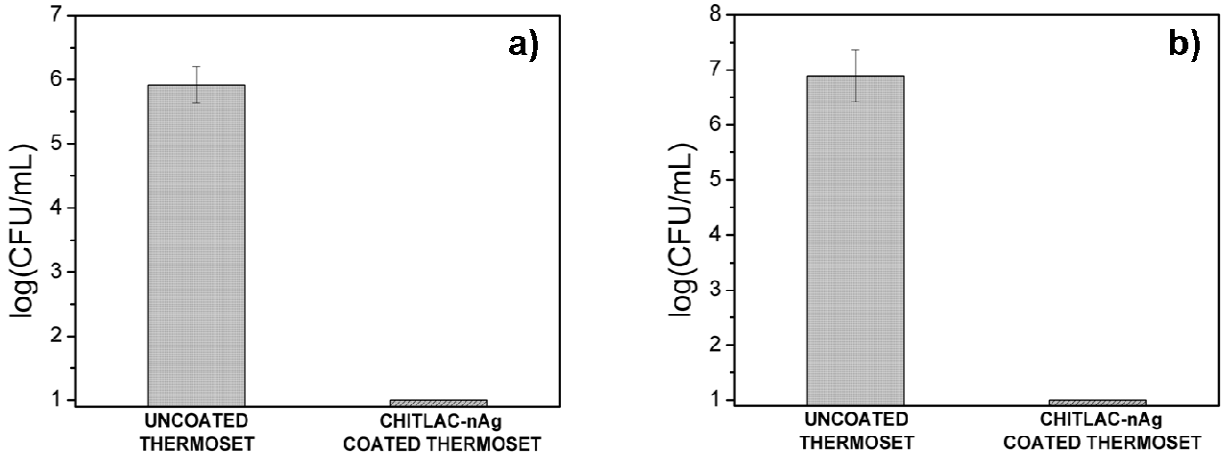

Figure 3. Antimicrobial efficacy tests on *S. aureus* (a) and *P. aeruginosa* (b) in direct contact with Chitlac-nAg coated and uncoated thermoset. The values are the mean ± standard deviation of three independent experiments.

It should be noticed that the biocidal activity of silver nanoparticles is not impaired by their incorporation in the polymer layer (Travan *et al.*, 2009), which implies that their immobilization does not significantly restrict access to bacteria. This means that the electrostatic deposition on acrylic supports represents an effective method to immobilize silver nanoparticles keeping their antibacterial activity.

Since antimicrobial biomaterials need to combine bactericidal activity with the lack of toxicity towards eukaryotic cells, LDH cytotoxicity tests were carried out with a osteoblasts-like cell line (MG63) and with primary human fibroblasts. Figure 4 (a,b) reports the percentage of lactate dehydrogenase released by cells in contact with both coated and uncoated thermosets, with the corresponding extracts and with control materials; the results show that Chitlac-nAg coated thermosets did not exert any considerable cytotoxic effect on the tested cells. In fact, although

MG63 cells exhibit after 24 h a minor increase of the LDH release for the coated samples in direct contact with cells, there was no considerable difference between silver-treated cells and control groups after 72 h. The slightly toxic effect observed in the case of MG63 cells during the first few hours could be presumably ascribed to an initial burst release of silver followed by recover of cell viability.

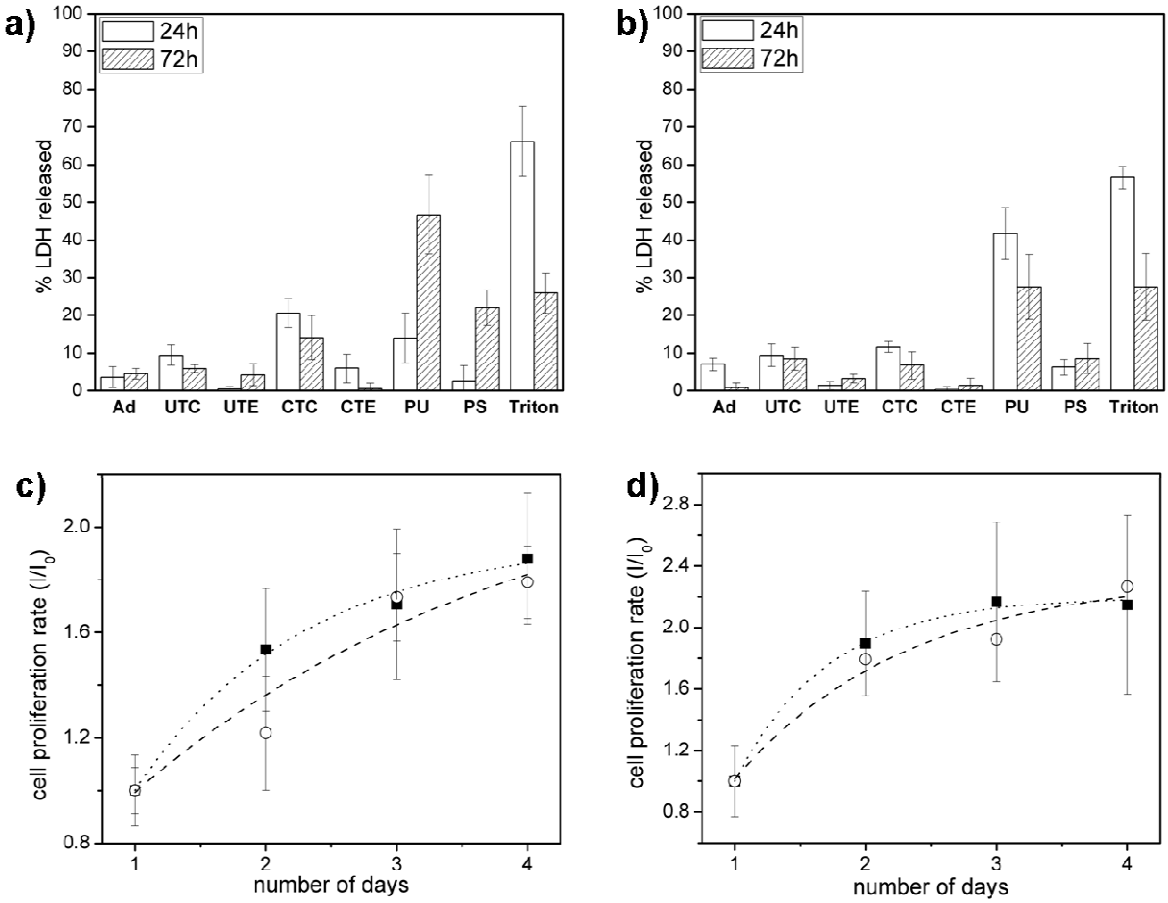

Figure 4: a, b) Cytotoxicity of osteoblast-like cells (MG63) (left) and primary fibroblasts (right). Ad = adhesion control on multiwell, UTE = uncoated thermoset extract, CTE = coated thermoset extract, UTC = uncoated thermoset contact, CTC = coated thermoset contact, PU = polyurethane positive control, PS = plastic sheet negative control. c, d) Cell proliferation of osteoblast-like cells (MG63) (left) and primary fibroblasts (right) on uncoated (circle symbols, dashed line) and coated thermosets (square symbols, dotted line); lines are drawn to guide the eye.

This result indicates that, despite the presence of silver nanoparticles, the nanocomposite coating does not represent a threat in terms of toxicity towards eukaryotic cells. Nevertheless, this information is not sufficient to state that mammalian cells can grow and proliferate on such material. Thus, in order to evaluate the cell proliferation, both osteoblasts and fibroblasts were plated on Chitlac-nAg coated and uncoated thermosets and their proliferation rate was evaluated by means of Alamar Blue assay over 4 days. Figure 4 (c,d) shows that for both osteoblasts MG63 and primary fibroblasts the proliferation rate is practically the same on uncoated and Chitlac-nAg coated thermosets, which indicates that the antimicrobial coating does not hamper cell proliferation with respect to the supporting biomaterial.

SEM and confocal characterizations were used in order to gain more information about the distribution and morphology of the eukaryotic cells cultured on the nanocomposite coating. Figure 5 refers to the tests carried out with MG63 cells: rows a) and b) display SEM images of the different surfaces without or with cell cultures, respectively, while row c) reports the confocal images at higher magnifications. SEM images indicate that the cells proliferate uniformly resulting in a layer well adhered to the substrate on both coated and uncoated surfaces. Confocal images clearly show that cells keep the same healthy morphology in the presence of the nanocomposite coating as on the uncoated surface. The actin filaments are seen to align along the grooves introduced with the polishing of the raw thermoset.

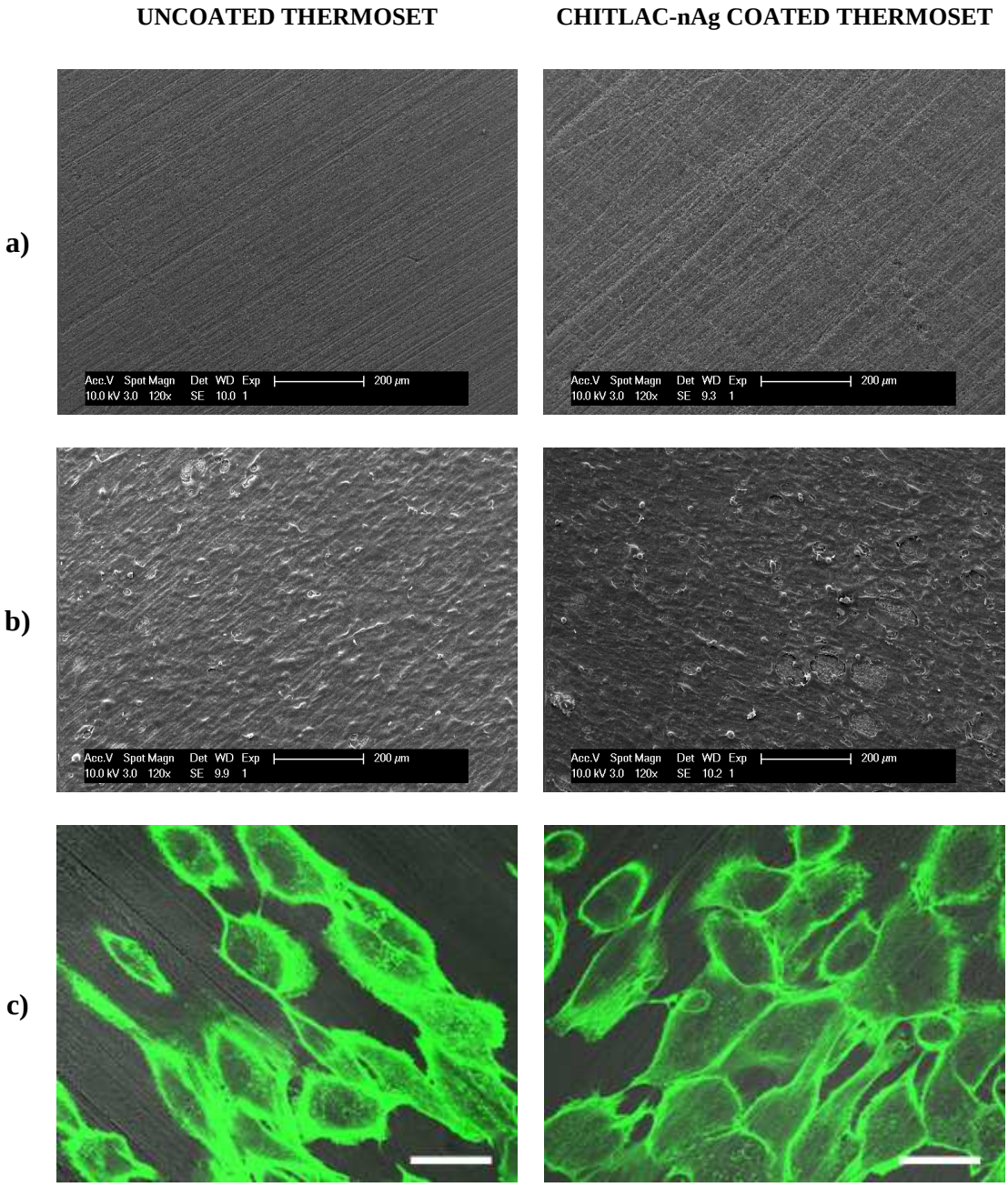

Figure 5. Micrographs of uncoated (left column) and Chitlac-nAg coated (right column) thermosets. a) SEM images of thermosets without cells. b) SEM images of MG63 cells grown for 72 h on thermosets. c) Confocal images of MG63 cells grown for 72 h on thermosets (ruler = 50 µm).

In order to assess if these qualitative results are not dependent on the cell line selected, SEM and confocal characterization were carried out also with another osteoblasts cell line, *i.e.* Saos-2. Figure

6 shows that also in this case the cells display an elongated morphology (Figure 6a and 6b) which follows the underlying ribbed structure (Figure 6c). The osteoblasts are firmly attached and spread on the polysaccharidic matrix as pointed out by the presence of numerous focal adhesions stained in red (Figure 6d). Cytoskeleton, in particular actin fibres appear well organized in the chitlac-nAg coated samples such as in uncoated samples. In the centre of Figure 6d it is possible to notice the chromosomes rearrangements that characterize cell mitosis, thus confirming the healthy condition of the cells in direct contact with the silver containing coating.

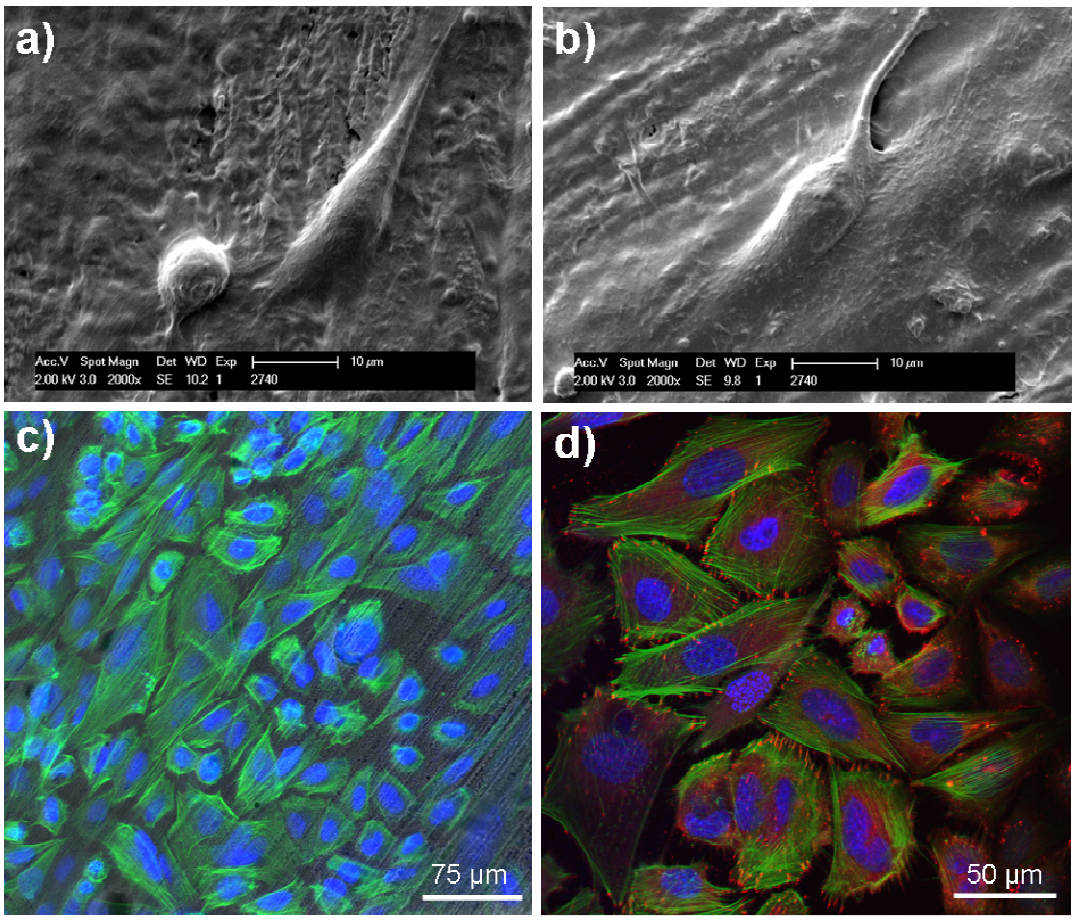

Figure 6. Saos-2 cell morphology and proliferation on uncoated and coated thermosets. Top: SEM images of cells grown on the uncoated thermoset (a), and on Chitlac-nAg coated thermoset (b). Bottom: confocal images of Saos-2 cell distribution over the Chitlac-nAg coating showing the underlying nanocomposite surface finishing (c), and highlighting the vinculin, a focal adhesion marker of cells (red spots) (d).

In analogy to what observed for osteoblast cell lines, also the morphology of primary fibroblasts grown on Chitlac-nAg coating does not appear modified in comparison with that of cells grown on uncoated samples; the cells appear uniformly spread and well adhered with a highly organized actin network (Figure 7a,b).

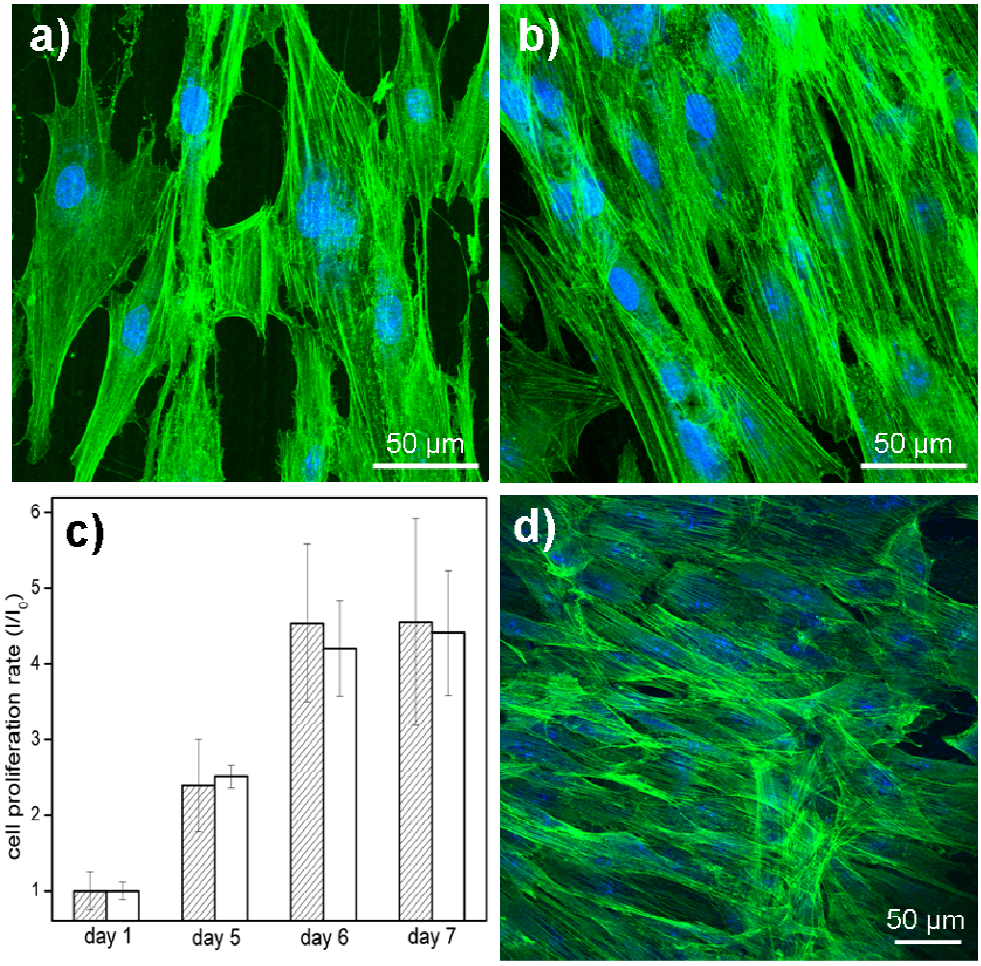

Figure 7. Top: Confocal images of human primary fibroblasts proliferated for 72 hours on uncoated (a) and Chitlac-nAg coated (b) thermosets. Bottom: c) Alamar Blue proliferation assay on human adipose-derived stem cells on Chitlac-nAg coated (striped bars) and uncoated (white bars) thermosets. d) Confocal image of human adipose-derived stem cells proliferated for 7 days on Chitlac-nAg coated thermoset.

Human adipose-derived stem cells were tested in order to preliminary evaluate the effect of the silver-containing nanocomposite coating on undifferentiated cells. Since these cells were expected

to have a lower proliferation rate with respect to the cell-lines tested, the Alamar Blue assay was performed on longer time range (seven days); the results reported in Figure 7c show that stem cells were able to attach and proliferate on Chitlac-nAg coating (striped bars) as well as on uncoated thermoset (white bars). Confocal images of stem cells grown on Chitlac-nAg coated thermoset confirmed the presence of well adhered cells all over the coating in direct contact with the substrate and also in overlapping layers (Figure 7d). Further studies are planned to study the differentiation of the stem cells proliferated on the nanocomposite coating.

Conclusions

A polysaccharide film containing silver nanoparticles was successfully prepared to coat a surface-hydrolyzed methacrylic thermoset exploiting electrostatic interactions. The nanocomposite film is effective in killing both Gram+ and Gram- bacteria; FE-SEM and TEM images reveal the presence of silver nanoparticles located on the surface of the coating allowing the direct contact between the metal and bacteria, while the considerable thickness of the nanocomposite layer could account for a long-term reservoir of the antimicrobial agent *in vivo*. This material does not exert any significant cytotoxic effect towards eukaryotic stem cells, primary cells and cell-lines, which are able to firmly attach and proliferate on the surface of the coating. Such biocompatible antimicrobial polymeric films containing silver nanoparticles may have good potentials for surface modification of medical devices, especially for prosthetic applications in orthopaedics and dentistry. The preparation technique is easy and inexpensive: in particular, the polyelectrolyte layer provides a convenient matrix for immobilizing accessible antimicrobial nanoparticles on methacrylic supports. The procedure can be adapted to almost any type of material as long as proper surface charges are present or can be produced thereon; such possibility to combine the system with other polyelectrolytes with specific biological properties could make this technique even more appealing.

Acknowledgments

The authors would like to acknowledge Prof. G. Adami for the ICP-AES measurements. This study was supported by grants from the Italian Ministry for University and Research (PRIN 2007), the Friuli Venezia Giulia Region (LR 26/2005, art. 23: "R3A2 network"), and the EU-FP6 Project "NEWBONE" (Contract Number 026279-2).

References

Ballo AM, Akca EA, Ozen T, Lassila L, Vallittu PK, Narhi TO (2009) Bone tissue responses to glass fiber-reinforced composite implants--a histomorphometric study. Clin Oral Implants Res **20**: 608-615

Ballo AM, Kokkari AK, Meretoja VV, Lassila LL, Vallittu PK, Narhi TO (2008) Osteoblast proliferation and maturation on bioactive fiber-reinforced composite surface. J Mater Sci Mater Med **19**: 3169-3177

Ballo AM, Lassila LV, Vallittu PK, Narhi TO (2007) Load bearing capacity of bone anchored fiber-reinforced composite device. J Mater Sci Mater Med **18**: 2025-2031

Balogh L, Swanson DR, Tomalia DA, Hagnauer GL, McManus AT (2001) Dendrimer-Silver Complexes and Nanocomposites as Antimicrobial Agents. Nano Lett **1**: 18-21

Chen X, Schluesener HJ (2008) Nanosilver: A nanoproduct in medical application. Toxicol Lett **176**: 1-12

Dai JH, Bruening ML (2002) Catalytic nanoparticles formed by reduction of metal ions in multilayered polyelectrolyte films. Nano Lett **2**: 497-501

Donati I, Stredanska S, Silvestrini G, Vetere A, Marcon P, Marsich E, Mozetic P, Gamini A, Paoletti S, Vittur F (2005) The aggregation of pig articular chondrocyte and synthesis of extracellular matrix by a lactose-modified chitosan. Biomaterials **26**: 987-998

Donati I, Travan A, Pelillo C, Scarpa T, Coslovi A, Bonifacio A, Sergo V, Paoletti S (2009) Polyol Synthesis of Silver Nanoparticles: Mechanism of Reduction by Alditol Bearing Polysaccharides. Biomacromolecules **10**: 210-213

dos Santos DS, Goulet PJG, Pieczonka NPW, Oliveira ON, Aroca RF (2004) Gold nanoparticle embedded, self-sustained chitosan films as substrates for surface-enhanced Raman scattering. Langmuir **20**: 10273-10277

Dotzauer DM, Dai J, Sun L, Bruening ML (2006) Catalytic Membranes Prepared Using Layer-by-Layer Adsorption of Polyelectrolyte/Metal Nanoparticle Films in Porous Supports. Nano Lett **6**: 2268-2272

Elechiguerra J, Burt J, Morones J, Camacho-Bragado A, Gao X, Lara H, Yacaman M (2005) Interaction of silver nanoparticles with HIV-1. Journal of Nanobiotechnology **3**: 6

Feng QL, Wu J, Chen GQ, Cui FZ, Kim TN, Kim JO (2000) A mechanistic study of the antibacterial effect of silver ions on *Escherichia coli* and *Staphylococcus aureus*. J Biomed Mater Res **52**: 662-668

Fu J, Ji J, Fan D, Shen J (2006) Construction of antibacterial multilayer films containing nanosilver via layer-by-layer assembly of heparin and chitosan-silver ions complex. J Biomed Mater Res A **79**: 665-674

Furr JR, Russell AD, Turner TD, Andrews A (1994) Antibacterial activity of Actisorb Plus, Actisorb and silver nitrate. J Hosp Infect **27**: 201-208

Geiser M, Rothen-Rutishauser B, Kapp N, Schurch S, Kreyling W, Schulz H, Semmler M, Im H, V, Heyder J, Gehr P (2005) Ultrafine particles cross cellular membranes by nonphagocytic mechanisms in lungs and in cultured cells. Environ Health Perspect **113**: 1555-1560

Grunlan JC, Choi JK, Lin A (2005) Antimicrobial Behavior of Polyelectrolyte Multilayer Films Containing Cetrimide and Silver. Biomacromolecules **6**: 1149-1153

Gupta A, Matsui K, Lo JF, Silver S (1999) Molecular basis for resistance to silver cations in Salmonella. Nat Med **5**: 183-188

Hachem RY, Wright KC, Zermeno A, Bodey GP, Raad II (2003) Evaluation of the silver iontophoretic catheter in an animal model. Biomaterials **24**: 3619-3622

Hernandez-Sierra JF, Ruiz F, Cruz Pena DC, Martinez-Gutierrez F, Martinez AE, de Jes·s Pozos Guillon A, Tapia-Perez H, Martinez Castanon G (2008) The antimicrobial sensitivity of Streptococcus mutans to nanoparticles of silver, zinc oxide, and gold. Nanomedicine: Nanotechnology, Biology and Medicine *In Press*,

Ho CH, Tobis J, Sprich C, Thomann R, Tiller JC (2004) Nanoseparated Plymeric Network with Multiple Antimicrobial Properties. Adv Mater **16**: 957-961

Huang H, Yang X (2004) Synthesis of polysaccharide-stabilized gold and silver nanoparticles: a green method. Carbohyd Res **339**: 2627-2631

Huang H, Yuan Q, Yang X (2004) Preparation and characterization of metal-chitosan nanocomposites. Colloids and Surfaces B: Biointerfaces **39**: 31-37

Hussain SM, Hess KL, Gearhart JM, Geiss KT, Schlager JJ (2005) In vitro toxicity of nanoparticles in BRL 3A rat liver cells. Toxicol In Vitro **19**: 975-983

Ignatova M, Voccia S, Gilbert B, Markova N, Cossement D, Gouttebaron R, Jerome R, Jerome C (2005) Combination of Electrografting and Atom-Transfer Radical Polymerization for Making the Stainless Steel Surface Antibacterial and Protein Antiadhesive. Langmuir **22**: 255-262

Ip M, Lui SL, Poon VK, Lung I, Burd A (2006) Antimicrobial activities of silver dressings: an in vitro comparison. J Med Microbiol **55**: 59-63

Kohnen W, Kolbenschlag C, Teske-Keiser S, Jansen B (2003) Development of a long-lasting ventricular catheter impregnated with a combination of antibiotics. Biomaterials **24**: 4865-4869

Kuo PL, Chen WF (2003) Formation of silver nanoparticles under structured amino groups in pseudo-dendritic poly(allylamine) derivatives. J Phys Chem B **107**: 11267-11272

Lee KJ, Nallathamby PD, Browning LM, Osgood CJ, Xu XHN (2007) In Vivo Imaging of Transport and Biocompatibility of Single Silver Nanoparticles in Early Development of Zebrafish Embryos. ACS Nano **1**: 133-143

Lee SB, Koepsel RR, Morley SW, Matyjaszewski K, Sun Y, Russell AJ (2004) Permanent, Nonleaching Antibacterial Surfaces. 1. Synthesis by Atom Transfer Radical Polymerization. Biomacromolecules **5**: 877-882

Lehtinen J, Laurila T, Lassila LVJ, Vallittu PK, Räty J, Hernberg R (2008) Optical characterization of bisphenol-A-glycidyldimethacrylate-triethyleneglycoldimethacrylate (BisGMA/TEGDMA) monomers and copolymer. Dental Materials **24**: 1324-1328

Morones JR, Elechiguerra JL, Camacho A, Holt K, Kouri JB, Ramirez JT, Yacaman MJ (2005) The bactericidal effect of silver nanoparticles. Nanotechnology **16**: 2346-2353

Multanen M, Talja M, Hallanvuo S, Siitonen A, Valimaa T, Tammela TL, Seppala J, Tormala P (2000) Bacterial adherence to silver nitrate coated poly-L-lactic acid urological stents in vitro. Urol Res **28**: 327-331

Panacek A, Kvitek L, Prucek R, Kolar M, Vecerova R, Pizurova N, Sharma VK, Nevecna T, Zboril R (2006) Silver Colloid Nanoparticles: Synthesis, Characterization, and Their Antibacterial Activity. J Phys Chem B **110**: 16248-16253

Rhim JW, Hong SI, Park HM, Ng PK (2006) Preparation and characterization of chitosan-based nanocomposite films with antimicrobial activity. J Agric Food Chem **54**: 5814-5822

Sambhy V, MacBride MM, Peterson BR, Sen A (2006) Silver Bromide Nanoparticle/Polymer Composites: Dual Action Tunable Antimicrobial Materials. J Am Chem Soc **128**: 9798-9808

Stevens KNJ, Crespo-Biel O, van den Bosch EEM, Dias AA, Knetsch MLW, Aldenhoff YBJ, van der Veen FH, Maessen JG, Stobberingh EE, Koole LH (2009) The relationship between the antimicrobial effect of catheter coatings containing silver nanoparticles and the coagulation of contacting blood. Biomaterials **30**: 3682-3690

Tezvergil A, Lassila LV, Vallittu PK (2005) The shear bond strength of bidirectional and random-oriented fibre-reinforced composite to tooth structure. J Dent **33**: 509-516

Tian J, Wong KK, Ho CM, Lok CN, Yu WY, Che CM, Chiu JF, Tam PK (2007) Topical delivery of silver nanoparticles promotes wound healing. ChemMedChem **2**: 129-136

Travan A, Donati I, Marsich E, Bellomo F, Achanta S, Toppazzini M, Semeraro S, Scarpa T, Spreafico V, Paoletti S (2010) Surface Modification and Polysaccharide Deposition on BisGMA/TEGDMA Thermoset. Biomacromolecules *In press*

Travan A, Pelillo C, Donati I, Marsich E, Benincasa M, Scarpa T, Semeraro S, Turco G, Gennaro R, Paoletti S (2009) Non-cytotoxic Silver Nanoparticle-Polysaccharide Nanocomposites with Antimicrobial Activity. Biomacromolecules **10**: 1429

Vakiparta M, Puska M, Vallittu PK (2006) Residual monomers and degree of conversion of partially bioresorbable fiber-reinforced composite. Acta Biomater **2**: 29-37

Wang YZ, Li YX, Yang ST, Zhang GL, An DM, Wang C, Yang QB, Chen XS, Jing XB, Wei Y (2006) A convenient route to polyvinyl pyrrolidone/silver nanocomposite by electrospinning. Nanotechnology **17**: 3304-3307

Yu H, Xu X, Chen X, Lu T, Zhang P, Jing X (2006) Preparation and Antibacterial Effects of PVA-PVP Hydrogels Containing Silver Nanoparticles. J Appl Polym Sci **103**: 125–133

Zhao DS, Moritz N, Laurila P, Mattila R, Lassila LVJ, Strandberg N, Mäntylä T, Vallittu PK, Aro HT (2009) Development of a multi-component fiber-reinforced composite implant for load-sharing conditions. Medical Engineering & Physics **31**: 461-469

Paper 5

Cytotoxicity Evaluation of Hydrogels Embedding Gold Nanoparticles

Eleonora Marsich*, Andrea Travan, Ivan Donati, Andrea Di Luca,

Monica Benincasa, Sergio Paoletti

Department of Life Sciences, University of Trieste, Via Giorgieri 1, Trieste I-34127, Italy

---

* To whom correspondence should be addressed. Tel.: +39 040 558

3682. Fax: +39 040 558 3692. E-mail: emarsich@units.it

Abstract

A nanocomposite hydrogel based on natural polysaccharides and gold nanoparticles (AC-nAu) has been prepared and its biological effects were tested *in vitro* with both bacteria and eukaryotic cells. Antimicrobial tests showed that AC-nAu gels are effective in killing both Gram+ (*S. aureus*) and Gram- (*P. aeruginosa*) bacteria. LDH assays pointed at a toxic effect towards eukaryotic cell-lines (HepG2 and MG63), at variance with silver-based hydrogels; cytofluorimetry studies demonstrated an apoptosis-related mechanism that leads to cell death after 24 hours of direct contact with AC-nAu gels. *In vivo* biocompatibility has been evaluated in a rat model: this study aimed at investigating the soft tissue peri-implant reaction after 1 month of implantation. The results show that silver-containing samples induced a soft tissue capsule of the same average thickness of the control sample (devoid of nanoparticles) (~50 µm), while in the case of gold-containing materials the fibrotic capsule was thicker (~100 µm), confirming a higher biocompatibility for silver-based samples than for gold-based ones.

Introduction

Bulk gold is the most noble of all metals and as such considered inert[1]. This behaviour is found only at a macroscopic level, since this metal exhibits different properties when moving to nanoscale structures that find increasing attention in plasmonics-related field. For instance, gold nanoparticles are being employed for molecular imaging applications[2], Surface Enhanced Raman Scattering[3;4], as catalyzing agents[5], tracers in diagnostics[6] and antimicrobial agents[7-10;10;11]. Gold compounds are also used for the treatment of rheumatoid arthritis[12] and were referred to inhibit bone-resorbing osteoclasts[13].

However, once reaching the nanoscale, certain materials (*e.g.* carbon) do exhibit significant toxicity to mammalian cells even if they are biochemically inert and biocompatible in bulk size[6;14-17]. When dealing with metal nanoparticles, only a few studies have provided insights on their interactions with eukaryotic cells and their relevant toxicological implications, in contrast to the attention paid to their applications [18]. In the last few years, despite the great excitement about the potential uses of gold nanoparticles, researchers have become increasingly aware that potential nanoparticle toxicity must be investigated before any *in vivo* applications of gold nanoparticles can move forward[6].

The recent literature contains conflicting data regarding the cytotoxicity of gold nanoparticles[19]. Shukla et al.[16] showed that gold nanoparticles are not cytotoxic to macrophage cells, reduce the production of reactive oxygen and nitrite species, and do not elicit secretion of proinflammatory cytokines TNF-R and IL1-α, underlining their non-immunogenic and biocompatible properties with the potential for application in nanobiotechnology and molecular medicine therapies. On the other hand, nanoparticles cytotoxicity directly related to their dimensions has been reported[20]. Jan et al.[21] pointed to the inhibitory effect of gold nanoparticles on HepG2 cell growth and Pan et al.[19] discussed the issue of size-dependence on the mechanism of gold nanoparticles cytotoxicity. Mitchell et al.[22] reported the toxicity of gold nanoparticles against a yeast (*Saccharomyces cerevisiae*).

Within this debate, metal nanoparticles like gold and silver have also been explored for their broad-spectrum antimicrobial activity[7]. Colloidal gold and silver (AuNPs and AgNPs) were successfully used to treat both Gram+ and Gram- bacteria[11]. Ray et al.[9] studied the antimicrobial efficacy of metallopharmaceutical agents based on gold complexes and Nomyia et al.[23] discussed the antimicrobial and antifungal activity of gold complexes.

A general way to prepare metal nanoparticles is by reducing metal ions in the presence of a stabilizing agent such as a polymer in order to prevent aggregation. Polymers like chitosan[24;25], methylcellulose[26] and amphiphilic block copolymers[27] have been used to stabilize gold nanoparticles. Yang et al.[28] reported a method to prepare gold nanoparticles using chitosan as both reducing and capping agent. Dinda et al.[29] reported a method for the formation of gold nanoparticles by using ionic liquids based on ascorbic acid. Esumi et al.[30]demonstrated that hydroxyl groups of Sugar-Persubstituted Poly(amidoamine) dendrimers reduce Au(III) to Au(0).

In the antimicrobial field, many efforts are aimed at the preparation of biocompatible and hydrated materials endowed with broad spectrum antibacterial activity for topic applications like the treatment of burns and chronic wounds; in this perspective, hydrogels appear as the ideal matrix for the selected biocidal agent. Recently, the *in vivo* evaluation of noble metal coatings (Ag, Au, Pd coated catheters) has pointed out a higher biocompatibility for silver coatings, while the addition of gold or palladium induced the formation of a thicker fibrotic capsule surrounding the implants[31].

A recent study of the authors[17] discussed the preparation of a nanocomposite hydrogel based on biocompatible polysaccharides (a lactose-modified chitosan, named “Chitlac”, and alginate) and silver nanoparticles that displays considerable antimicrobial efficacy without exerting any cytotoxic activity towards eukaryotic cells in vitro.

In the present study we describe the preparation of 3D hydrogels structures based on polysaccharides and gold nanoparticles and we assess their antimicrobial properties and cytotoxicity. The results obtained in the case of hydrogels containing gold nanoparticles are compared with those loaded with silver nanoparticles in order to evaluate the biological effects of

the two nanocomposite systems based on different metal nanoparticles; *in vitro* studies were carried out to elucidate antimicrobial activity and cytotoxic mechanism, while *in vivo* tests evaluated interfacial soft tissue response in a rat model.

Materials and methods

Materials

Chitosan was purchased from Sigma Chemical Co (St. Luois, MO) and purified according to the procedure reported elsewhere[32]. Chitlac (1-Deoxylactit-1-yl chitosan, CAS registry number 85941-43-1) sample was prepared according to the procedure reported elsewhere[33] starting from a highly deacetylated chitosan (residual acetylation degree = 11.3%, Aldrich Chemical Co. (USA). The relative molar mass of Chitlac was estimated to be approximately 1.5×10^6. Ultrapure alginate ($F_G = 0.65$, $F_{GG} = 0.53$) was purchased from Novamatrix. Chloroauric acid ($HAuCl_4$), Ascorbic acid, 4-(2-hydroxyethyl)-1-piperazineethanesulfonic acid, $CaCO_3$ (mean particle size 3 µm), Glucono-d-lactone (GDL) and LDH based TOX-7 kit (Sigma-Aldrich) were purchased from Sigma Chemical Co (St. Luois, MO). The colloidal solution of Chitlac and with silver nanoparticles (Chitlac-nAg) was prepared as reported elsewhere[17].

Gold nanoparticles preparation in the presence of Chitlac or chitosan

Gold nanoparticles were obtained by reducing gold ions in polysaccharides solutions according to the following procedures: freeze-dried Chitlac or chitosan was dissolved in deionized water at different concentrations (2, 4, 8 and 12 g/L). Chitlac and chitosan solutions were mixed with $HAuCl_4$ solutions to achieve the final concentration of 1 mM $HAuCl_4$; the samples were then heated for 24 hours at 55°C and a red-violet colloidal solution was obtained. When the polysaccharide concentration was 4 g/L the colloidal solution is referred to as “Chitlac-nAu” or “chitosan-nAu”. For antibacterial tests 20% Muller-Hinton broth was added to the colloidal solutions.

Hydrogel preparation

Alginate-Chitlac (AC) hydrogel: for the preparation of alginate-Chitlac hydrogels an *in-situ* calcium release approach was used. Briefly, a Chitlac solution was added to an alginate solution (final concentrations: alginate 15 g/L, Chitlac 2 g/L, NaCl 0.15 M, HEPES 0.01 M, pH 7.4) and the mixture was blended with an inactivated form of Ca^{2+} ($CaCO_3$, 15 mM) followed by the addition of the slowly hydrolyzing D-glucono-δ-lactone (GDL) ([GDL]/[Ca^{2+}] = 2). Aliquots of this gelling solution were poured in well tissue culture plates. Finally, the gels were washed with $CaCl_2$ solution 5 mM to remove residual GDL.

Alginate-Chitlac-nAu (AC-nAu) hydrogel: alginate-Chitlac hydrogels containing gold nanoparticles were prepared according to the procedure of the AC-Gels using Chitlac-nAu instead of Chitlac solutions. For antibacterial tests, 20% Muller-Hinton broth was added to both Chitlac and alginate solutions.

Alginate-Chitlac-nAg (AC-nAg) hydrogel: alginate-Chitlac hydrogels containing silver nanoparticles were prepared according to the procedure of the AC-Gels using Chitlac-nAg instead of Chitlac solutions, as previously reported[17].

UV-Vis spectroscopy

UV-Visible (UV-Vis) spectroscopy measurements were performed with a Cary 400 Spectrophotometer (data interval: 0.5 nm; scan speed: 300 nm/min). All samples solutions were diluted 1:2.

Transmission Electron Microscopy (TEM)

TEM images were taken by means of a PHILIPS EM 208 Microscope; the solutions were deposited onto Nickel grids coated with a carbon film and dried overnight.

Bacterial growth Inhibition Tests

Bacterial growth Inhibition Tests were performed using bacteria stains of *S. aureus* (ATCC 25923) and *P. aeruginosa* (ATCC 27853) diluted in 20% Muller-Hinton broth to give 1 x 10^6 Colony Forming Units (CFU/mL), in presence or absence of Chitlac-nAu. Bacteria growth was monitored

for 4 hours by measuring the absorbance at 620 nm 10 min with a microtiter plate reader (Tecan Trading AG, Switzerland).

Growth Inhibition Assays in Solid Medium

The growth inhibition in solid medium was evaluated by smearing with sterile cotton swabs bacterial suspensions (10^6 CFU/mL) on Petri dishes prepared as described above (Hydrogel preparation). After overnight incubation at 37°C, the presence of visible colonies was evaluated. Growth controls were carried out on Muller-Hinton agar plates and AC gels in the presence of Muller-Hinton medium.

LDH cytotoxicity assay

In vitro cytotoxicity of AC-nAu gels was evaluated by using the lactate dehydrogenase assay (LDH assay- TOX-7 Sigma) on human hepatocarcinoma (HepG2) and human osteosarcoma (MG63) cell lines. Cylindrical samples with a length of 5 mm and a diameter of 4 mm were used and the tests were performed by direct contact and on liquid extract of material. For direct contact test, 50000 cells were plated on 24-well plates and after complete adhesion, culture medium was changed with 250 µL of fresh medium. Tested materials (in quadruplicate) were directly deposited on the cell layer. After 24 and 72 hours, medium was collected and the LDH assay was performed according to the manufacture's protocol. In extraction test, samples were incubated in extraction medium (Dulbecco's modified Eagle's medium, inactivated fetal bovine serum 10%, penicillin 100 U/ml, streptomycin 100 µg/ml and L-glutamine 2 mM) for 24 h at 37 °C and 5% pCO_2. The surface/volume ratio of the samples and the medium was 1.25 cm^2/mL. After incubation, extraction media were added on cells seeded on 24-well plates (50000 cells/well). Tested materials (in quadruplicate) were directly deposited on the cell layer. After 24 and 72 hours, medium was collected and the LDH assay was performed according to the manufacture's protocol. As a positive control material, polyurethane films (PU) containing 0.25% zinc dibuthyldithiocarbamate (ZDBC) (8 mm discs) were used. As negative control material, plastic sheet (8 mm discs) were used (PS). For the extraction test, each sample (in quadruplicate) was incubated in cell culture medium (1 mL)

for 24 h at 37 °C and 5 % pCO2. After incubation, the extraction media were added on cells seeded on 24-well plates (50000 cells/well). As positive control, Triton 1% was used. The LDH assays were performed after 24 h and 72 hours as described above. Each material test was performed in quadruplicate. Evaluation of cytotoxicity was calculated according to the formula: % LDH released = [(A-B)/(C-B)] x 100 %, with A = LDH content from sample; B = LDH content of culture medium; C = maximal LDH content after cell lysis).

Apoptosis assays

Annexin V assay was used to evaluate cell apoptosis. Apoptosis was estimated in MG63 cells after 18 hours of incubation with AC-nAU hydrogels directly deposited on cell layer. Azacitidine (50 μM) was used as apoptosis positive control. Annexin V assay was performed using the Annexin V-FITC Apoptosis Detection kit by Sigma according to the manufacture's protocol and data collected by cytofluorimetric analysis.

In vivo tests and histological analyses

For *in vivo* test, the hydrogels were prepared according to the protocol reported above using ultrapure endotoxin-free alginate. After gelification, the hydrogels were dried under hood, cut in circular films with diameter 8 mm and thickness 1 mm and UV sterilized.

The animal model

Wistar rats (200–250 g) had free access to water and a standard pellet diet (hatlan Teklad 2018); they were anesthetized using Tribromoethanol (Sigma, 250 mg/kg i.p.) and xilazin (Virbaxil 2 %, 10 mg/kg i.p.). Rats were shaved on the back and cleaned with betadine. Four rats were used for each type of material (AC-nAg and AC-nAu). Each rat received one nanocomposite sample and one control sample (AC) subcutaneously on the back. Separate incisions were made for each implant type. The wounds were closed with two sutures (Ethilon 5-0 FS-3, Ethicon1, Johnson & Johnson, Belgium). The implants were kept for 1 month, in order to evaluate the fibrous capsule formation and the late inflammatory response. For explantation, the animals were sacrificed by CO_2 inhalation. The animal experiment was in compliance with Italian National law D.L.vo 116/92.

Histological analysis

After 1 month, the implants together with surrounding tissues were excised *en bloc* and immersed in 10% buffered formalin for 3-5 days. The specimens were dehydrated in a graded series of ethanol and embedded in Paraplast® Plus Tissue Embedding Medium added with dimethyl sulphoxide (DMSO) (McCormick).The embedded tissue was sectioned in 3-4 µm thick section and stained with ematoxylin-eosin for light microscopy. The thickness of the fibrous capsule around each implant was analyzed at equally located points on both sides of the implant disk by light microscopy (Leica DMLB) equipped with photographic system (Leica DC100).

Results and discussion

Colloidal solutions containing gold nanoparticles were prepared by reduction of corresponding metal ions (Au^{+++}) to zeroth-valent metal nanoparticles in the presence of polysaccharides solutions (Chitlac or chitosan). The reduction of gold ions occurred upon heating the polysaccharide solution with $HAuCl_4$ at 55°C, according to the procedure proposed by Huang et al.[25]. During the thermal treatment the solutions turned from light yellow to red-violet, suggesting the formation of the metallic nanoparticles. The formation of a surface plasmon resonance band arising from gold nanoparticles was monitored by means of UV-Vis absorption spectroscopy after 24 hours of incubation at 55°C (Figure 1a). Figure1b shows the variation of the plasmon band intensity as a function of the heating time in the case of nanoparticles formation in Chitlac (4 g/L); after about 24 hours the intensity reaches a plateau, suggesting the completion of nanoparticles formation. The effect of Chitlac concentration on the plasmon resonance band was also explored (Figure 1a, solid lines): the changes in absorption spectra indicate that size and dispersion of gold nanoparticles are strongly affected by polysaccharide concentration. In particular, the highest peak was recorded for the Chitlac concentration of 4 g/L and was centred at about 530 nm, while lower or higher concentrations were associated with lower peak intensities (8 g/L, 12 g/L) or red shifted non-symmetrical curves (2 g/L). As a comparison, the UV-Vis spectrum after 24 h in the case of

chitosan 4 g/L was recorded (Figure 1a, dashed line): the spectrum is less intense and asymmetrical and the plasmon peak is red-shifted with respect to Chitlac. These data suggest the formation of smaller and better stabilized nanoparticles in Chitlac, whereas in chitosan there is a higher tendency to aggregation. TEM images confirmed this indication: Figure 1c,d shows the presence of well dispersed nanoparticles in Chitlac smaller than 20 nm, while in chitosan we can observe both dispersed nanoparticles and large aggregates with branched structures (Figure 1e,f).

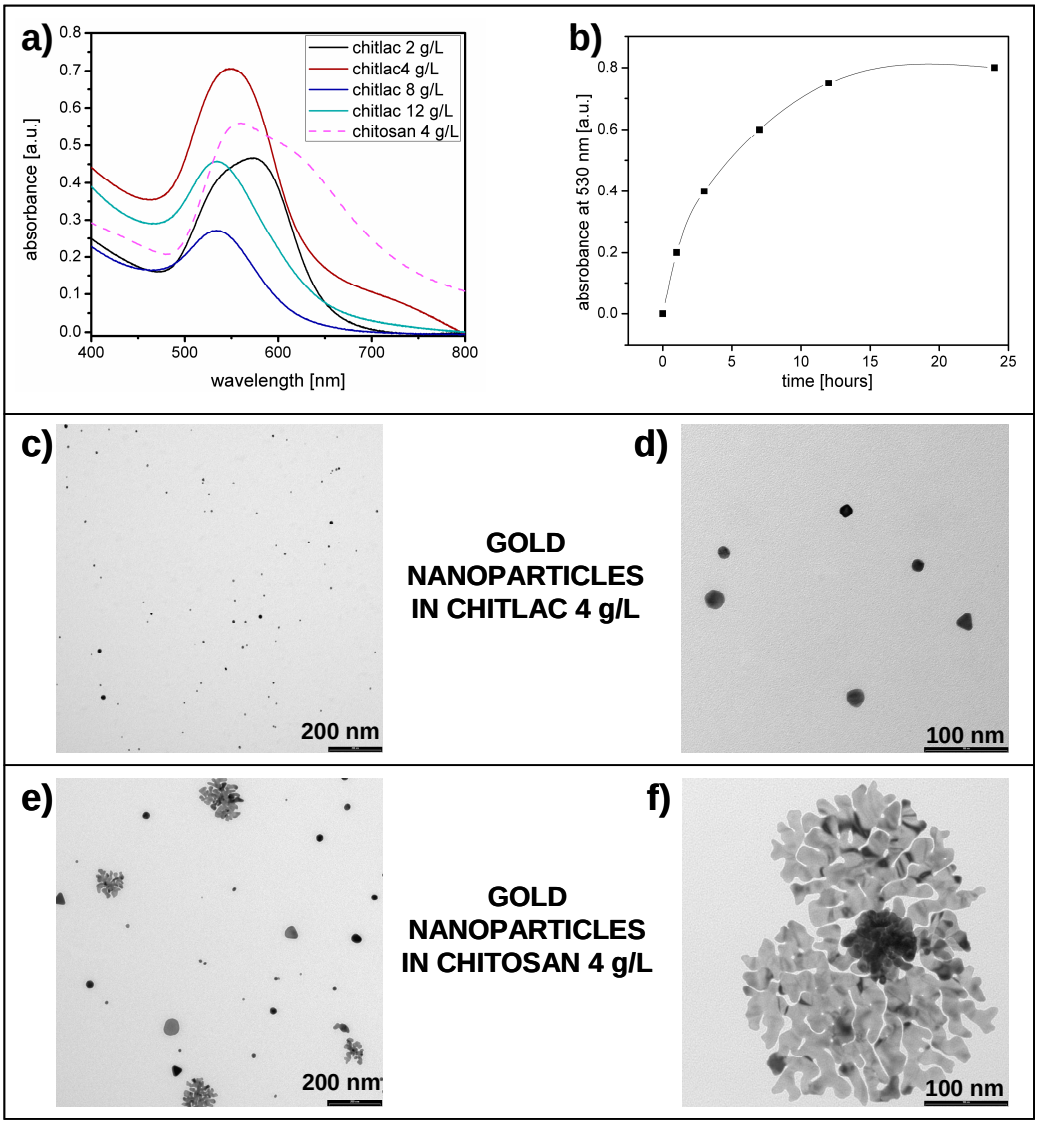

Figure 1: a) UV-Vis spectra of gold nanoparticles in Chitlac at various polysaccharide concentration (solid lines) and of gold nanoparticles in chitosan (dashed line). b) Evolution of the plasmon peak intensity in Chitlac-nAu (Chitlac = 4 g/L) as a function of incubation time at 55°C. c,d) Gold nanoparticles formed in Chitlac 4 g/L. e,f) Separate gold nanoparticles and branched aggregates formed in chitosan 4 g/L.

The better performance of Chitlac with respect to chitosan might be attributed to the presence of the hydrophilic and bulky lactitol groups decorating the modified polysaccharide[17]; they account for a higher steric hindrance toward nanoparticle aggregation and formation of larger structures. Given the UV-Vis results, the Chitlac concentration was set at 4 g/L for the preparation of the colloidal system used for all subsequent biological characterizations (hereafter named "Chitlac-nAu").

In order to evaluate the antimicrobial activity of the Chitlac-nAu colloidal solution, both Gram+ and Gram- strains were considered. Bacteria growth inhibition tests were performed incubating *S. aureus* and *P. aeruginosa* in 20% Mueller-Hinton broth in the presence of Chitlac-nAu. Bacterial growth was followed as increase of absorbance at 620 nm. A marked inhibition of the bacterial growth is achieved in the presence of Chitlac-nAu in comparison with the growth control (Figure 2a,b): in fact, the bacterial growth curve remained close to zero in the case of gold-treated runs, thus indicating the effective bacterial inhibition associated with Chitlac-nAu. Similar results were obtained for *E. coli* and *S. epidermidis* (data not shown).

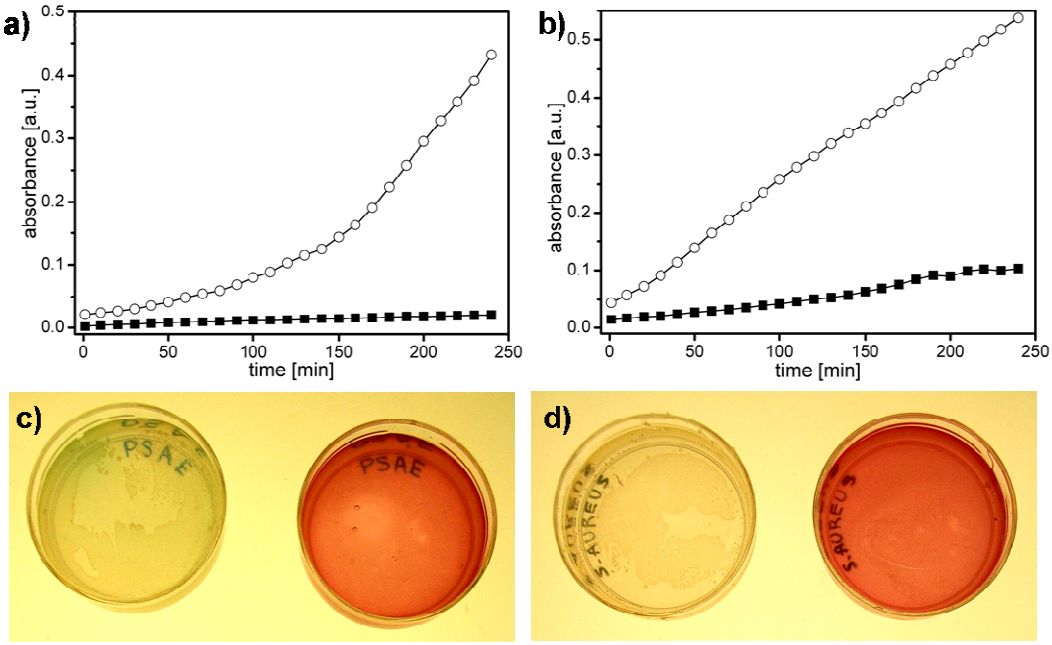

Figure 2. Top: Bacteria growth kinetics of *P. aeruginosa* (a) and *S. aureus* (b) treated with the colloidal solution Chitlac-nAu (square) and with Mueller-Hinton broth (circles). Bottom: Growth of *P. aeruginosa* (c) and *S. aureus* (d) on AC-nAu nanocomposite hydrogels (violet gels) and on agar plates (transparent gels).

The Chitlac-nAu colloidal solution was also tested *in vitro* on eukaryotic cells: LDH cytotoxicity assays pointed out a cytotoxic effect both on human hepatocarcinoma (HepG2) and human osteosarcoma (MG63) cell lines leading to cell death after 24 hours (data not shown). This result was expected since also in the case of silver the Chitlac-nAg colloidal solution was toxic towards the same cell lines[17]; this fact was attributed to the lack of physical barriers to nanoparticle diffusion into cells which determines their generalized (bio)availability, with the risk of a massive nanoparticles uptake by eukaryotic cells. For this reason, we prepared three dimensional structures to entrap gold nanoparticles by exploiting the gel forming properties of alginate and its miscibility with Chitlac-nAu colloidal solutions. In an ideal case, as already demonstrated for AC-nAg gels[17], such nanocomposite hydrogel could prevent nanoparticles from being available for cell uptake and, at the same time, preserve their antimicrobial activity allowing the direct interaction of the nanoparticles with bacteria surface proteins, which are considered the main molecular targets of nanoparticles[34]. The binary mixture of alginate and Chitlac-nAu allowed for the preparation of homogeneous hydrogels by exploiting the *in situ* gelification technique[35;36]: the result was a violet semi-transparent construct (Figure 4b). It is also important to underline that neither nanoparticle aggregation or polymer phase separation were observed during and after gel formation.
To assess the extent of bacterial growth on the nanocomposite hydrogel, bacteria were smeared on the surface of AC-nAu gels while agar plates were used as controls. After overnight incubation, bacterial colonies were clearly visible on agar plates, while they were completely absent on the gold nanoparticles-containing gels (Figure 2c,d), showing that the antibacterial activity persists also in the semi-solid structure.
In vitro cytotoxicity of the nanocomposite hydrogel (AC-nAu) towards HepG2 and MG63 cell-lines was tested by means of LDH assay (Figure 3). A similar approach was previously followed by the authors in the case of AC-nAg gels where no cytotoxic effect was detected on the same cell-lines[17]. At variance, the gold-nanoparticles containing gels were found to exert cytotoxic activity both by direct contact with cells and as extraction media solutions from the gel. As a matter of fact,

there was a significant difference in the release of lactate dehydrogenase (LDH) between the AC-nAu treated cells and control groups after 24 hours (Figure 3).

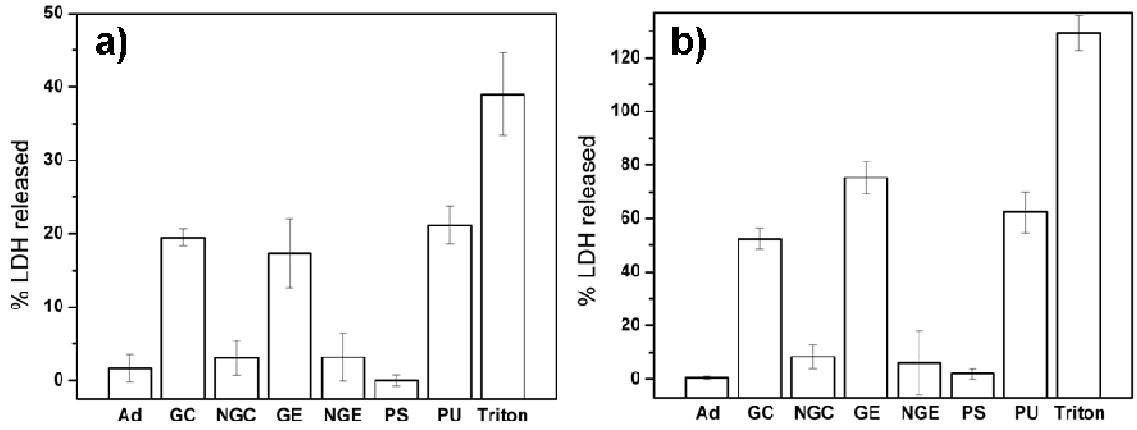

Figure 3. Effect of AC-nAu gels on LDH leakage from (a) human hepatocarcinoma (HepG2), and (b) human osteosarcoma (MG63) cell lines. The cytotoxicity test was performed both with the extract from gel material (GE) and with the gel material itself by direct contact with cell layer (GC). Control cells cultured in adhesion in complete DMEM medium and cells treated with AC gels lacking gold nanoparticles (NGC and NGE extract) were run in parallel to AC-nAu gels treated groups. The percentage of LDH release was calculated by dividing the amount of activity in the medium by the total activity (medium and cell lysate) after subtraction of the control. Polyurethane sheets (PU) were used as contact positive control, plastic sheets (PS) were used as contact negative control and Triton was used as extract positive control. The data are expressed as mean ±SD of four independent experiments.

This was an interesting finding because, in the case of AC-nAg, the gel structure was able to embed silver within the structure and the cell viability was not affected. Thus, in the case of gold, the metal (both as nanoparticles and ionic species) does not seem to be entrapped within the gel matrix as efficiently as in the case of silver. One could speculate that this effect is caused by different coordination ability of the polysaccharides towards the two metals. Hence, at this point of the research, the cause of AC-nAu gel toxicity might in principle be ascribed to the release of both metallic (nanoparticles) and anionic species of gold; further studies are required for a deeper understanding of this complex mechanism.

A study on cellular death mechanism was tackled in order to elucidate whether it is related with cell necrosis or apoptosis. To this aim, the cells were incubated with AC-nAu gels for 18 hours and then

processed for cytofluorimetric analysis (Figure 4a,c). The results showed that, after 18 hours of incubation with AC-nAu gels, the late apoptotic cells increased from 2.8 % to 10.8 % (Q2 quadrant), while cells in early apoptosis increased from 0.5 % to 4.9 % (Q4 quadrant) with respect to non-treated cells. In view of these results, the hypothesis of cell necrosis can be ruled out since the death mechanism associated with metal release can be ascribed to apoptosis.

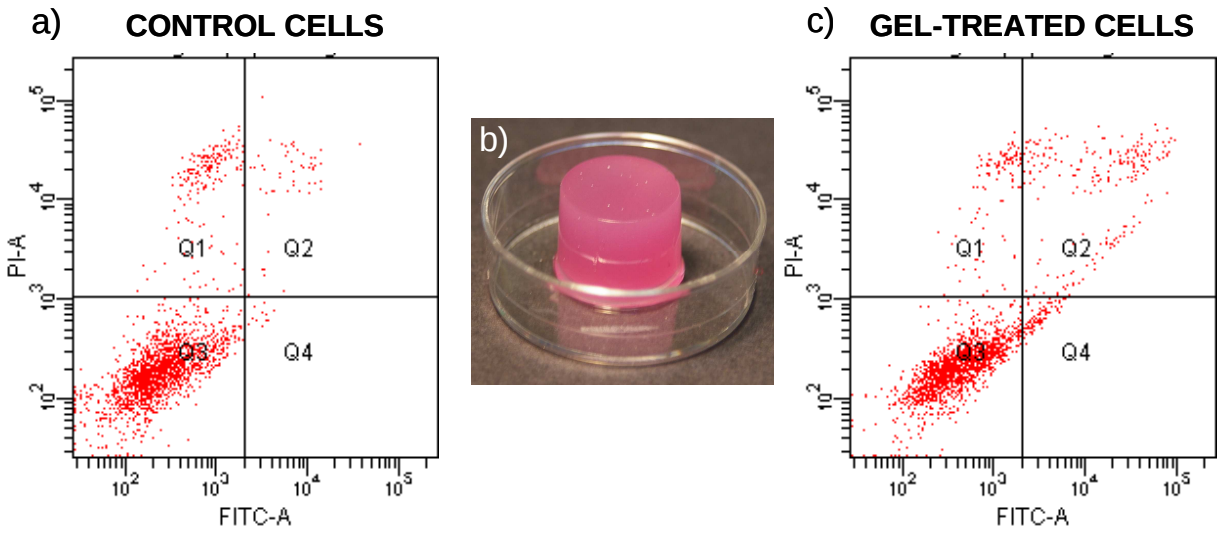

Figure 4. a,c) Cytofluorimetry plots of MG63 cells respectively untreated (a) and treated (c) for 24 h with AC-nAu. b) The semi-transparent nanocomposite hydrogel embedding gold nanoparticles (AC-nAu)

The biological behaviour of the nanocomposite hydrogels was further explored by means of *in vivo* tests in a rat model; for this test, the samples were dried, sterilized and implanted subcutaneously and after 1 month histological analyses were carried out (Figure 5). As control materials, both AC and AC-nAg were considered. The images show, from the inside tissues towards the implant (white zone on top), the cutaneous muscle, the connective soft tissues and a fibrotic tissue composed by fibroblast cells and collagen fibres: the three different samples have all induced the formation of a fibrotic capsule, while no damage, inflammation or morphological alteration of the surrounding tissues were observed.

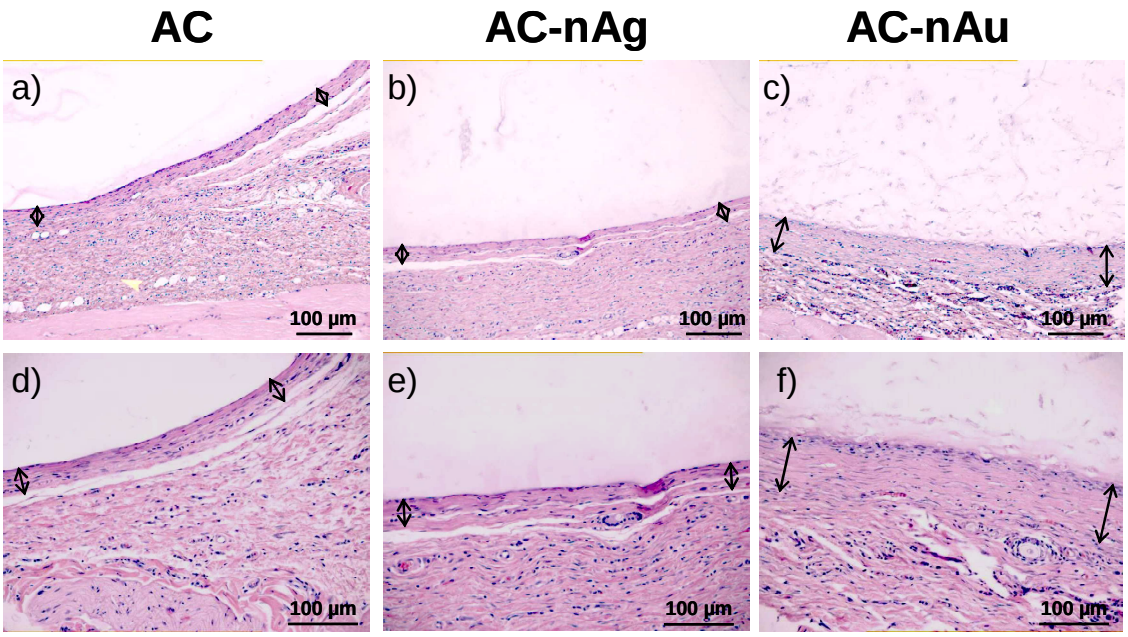

Figure 5. Histological analyses of the fibrous capsule surrounding the implants; the arrows indicate the section of the fibrous capsules formed after 1 month at the interface with the samples (white zones on top). Top: peri-implant tissues in the case of AC (a), AC-nAg (b) e AC-nAu (c). Bottom (d,e,f): magnifications of the fibrotic capsules near the three different samples.

This capsule is thinner in the case of AC and AC-nAg (~ 50 µm) while in the case of AC-nAu the thickness is higher (~ 80÷100 µm). The increased thickness of the capsule in the case of gold is in line with its *in vitro* cytotoxicity. In facts, although for the *in vivo* test the material is in contact with a much more complex biological system, the higher level of toxicity revealed by LDH assays seems to be confirmed in the rat model in terms of a thicker fibrotic capsule formation. In the literature, the fibrous capsule thickness has been correlated to enhanced ion release and ion toxicity when metals and their alloys were inserted in rabbit muscle[37]; toxic materials, like copper-coated implants, induced a dense fibrous capsule of thickness about 150–200 µm with newly formed blood vessels and inflammatory cells, while a capsule around titanium (standard control material clinically used) exhibited a well organized thin capsule of only 90 µm[38]. These data strengthen the hypothesis that in the case of AC-nAu samples the release of gold causes adverse effects displayed

by cytotoxicity *in vitro*, and by the increased thickness of fibrotic capsules *in vivo*. The issue regarding the form and amount of gold release remains to be elucidated.

Conclusions

In the present study we have obtained homogeneous nanocomposite systems based on natural polysaccharides and gold nanoparticles formed in Chitlac solutions, whose lactose moieties account for the preparation of smaller and better dispersed particles with respect to chitosan. Although these mixed hydrogels displayed considerable antimicrobial activity, they exerted also toxic effect towards eukaryotic cells as demonstrated by *in vitro* assays, at variance with similar gels containing silver nanoparticles; the gold-related cytotoxicity is due apoptotic mechanisms as demonstrated by cytofluorimetric studies. *In vivo* tests showed a good biocompatibility of these metal nanocomposites that caused only the formation of a limited fibrous capsules around the implant without signs of chronic inflammation, although gold-based nanocomposites displayed the highest fibrogenic potential, thus confirming the *in vitro* indications.

Bibliography

[1] C. Brown, M. Whitehouse, E. Tiekink, and G. Bushell, "Colloidal metallic gold is not bio-inert," *Inflammopharmacology*, vol. 16, no. 3, pp. 133-137, June2008.

[2] J. F. Hainfeld, D. N. Slatkin, T. M. Focella, and H. M. Smilowitz, "Gold nanoparticles: a new X-ray contrast agent," *Br J Radiol*, vol. 79, no. 939, pp. 248-253, Mar.2006.

[3] S. Saha, A. Pal, S. Pande, S. Sarkar, S. Panigrahi, and T. Pal, "Alginate Gel-Mediated Photochemical Growth of Mono- and Bimetallic Gold and Silver Nanoclusters and Their Application to Surface-Enhanced Raman Scattering," *The Journal of Physical Chemistry C*, vol. 113, no. 18, pp. 7553-7560, Apr.2009.

[4] O. Siiman and S. Ledis, "Surface-enhanced Raman scattering (SERS) of random silver or gold particle arrays on aminodextran-coated polystyrene beads," *Journal of Raman Spectroscopy*, vol. 36, no. 12, pp. 1125-1133, 2005.

[5] D. M. Dotzauer, J. Dai, L. Sun, and M. L. Bruening, "Catalytic Membranes Prepared Using Layer-by-Layer Adsorption of Polyelectrolyte/Metal Nanoparticle Films in Porous Supports," *Nano Lett.*, vol. 6, no. 10, pp. 2268-2272, Oct.2006.

[6] C. J. Murphy, A. M. Gole, J. W. Stone, P. N. Sisco, A. M. Alkilany, E. C. Goldsmith, and S. C. Baxter, "Gold Nanoparticles in Biology: Beyond Toxicity to Cellular Imaging," *Acc. Chem. Res.*, Aug.2008.

[7] J. F. Hernandez-Sierra, F. Ruiz, D. C. Cruz Pena, F. Martinez-Gutierrez, A. E. Martinez, A. de Jes·s Pozos Guillon, H. Tapia-Perez, and G. Martinez Castanon, "The antimicrobial sensitivity of Streptococcus mutans to nanoparticles of silver, zinc oxide, and gold," *Nanomedicine: Nanotechnology, Biology and Medicine*, vol. In Press, Corrected Proof Nov.2008.

[8] S. Nath, C. Kaittanis, A. Tinkham, and J. M. Perez, "Dextran-Coated Gold Nanoparticles for the Assessment of Antimicrobial Susceptibility," *Anal. Chem.*, Jan.2008.

[9] S. Ray, R. Mohan, J. K. Singh, M. K. Samantaray, M. M. Shaikh, D. Panda, and P. Ghosh, "Anticancer and Antimicrobial Metallopharmaceutical Agents Based on Palladium, Gold, and Silver N-Heterocyclic Carbene Complexes," *J. Am. Chem. Soc.*, vol. 129, no. 48, pp. 15042-15053, Dec.2007.

[10] V. P. Zharov, K. E. Mercer, E. N. Galitovskaya, and M. S. Smeltzer, "Photothermal nanotherapeutics and nanodiagnostics for selective killing of bacteria targeted with gold nanoparticles," *Biophys. J.*, p. biophysj, Oct.2005.

[11] Y. Zhang, H. Peng, W. Huang, Y. Zhou, and D. Yan, "Facile preparation and characterization of highly antimicrobial colloid Ag or Au nanoparticles," *J. Colloid Interf. Sci.*, vol. 325, no. 2, pp. 371-376, Sept.2008.

[12] J. D. Jessop, "Gold in the treatment of rheumatoid arthritis -- why, when and how?," *J Rheumatol Suppl*, vol. 5, pp. 12-17, 1979.

[13] T. Hall, H. Jeker, H. Nyugen, and M. Schaeublin, "Gold salts inhibit osteoclastic bone resorption in vitro," *Inflammation Research*, vol. 45, no. 5, pp. 230-233, May1996.

[14] O. Bar-Ilan, R. M. Albrecht, V. E. Fako, and D. Y. Furgeson, "Toxicity assessments of multisized gold and silver nanoparticles in zebrafish embryos," *Small*, vol. 5, no. 16, pp. 1897-1910, Aug.2009.

[15] B. D. Chithrani, A. A. Ghazani, and W. C. W. Chan, "Determining the Size and Shape Dependence of Gold Nanoparticle Uptake into Mammalian Cells," *Nano Lett.*, vol. 6, no. 4, pp. 662-668, Apr.2006.

[16] R. Shukla, V. Bansal, M. Chaudhary, A. Basu, R. R. Bhonde, and M. Sastry, "Biocompatibility of Gold Nanoparticles and Their Endocytotic Fate Inside the Cellular Compartment: A Microscopic Overview," *Langmuir*, vol. 21, no. 23, pp. 10644-10654, Nov.2005.

[17] A. Travan, C. Pelillo, I. Donati, E. Marsich, M. Benincasa, T. Scarpa, S. Semeraro, G. Turco, R. Gennaro, and S. Paoletti, "Non-cytotoxic Silver Nanoparticle-Polysaccharide Nanocomposites with Antimicrobial Activity," *Biomacromolecules*, vol. 10, no. 6, p. 1429, Apr.2009.

[18] X. Chen and H. J. Schluesener, "Nanosilver: A nanoproduct in medical application," *Toxicolol Lett*, vol. 176, no. 1, pp. 1-12, Jan.2008.

[19] Yu Pan, "Size-Dependent Cytotoxicity of Gold Nanoparticles," *Small*, vol. 3, no. 11, pp. 1941-1949, 2007.

[20] L. C. Renwick, D. Brown, A. Clouter, and K. Donaldson, "Increased inflammation and altered macrophage chemotactic responses caused by two ultrafine particle types," *Occup. Environ. Med.*, vol. 61, no. 5, pp. 442-447, May2004.

[21] E. Jan, S. J. Byrne, M. Cuddihy, A. M. Davies, Y. Volkov, Y. K. ko, and N. A. Kotov, "High-Content Screening as a Universal Tool for Fingerprinting of Cytotoxicity of Nanoparticles," *ACS Nano*, vol. 2, no. 5, pp. 928-938, May2008.

[22] D. Mitchell and E. Claudio, "Nanoparticle Toxicity in *Saccharomyces cerevisiae*: A Comparative Study Using Au Colloid, Ag Colloid, and HAuCl4 • 3H2O in Solution," 2008.

[23] K. Nomiya, R. Noguchi, K. Ohsawa, K. Tsuda, and M. Oda, "Synthesis, crystal structure and antimicrobial activities of two isomeric gold(I) complexes with nitrogen-containing heterocycle and triphenylphosphine ligands, [Au(L)(PPh3)] (HL = pyrazole and imidazole)," *J Inorg. Biochem.*, vol. 78, no. 4, pp. 363-370, Mar.2000.

[24] K. Esumi, N. Takei, and T. Yoshimura, "Antioxidant-potentiality of gold-chitosan nanocomposites," *Colloids and Surfaces B: Biointerfaces*, vol. 32, no. 2, pp. 117-123, Oct.2003.

[25] H. Huang, Q. Yuan, and X. Yang, "Preparation and characterization of metal-chitosan nanocomposites," *Colloid Surface B*, vol. 39, no. 1-2, pp. 31-37, Nov.2004.

[26] A. Pal, D. L. Stokes, and T. Vo-Dinh, "Photochemically prepared gold metal film in a carbohydrate-based polymer: A practical, solid substrate for surface-enhanced Raman scattering," *Current Science*, vol. 87, no. 4, pp. 486-491, 2004.

[27] T. Sakai and P. Alexandridis, "Mechanism of Gold Metal Ion Reduction, Nanoparticle Growth and Size Control in Aqueous Amphiphilic Block Copolymer Solutions at Ambient Conditions," *J. Phys. Chem. B*, vol. 109, no. 16, pp. 7766-7777, Apr.2005.

[28] K. Yang, X. Wang, Z. Zhou, J. Xu, J. Weng, and Q. Zhang, "One-step synthesis and characterisation of chitosan-mediated micro-sized gold nanoplates through a thermal process," *IET Nanobiotechnology*, vol. 1, no. 6, pp. 107-111, Dec.2007.

[29] E. Dinda, S. Si, A. Kotal, and T. K. Mandal, "Novel ascorbic acid based ionic liquids for the in situ synthesis of quasi-spherical and anisotropic gold nanostructures in aqueous medium," *Chemistry.*, vol. 14, no. 18, pp. 5528-5537, 2008.

[30] K. Esumi, T. Hosoya, A. Suzuki, and K. Torigoe, "Spontaneous Formation of Gold Nanoparticles in Aqueous Solution of Sugar-Persubstituted Poly(amidoamine)dendrimers," *Langmuir*, vol. 16, no. 6, pp. 2978-2980, Jan.2000.

[31] F. Suska, S. Svensson, A. Johansson, L. Emanuelsson, H. Karlholm, M. Ohrlander, and P. Thomsen, "In vivo evaluation of noble metal coatings," *J Biomed. Mater. Res B Appl. Biomater.*, Aug.2009.

[32] I. Donati, S. Stredanska, G. Silvestrini, A. Vetere, P. Marcon, E. Marsich, P. Mozetic, A. Gamini, S. Paoletti, and F. Vittur, "The aggregation of pig articular chondrocyte and synthesis of extracellular matrix by a lactose-modified chitosan," *Biomaterials*, vol. 26, no. 9, pp. 987-998, Mar.2005.

[33] M. Yalpani and L. D. Hall, "Some chemical and analytical aspects of polysaccharide modifications. Formation of branched-chain, soluble chitosan derivatives," *Macromolecules*, vol. 17, no. 3, pp. 272-281, May1984.

[34] J. R. Morones, J. L. Elechiguerra, A. Camacho, K. Holt, J. B. Kouri, J. T. Ramirez, and M. J. Yacaman, "The bactericidal effect of silver nanoparticles," *Nanotechnology*, vol. 16, no. 10, pp. 2346-2353, 2005.

[35] I. Donati, S. Holtan, Y. A. Mørch, M. Borgogna, M. Dentini, and G. Skjåk-Bræk, "New hypothesis on the role of alternating sequences in calcium-alginate gels," *Biomacromolecules*, vol. 6, no. 2, pp. 1031-1040, Mar.2005.

[36] K. I. Draget, K. Østagaard, and O. Smidsrød, "Homogeneous alginate gels: A technical approach," *Carbohydrate Polymers*, vol. 14, no. 2, pp. 159-178, 1991.

[37] P. G. Laing, A. B. Ferguson, Jr., and E. S. Hodge, "Tissue reaction in rabbit muscle exposed to metallic implants," *J Biomed. Mater Res*, vol. 1, no. 1, pp. 135-149, Mar.1967.

[38] F. Suska, "On the initial inflammatory response to variations in biomaterial surface chemistry." Goteborg University, 2004.

Paper 6

SILVER NANOCOMPOSITES AND THEIR BIOMEDICAL APPLICATIONS

Andrea Travan, Eleonora Marsich, Ivan Donati, Sergio Paoletti

Department of Life Sciences, University of Trieste, Via Giorgieri 1, Trieste I-34127, Italy

Chapter of the Book “Nanocomposites for the Life Sciences” (Wiley-VCH 2010). *In Press*.

1.0 INTRODUCTION TO SILVER NANOCOMPOSITES

By definition, nanocomposites are materials containing domains or inclusions that are of nanometer size scale[1]. Nanocomposite materials that exploit the properties of silver at the nanoscale for biomedical applications are of increasing interest in the scientific literature (Figure 1) and today they can be found in many commercial products, like wound dressings and creams.

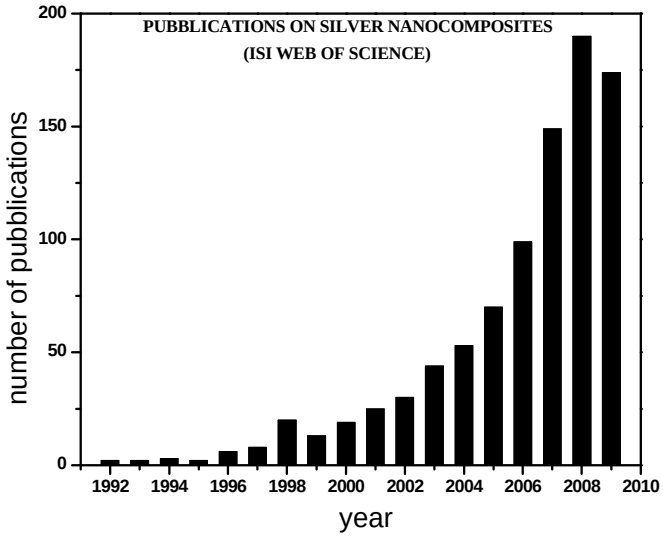

Figure 1. Publication counts derived from the Thompson ISI Web of Science database on October 2009, using the key word “silver nanocomposites”.

The idea behind these novel materials is that silver at the nanometer scale displays unique properties that can be used for different purposes, ranging from antimicrobial to optical and catalytic applications[2,3].

This section overviews the state-of-the-art of silver nanocomposites for the most promising pathways in the biomedical field; it is structured in 5 main parts. Chapter 1 gives a brief introduction about the new class of materials referred to as “silver nanocomposites”, while Chapter 2 discusses the main routes of preparation of silver nanoparticles and the final composite constructs. Chapter 3 presents the main results and applications of these materials over the last few years, with a particular attention to the antimicrobial field: in fact, as the largest efforts aim at exploiting the antimicrobial properties of silver, chapter 3.1 is meant to sum up results and hypothesis about the detailed antimicrobial mechanism, which is today only partially understood.

Paragraphs 3.2 to 3.4 specifically consider the use of silver nanocomposites for applications related to wound healing, inflammations and biological sensing. Chapter 4 deals with the possible biological hazards of such materials, which are rarely taken into account and often represent a matter of controversy in terms of contradictory results. Finally, Chapter 5 suggests possible upcoming biomedical applications of this class of materials.

2.0 PREPARATION AND CHARACTERIZATION OF SILVER NANOCOMPOSITES

2.1 PREPARATION TECHNIQUES

Since silver nanocomposite constructs are meant to exploit the properties of silver at the nano-scale, many efforts are aimed at finding efficient and reproducible routes to produce silver nanoparticles (hereafter AgNPs). Many potential uses for these novel materials are being explored, ranging from antimicrobial purposes to molecular imaging. When preparing homogeneous nanocomposite materials containing AgNPs, a crucial issue is the tendency of nanoparticles to aggregate, which leads to the loss of the peculiar properties associated with the nano-scale. For instance, in the antimicrobial field, studies by Lok *et al.*[4] revealed that non-stabilized AgNPs prepared by standard chemical methods (reduction of silver salt solutions) tend to aggregate in culture media and biological buffers which have high salt contents (chloride and phosphate being considered the most problematic anions): the aggregation leads to a decrease in the effective surface of the nanoparticles or the degree to which they can associate to bacteria. The so called "*ex situ*" preparation methods consist in the synthesis of nanoparticles as a first step, and then in mixing the pre-formed nanoparticles with a matrix (typically a polymer); however with this conventional technique it is difficult to disperse homogeneously the nanoparticles[5]. At variance, an "*in situ*" approach aims at synthesizing the nanoparticles within a suitable matrix in order to achieve a homogeneous dispersion in the composite materials. To date, the preparation and stabilization of metal nanoparticles represent an open challenge. The methods for preparing non-aggregated AgNPs for biomedical applications can be divided into two groups[6]:

- wet chemical synthesis in the presence of a reducing agent and a stabilizing agent;
- synthesis through physical processes

The chemical approach is based on the use of a silver salt in an aqueous environment; silver ions are then reduced to zeroth-valent silver in the presence of a stabilizing agent in order to limit aggregation of the so-formed nanoparticles. The stabilizing agent is meant to cap the particles and prevent further growth. The most accepted mechanism for the synthesis of a particle suggests a two-step process, i.e., nucleation followed by successive growth. In the first step, part of the metal ions in solution is reduced by a suitable reducing agent. The atoms thus produced act as nucleation centres and catalyze the reduction of the remaining metal ions present in the bulk solution. The atomic coalescence leads to the formation of metal clusters whose dimensions can be controlled by ligands, surfactants or polymers; in the absence of a stabilizer, clusters in aqueous solution undergo further growth leading ultimately to precipitation of the metal [7].

Polymers and more generally many organic molecules can bind to the particle surface and thus serve the role of stabilizer. In general, the stabilization of metal nanoparticles is explained by the electronic interaction of the polymer functional groups with the metal particles. In fact, nucleophilic groups can bind the metal particles by donating electrons [3]. A common approach to prepare stable AgNPs involves the use of polymer solutions: to this end, a variety of polymers can be used, ranging from synthetic to natural ones. Nitrogen-

containing stabilizing polymers, such as poly-(ethyleneimine) and poly(vinylpyrrolidone), act via lone electron pairs. Protective polymers can coordinate metal ions before reduction, forming a polymer-ion complex; such a complex can then be reduced under mild conditions, resulting in metal particles of smaller dimensions and a narrower size distribution than those obtained without protective polymers [8]. Once the reduction occurred, the stabilizing effect of these macromolecules is attributable to the fact that either the particles are attached to the much larger protecting polymers or the protecting molecules cover or encapsulate the metal particles [9]. This chemical approach can be generalized in Figure 2.

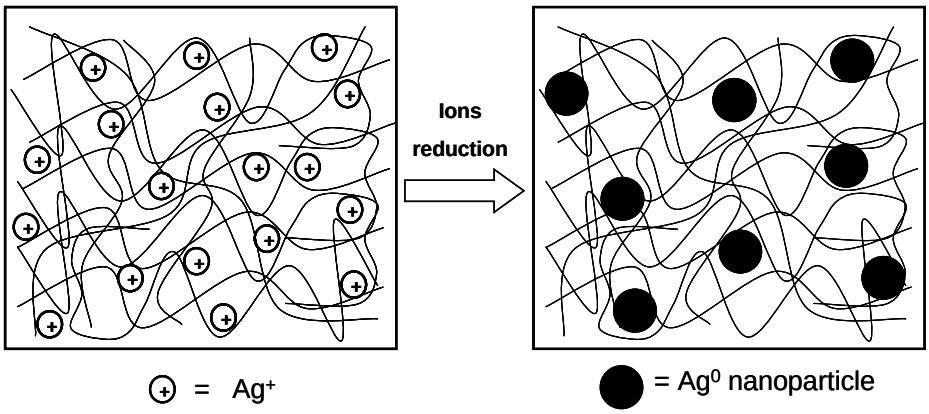

Figure 2. Preparation of AgNPs in the presence of a stabilizing polymer (wet synthesis)

In particular, owing to the presence of many different functional groups, polyelectrolytes are successfully used in the preparation of stable AgNPs. Polyelectrolytes at low concentrations (such as polyphosphate, polyacrylate, poly-(vinyl-sulfate), poly-(ethylene-imine) [2,3,10], poly-(allyl-amine) [9], and chitosan [11-13]) have been used with different outcomes to stabilize nanoparticles preventing the growth of aggregates. As already mentioned, poly-(vinyl-pyrrolidone) [5,14], a neutral polymer, has been widely used for the stabilization of silver nanoparticles. It must be noticed that in order to find applications in the field of biomaterials, both the stabilizing and the reducing agents must not represent a biological hazard [15].

Considering the reduction step, various exogenous agents can be used, such as ascorbic acid[16,17], sodium borohydride[18], sodium citrate[19,20], alcohols[20], hydrogen[21], polyols, hydroxyalkyl radicals, and aldehyde groups of reducing sugars[22-24]. For a "green synthesis" of nanoparticles[15], reducing saccharides can be used as non-toxic and environmental-friendly reducing agents. In this case the synthesis is based on a Tollens reaction that involves the reduction of a silver ammoniacal solution with a reducing sugar (*e.g.,* glucose, maltose, xylose…)[25].

By the choice of the stabilizer and the reducing agent, one can control the growth process and manipulate shape and size of the metal nanoparticles in the nanocomposites. For instance, a lactose-substituted chitosan (1-deoxylactit-1-yl chitosan) was successfully used to prepare stable silver nanoparticles using this particular polymer either as stabilizing agent only, or as both reducing and stabilizing agent at the same time[26,27]. In the first case, the nanoparticles are obtained in a polysaccharide solution with silver ions reduced by ascorbic acid ($C_6H_8O_6$) according to the following stoichiometry[16,17]:

$$2Ag^{+} + C_6H_8O_6 \rightleftharpoons 2Ag^{0} + C_6H_6O_6 + 2H^{+}$$

The nanoparticles thus obtained were mostly round-shaped and well dispersed with an average diameter of 30 nm as revealed by image analysis based on transmission electron micrographs.

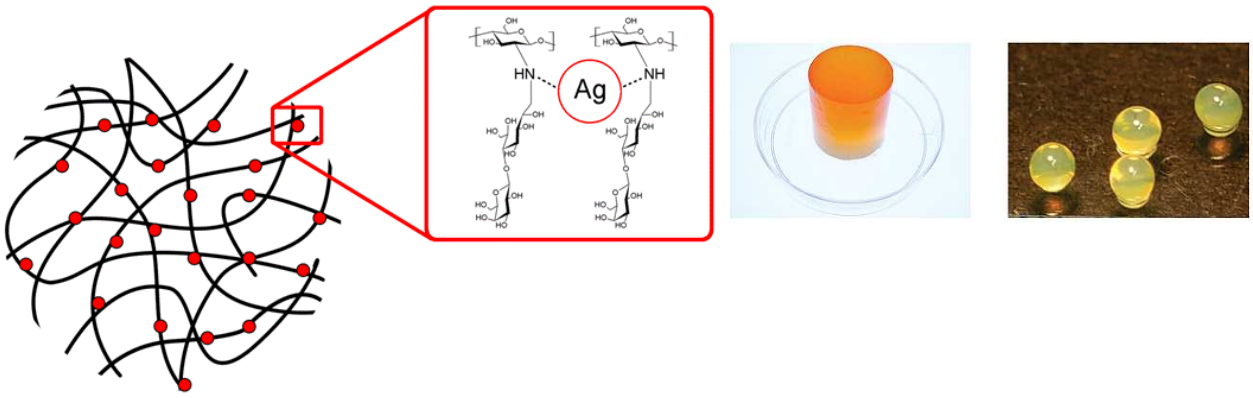

Figure 3: Left) Schematic representation of the polymeric chains of lactose-modified chitosan providing the nitrogen atoms for the coordination and stabilization of silver nanoparticles. From Travan *et al.* (2009), reproduced with permission. Center and right) Nanocomposite hydrogels based on AgNPs and polysaccharides. From Travan *et al.* (2009), reproduced with permission.

This polysaccharide acts as an efficient stabilizing ligand for silver ions and AgNPs thanks to the presence of amino groups. Esumi *et al.*[8] demonstrated that metal nanoparticles can be protected by the exterior amino groups of dendrimers which act as stabilizers. In the case of the lactose-modified chitosan (chitlac) it was suggested that when $AgNO_3$ is mixed with the polyelectrolyte solutions, Ag^{+} ions give rise to a localized binding to the polymer macromolecules *via* amino groups chelation that persists also with the formed AgNPs. The hydrophilic lactitol side-chains also play a fundamental role in the stabilization by embedding the AgNPs bound in the proximity of the polymer backbone and isolating them from the surrounding species (Figure 3, left). Furthermore, the complete miscibility of this colloidal solution with the anionic polysaccharide alginate can lead to the preparation of homogeneous nanocomposite hydrogels that entrap highly stabilized silver nanoparticles, the yellow colour witnessing the good dispersion of the AgNPs within the gel matrix (Figure 3, center and right). Huang *et al.*[12]discussed the preparation of silver-chitosan nanocomposites obtained by chemical synthesis from a chitosan solution in the presence of $AgNO_3$ reduced by $NaBH_4$; the evaporation of the solvent in this colloidal solution brings to the formation of a nanocomposite film. The morphology of the film shows a rod-like structure, whose formation is attributed to the presence of the silver clusters that act as an accelerant to the precipitation of polymer crystallites. Silver nanocomposites can be prepared in the form of nanofibres by means of the electrospinning technique, a process by which a suspended droplet of polymer solution is charged to high voltage to produce fibres with a diameter typically smaller than 500 nm. If the solution contains AgNPs stabilized by the polymer, it is

possible to obtain nanocomposite fibres. Wang *et al.*[5] successfully prepared AgNPs through reduction of $AgNO_3$ by ethanol in PVP/ethanol solution and managed to obtain nanocomposite fibres with AgNPs smaller than 10 nm (Figure 5, left).

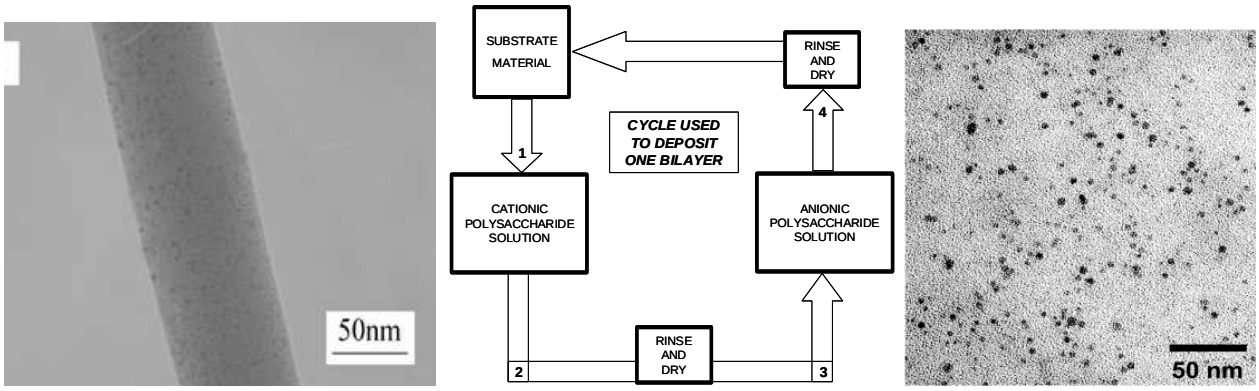

Figure 5. Left) TEM image of Ag/PVP nanocomposite electrospun fibre. From Wang *et al.* (2006), reproduced with permission. Center) Schematics of the layer-by-layer self-assembly procedure for creating antimicrobial thin films, adapted from Grunlan *et al.* (2005). Right) TEM image of a silver-PEI-PAA film that shows the dispersion of spherical AgNPs with a mean diameter of 4 nm. From Dai *et al.* (2002), reproduced with permission.

The need to obtain antimicrobial coatings and films can be fulfilled by incorporating AgNPs into polymeric matrixes by means of the so-called "layer-by-layer" technique. This is a simple and straightforward approach based on the alternate deposition on a substrate of layers of polyelectrolytes with opposite charges through a dipping process (Figure 5, center). The dipping process is repeated until a desired number of layers is obtained, each layer having a thickness in the range of a few nanometers. With this method it is possible to incorporate in one or more layers bioactive agents like silver. According to this approach, Grunlan *et al.*[10] prepared polyelectrolyte multilayers using silver nitrate and/or cetrimide (antiseptic agent) as antimicrobial agents. The films were prepared by alternately dipping poly(ethylene terephtalate) (PET) substrate into solutions of poly(acrylic acid) (PAA) and poly(ethylene imine) in mixture with the bioactive agents. Dai *et al.*[2] followed the layer-by-layer approach to obtain multilayered polyelectrolyte films that incorporate homogeneously dispersed AgNPs; in this work a polyethyleneimmine (PEI) solution was used to prepare stabilized silver ions from $AgNO_3$. Then, the alternated deposition on a substrate of the PEI-silver layer and of a poly(acrylic acid) (PAA) solution followed by reduction with $NaBH_4$ led to the formation of a multilayered film based on the two oppositely charged polysaccharides containing finely dispersed AgNPs (Figure 5, right). Multilayers can be fabricated by means of the layer-by-layer technique not only on planar substrates, but also on three-dimensional templates. In the case of a spherical template, its eventual dissolution after the film formation allows obtaining multlayered capsules that can embed bioactive agents like AgNPs; Choi *et al.*[28]synthesised polyelectrolyte capsules with two types of nanoparticles embedded: AgNPs for the antimicrobial activity and goethite nanoparticles to endow the capsules with the possibility to be moved by external magnetic fields. The capsules were prepared by means of copolymerized polyelectrolytes composed of poly(styrene sulfonate) (PSS) and poly(acrylic acid) (PAA) in addition to

poly(allylamine hydrochloride) (PAH). Then, metal ions were loaded from aqueous solution into the capsules and were finally let react to create the two different types of nanoparticles. Ho *et al.*[29]developed a nanocomposite film where a polymer network based on poly(ethylene imine) derivatized with double bonds was copolymerized with 2-hydroxyethyl acrylate; after a UV-initiated polymerization the film was loaded with silver ions that were subsequently reduced to form AgNPs. After immersing the film in $AgNO_3$ solution, the chemical reduction of Ag^+ complexed within the polymer network occurred by treating the film in ascorbic acid solution until the film turned to yellowish-brown, which suggests the formation of well dispersed nanoparticles. Polyols can be used as reducing agents for silver ions: in this case, the silver-reduction mechanism typically involves a heat treatment. Wiley *et al.*[23,30] prepared AgNPs with different shapes (quasi-spherical particles, single-crystal cubes, tetrahedrons, rods, triangular nanoplates, nanowires with pentagonal cross sections, twinned structures…) by reducing $AgNO_3$ with ethylene glycol at high temperature in the presence of PVP.

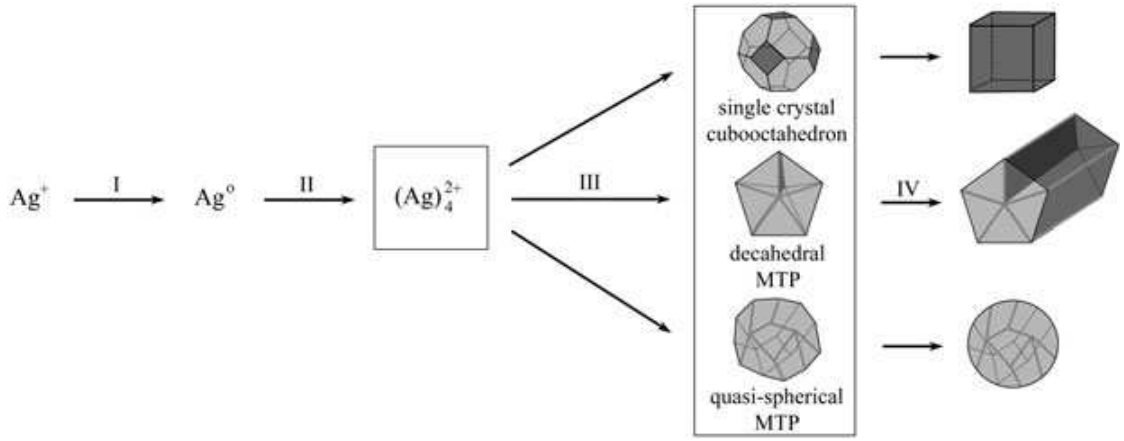

Figure 6. Schematic showing the reduction of silver ions by ethylene glycol (I); the formation of silver clusters (II); the nucleation of seeds (III); and the growth of seeds into nanocubes, nanorods or nanowires, and nanospheres (IV). From Wiley *et al.* (2005), reproduced with permission.

These studies showed how the crystallinity of seeds was determined by the molar ratio between the capping agent (PVP) and $AgNO_3$ as well as by the strength of the chemical interaction between the polymer and various crystallographic planes of silver (Figure 6). Silver nanocomposites can be prepared using polymeric dendrimers as stabilizing agents. In fact dendrimers are branched macromolecules that possess architecture and ligand sites that allow the pre-organization of metal ions and an effective stabilization of silver owing to the formation of stable complexes at atomic/molecular level dispersion. Balogh *et al.*[31] discussed the preparation of silver complexes within poly(amidoamine) dendrimers for antimicrobial applications. Kuo *et al.*[9] reported the formation of AgNPs stabilized in pseudo-dendritic poly(allylamine) derivates. Following the same strategy, other organic macromolecules can be used to stabilize AgNPs: for instance Lok *et al.*[4] reported the preparation of antimicrobial AgNPs stabilized by bovine serum albumin (BSA). Inorganic stabilizers are also being explored for the preparation of silver nanocomposites. Su *et al.*[6] prepared AgNPs immobilized within inorganic phyllosilicate clays in order to obtain nanohybrids exploiting an ion exchange between Ag^+ (provided by $AgNO_3$) and Na^+ from the clay, followed by *in situ* reduction of silver ions by

methanol at 80°C. In this case the nanoparticles thus formed are free of polymeric surfactants and have a narrow size distribution with an average diameter around 30 nm (Figure 7).

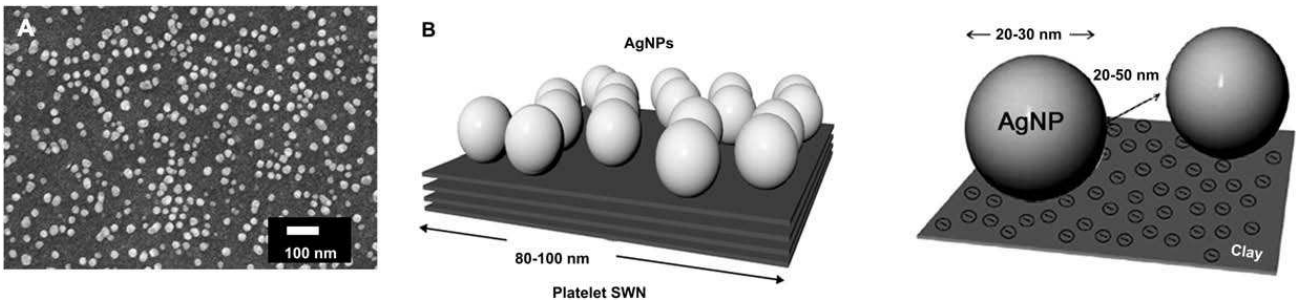

Figure 7. Silver nanoparticles dispersed on silicate clay. (A) The surface structure of the AgNP/Clay is characterized by Field-Emission SEM. (B) Representations of the nanocomposite structure. From Su *et al.* (2009), reproduced with permission.

Silver nanocomposites can be obtained in the form of bioceramics in order to endow osteoconductive materials with antimicrobial properties. Rameshbabu *et al.*[32] prepared silver-substituted hydroxyapatite nanocrystals by microwave processing.

Although the conventional chemical synthesis represents to date the most popular approach for the preparation of silver nanocomposites, other techniques are being explored which are based on physical processes. A promising technique is the radiolytic method used for the generation of AgNPs in solution; with this technique, radiolytically generated species, solvated electrons and secondary radicals, exhibit strong reducing potentials towards metal ions. Krkljes *et al.*[33] reported the preparation of Ag-PVA nanocomposites by radiolytic procedure using steady state gamma irradiation. Alternatively, ablation of a metal surface immersed in a liquid can produce nanoparticles of the metal in the liquid. In the laser ablation technique metal atoms and small metal clusters are ablated from a metal rod by laser irradiation; self-aggregation of the nanoparticles suspended in the liquid can be prevented by hindering direct contact of the nanoparticles by means of a surfactant. Mafunè *et al.*[34] performed the preparation of AgNPs by laser ablation against a silver plate in an aqueous solution of sodium dodecyl sulphate. Photochemical methods can be used to prepare polymer-stabilized AgNPs[35]. Mallick *et al.*[7] prepared colloidal silver under UV photo irradiation of silver nitrate solution in the presence of methoxy poly(ethylene glycol) which acts as a reducing and stabilizing agent. Further interesting routes to prepare silver nanocomposites are sonochemical treatments[36], potentiostatic and galvanostatic methods[37], vapour deposition[38], microwave irradiation[39], electron beam irradiation[40], synthesis templated by DNA[41], Langmuir-Blodgett-based techniques [42], ion implantation, sputtering, vapor-phase co-deposition, and vacuum co-condensation[43].

2.2 CHARACTERIZATION TECHNIQUES

The characterization of silver nanocomposites can be performed by means of different techniques; the most important ones are spectroscopic techniques (UV-Vis, infrared and X-ray photoelectron spectroscopy), X-ray diffraction and microscopic techniques (TEM, SEM, Dark-Field, AFM, NSOM).

In the chemical synthesis, colloidal solutions of AgNPs are obtained upon reduction of Ag^+ to the metal atom and consecutive coalescence of atoms yelding larger particles. The transition from atom to metal nanoparticle can be studied by pulse radiolysis techniques[3,20]. When a sufficient number of atoms coalesce, the particles start to display a typical property called "Surface Plasmon Resonance", which is produced by a collective excitation of all the free electrons in the particles[3]. Under the influence of the electric field due to the incoming light, the movement of electrons leads to a dipole excitation across the particle sphere that makes the electrons oscillate (Figure 8, left).

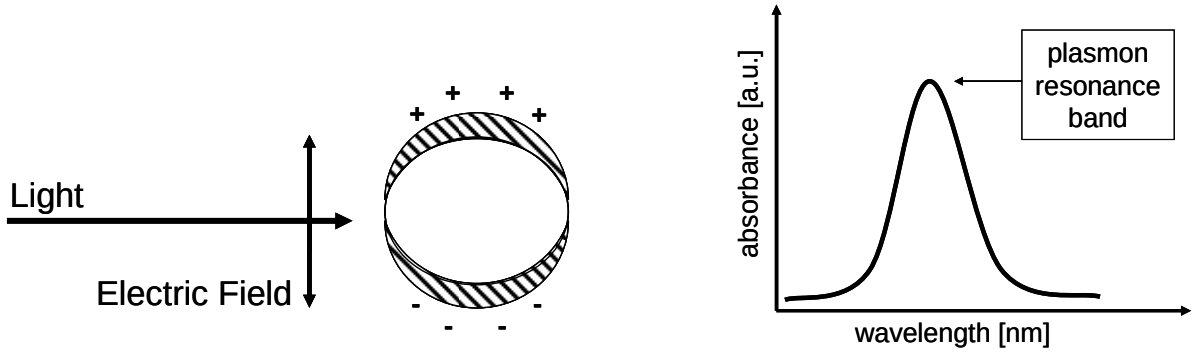

Figure 8. Left) Polarization of a spherical metal particle by the electrical field vector of the incoming light. Adapted from Henglein (1993). Right) A plasmon resonance band in the UV-Vis spectrum accounts for the presence of metallic nanoparticles.

The electron density within a surface layer (a few angstroms thick) oscillates, while the density in the interior of the particle remains constant. When the condition of resonance is reached, the UV-Vis spectrum displays an intense absorption band called "Surface Plasmon Resonance Band" (Figure 8, right).

A typical example is given by the formation of the plasmon resonance peak at about 400 nm during the chemical synthesis of AgNPs in a chitosan-derivative (chitlac) solution[27]; the absorption peak increases with time after the addition of the reducing agent, which indicates the coalescence of the reduced ions to form the metallic nanoparticles (Figure 9, left)

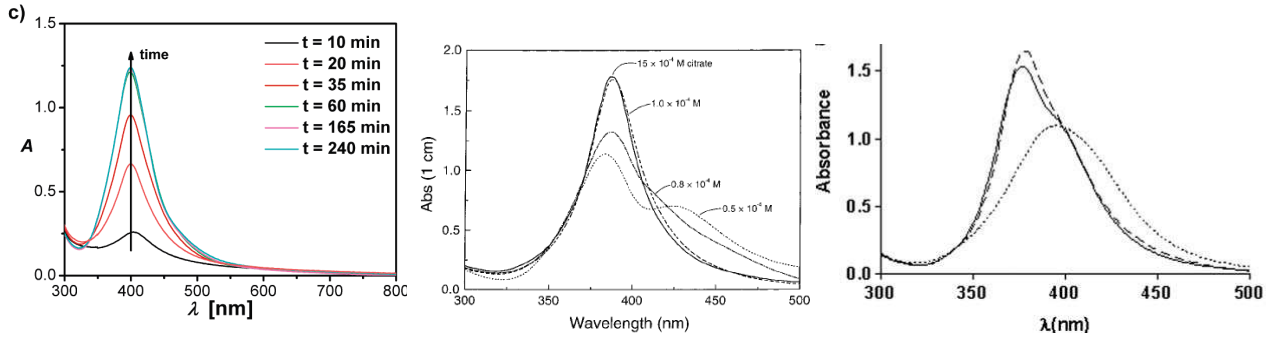

Figure 9. Left) Time dependence of UV-vis spectra variations of polymer-stabilized silver nanoparticles after the addition of the reducing agent. From Travan *et al.* (2009), reproduced with permission. Centre) Absorption spectra of silver colloids obtained at various citrate concentrations. From Henglein *et al.* (1999), reproduced with permission. Right) The surface plasmon resonance absorption of reduced AgNPs (solid line), oxidized AgNPs (dotted line), and oxidized AgNPs re-reduced by NaBH4 (dashed line). From Lok *et al.* (2007), reproduced with permission.

A symmetrical shape of the plasmon band suggests that the nanoparticles are well dispersed and spherical[9]. At variance, the aggregation of nanoparticles leads to a broader plasmon band, with a red-shifted maximum[44]. A systematic study on the formation of silver nanoparticles by absorption spectroscopy was tackled by Henglein[45] who reported the preparation of AgNPs from $AgClO_4$ solutions at a fixed concentration and studied the variations of the UV-Vis spectra as a function of the concentration of sodium citrate used as both reducing and capping agent. The UV-Vis spectra in Figure 9 (center) suggest that sodium citrate plays a drastic effect on the formation of AgNPs with different size; in fact according to its concentration it can determine the formation of well stabilized AgNPs or the coalescence of poorly stabilized polycrystallites. Excess charge carriers influence the wavelength of the plasmon resonance band; a blue shift of the plasmon peak occurs upon electron donation to the particles, while a red shift occurs upon injection of positive holes into the particles. Furthermore, chemical modification on the surface of the particles, like interaction with organic molecules, strongly affects the plasmon absorption band.

Anions able to form complexes or insoluble salts with silver ions are strongly adsorbed on silver particles. Also the Fermi level floats upon chemisorption, depending whether the adsorbed molecule is nucleophilic or electrophilic. A surface atom carrying an adsorbed nucleophile molecule acquires a slightly positive charge ("preoxidation state"); the excess electron density is simultaneously transferred into the metal particle. Thus, the chemisorption of a nucleophile is accompanied by a shift of the Fermi potential to a more negative value. AgNPs are highly sensitive to oxygen, resulting in the formation of partially oxidized AgNPs with chemisorbed Ag^+ on the surface. In the absorption spectra this partial oxidation leads to a red-shift of the surface plasmon resonance band, according to the following equation[44]:

$$\lambda = \lambda_0(1 + [Ag^+]/[Ag])^{1/2}$$

where λ_0 is the wavelength of the plasmon peak before oxidation, and λ after oxidation.

Lok *et al.*[4] reported that borohydride reduced (zeroth-valent) AgNPs in the presence of citrate exhibit a surface plasmon resonance peak at 375 nm, while subsequent exposure to oxygen led to a rapid shift of the absorption peak to 398 nm, with broadening of the band width and lowering of the maximum absorption. These changes in the absorption spectrum can be attributed to the partial oxidation of the nanoparticles with the formation of chemisorbed Ag^+ on thier surface, indicating the sensitivity of AgNPs to oxygen. Further addition of borohydride induced a shift in the plasmon resonance band to the intensity and shape of non-oxidized zeroth-valent nanoparticles (Figure 9, right). It is important to notice that the presence of oxidized (or partially oxidized) atoms on the surface of the nanoparticle affects its biological properties, as discussed in chapter 3.1.4. Infrared spectroscopy (IR) can provide information about the interaction (chemical bonding) between the nanoparticles and the matrix in a silver nanocomposite structure. Krkljes *et al.*[33] carried out IR analysis to point out the interaction between AgNPs and PVA chains *via* its OH groups. By means of Fourier Transform IR Dai *et al.*[2] characterized poly(acrylic acid)/polyethyleneimine-silver nanocomposites in order to evaluate the influence of silver reduction on the polymer matrix and Zhang *et al.*[46] verified the formation of coordination bonds between the amino/amide groups of a poly(amidoamine) derivative and AgNPs.

Transmission Electron Microscopy (TEM) is commonly used to investigate size, structure (crystallography, existence of twin planes, stacking faults…) and dimensional distribution of AgNPs: AgNPs prepared upon chemical reduction in the presence of chitlac[27] appeared as spheroidal particles with average dimensions between 20 and 30 nm (Figure 10, left).

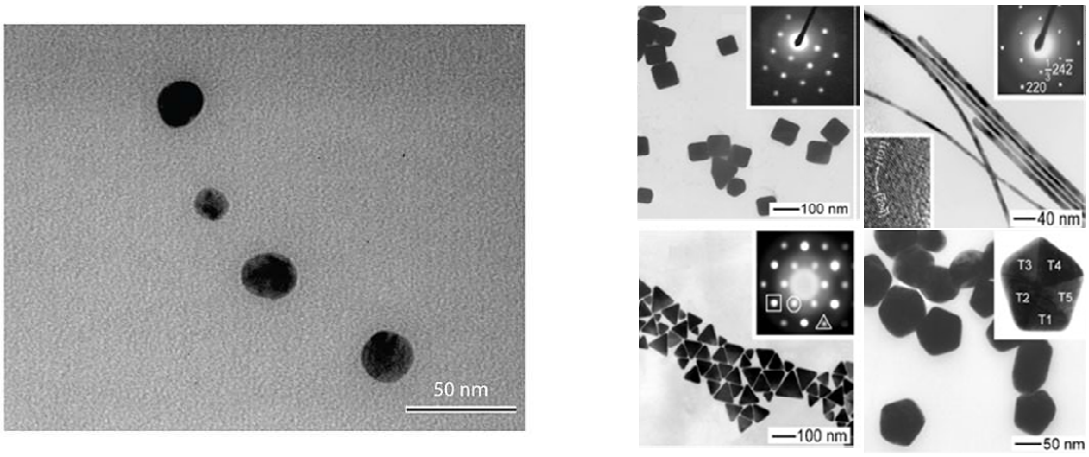

Figure 10. Left) TEM image of silver nanoparticles stabilized by a lactose-modified chitosan. From Travan *et al.* (2009), reproduced with permission. Right) TEM characterization of AgNPs with different morphologies obtained by polyol synthesis. From Wiley *et al.* (2005), reproduced with permission.

Wiley *et al.*[30,47] carried out TEM investigations to study a polymer-mediated polyol process that allows for the preparation of silver nanostructures with a number of different morphologies (*e.g.*, cubes, rods, wires, and spheres) as reported in Figure 10, right.

Wang *et al.*[48] prepared polyelectrolyte multilayer films containing AgNPs and evaluated the distribution of the particles in the polymer matrix by means of cross-sectional TEM imaging. The pictures show spherical particles uniformly and randomly distributed throughout the film (Figure 11, left).

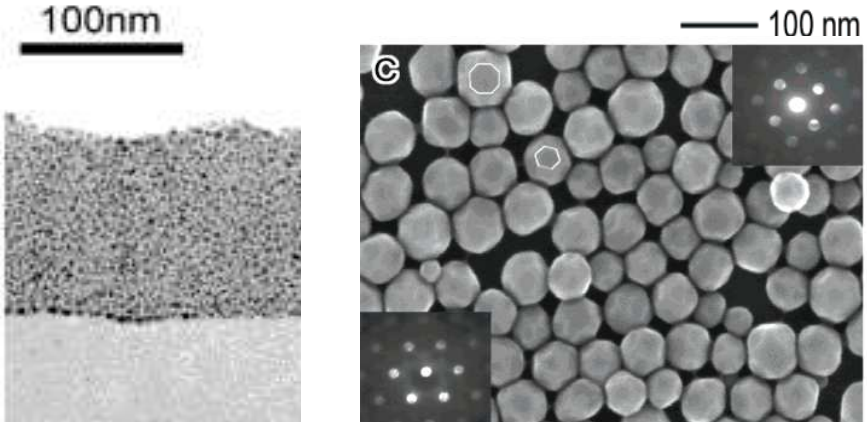

Figure 11. Left) Cross-sectional TEM image of a polyelectrolyte multilayer containing AgNPs. From Wang *et al.* (2002), reproduced with permission. Right) FE-SEM image of AgNPs obtained by polyol synthesis. The main image shows truncated cubes (indicated by an octagon) and truncated tetrahedrons (indicated by a hexagon), while the insets show the convergent beam electron diffraction patterns showing that these particles are single crystals. From Wiley *et al.* (2004), reproduced with permission.

Metal nanocomposites have been studied by means of Scanning Electron Microscopy (SEM), especially equipped with field-emission guns (FE-SEM) that allow avoiding the sputtering step of conventional SEM which could cover or affect the nanoparticles on the surface of the nanocomposite material[28,49]. Wiley *et al.*[23] carried out a polyol synthesis of AgNPs whose structure was analysed by FE-SEM: the images proved the formation of single-crystal, truncated cubes and tetrahedrons (Figure 11, right).

Among other techniques, Atomic Force Microscopy (AFM) is a useful means to characterize the morphology of nanocomposites materials containing a dispersion of nanoparticles[50,51]. Deshmukh *et al.*[43] explored by AFM the surface and bulk morphology of poly(methyl methacrylate) (PMMA) nanocomposite films containing AgNPs. Figure12 (left) shows AFM image of the nanoparticles on the surface of the polymer film.

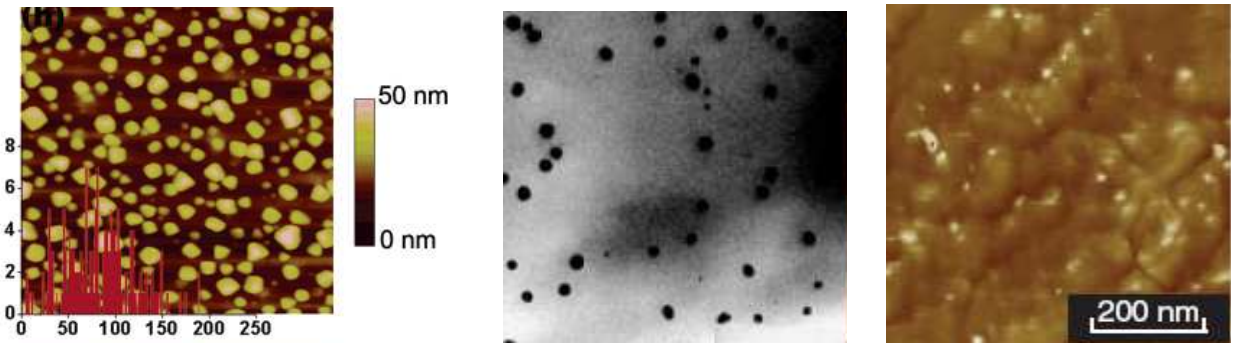

Figure 12. Left) AFM image and size distribution of silver nanoparticles dispersed in a PMMA film. The x-axis corresponds to the size of the protruding nanoparticles covered by the PMMA layer. From Deshmukh *et al.* (2007), reproduced with permission. Centre and Right)TEM image of a cross section and AFM (phase mode) image of the surface of poly(ethylene imine)-based films containing silver nanoparticles. From Ho *et al.* (2004), reproduced with permission.

Ho *et al.*[29]compared AFM and TEM techniques to characterize nanocomposite films based on poly(ethylene imine) and AgNPs. AFM images in the phase-contrast mode show the dispersion of nanoparticles that appear as bright spots on the surface of the film, while the corresponding TEM image of a cross-section of the film indicates the presence of non-aggregated nanoparticles with a size that ranges from 4 to 50 nm (Figure 12, center an right).

The crystallographic structure of AgNPs formed within a matrix can be studied by means of XRD. Wang *et al.*[5] used such technique to carachterize Ag/PVP nanocomposite films: the XRD pattern revealed the presence of face-centred cubic (fcc) nanocrystals formed within the polymer matrix (Figure 13, left).

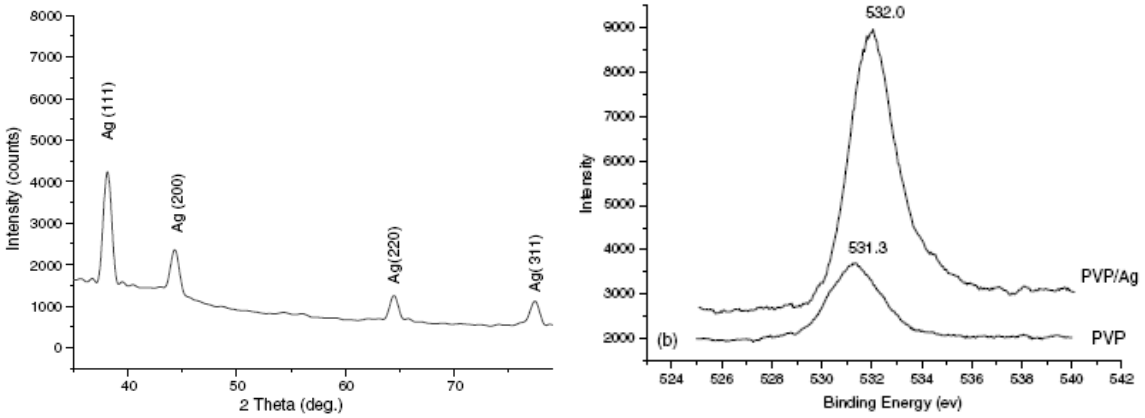

Figure 13. Left) XRD pattern of Ag/PVP nanocomposite film. From Wang *et al.* (2006), reproduced with permission. Right) X-ray photoelectron spectra of O 1s of pure PVP and PVP/Ag nanocomposite. From Wang *et al.* (2006), reproduced with permission.

X-ray photoelectron spectroscopy (XPS) is a surface chemical analysis technique that can be used to analyze silver-nanocomposite materials. XPS was used by Zeng *et al.*[52] to characterize polymer films (poly(styrene) and acrylonitrile–styrene copolymer) filled with silver nanoparticles: this technique pointed to the existence of charge transfer interaction between AgNPs and acrylonitrile segments, while no obvious interaction between silver and styrene segments was found. Stofik *et al.*[53]prepared silver-dendrimer nanocomposites for immunosensors application and confirmed with XPS the synthesis of AgNP. XPS studies on PVP-silver nanocomposite fibres showed the interaction between silver and the carbonyl oxygen; this strong Ag:O coordination can prevent AgNPs from aggregation within the polymer matrix[5](Figure 13, right).

Silver nanoparticles are extremely bright and can be directly observed using dark-field single nanoparticle optical microscopy and spectroscopy; with this technique Lee *et al.*[54] characterized AgNPs embedded in zebrafish embryos for studying their transport, biocompatibility, and toxicity in real time. Lu *et al.*[42] reported dark-field images of a high-density nanocomposite film obtained from poly (*N*-isopropylacrylamide) and AgNP (Figure 14, left).

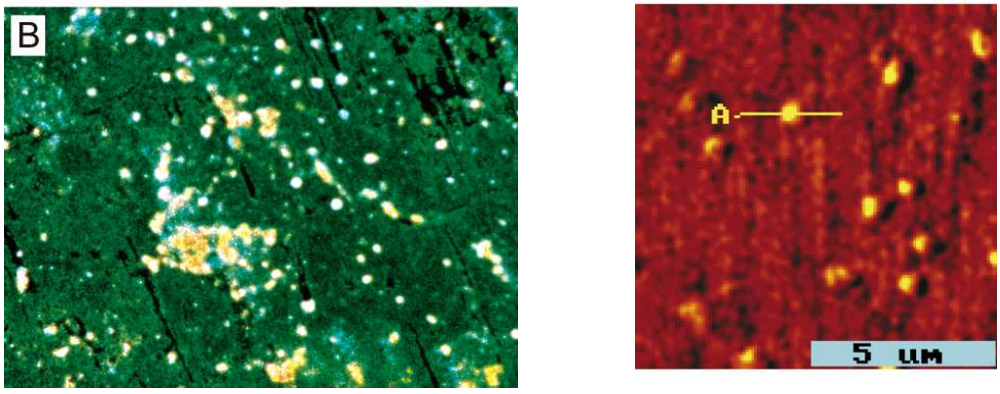

Figure 14. Left) Optical dark-field microscope images of silver nanoparticles on a poly(*N*-isopropylacrylamide film. From Lu *et al.* (2005), reproduced with permission. Right) Near-field scanning optical image of azo film sample doped with silver nanoparticles. From Zhou *et al.* (2007), reproduced with permission.

Silver nanocomposites have also been characterized by means of Near-Field Scanning Optical Microscopy (NSOM), a microscopic technique that allows for performing a surface inspection with high spatial, spectral and temporal resolution overcoming the far-field resolution limit by exploiting the properties of evanescent waves. Zhou *et al.*[55] studied the dispersion of AgNPs in polymer films containing azo groups by NSOM (Figure 14, right).

All the above mentioned techniques are the most widely used means of characterization for biomedical silver nanocomposites. Nevertheless, other techniques can provide valuable information regarding this new class of materials; to name a few, DSC[33], TGA[56], Dynamic Light Scattering[57,58] and Zeta Potential measurements[58]can also provide a deeper insight into some specific properties of the constructs, like thermodynamic properties and thermal stability, size, surface charge and diffusion.

3.0 BIOMEDICAL APPLICATIONS

3.1 SILVER NANOCOMPOSITES FOR BIOCIDAL APPLICATIONS (ANTIMICROBIAL, ANTIVIRAL, ANTIFUNGINE)

3.1.1 General considerations

Nanoscale materials have emerged as novel bioactive agents thanks to their unique physical-chemical properties and their high surface area-to-volume ratio. A large interest in silver-based nanocomposites is due to silver biocidal properties [59,60]. In fact, silver has been extensively used to control infections since ancient times. For centauries it has been in use for the treatment of burns and chronic wounds. In the 1940s penicillin was introduced and the use of silver for the treatment of bacterial infections diminished. In 1968 silver nitrate was combined with sulphonamide to obtain silver sulfadizine cream to treat burns [59]. Nowadays antibiotic-resistant bacterial strains have become a major issue in public health care and this is why silver-based nanocomposites in a variety of forms (i.e. wound dressings, coated medical devices, hydrogels) have

made a tremendous comeback for anti-infective applications[27]. Silver-based medical products, ranging from topical ointments and bandages for wound healing to coated stents, have been proven to be effective in retarding and preventing bacterial infections [61]. Improvements in the development of novel silver nanoparticles-containing products are continuously sought. In particular, there is an increasing interest towards the exploitation of silver nanoparticles technology in the development of new bioactive biomaterials, aiming at combining the unique antibacterial properties of the metal at the nano-scale with the performance of the biomaterial [9,12,16,31,62]. Silver containing nanomaterials represent a promising strategy to combat infections related to indwelling medical devices like catheters, stents and bone prosthesis. These infections are the fifth leading-cause of hospital patients' death it the US[63]. Although silver is known and used primarily for its antibacterial properties, silver nanoparticles have been shown to exhibit also promising antiviral and antifungal properties. Ag-NPs exert cytoprotective activities towards HIV-infected T-cells by inhibiting the *in vitro* production of extracellular virions. It is hypothesized that the direct interaction between these nanoparticles and double-stranded DNA of HBV viral particles is responsible for their antiviral mechanism [64]; however, the effects of silver nanoparticles towards other kinds of viruses remain largely unexplored. Although antifungal drug resistance does not seem to be as much of a problem as resistance to antibacterial agents in bacteria, one long-term concern is that the number of fundamentally different types of antifungal agents that are available for treatment remains extremely limited. There is an inevitable and urgent medical need for drugs with novel antifungal mechanisms. In the last years attention has been focused on the potential use of silver as an antifungal agent. Experimental results evidence that AgNPs exhibit potent antifungal effects on tested fungi, probably through destruction of membrane integrity [65-67].

3.1.2 Overview of *in vitro* results

This section overviews the most promising applications of silver nanocomposites as biocidal systems developed during the last few years. Silver-based materials are generally considered as good candidate for coating medical devices and many recent literature data deal with the preparation of nanocomposite-coatings based on polymers and silver nanoparticles. As it will be discussed in chapter 3.1.3, the mechanism by which silver-based materials exert biocidal activity is only partially understood; this fact often leads to different interpretations of experimental results. For this reason, the results and discussions summarized in this paragraph in some cases may appear conflicting. For central venous catheter (CVCs) applications, Stevens *et al.*[63] reported the use of various hydrophilic polymer coatings loaded with silver nanoparticles in order to assess both the antimicrobial efficacy and the impact of silver on the coagulation of contacting blood. The roll-plate assay[68] showed that bacteria inhibition begins when silver ions released from the nanoparticles into the suspension exceeds 100 nM and no bacteria are found for Ag^+ concentrations higher than 10 µM. On the other hand, thrombin generation and platelet activation starts at Ag^+ concentrations higher than 100 µM. Interestingly, thrombin generation can occur also upon activation of blood platelets through collision (direct contact) with silver particles exposed on the surface, so it was suggested that the use of silver nanocomposite

coatings for CVCs may enhance thrombus formation. Su *et al.*[6] successfully prepared AgNPs/Clay nanocomposites and by inductively coupled plasma mass spectrometry (ICP-MS) analysis showed that the immersion of the nanocomposite in water at 0.1 wt% after centrifugation causes a release of silver ions of only 139 ppb. A nanocomposite concentration of 0.05 wt% was enough for a complete inhibition of *S. aureus*, *S. pyogenes*, *P. aeruginosa* and *E. coli*. It must be noticed that the solution obtained from 0.5 wt% dispersion after centrifugation of the slurry was not effective for the inihition of *S. aureus*. This fact means that in this case AgNPs, and not the released Ag^{+}, appear to be involved in the antibacterial mechanism. In the case of multilayered nanocomposites, Dai *et al.*[2]demonstrated that their film based on the alternated deposition of poly(ethylene imine) and poly(acrylic acid) including AgNPs was effective in inhibiting *E. coli* growth. Remarkably, the effect was the same when the film contained silver ions or when it contained AgNPs; the latter case may be more desirable because it should minimize the amount of Ag^{+} absorbed in the body. Grunlan *et al.*[10]prepared a multilayered film based on poly(acrylic acid) and poly(ethylene imine) containing silver ions and cetrimide (an organic quaternary ammonium molecule) as antimicrobial agents. The biocidal activity was studied by means of the Zone Of Inhibition (ZOI) test with *E. coli* and *S. aureus* (Figure 15, left).

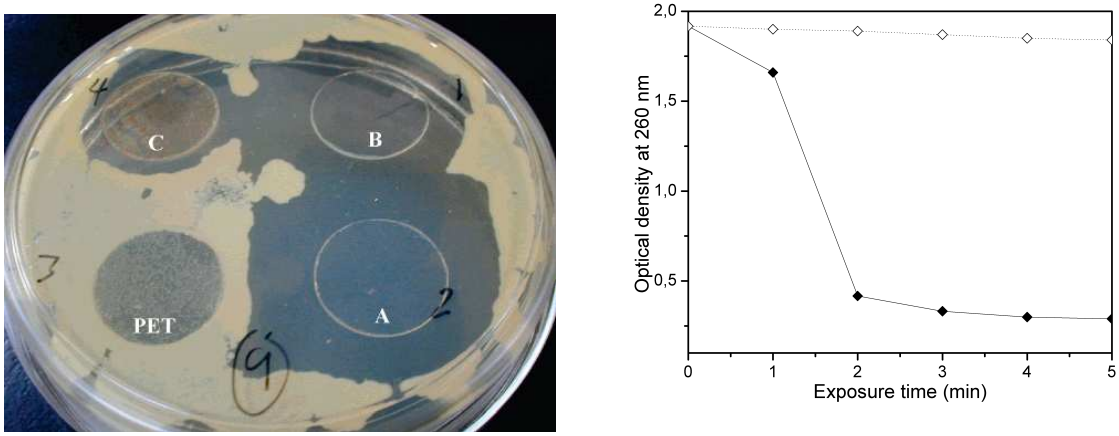

Figure 15. Left) Kirby-Bauer test performed to evaluate the Zone Of Inhibition (ZOI) after 24 h of *S. aureus* incubation. Letters (A-B-C) associated with the test films refer to different amounts of silver and cetrimide. The film in the lower left corner of the plate is a PET film with no antimicrobial coating. From Grunlan *et al.* (2005), reproduced with permission. Right) Optical density of a suspension of *E. coli* with silver-embedded (filled diamond) or without silver (nonfilled diamond) capsules as a function of exposure time (redrawn from Choi *et al.* 2005)

It was shown that such materials were effective in preventing bacteria growth and the antimicrobial efficacy of the silver containing films was further enhanced by the use of cetrimide. Choi *et al.*[28] tested nanocomposite capsules based on polyelectrolytes with AgNPs with a suspension of *E. coli*; optical density measurements at 260 nm, which are proportional to the number of bacteria, showed that the amount of bacteria decreased after only 1 min exposure to silver-embedded capsules. As a control, in the absence of silver the optical density of the *E. coli* suspension remained almost unchanged (Figure 15, right).

Antimicrobial studies were carried out on a nanocomposite systems based on lactose-modified chitosan (chitlac) and AgNPs either as a colloidal solution or as hydrogels obtained in association with alginate[27]. In both cases the materials displayed a remarkable bactericidal effect on four types of bacteria strains: *S. epidermidis*, *E. coli*, *S. aureus*, and *P. aeruginosa*. Figure 16 (left) reports the results for the *S. epidermidis* strain, as representative data. The number of viable cells drastically decreased (a drop of 3 log units in CFU/mL) after only 30 min of incubation with the colloidal system and a complete inactivation of bacterial cells was found after 2 h of treatment. The activity was preserved also in the hydrogel state; Figure 16 (center) shows that bacteria, smeared on the surface of hydrogels without silver, could grow (control gel), but they were completely absent on the AgNPs-containing gels.

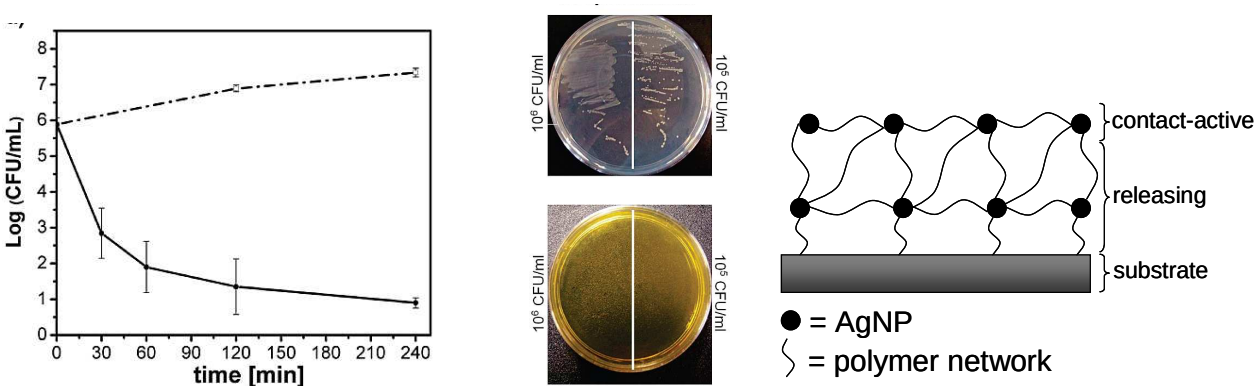

Figure 16. Left) killing kinetics of polymer-stabilized silver colloidal solution (solid line) against *S. epidermidis*; the dashed line indicates control runs in the absence silver. Center) growth of *S. epidermidis* on polysaccharide-based hydrogels without (upper Petri dish) and with (lower Petri dish) silver nanoparticles. From Travan *et al.* (2009), reproduced with permission. Right) Representation of an antimicrobial nanocomposite coating that exploits both the release of silver ions and the direct contact of silver nanoparticles within a polymer matrix (adapted from Ho *et al.* 2004)

The release of silver ions from the hydrogels into a saline solution was measured by means of ICP-MS; the concentration after 4 weeks was quite low (58 μg/L) and MTT essays proved that such amount was not toxic to three different eukaryotic cell-lines (fibroblasts NIH-3T3, osteoblasts MG63, and hepatocytes HepG2). Interestingly, LDH cytotoxicity assays revealed that the polysaccharide-AgNPs colloidal system in solution was toxic to these eukaryotic cell-lines, whereas the hydrogel system obtained from its combination with alginate was not. This fact suggests that the 3D system could prevent nanoparticles from being available for eukaryotic cellular uptake but, at the same time, preserve its antimicrobial activity allowing the direct interaction of the nanoparticles with the proteins localized on the bacterial surface. Ho *et al.*[29] reported the preparation of antimicrobial nanocomposite films based on poly(ethylene imine) and AgNPs which exploit both the release of silver ions and the direct contact between bacteria and nanoparticles (Figure 16, right). *S. aureus* was allowed to adhere to the film surface and then cultivated in agar to evaluate the viable cells. Results show that the film inhibits bacteria growth for 12 hours. When the amount of silver in the film

reached the value of 10 μg/cm^2 no bacteria could grow even after two weeks, indicating a bactericidal effect of the nanocomposite material.

3.1.3 Effects of nanoparticles properties and role of the matrix

Many factors influence the biocidal activity associated with AgNPs-based constructs, which may complicate the understanding of the antibacterial mechanism, as discussed in chapter 3.1.4; for this reason it is not easy to evaluate one property at a time, which can lead to conflicting results in the literature. Moreover the biological effects of AgNPs are affected by the dispersing agent or matrix of each particular nanocomposite system. In general, it can be stated that nanoparticles size, shape, surface properties, dispersion and stability are important issues for tailoring their biological performances. In particular, the effect of the particles dimensions has often been taken into account while characterizing the antibacterial activity: various researchers have documented that the size of AgNPs affects the biocidal effectiveness[46,69]. The antibacterial activity of AgNPs can be related to their size since the activity of smaller particles is higher due to the increase in surface area when compared on the basis of equivalent silver mass content. For such speculations it can be useful to evaluate the number of silver atoms in a nanoparticle (n) from the following relation[45]:

$$n = \frac{0.5 \cdot \pi \cdot \mathrm{N_A} \cdot \mathrm{dm}^3}{3 \cdot \mathrm{V_m}}$$

where dm is the particle diameter in nanometres, Na is Avogadro's number and V_m is the molar volume of silver (mL/mol). Considering the effect of AgNPs dimensions against *E. coli*, Lok *et al.*[4] showed that AgNPs with an average diameter of 9.2 nm were 9 times more active than particles with an average diameter of 62 nm. Morones *et al.*[70] reported that the bactericidal properties of the carbon-stabilized AgNPs are size dependent in four types of Gram-negative bacteria, since the only nanoparticles that displayed a direct interaction with bacteria preferentially had a diameter of 1–10 nm. At variance, Su *et al.*[6] prepared silver nanocomposites of different sizes (45.7 nm and 25.9 nm) within a silicate clay and found that the bacterial growth inhibition was not significantly dependent on the particle size but only on the silver amount (Figure 17, left).

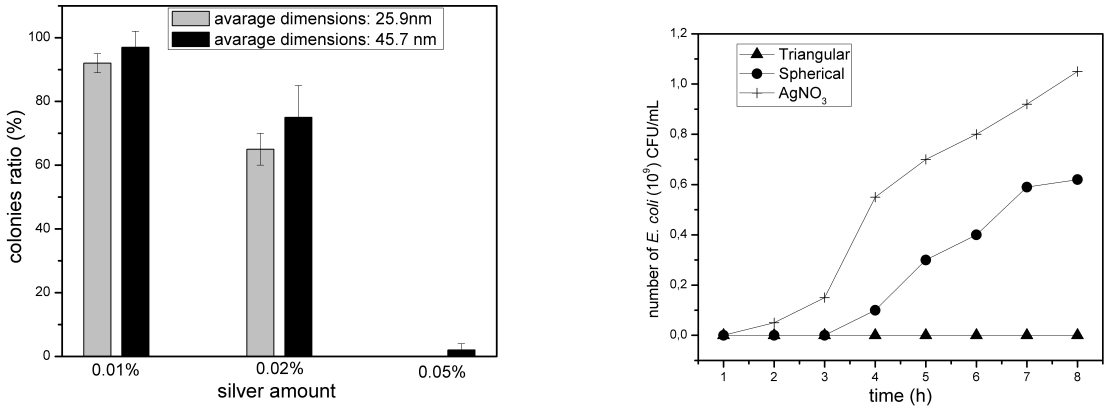

Figure 17. Left) Antimicrobial study on AgNP/Clay nanocomposites: in this system the biocidal effect depends on the silver content and not on particles size (redrawn from Su *et al.* 2009). Right) Comparative graph of the dynamics of *E. coli* growth in the presence of spherical silver nanoparticles, triangular nanoparticles and of ionic silver ($AgNO_3$) (redrawn from Pal *et al.* 2007)

The crystallographic structure and shape of the nanoparticles are considered as important properties affecting the antimicrobial behaviour. Recent works have demonstrated that the reactivity is favoured by high atom density facets such as {111}[70]. According to Pal *et al.*[71] truncated triangular nanoparticles display a higher antibacterial activity as compared to spherical nanoparticles and ionic silver (Figure 17, right).

Comparing the antibacterial activities of metallic and partially oxidized AgNPs, Lok *et al.*[4] indicated that only partially oxidized particles exhibited antibacterial activities and since smaller AgNPs have a higher surface area-to-mass ratio, they provide higher relative concentration of chemisorbed silver ions. The matrix where the nanoparticles are dispersed is of primary importance to determine the performance of the material; in fact, in the final nanocomposite constructs, stabilizers play a fundamental role to control the formation of nanoparticles as well as their dispersion stability. For example, in the case of polymer solutions, the concentration of the stabilizer operates as a controller of nucleation, affecting the size of the final nanoparticles as can be monitored by UV-Vis spectra and TEM observations. Polymeric dispersants or capping agents are generally used to stabilize AgNPs, but it must also be considered that they may deactivate the nanoparticles functions because the organic wrapping on the metal surface can limit or prevent its surface reactivity[6].

3.1.4 Antimicrobial mechanism

Three main strategies can be pursued to render materials antimicrobial[29], by choosing:

1. the anti-adhesiveness;
2. the biocide-release activity;
3. the activity by contact.

Silver-based systems can be developed both as biocide-releasing systems (Ag^+) and as contact-active materials. Although the toxic effects of silver on bacteria have been investigated for more than 60 years, the mechanism by which silver is able to kill bacteria is still only partially understood [59,70]. Several investigations have suggested possible mechanisms involving the interaction of silver ions with biological macromolecules.

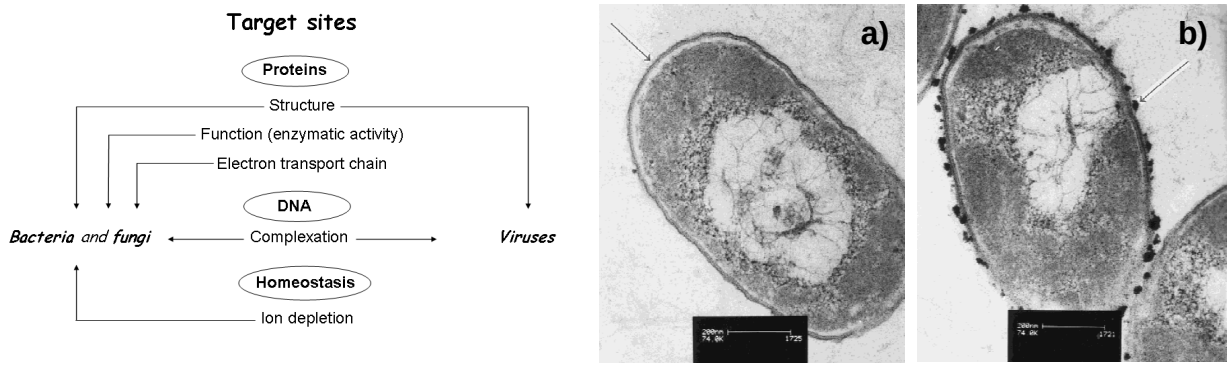

Figure 18: Left) Interaction sites of silver ions on microorganisms. Right) Internal structure of *E.coli* cells treated with silver ions. a) Cytoplasm membrane detachment from cell wall (arrow). B) Electro-dense granules around the cell wall (arrow). From Feng *et al.* (2000), reproduced with permission.

Most of the Ag^+ sensitive sites are likely to be proteins and their alterations will result in cell disruption due to structural and/or severe metabolic damage (Figure 18, left). Silver ions inhibit a number of enzymatic activities reacting with electron donor groups containing sulfur, oxygen, or nitrogen such as carboxylates, phosphates, hydroxyl, amines, imidazoles, indoles and especially sulfhydryl groups[72-75]. In the bacterial cell wall, free sulfhydryl groups are localized on transmembrane and outer-membrane proteins, including proteins of the electron transport chain, and they protrude in the extracellular portion of the membrane where they represent a very accessible interaction site for silver ions [70,73,76-78].

The Na^+-translocating NADH:ubiquinone oxydoreductase (NQR) has been recognized as one of the primary targets for Ag^+ ions. It is a component of the respiratory chain of various bacteria and it generates a redox-driven transmembrane electrochemical Na^+ potential. In two independent studies, submicromolar concentrations of Ag^+ ions were demonstrated to inhibit energy-dependent Na^+ transport in membrane vesicles of the NQR-possessing *Bacillus sp.* strain [79] and to inhibit purified NQR of *V. alginolyticus* [80]. Dibrov *et al.* [81] showed that low concentrations of Ag^+ (submicromolar) induce a massive proton leakage through the *Vibrio cholerae* membrane, which results into a complete alteration and elimination of transmembrane proton gradient, de-energization, followed by cell death.

A study performed on *E. coli* as a bacterial model pointed out that the bactericidal action of silver ions is correlated with the interaction with ribosomal subunit proteins and with the suppression of enzymes and proteins necessary for ATP production[82].

Ag^+ also forms complexes with the DNA bases, inducing DNA condensation. It is known that the replication of DNA molecules is effectively conducted only when DNA molecules are in a relaxed state. In a condensed form, DNA molecules lose their replicating abilities [59,70,73].

Feng *et al.* [73] have provided a morphological and structural study on the changes that occur on bacteria when treated with silver ions. They observed detachment of the cytoplasm membrane from the cell and the presence of dense electron granules around the cell wall and in the cytoplasm. As explained by Feng, these electron-dense granules, likely formed by the combination of silver and proteins, are prevented from permeating through the membrane, denying electron transport. Silver ions produce the formation of a low molecular weight region in the centre of the bacteria, which is considered a defense mechanism by which the bacteria conglomerates its DNA to protect it from toxic compounds when the bacteria senses a disturbance of the membrane (Figure 18, right).

As to silver nanocomposite materials, it is still not clear whether the biocidal mechanism of the AgNPs involves only silver ions or it also follows different routes [6]. Various mechanisms have been suggested according to the morphological and structural changes of bacteria. Generally, silver is believed to interact with the bacterial membrane either by direct contact between the nanoparticle and the membrane causing a direct transfer (solvent free) of Ag^+ ions, or by means of silver ions released into the medium. A combination of the two mechanisms is also possible. Stevens *et al.* [63] suggested that when bacteria are in direct contact with silver nanoparticles in the medium they locally encounter high amounts of silver ions resulting in their death. In fact, the high surface-to-volume ratio of the nanoparticles accounts for a sustained local supply of silver ions at the material-bacterium interface, preventing bacterial adhesion and biofilm formation (Figure 19, left). It must be also taken into account that if plasma proteins adsorb onto the biomaterial surface, the release of Ag^+ can be hampered as well as the direct contact between nanoparticles and bacteria can be prevented.

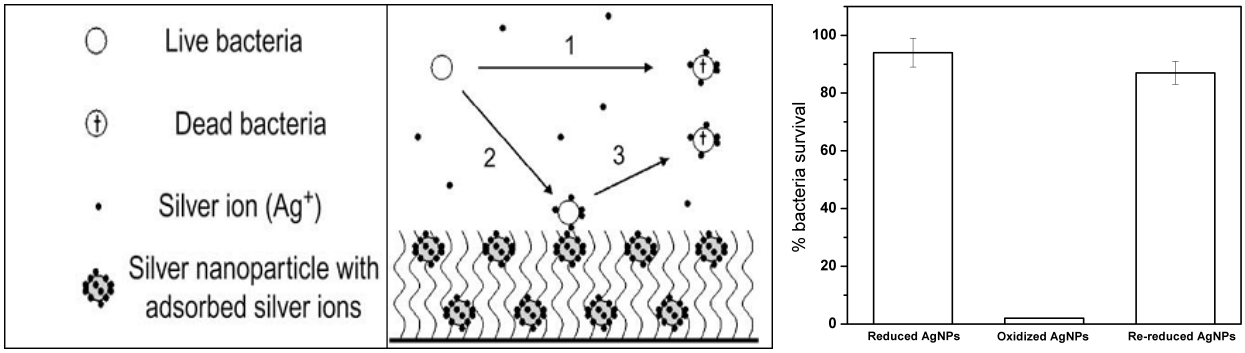

Figure 19. Left) Schematic representation of the possible antimicrobial mechanisms by ions elution or by contact-dependent transfer of silver ions following collision with the silver nanoparticle-containing surface. From Stevens *et al.* (2009), reproduced with permission. Right) Antibacterial activity of reduced, oxidized and re-reduced silver nanoparticles (redrawn from Lok *et al.* 2007)

Catellano *et al.*[83] suggested that when metallic silver reacts with the moisture in the wounded skin it gets ionized and binds to bacterial membrane proteins, DNA and RNA, leading to bacteria death. Lok *et al.*[4]

reported that the antibacterial activity of AgNPs is dependent on surface oxidation; in contrast with zeroth-valent nanoparticles, only partially oxidized AgNPs exhibit antibacterial activities suggesting that partially oxidized AgNPs may be carriers of chemisorbed Ag^+ in quantities that are sufficient to cause bacterial damage (Figure 19, right). A possible way of delivery of Ag^+ from oxidized AgNPs may involve a direct interaction with the bacterial membrane. Su *et al.*[6] studied the antimicrobial mechanism of AgNPs/Silicate Clay nanocomposites; these constructs appear to exert their biocidal effect by means of a direct contact with the nanoparticles and not by means of the silver ions released, which indicates that in this system a simple contact with AgNPs is sufficient to trigger membrane leakage and cell death.

One of the main target sites of silver nanoparticles is the bacterial membrane where deep morphological changes are induced leading to a significant increase of permeability and to the alteration of transport mechanisms through the plasma membrane [27,84]. As reported by the authors[27], a colloidal system based on a lactose-modified chitosan and AgNPs, noticeably affects membrane potential and permeability. Cell membrane depolarization has been assessed by addition of a fluorescent probe (DiBAC4(3)) able to selectively enter and label bacteria whose membrane potential has collapsed. The fluorescence intensity of AgNPs-treated bacteria increases with respect to untreated cells after only 10 min of incubation with the silver-based colloidal solution, revealing a remarkable depolarization of the cell population (97.5 % of cells) that boosts to 99.6% after 30 min, proving a strong interaction with the bacterial membrane. Since the antimicrobial mechanism is supposed to involve a damage of the bacterial membrane, the membrane integrity has been also evaluated by means of the fluorescent probe propidium iodide (PI), which allowed to reveal a remarkable permeabilizing effect as a function of time of incubation (Figure 20, left).

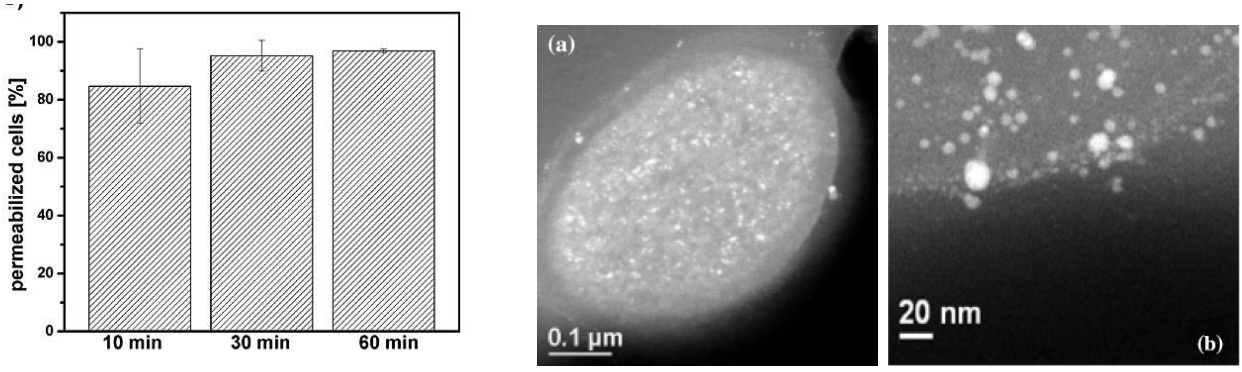

Figure 20. Left) Effect of polymer-stabilized silver nanoparticles on the membrane integrity of *S. epidermidis*. From Travan *et al.* (2009), reproduced with permission. Right) (a) Silver nanoparticles on the membrane and inside *E. coli* bacteria. (b) Magnification of *E. coli* membrane, where the presence of silver nanoparticles is clearly observed. From Morones *et al.* (2005), reproduced with permission.

Morones *et al.* [70] have tested silver nanoparticles on four types of Gram-negative bacteria: *E. coli, V. cholera, P. aeruginosa* and *S. typhus.* They observed silver nanoparticles attached to the cell membrane and in the cytoplasm of the bacteria (Figure 20, right). The mechanism by which the nanoparticles are able to penetrate into the bacteria is not totally understood, but the observation of silver nanoparticles on the cell surface and inside the bacteria is fundamental in the understanding of the bactericidal mechanism. In analogy with the

mechanism suggested for silver ions, nanoparticles might tend to react with sulfur-containing proteins, as well as with phosphorus-containing compounds such as DNA, inducing irreversible cellular damages. Proteomic data revealed that a short exposure of *E. coli* cells to antibacterial concentration of AgNPs resulted in an accumulation of envelope proteins precursors, indicative of the dissipation of proton motive force. Consistent with these proteomic findings, nano-Ag was shown to destabilize the outer membrane, to collapse the plasma membrane potential and to deplete the levels of intracellular ATP[85]. As free-radicals increase is considered as one of the possible explanation of the antimicrobial mechanism [86,87], Su *et al.*[6]studied the burst of free radicals and reactive species of oxygen (ROS) in AgNPs/Clay-treated bacteria by measuring 2,7-dichlorofluorescin-diacetate (DCFH-DA) as intracellular-ROS indicator. Results show that 40.3% of the AgNPs/Clay-treated bacteria became DCF^+, indicating that ROS were generated and played a role in the killing mechanism. In addition it was observed that bacteria lost their mobility upon treatment with the nanocomposites, meaning that the motor function of the cytoskeleton is hampered with a consequent prevention of cytokinesis (Figure 21). Nanocrystalline silver-supported activated carbon [88] show kinetics of bacterial inactivation, in the presence of hydroxyl radical scavengers and superoxide anion radical inducer that suggest the contribution of the reactive oxygen species (ROS) to antibacterial effect. However, these ROS scavengers did not show any inhibition of bactericidal activity after approximately 1 hour, suggesting that generated ROS are responsible for *E. coli* inactivation only during the initial hour of the incubation time. The antibacterial process was found to be highly increased at higher temperature, which was ascribed to the enhanced ROS formation and Ag^+ elution.

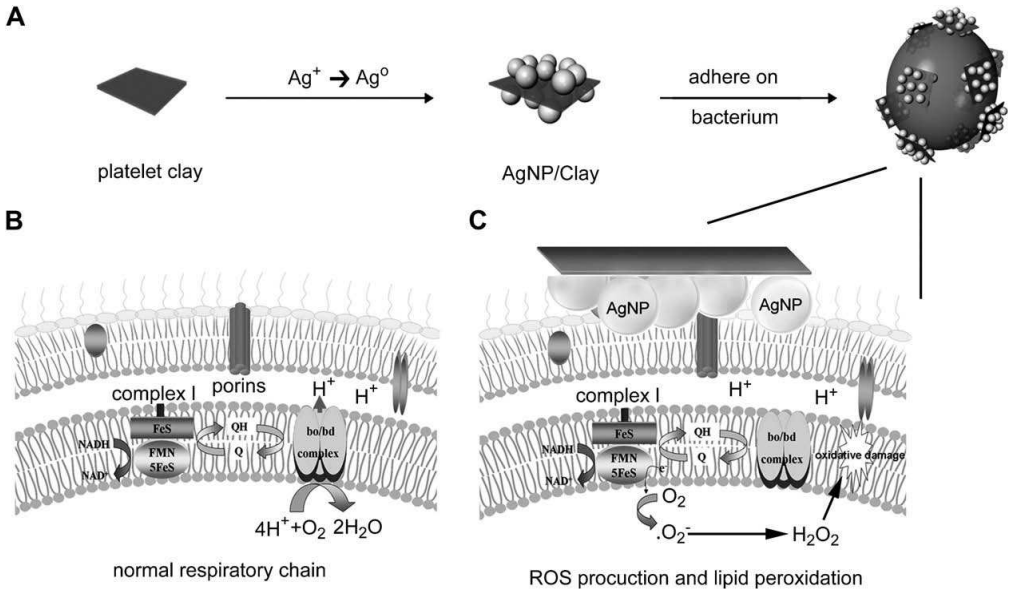

Figure 21. Possible mechanisms of AgNP/Clay-mediated cytotoxicity. (A) AgNPs on synthetic platelet clay show electrostatic attraction to bacteria and form AgNP clusters on the bacterial cell wall. (B) Electronic transport through the respiratory chain on plasma membrane of *E. coli* through complex I, ubiquinone oxidoreductase (Q) and cytochrome bo/bd ubiquinone oxidase (bo/bd complex). (C) AgNP/Clay on the cell wall interacts with transmembrane proteins and consequently interferes with the proton pool in the intermembrane space or the electronic flow through the respiratory chain. Accumulated electrons due to a disturbance of complex I are transferred to oxygen to form O_2 and H_2O_2, contributing to oxidative damage and membrane leakage in bacteria. From Su *et al.* (2009), reproduced with permission.

3.2 SILVER NANOCOMPOSITES IN WOUND HEALING

Non-healing chronic wounds (*e.g.*, diabetic ulcerations, pressure, venous and arterial ulcers and burn wound) are a serious problem in the healthcare system all over the world; they cause great pain and suffering to patients, affecting their quality of life; moreover they have a serious financial impact on health systems. When the wound bio-burden exceeds a host-manageable level, a wound may become infected. Chronic wounds can be easily contaminated with several species and the progression to local infection occurs in stages, often leading to critical colonisation [89]. Chronic infections are clearly detrimental to wound healing and they are one of the main factors that contribute to the formation of a non-healing wound [90]. When they occur and the host response is depressed, the normal healing process is broken off because of a prolonged inflammatory response, molecular and cellular abnormalities in the wound bed and granulation tissue disruption, resulting in a deteriorating wound [91]. Appropriate management of infected and critically colonised wounds is therefore essential to encourage wound healing progression [92]. Unfortunately, not only critical colonisation or infection are difficult in diagnosing, but traditional topical antimicrobials can be toxic to granulation tissues or increase the chance of resistant organisms. Silver, in its ionic form or as nanoparticles, is particularly attractive as an antibacterial agent for infected wound treatments because it can be readily incorporated into dressing materials or included in topic antimicrobial ointments. Topical antimicrobial agents, such as silver-based formulations, are often used to prepare the wound for healing. Silver ions are effective against a broad range of micro-organisms such as yeast, mold, and bacteria, including MRSA (Methicillin-Resistant *Staphylococcus aureus*) and VRE (Vancomycin-Resistant Enterococci) when they are provided at an appropriate concentration. The commonly used forms are silver-coated dressings, which have been demonstrated to be more effective in killing a broader range of bacteria than cream-based silver applications. They are less irritating than silver nitrate solution and better tolerated [93]. Chronic wounds take advantages by the use of AgNPs-based devices not only for their antimicrobial activity but also for the additional biological properties displayed by metal nanoparticles which improve the opportunity for wound healing by creating conditions that are unfavourable to micro-organisms and favourable for the host repair mechanisms. One of the major contributors to delayed wound healing is a prolonged inflammatory response in the wound [94]. Normally, the inflammatory response occurs immediately following wounding and it starts to induce phagocytosis and removal of bacteria and tissue debris. It also releases factors that cause the migration and division of cells involved in the proliferative phase and in the deposition of new tissues components. A prolonged inflammatory response, however, may result in the destruction of tissue by the same processes that normally have protective and restorative functions. Increasing evidence from *in vivo* and *in vitro* studies indicates that AgNPs promote wound healing thanks to their potent anti-inflammatory activity [95-98]. This activity seems to be correlated to increased expression of anti-inflammatory molecular signals such as vascular endothelial growth factor (VEGF), IL-10 and to reduction of pro-inflammatory cytokines as IL-6 and interferon-γ. VEGF promote wound healing inducing vascular permeability and endothelial cell proliferation. IL-10 is a vital mediator of the anti-inflammatory cascade produced by keratinocytes as well as inflammatory cells involved in the healing process, including T

lymphocytes, macrophages, and B lymphocytes. One of the unique actions of IL-10 is its ability to inhibit the synthesis of pro-inflammatory cytokines including IL-6. IL-6 is secreted by polymorphonuclear cells and fibroblasts and it has been recognized as an initiator of events in the physiological alterations of inflammation after thermal injury [99]. It promotes inflammation through monocyte and macrophage chemotaxis and activation [100]. Decreased levels of IL-6 may results in fewer neutrophils and macrophages recruited to the wound and less cytokines being released into the wound with, subsequently, a lower paracrine stimulation of cellular proliferation, fibroblast and keratinocyte migration, and extracellular matrix production. This lack of amplification of the inflammatory cytokine cascade may be important in providing a permissive environment for scarless wound repair to proceed. Moreover, silver-induced neutrophil apoptosis, decreased matrix metalloproteinases (MMPs) activity, and inhibition of free radicals formations (ROS/RNS) also contribute to the overall decrease in the inflammatory response and, as a consequence, an increased rate of wound healing[97,101-104]. MMPs are a group of proteinases including collagenases, elastase, and gelatinases that can be endogenous (cellular) or exogenous (bacterial) in origin and that have been shown to be present in chronic ulcers at abnormally high levels, as compared with acute wounds and may contribute to the chronicity of the wounds [105]. MMPs function in the controlled degradation of the extracellular matrix to remove damaged components and to allow cell migration and angiogenesis to occur [106]. However, it has been proposed that elevated activities of these enzymes may contribute to excessive matrix destruction and therefore to wound repair delay. In the biomedical field, market offer a large select of wound dressing containing silver in different chemical forms such as silver salts, silver oxides and metallic silver. With the advent of the nanotechnologies the interest has been focused primarily on silver salts, since, in comparison with silver ions and metallic silver, they exhibit both improved bactericidal and fungicidal effectiveness due to their nanoscale dimensions and good silver release kinetics because of their slight solubility. Table 1 offers a list of type and composition of some commercially available silver-based dressing. All new commercial wound care products have typically a multilayer structure. From the top, they include an outer acrylic adhesive layer that protects wound from the external environment, a middle layer to absorb the exudates and finally a wound contact layer where are incorporated silver particles. The selection of suitable silver substrate depends upon many factors like designing of wound care product, type of wound, fabric strength, thickness etc. The substrate materials may include cotton, viscose, silk, polyamide fibers, hydrogels (alginate and agarose) and hydrophilic polyuretane foam.

Silver formulation	***Product name***	***Manufacturer***
SILCRYST Nanocrystalline (Patented Silver technology)	Acticoat ®	Smith&Nephew
Nanocrystals of metallic silver	Acticoat 7 ®	Smith&Nephew
Ionic silver	Aquagel Ag ®	Convatec
Metallic silver	Actisorb Silver 220®	Johnson&Johnson
Silver particles	Polymem Silver®	Ferris Mfg. Corp.
Ionic silver	Suprasorb A+Ag®	Activa Healthcare
Silver sulphadiazine	Urgotul SSD ®	Urgo Medical

Table 1: Commercially available silver-based dressings

3.3 SILVER NANOCOMPOSITES AND INFLAMMATION

Besides the anti-inflammatory activity of AgNPs related to wound healing, numerous studies have suggested that nanocrystalline silver have a general anti-inflammatory effect, but its molecular and cellular mechanism of action have not been fully elucidated [107-111]. On allergic contact dermatitis models, anti-inflammatory activity of topical nanocrystalline silver cream is comparable with the effects of topical steroids and currently available immunosuppressant [107-109,112]. This study shows that nanocrystalline silver treatments uniquely decrease induced erythema and edema, increasing apoptosis in inflammatory cells, decreasing MMPs activity and inhibiting proinflammatory cytokine expression such as TNF-α, TGF-β, interleukin-12 and -8.

The reduction of pro-inflammatory factors and MMPs activity is ascribed both to a specific inhibition of gene expression [108] and to the reduction of inflammatory cells via apoptosis [109]. Programmed cell death, or apoptosis, occurs in various physiological and pathological conditions, and takes place through a characteristic mechanism of intercellular sequential reactions. During inflammation events, apoptosis contributes to the elimination of inflammatory cells from the inflamed area. When cells, like neutrophils and T-lymphocytes, die by apoptosis, they initially maintain plasma membrane integrity, and granulocytes lose the ability to secrete granular contents consisting of numerous cytotoxic and pro-inflammation factors [113,114]. Apoptotic cells are recognized and phagocytised by neighbouring macrophages, further minimizing local inflammation and tissue injury[114]. In contrast, when inflammatory cells die by necrosis they burst and release numerous cytotoxic compounds, including proteases, oxygen radicals, and various acids, which further amplify local inflammation[115-118]. In this perspective, cell death by apoptosis represents an injury-limiting clearance mechanism and plays an important role in the resolution of local inflammation. Interestingly, anti-inflammatory effects were observed only or mostly for silver nanoparticles and not for comparable concentrations of silver salts [102,109]. Moreover, silver salts such as $AgNO_3$ may even have an opposite effect, being pro-inflammatory with subsequent delay healing [119,120]. The apparent discrepancy may be solved by the hypothesis proposed in a recent work by Nadworny *et al.* [109] who demonstrated that in porcine models of contact dermatitis, dressings containing nanostructured silver induce apoptotic processes in a discriminatory way toward dermal cells and did not target keratinocytes. Otherwise, apoptotic activity was induced indiscriminately by $AgNO_3$-based dressings in all cell types at the tissue surface, including keratinocytes. The authors therefore assume that the anti-inflammatory activity displayed by nanocrystalline silver is not due to Ag^+ form but it may be related to Ag^0 form. This species may be anti-inflammatory such as other noble metals. For instance, colloidal gold is successfully used as rheumatoid arthritis treatment[121,122]. Various gold-containing compounds, used as anti-inflammatory agents in the treatment of rheumatoid arthritis, induce apoptosis in cells including T cells and macrophages through multiple mechanisms. Moreover Au^0 nanoparticles suppress the activity of IL-6 and TNF-α thus relieving rheumatoid arthritis symptoms [123,124]. *In vitro* and in *vivo* studies indicate that in a biological environment, gold in its monovalent state (Au(I)) when not tightly bound to ligands, such as cyanide, a phosphine, or molecules containing sulphur(II), spontaneously dismutate to finely divided metallic gold (Au^0) and auric (Au(III)) complexes. The crystal structures (face-centered cubic) and Pauling covalent raddii for silver and gold are equal; thus they conclude

that silver and gold can replace each other in crystal lattices, suggesting that Au^0 and Ag^0 clusters should be physically identical, and therefore may have similar biological activity.

3.4 SILVER NANOCOMPOSITES FOR APPLICATIONS IN BIOLOGICAL SENSING AND NANOSCALE PHOTONICS

Metal nanocomposites are being studied also with respect to nanoparticle plasmonics, an emerging research field related to the optical properties of noble metal nanoparticles of various size, shape and structure. In particular, the scattering of plasmon-resonant nanoparticles and their colours in dark-filed microscopy allow for many applications in biomedical imaging. Depending on the type of nanoparticles and on nature of the stabilizing shell on their surface, plasmon resonant nanoparticles can emit bright resonance light scattering of various wavelengths[125]. These nanoparticles can be addressed to well defined biological targets by means of surface functionalization with proper molecular signals; selected biomacromolecules can be attached to the metal nanoparticles, used as optical labels, to target specific receptors. According to this rationale, noble metal nanoparticles, especially gold and silver are being studied for *in vivo* imaging applications in order to overcome the limitations associated with traditional fluorescence probes (photobleaching, autofluorescence of living cells, ect…).

Among noble metal nanoparticles, AgNPs offer the highest quantum yield of Rayleigh scattering and for this reason colloidal silver can be efficiently used as optical probe for *in vivo* imaging in real time with sub-100 nm spatial resolution and millisecond time resolution[54]. Schrand *et al.*[126] demonstrated that low concentrations of AgNPs (<25 $\mu g\ ml^{-1}$) bind to the plasma membranes of living cells, and intensely scattered light when imaged at submicron resolution with high illumination light microscopy, thereby demonstrating their potential use as biological labels. Lee *et al.*[54] reported the use of silver colloids for the study of nanoparticles transport, biocompatibility, and toxicity in early development of zebrafish embryos in real time by means of dark-field single nanoparticle optical microscopy and spectroscopy. Huang *et al.*[57] have developed functionalized silver nanoparticle biosensors to quantitatively measure the binding kinetics and affinity of single protein molecules on single living cells for an extended period of time (hours) using single-nanoparticle optical microscopy and spectroscopy (Figure 22). These silver nanocomposites offer the possibility to monitor cascades of biochemical reactions in real time through a quantitative molecular imaging.

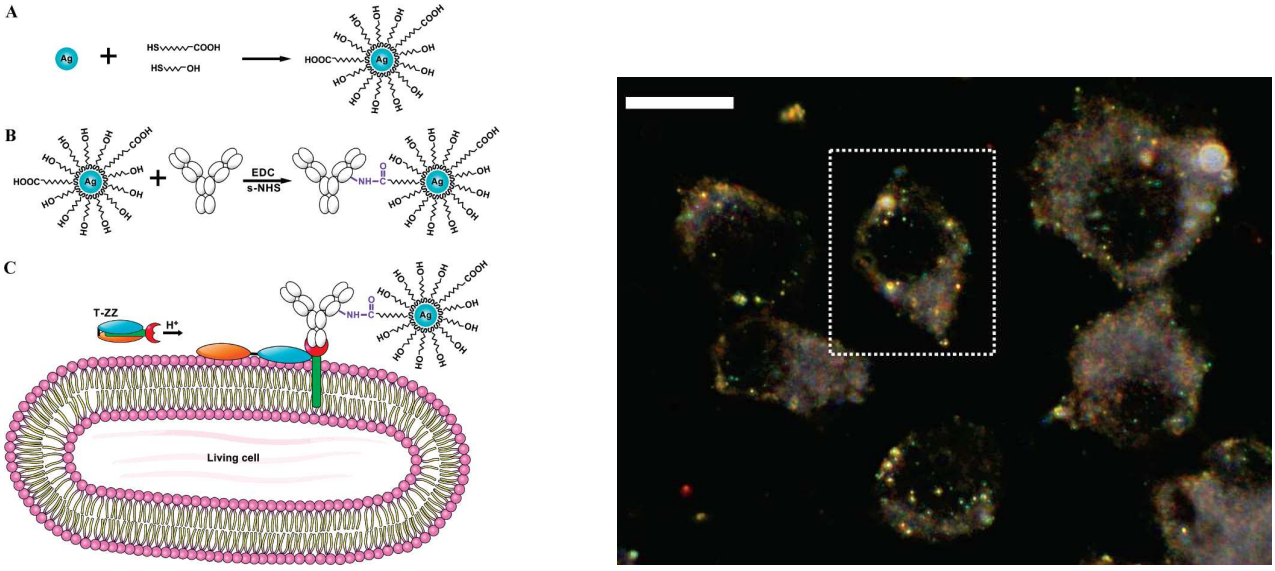

Figure 22. Left) Schematic illustration of preparation of single-nanoparticle biosensors to image and detect single T-ZZ molecules on single living cells. (A) Functionalizing AgNPs. (B) Covalently linking with immunoglobulin G. (C) Attaching T-ZZ onto living cells to detect single T-ZZ molecules on single living cells. Right) Imaging and sensing of single T-ZZ molecules on single living cells using single AgMMUA-IgG nanoparticle biosensors by SNOMS imaging system. The scale bar is 10 μm. From Huang *et al.* (2007), reproduced with permission.

Hu *et al.*[127] have developed biocompatible polyelectrolyte-coated AgNPs for targeted *in vitro* labelling of pancreatic cancer cells; these particles can be conjugated with monoclonal antibodies and proteins and act like plasmon enhanced scattering probes for dark-field multiplex and TEM imaging of pancreatic cancer cells. Nanoparticle optics can be also employed as a tool for real-time monitoring of the effect of antibiotics in living bacteria cells with millisecond temporal and nanometer-sized resolution; Kyriacou *et al.*[128] studied the modes of action and the pharmacokinetics of antibiotics in *P. aeruginosa* treating bacteria with silver colloidal solutions and evaluating the membrane permeability and the disruption of the cell wall by means of optical darkfield microscopy and spectroscopy. Lesniak *et al.*[58] synthesized fluorescent and biocompatible silver/ poly(amidoamine) dendrimers carrying various surface functionalities for applications as cell labelling agents as demonstrated by *in vitro* assays with four different cell lines.

Aside of the bioimaging field, the strong plasmon resonance of silver nanoparticles can find other applications in the field of nanophotonics. A particular area of interest of silver nanocomposites constructs for biomedical purposes is in the field of Raman Spectroscopy, since a significant enhancement of the Raman signal can be achieved in the presence of plasmon resonant nanoparticles. This phenomenon called "Surface Enhanced Raman Scattering" (SERS) provides chemical information of molecules in the proximity of metal nanostructures. Since the enhancement factor can be as much as 10^{14}-10^{15}, this technique can be used for the detection of very diluted compounds or even single molecules[129]. The size and arrangement of the nanoparticles strongly affect the enhancement factor, thus the structural properties of the nanocomposite system determine its efficient use in SERS applications. Jia *et al.*[130] developed a "green synthesis" preparation of silver nanocomposites based on the formation of AgNPs within a cuttlebone-derived organic matrix as a natural macroporous dispersing material. It was shown that the resulting nanocomposite films can

be successfully employed for trace analysis in SERS applications. Many efforts aim at developing effective ways to organize the nanoscale particles into functional structures and devices. In particular efficient routes for the fabrication of films characterized by a high density of nanoparticles with controllable spacing on solid substrates are sought; Lu *et al.*[42] developed a silver nanocomposite film with temperature-controllable interparticle spacing for a tuneable SERS substrate. In such constructs, the scattering signal enhancement factor can be dynamically tuned by thermal activation; in fact, the spacing between nanoparticles can be controlled by adjusting the temperature in order to approach strongest coupling between adjacent particles and match the plasmon resonance wavelength to the laser excitation wavelength (Figure 23). This nanocomposite system can find applications in label-free biomolecular detections, environmental monitoring, and biological warfare agents sensing.

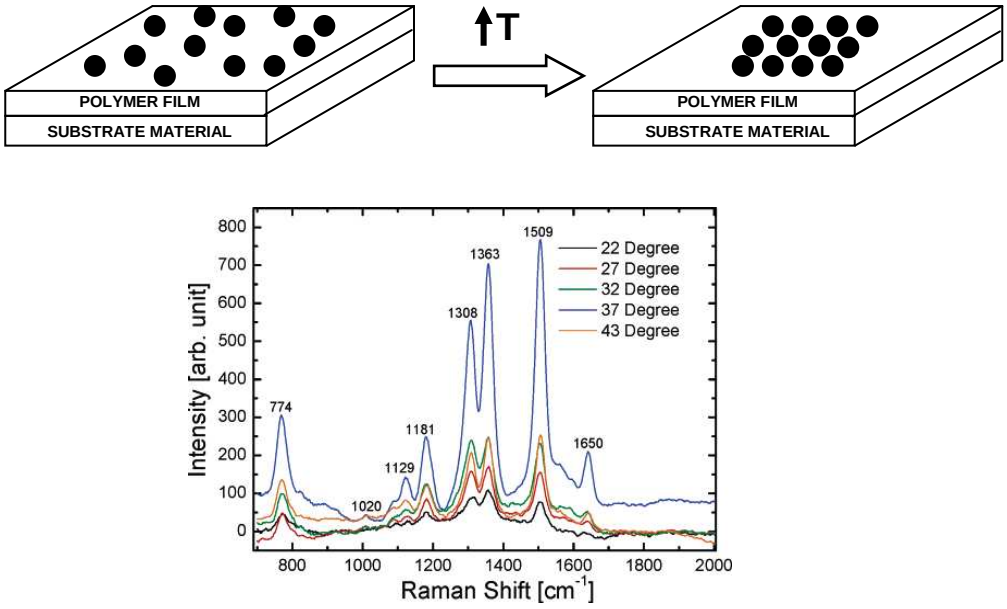

Figure 23. Top: schematic illustration of a nanoparticle monolayer on a thermo-responsive polymer film. Bottom: SERS spectra of Rhodamine 6G on the nanocomposite film at different temperatures. From Lu *et al.* (2005), reproduced with permission.

Biocompatible SERS substrates based on chitin (cicada wings) and silver were prepared by Stoddart *et al.*[131] who propose a molecular detection limit as low as nanomolar level.

4.0 BIOLOGICAL HAZARDS OF SILVER NANOCOMPOSITES

Nano-sized materials are currently being used in medicine, biotechnology, energy and environmental technology. Given the wide variety and growing number of applications on the market, there is a lack of studies and information regarding the effects of nano-sized materials (silver nanoparticles included) on

general human health and environment. At present silver-based products are widespread available on the market primarily as formulations for topical applications, both in the medical areas such as wound dressing and surgical instruments, coated or embedded with AgNPs, and in daily life where consumers have access to silver containing detergents and soaps, room sprays, water purificants, textiles, personal care products, handles and furniture for public places. Silver-based systems are also used in some food processing industry where pipelines are susceptible to biofilm formation. Besides, more recently AgNPs have been studied to be exploited for systemic applications and for the preparation of internal prosthesis and devices (e.g. bone cement, catheters). Hundreds of silver-based products are currently on the market, but there are not specific reporting requirements, risk assessments or official government indications for the commercialization of these kinds of products. The widespread use of AgNPs and silver ion-based products is partially justified by the fact that till few years ago and even nowadays, many researchers associated to ionic silver low toxicity in the human body and expected minimal risk with respect to clinical exposure by inhalation, ingestion, dermal application or through the urological or haematogenous routes. Silver is not known as a systemic toxic agent for humans, except at extreme doses. The most evident secondary effects derived by chronic ingestion or inhalation of silver preparations (especially colloidal silver) is the deposition of particles in the skin (argyria), eye (argyrosis) and other organs. These conditions are generally not considered life-threatening but simply cosmetically undesirable. Silver in form of ions is absorbed into the human body and enters the systemic circulation as a protein complex to be eliminated by the liver and kidneys with a metabolism modulated by induction and binding to metallothioneins. These protein complexes can mitigate the cellular toxicity of silver and contributes to tissue repair[132]. Literature does not report cases of people specifically harmed by the use or exposure AgNPs: this fact could be attributed to the lack of knowledge about what effects to expect. A recent work by Larese et al., demonstrated the absorption of silver nanoparticles through intact and damaged skin, detecting the presence of nanoparticles in the stratum corneum and the outermost surface of the epidermis [133]. In fact, in sharp contrast with the attention paid to new applications of silver nanocomposites, few studies provide insights (and only scant ones) into the possible interaction of AgNPs with the human body after entering *via* different routes, and not only through skin. Systemic distribution and translocation, organ accumulation, degradation, possible adverse effects and toxicity in human tissues start to be considered and open major questions associated with the increased medical use of silver nanocomposites.

An important and often disregarded aspect to be considered when studying the biological effect of silver nanocomposites is that nanoparticles show an impressive array of unusual physical-chemical properties that confer them higher and often unpredictable bioactivity when compared to the identical bulk materials. For instance, based upon size alone and not upon physical or chemical properties, nanomaterials have capabilities (normally attributed to micro-organisms like viruses) to penetrate circulatory system and to reach and to translocate in all living organs including the blood-brain barrier. In the last 5 years most of the *in vitro* studies regarding the exposure of cellular cell lines to silver nanoparticles have evidenced the presence of a potential cytotoxic mechanism that is strictly dependent on particle size and concentration. In spite of the limited number of cell lines tested, all experimental data agree that the mitochondria are the main intracellular target of silver nanoparticles. AgNPs mediate their toxicity through an oxidative stress with increase of ROS levels and following activation of the apoptotic mitochondrial pathway [134-138]. This is a mechanism shared by all cell lines tested [139-145], in which apoptosis and apoptosis-like change of morphology occur when AgNPs are applied. Ag NPs induce mitochondrial membrane perturbation, generation of ROS, depletion of antioxidant GSH and reduction of mitochondrial function in BRL 3A rat liver cells [143], rat alveolar macrophages [140] and human THP-1 monocytic cells[141]. Furthermore, GSH depletion in human skin carcinoma and fibrosarcoma cell lines is associated to expression of apoptotic markers [146] and in human hepatoma cells HepG2 to the over expression of oxidative stress-related genes such us catalase and superoxide dismutase[144].It is to note a report where four commercially available silver dressings were tested in terms of cytotoxicity towards keratinocyte HaCaT and fibroblast 142BR cells[147]; the results, as similarly observed by Burd *et al.*[148], showed that all tested dressings induce, albeit to a different degree, apoptotic cell death in a way dependent on the cell line and type of dressing investigated.

Although the molecular mechanism at the base of silver nanoparticles potential toxicity is yet to be completely elucidated, a work by Hsin *et al.*[142] shed partially light on it. The mitochondria-dependent apoptotic mechanisms identified in eukaryotic cells constitute an intrinsic and an extrinsic pathway characterized by the activation of pro-apoptotic proteins such as Bid, Bad, Bak and the inactivation of anti-apoptotic proteins as Bcl-2 e Bcl-Xl. Activation of Bad and Bak results in their traslocation and oligomerization on mitochondria membrane, to form ion channels allowing exit of cytochome C and other apoptotic factors. The tumour suppressor protein p53 is able to exert a pro-apoptotic effect both by direct

transcriptional activation of pro-apoptotic genes as BAK and inhibition of expression of anti-apoptotic protein as Bcl-2 and Bcl-X and by direct binding to pro-apoptotic (Bax and Bak) and anti-apoptotic protein effectors (Bcl-2 , BcXL) [149,150,150,151]. In NIH-3T3 (mouse fibroblast) cells, pro-apoptotic internalized AgNPs induce intracellular ROS generation leading to the activation of JNK and p53 genes, and subsequently, to Bax translocation, cytochrome c release and PARP cleavage. Moreover, the elevated expression of the anti-apoptotic Bcl-2 protein induced in HCT116 (human colon cancer) cells, apparently shields these cells from silver-mediated apoptosis. In the same way, a study[152] comparing the biological effects of uncoated and polysaccharide-coated AgNPs in mouse embryonic stem cells (mES) and in embryonic fibroblast (MEF) has shown p53 upregulation in both cell lines and p53 phosphorylation in mES cells. By the experimental data so far collected by the researches till now, the prevailing hypothesis is that AgNPs interact with thiol groups of proteins and enzymes after passing through eukaryotic cell membrane. Most of those proteins can be involved in the antioxidant defense mechanism, like reduced glutathione, catalase, superoxide dismutase, that prevent tissue damage under normal conditions neutralizing ROS produced by the aerobic energy metabolism [153,154]. Over accumulation of ROS, an inflammatory response is induced and irreversible mitochondrial membrane damage and pemeabilization occurs, with following release of cytochrome C and of others apoptogenic factors [155]. Besides mitochondrial pathway activation, cell membrane destruction and lipoperoxidation can also take place and they represent another aspect of AgNPs toxicity (Figure 24).

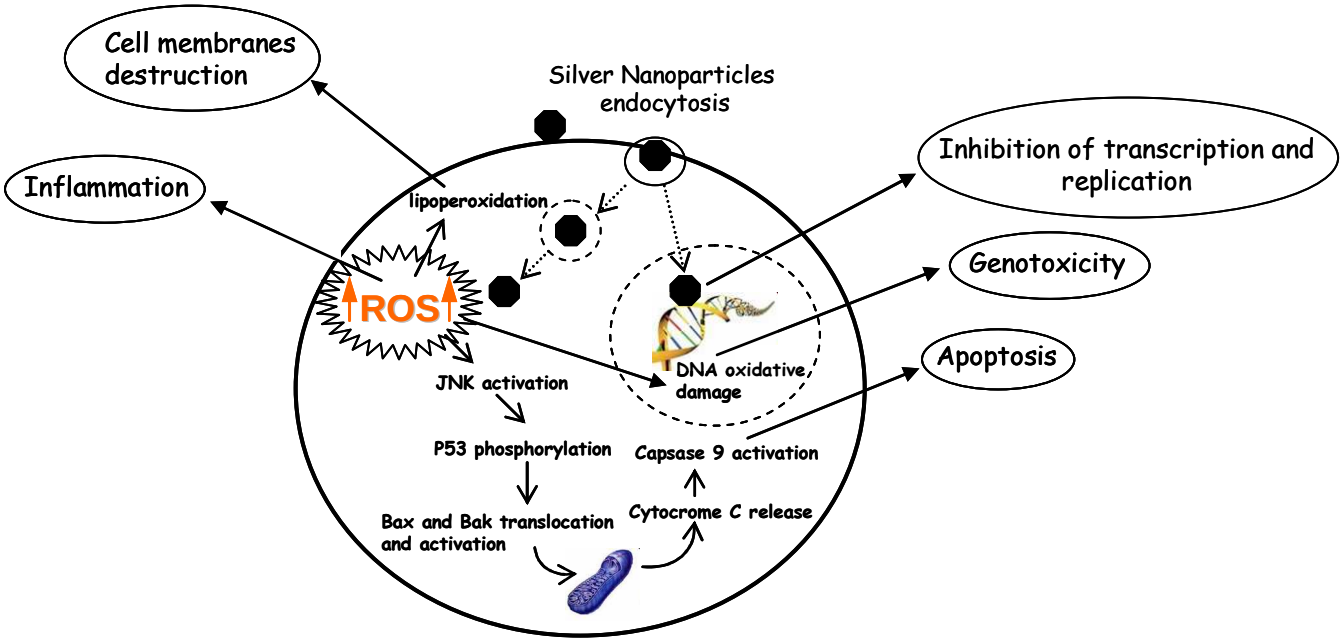

Figure 24: Cytotoxic effect of silver nanoparticles on eukaryote cells

Silver nanoparticles can be internalized through the membrane by different mechanisms that include passive diffusion, receptor-mediated endocytosis and clathrin- or caveolae-mediated endocytosis[140,144,152,156] (Figure 25).

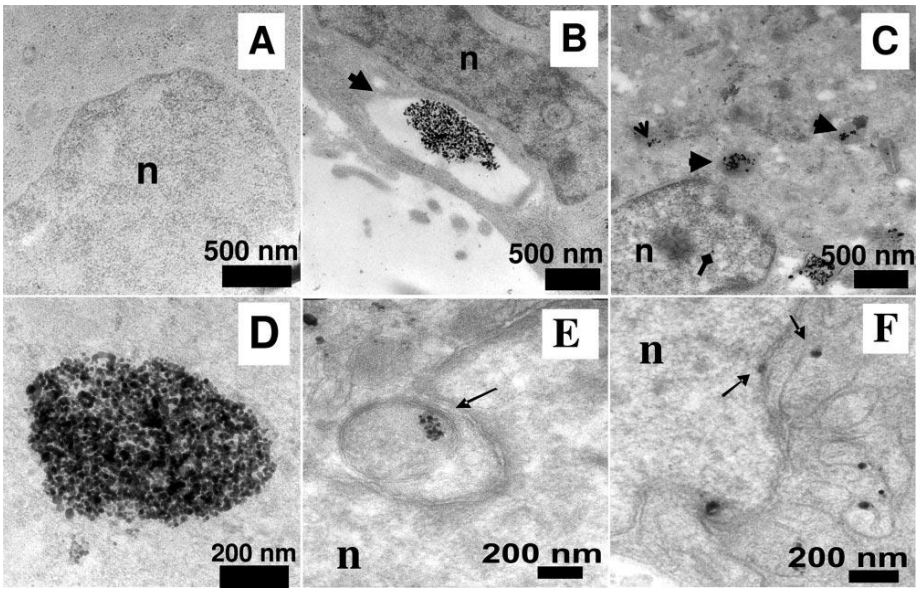

Figure 25: TEM images of ultrathin sections of cells. Untreated cells showed no abnormalities (A), whereas cells treated with Ag-NP showed large endosomes near the cell membrane with many nanoparticlesinside (B). Electron micrographs showing lysosomes with nanoparticles inside (thick arrows) and scattered in cytoplasm (open arrow). Diamond arrow shows the presence of the nanoparticle in the nucleus (C). Magnified images of nanogroups showed that the cluster is composed of individual nanoparticles rather than clumps (D). Image shows endosomes in cytosol that are lodged in the nuclear membrane invaginations (E) and the presence of nanoparticles in mitochondria and on the nuclear membrane (F). From AshaRani 2009, reproduced with permission.

The mechanism of action of AgNPs described above seems to be shared by silver ions[157], and supports the hypothesis that part of the toxic potentiality of silver nanoparticles is due to the Ag^+ release from them.

The literature survey clearly shows that over the last years studies were mainly focused to asses the adverse biological affects of AgNPs by administering them at dose and concentrations that lead to cell death or irreversible cellular damage. These studies fail to consider concentrations of nanoparticles that may not result in cellular death but may cause sub-lethal cellular alterations leading to serious consequences on human health. The most important examples are DNA damage and induction of inflammation processes. Mutation of DNA, induced by genotoxic materials, leads to carcinogenesis and has a deep impact on the biology of reproductive cells. As recently reviewed by Singh *et al.*[145], metal nanoparticles can generate DNA damage indirectly, by inducing oxidative stress and inflammation responses. ROS, whose increase is associated to an

oxidative stress and subsequence redox imbalance, react with many biological macromolecules, including DNA, enzymes and lipids; in particular, they cause oxidative damage on DNA in the form of breads of single and double-strands, purine, pyrimidine and deoxyribose modifications, abasic sites and DNA-DNA coupling[158]. At the same time, if small enough, nanoparticles can gain direct access to the nucleus either though passive diffusion or transport across the nuclear pore complexes. Within this site they can trigger aggregation of nuclear proteins with subsequent inhibition of transcription, replication and cell proliferation [159-162]. Although there is a substantial experimental evidence on the genotoxic potential of many metal-based nanomaterials, the data accumulated on silver NPs point only very marginally on their genotoxicity. The detection of γ-H2AX phosphorylation, which is indicative of DNA double strand break, was described in HepG2 cells treated with 2 μg/ml of AgNPs[144], and mouse embryonic stem and fibroblast cells exhibit a severe DNA damage response suggested by increased expression of Rad51, a key double strand break repair protein and phosphorilation at serine 139 of histone H2AX[152]. An initial screen of nanomaterials toxicity must be always accomplished using *in vitro* studies, but they must be always supported by *in vivo* test, since the *in vitro-in vivo* gap is associated with the complexity of biological interactions in a higher order organism that are not reproducible by an *in vitro* system. *In vivo* tests require animal models to evaluate markers of inflammation, oxidant stress, and cell proliferation in portal-of-entry and selected remote organs and tissues, deposition, translocation of the materials and its degradation products, toxicokinetics and biopersistence studies, effects of multiple exposures and finally potential effects on the reproductive system, placenta, and fetus. In the field of silver nanocomposite materials the scarcity of toxicity data obtained on cellular models goes in parallel with the almost lack of exhaustive studies performed using *in vivo* models. In Zebrafish embryos, AgNPs in a concentration range between 250 and 0,25 μM cause toxic lethal and sub-lethal (morphological malformations) effects albeit in a size-dependent manner for some concentrations and time points[163]. Silver nanoparticles administrated via intra-peritoneal injection in adult mice are able to traslocate to the circulatory system and reach the brain were they generate neurotoxicity by inducing free-radical oxidative stress and by altering gene expression and by producing apoptosis[164]. A study performed to compare the effects on liver caused on mice fed with nano- and micro-sized silver particles, revealed in both cases induction of liver inflammation[156]. Micro- and nano-silver particles implanted into rat's back muscle

reveal a good biological effect on days 7 and 14 but an inflammation process at day 30, more serious in AgNPs-treated rats than in the micro-silver treated ones[165].

All the studies are acute toxicity tests and no information was obtained from more informative chronic tests.

An increasing number of papers take into consideration the development and characterization of materials based on silver nanocomposites and their interaction with eukaryotic systems. As examples, Fu *et al.*[16] describe the realization of antibacterial multilayer films containing AgNPs via layer-by-layer assembly of heparin and chitosan, lacking of toxic effects on osteoblasts. Nanocomposite materials based on acrylic resins and Ag NPs stimulate fibroblast and osteoblast aggregation and growth without displaying any toxic effect[166,167], and stainless steel orthopaedic materials already commonly used in the biomedical field, when coated with silver, efficiently sustain the growth of osteoblasts and do not show genotoxicity[168]. Recently, *Travan et al*.[27] used silver nanoparticles formed and stabilized by a bioactive chitosan-derived to develop alginate-based hydrogel structures that display antimicrobial properties, but not cytotoxicity on different eukaryotic cell lines. The same nanocomposite systems based on chitosan- derived and on silver nanoparticles has been exploited to realize a non-cytotoxic coating for acrylic resins (manuscript in preparation by the authors).

However, beside to the potential toxicity of silver when topically or systematically administrated, a general concern must be also considered on the hazardous effects of nanoparticles accumulation in the environment. As the scientific literature often points out, there is a great lack of knowledge about AgNPs impact on human health but even less is what we know about its environmental pathways and its environmental effects. At present, silver is classified by EPA (US Environmental Protection Agency) as an environmental hazard because in some circumstances it is toxic, persistent, and bio-accumulative. Nanotechnology is not well researched or regulated, so the environmental impact and risks of silver nanoparticles is not known.

Nanoparticles can accumulate in air and soil but primarily in water where many substances have their most significant effects since in this environment materials can be more easily degraded, transformed and accumulated in a number of ways. When silver is present in a bioavailable chemical form [169,170] it is more toxic to aquatic organism than any other metal except mercury[171], but no comparable information are available for AgNPs. The environmental hazard of silver can be mitigated by its complexation with other compounds especially sulfide that reduce their bioavaibility. Nitrification inhibition by silver nanoparticles

was demonstrated in nitrifying bacteria isolated from wastewater treatment plants. Moreover, the results suggest that AgNPs have the same behaviour of surface complexation as silver ions, and inhibition by nanosilver in wastewater treatment may be removed by reaction of AgNPs with soluble sulfide species[87,172]. Exposure of bacteria, algae, invertebrates and fishes to AgNPs proved that organism models of various trophic levels and feeding strategies (zebrafish, daphnis and algal species) show differential susceptibility to AgNPs, with filter-feeding invertebrates being markedly more susceptible compared with larger organism (i.e. zebrafish)[173]. Although the scientific community is in agreement to retain that the paucity of data renders it premature to formulate any definite risk assessment about silver-based materials, an increasing public debate is emerging, and very contradictory opinions and experimental evidences about the potential impact of these nanomaterials on health [174,175]are often presented. A central point is that silver nanocomposites should not be considered as a uniform group of materials. The toxicity of nanocomposite materials may be influenced by particle concentration, size distribution, agglomeration state, shape, chemical and physical nature of the matrix, physical status of the composite and finally site and time of exposure. The ultimate and main goal in the field of silver nanotechnology remains still the development and choice of products with a superior profile of functionality *e.g.*, high infection control, associated to reduced host cell cytotoxicity and a moderate environmental risk to fully exploit the potential benefits and limit the unnecessary risks of this technology. In general, the rapid proliferation of many different engineered nanomaterials presents at a moment a dilemma to regulators regarding hazard identification. The International Life Sciences Institute Research Foundation/Risk Science Institute [176] convened an expert working group to develop a screening strategy for the hazard identification of engineered nanomaterials. Based on the evaluation of the limited data currently available, the report presents only a broad data gathering strategy applicable to this very early stage in the development of a risk assessment process for nanomaterials. Oral and dermal inhalation as well as injection routes of exposure must be considered recognizing that, depending on use patterns, exposure to nanomaterials may occur by any of these routes. In particular, three key elements of the toxicity screening strategy have been identified: 1) Physicochemical Characteristics, 2) In Vitro Assays (cellular and non-cellular), 3) In Vivo Assays. It is common opinion that in the next future every new nanomaterial entering the market will need to be screened for toxicity and biopersistence, using low-cost, fast-throughput but scientifically rigorous and standardized tests.

5.0 PERSPECTIVES

Novel potential applications of silver nanocomposites are continuously sought in particular in the biomedical field. Metal nanoparticles-based systems are being considered as a means of minimally invasive diagnostics for early detection of diseases, to facilitate targeted drug delivery and to enhance the effectiveness of selected therapies[177,178]. More specifically, by combining the scattering brightness and biocompatibility of silver nanocomposites, these systems could be employed as a new generation of contrast agents for early diagnosis of human cancer[127].

Liong *et al.*[179] have recently been studying multifunctional silica nanoparticles that incorporate iron oxide, gold or silver for applications in drug delivery, magnetic resonance and fluorescence imaging, magnetic manipulation, and cell targeting. These versatile multifunctional nanoparticles could potentially be used for simultaneous imaging and therapeutic towards cancer cells.

In a different approach, Balogh *et al.*[180] synthesized, by reactive encapsulation, fluorescent poly(amidoamine) dendrimer/silver nanocomposite particles for labeling and selective destruction of cancer cells. To explore biochemical targeting, B16 melanoma cancer cells and KB cells were incubated with the nanocomposite particles; subsequently a laser-induced optical breakdown was able to selectively destroy targeted cells, without affecting viability of others. With this technique a range of effects can be monitored by simultaneous real-time acoustic and optical microscopy. Huang *et al.*[57] suggested the use single-nanoparticle biosensors to quantitatively analyze single ligand and single receptor molecules on single living cells for effective characterization of anticancer vaccines and for a deeper understanding of their biological functions.

The tailorability of the Ag nanoparticles through surface engineering allows for a great variety of *in vivo* applications[126]; therefore, taking advantage of the various desirable properties of AgNPs while protecting the body from harmful side effects is a worthwhile long-term goal. The surface modification of silver nanoparticles appears to be one of the key factors in order to design nanocomposites that can fulfil these expectations.

6.0 BIBLIOGRAPHY

Reference List

1. Prasad, P. N. *Nanophotonics;* Wiley Interscience: 2004.

2. Dai, J. H.; Bruening, M. L. Catalytic nanoparticles formed by reduction of metal ions in multilayered polyelectrolyte films. *Nano Lett.* **2002,** *2* (5), 497-501.

3. Henglein, A. Physicochemical properties of small metal particles in solution: "microelectrode" reactions, chemisorption, composite metal particles, and the atom-to-metal transition. *J. Phys. Chem.* **1993,** *97* (21), 5457-5471.

4. Lok, C. N.; Ho, C. M.; Chen, R.; He, Q. Y.; Yu, W. Y.; Sun, H.; Tam, P.; Chiu, J. F.; Che, C. M. Silver nanoparticles: partial oxidation and antibacterial activities. *Journal of Biological Inorganic Chemistry* **2007,** *12* (4), 527-534.

5. Wang, Y. Z.; Li, Y. X.; Yang, S. T.; Zhang, G. L.; An, D. M.; Wang, C.; Yang, Q. B.; Chen, X. S.; Jing, X. B.; Wei, Y. A convenient route to polyvinyl pyrrolidone/silver nanocomposite by electrospinning. *Nanotechnology* **2006,** *17* (13), 3304-3307.

6. Su, H. L.; Chou, C. C.; Hung, D. J.; Lin, S. H.; Pao, I. C.; Lin, J. H.; Huang, F. L.; Dong, R. X.; Lin, J. J. The disruption of bacterial membrane integrity through ROS generation induced by nanohybrids of silver and clay. *Biomaterials* **2009,** *In Press, Corrected Proof*.

7. Mallick, K.; Witcomb, M. J.; Scurrell, M. S. Polymer stabilized silver nanoparticles: A photochemical synthesis route. *Journal of Materials Science* **2004,** *39* (14), 4459-4463.

8. Esumi, K.; Suzuki, A.; Aihara, N.; Usui, K.; Torigoe, K. Preparation of Gold Colloids with UV Irradiation Using Dendrimers as Stabilizer. *Langmuir* **1998,** *14* (12), 3157-3159.

9. Kuo, P. L.; Chen, W. F. Formation of silver nanoparticles under structured amino groups in pseudo-dendritic poly(allylamine) derivatives. *J. Phys. Chem. B* **2003,** *107* (41), 11267-11272.

10. Grunlan, J. C.; Choi, J. K.; Lin, A. Antimicrobial Behavior of Polyelectrolyte Multilayer Films Containing Cetrimide and Silver. *Biomacromolecules* **2005,** *6* (2), 1149-1153.

11. dos Santos, D. S.; Goulet, P. J. G.; Pieczonka, N. P. W.; Oliveira, O. N.; Aroca, R. F. Gold nanoparticle embedded, self-sustained chitosan films as substrates for surface-enhanced Raman scattering. *Langmuir* **2004,** *20* (23), 10273-10277.

12. Huang, H.; Yuan, Q.; Yang, X. Preparation and characterization of metal-chitosan nanocomposites. *Colloids and Surfaces B: Biointerfaces* **2004,** *39* (1-2), 31-37.

13. Yi, Y.; Wang, Y.; Liu, H. Preparation of new crosslinked chitosan with crown ether and their adsorption for silver ion for antibacterial activities. *Carbohyd. Polym.* **2003,** *53* (4), 425-430.

14. Yu, H.; Xu, X.; Chen, X.; Lu, T.; Zhang, P.; Jing, X. Preparation and Antibacterial Effects of PVA-PVP Hydrogels Containing Silver Nanoparticles. *J Appl Polym Sci* **2006**.

15. Huang, H.; Yang, X. Synthesis of polysaccharide-stabilized gold and silver nanoparticles: a green method. *Carbohyd Res* **2004,** *339* (15), 2627-2631.

16. Fu, J.; Ji, J.; Fan, D.; Shen, J. Construction of antibacterial multilayer films containing nanosilver via layer-by-layer assembly of heparin and chitosan-silver ions complex. *J. Biomed. Mater. Res. A* **2006,** *79* (3), 665-674.

17. Sondi, I.; Goia, D. V.; Matijevic, E. Preparation of highly concentrated stable dispersions of uniform silver nanoparticles. *J. Colloid Interf. Sci.* **2003,** *260* (1), 75-81.

18. Huang, H.; Yuan, Q.; Yang, X. Morphology study of gold-chitosan nanocomposites. *J. Colloid Interf. Sci.* **2005,** *282* (1), 26-31.

19. Bonifacio, A.; van der Sneppen, L.; Gooijer, C.; van der Zwan, G. Citrate-reduced silver hydrosol modified with ω-mercaptoalkanoic acids self-assembled monolayers as a substrate for surface-enhanced resonance raman scattering. A study with cytochrome c. *Langmuir* **2004,** *20* (14), 5858-5864.

20. Pillai, Z. S.; Kamat, P. V. What Factors Control the Size and Shape of Silver Nanoparticles in the Citrate Ion Reduction Method? *The Journal of Physical Chemistry B* **2003,** *108* (3), 945-951.

21. Liu, Z.; Wang, X.; Wu, H.; Li, C. Silver nanocomposite layer-by-layer films based on assembled polyelectrolyte/dendrimer. *Journal of Colloid and Interface Science* **2005,** *287* (2), 604-611.

22. Sun, Y.; Mayers, B.; Herricks, T.; Xia, Y. Polyol Synthesis of Uniform Silver Nanowires: A Plausible Growth Mechanism and the Supporting Evidence. *Nano Lett.* **2003,** *3*, 955-960.

23. Wiley, B.; Herricks, T.; Sun, Y.; Xia, Y. Polyol synthesis of silver nanoparticles: use of chloride and oxygen to promote the formation of single-crystal, truncated cubes and tetrahedrons. *Nano Lett.* **2004,** *4* (9), 1733-1739.

24. Yin, Y.; Lu, Y.; Sun, Y.; Xia, Y. Silver nanowires can be directly coated with amorphous silica to generate well-controlled coaxial nanocables of silver/silica. *Nano Lett.* **2002,** *2* (4), 427-430.

25. Panacek, A.; Kvitek, L.; Prucek, R.; Kolar, M.; Vecerova, R.; Pizurova, N.; Sharma, V. K.; Nevecna, T.; Zboril, R. Silver Colloid Nanoparticles: Synthesis, Characterization, and Their Antibacterial Activity. *J. Phys. Chem. B* **2006,** *110* (33), 16248-16253.

26. Donati, I.; Travan, A.; Pelillo, C.; Scarpa, T.; Coslovi, A.; Bonifacio, A.; Sergo, V.; Paoletti, S. Polyol Synthesis of Silver Nanoparticles: Mechanism of Reduction by Alditol Bearing Polysaccharides. *Biomacromolecules* **2009,** *10* (2), 210-213.

27. Travan, A.; Pelillo, C.; Donati, I.; Marsich, E.; Benincasa, M.; Scarpa, T.; Semeraro, S.; Turco, G.; Gennaro, R.; Paoletti, S. Non-cytotoxic Silver Nanoparticle-Polysaccharide Nanocomposites with Antimicrobial Activity. *Biomacromolecules* **2009,** *10* (6), 1429.

28. Choi, W. S.; Koo, H. Y.; Park, J. H.; Kim, D. Y. Synthesis of Two Types of Nanoparticles in Polyelectrolyte Capsule Nanoreactors and Their Dual Functionality. *J. Am. Chem. Soc.* **2005,** *127* (46), 16136-16142.

29. Ho, C. H.; Tobis, J.; Sprich, C.; Thomann, R.; Tiller, J. C. Nanoseparated Plymeric Network with Multiple Antimicrobial Properties. *Advanced Materials* **2004,** *16* (12), 957-961.

30. Wiley, B.; Sun, Y.; Mayers, B.; Xia, Y. Shape-controlled synthesis of metal nanostructures: the case of silver. *Chem. -Eur. J.* **2005,** *11* (2), 454-463.

31. Balogh, L.; Swanson, D. R.; Tomalia, D. A.; Hagnauer, G. L.; McManus, A. T. Dendrimer-Silver Complexes and Nanocomposites as Antimicrobial Agents. *Nano Lett.* **2001,** *1* (1), 18-21.

32. Rameshbabu, N.; Sampath Kumar, T. S.; Prabhakar, T. G.; Sastry, V. S.; Murty, K. V.; Prasad, R. K. Antibacterial nanosized silver substituted hydroxyapatite: Synthesis and characterization. *J Biomed. Mater. Res. A* **2007,** *80* (3), 581-591.

33. Krkljes, A. N.; Marinovic-Cincovic, M. T.; Kacarevic-Popovic, Z. M.; Nedeljkovic, J. M. Radiolytic synthesis and characterization of Ag-PVA nanocomposites. *European Polymer Journal* **2007,** *43* (6), 2171-2176.

34. Mafune, F.; Kohno, J. y.; Takeda, Y.; Kondow, T.; Sawabe, H. Formation and Size Control of Silver Nanoparticles by Laser Ablation in Aqueous Solution. *The Journal of Physical Chemistry B* **2000,** *104* (39), 9111-9117.

35. Kundu, S.; Mandal, M.; Ghosh, S. K.; Pal, T. Photochemical deposition of SERS active silver nanoparticles on silica gel and their application as catalysts for the reduction of aromatic nitro compounds. *Journal of Colloid and Interface Science* **2004,** *272* (1), 134-144.

36. Zhu, J.; Liu, S.; Palchik, O.; Koltypin, Y.; Gedanken, A. Shape-Controlled Synthesis of Silver Nanoparticles by Pulse Sonoelectrochemical Methods. *Langmuir* **2000,** *16* (16), 6396-6399.

37. Starowicz, M.; Stypula, B.; Banas, J. Electrochemical synthesis of silver nanoparticles. *Electrochemistry Communications* **2006,** *8* (2), 227-230.

38. Yan, X. M.; Ni, J.; Robbins, M.; Park, H. J.; Zhao, W.; White, J. M. Silver Nanoparticles Synthesized by Vapor Deposition onto an Ice Matrix. *Journal of Nanoparticle Research* **2002,** *4* (6), 525-533.

39. Yin, H.; Yamamoto, T.; Wada, Y.; Yanagida, S. Large-scale and size-controlled synthesis of silver nanoparticles under microwave irradiation. *Materials Chemistry and Physics* **2004,** *83* (1), 66-70.

40. Li, K.; Zhang, F. S. A novel approach for preparing silver nanoparticles under electron beam irradiation. *Journal of Nanoparticle Research* **2009**.

41. Braun, E.; Eichen, Y.; Sivan, U.; Ben-Yoseph, G. DNA-templated assembly and electrode attachment of a conducting silver wire. *Nature* **1998,** *391* (6669), 775-778.

42. Lu, Y.; Liu, G. L.; Lee, L. P. High-Density Silver Nanoparticle Film with Temperature-Controllable Interparticle Spacing for a Tunable Surface Enhanced Raman Scattering Substrate. *Nano Lett.* **2005,** *5* (1), 5-9.

43. Deshmukh, R. D.; Composto, R. J. Surface Segregation and Formation of Silver Nanoparticles Created In situ in Poly(methyl Methacrylate) Films. *Chem. Mater.* **2007,** *19* (4), 745-754.

44. Henglein, A. Colloidal Silver Nanoparticles: Photochemical Preparation and Interaction with O2, CCl4, and Some Metal Ions. *Chem. Mater.* **1998,** *10* (1), 444-450.

45. Henglein, A.; Giersig, M. Formation of Colloidal Silver Nanoparticles: Capping Action of Citrate. *J. Phys. Chem. B* **1999,** *103* (44), 9533-9539.

46. Zhang, Y.; Peng, H.; Huang, W.; Zhou, Y.; Yan, D. Facile preparation and characterization of highly antimicrobial colloid Ag or Au nanoparticles. *Journal of Colloid and Interface Science* **2008,** *325* (2), 371-376.

47. Wiley, B.; Sun, Y.; Xia, Y. Synthesis of Silver Nanostructures with Controlled Shapes and Properties. *Accounts of Chemical Research* **2007,** *40* (10), 1067-1076.

48. Wang, T. C.; Rubner, M. F.; Cohen, R. E. Polyelectrolyte Multilayer Nanoreactors for Preparing Silver Nanoparticle Composites: Controlling Metal Concentration and Nanoparticle Size. *Langmuir* **2002,** *18* (8), 3370-3375.

49. Dotzauer, D. M.; Dai, J.; Sun, L.; Bruening, M. L. Catalytic Membranes Prepared Using Layer-by-Layer Adsorption of Polyelectrolyte/Metal Nanoparticle Films in Porous Supports. *Nano Lett.* **2006,** *6* (10), 2268-2272.

50. Malikova, N.; Pastoriza-Santos, I.; Schierhorn, M.; Kotov, N. A.; Liz-Marzan, L. M. Layer-by-Layer Assembled Mixed Spherical and Planar Gold Nanoparticles: Control of Interparticle Interactions. *Langmuir* **2002,** *18* (9), 3694-3697.

51. Csaki, A.; Garwe, F.; Steinbruck, A.; Maubach, G.; Festag, G.; Weise, A.; Riemann, I.; Konig, K.; Fritzsche, W. A Parallel Approach for Subwavelength Molecular Surgery Using Gene-Specific Positioned Metal Nanoparticles as Laser Light Antennas. *Nano Lett.* **2007,** *7* (2), 247-253.

52. Zeng, R.; Rong, M. Z.; Zhang, M. Q.; Liang, H. C.; Zeng, H. M. Laser ablation of polymer-based silver nanocomposites. *Applied Surface Science* **2002,** *187* (3-4), 239-247.

53. Stofik, M.; Str²hal, Z.; Mal², J. Dendrimer-encapsulated silver nanoparticles as a novel electrochemical label for sensitive immunosensors. *Biosensors and Bioelectronics* **2009,** *24* (7), 1918-1923.

54. Lee, K. J.; Nallathamby, P. D.; Browning, L. M.; Osgood, C. J.; Xu, X. H. N. In Vivo Imaging of Transport and Biocompatibility of Single Silver Nanoparticles in Early Development of Zebrafish Embryos. *ACS Nano* **2007,** *1* (2), 133-143.

55. Zhou, J.; Yang, J.; Sun, Y.; Zhang, D.; Shen, J.; Zhang, Q.; Wang, K. Effect of silver nanoparticles on photo-induced reorientation of azo groups in polymer films. *Thin Solid Films* **2007,** *515* (18), 7242-7246.

56. Murthy, P. S. K.; Murali Mohan, Y.; Varaprasad, K.; Sreedhar, B.; Mohana Raju, K. First successful design of semi-IPN hydrogel-silver nanocomposites: A facile approach for antibacterial application. *Journal of Colloid and Interface Science* **2008,** *318* (2), 217-224.

57. Huang, T.; Nallathamby, P. D.; Gillet, D.; Xu, X. H. N. Design and Synthesis of Single-Nanoparticle Optical Biosensors for Imaging and Characterization of Single Receptor Molecules on Single Living Cells. *Anal. Chem.* **2007,** *79* (20), 7708-7718.

58. Lesniak, W.; Bielinska, A. U.; Sun, K.; Janczak, K. W.; Shi, X.; Baker, J. R.; Balogh, L. P. Silver/Dendrimer Nanocomposites as Biomarkers: Fabrication, Characterization, in Vitro Toxicity, and Intracellular Detection. *Nano Lett.* 2005, *5* (11), 2123-2130.

59. Rai, M.; Yadav, A.; Gade, A. Silver nanoparticles as a new generation of antimicrobials. *Biotechnology Advances* **2001,** *27* (1), 76-83.

60. Grishchenko, L.; Medvedeva, S.; Aleksandrova, G.; Feoktistova, L.; Sapozhnikov, A.; Sukhov, B.; Trofimov, B. Redox reactions of arabinogalactan with silver ions and formation of nanocomposites. *Russian Journal of General Chemistry* **2006,** *76* (7), 1111-1116.

61. Chen, J. P. Late angiographic stent thrombosis (LAST): the cloud behind the drug-eluting stent silver lining? *J. Invasive. Cardiol.* **2007,** *19* (9), 395-400.

62. Sanpui, P.; Murugadoss, A.; Prasad, P. V. D.; Ghosh, S. S.; Chattopadhyay, A. The antibacterial properties of a novel chitosan-Ag-nanoparticle composite. *International Journal of Food Microbiology* **2008,** *124* (2), 142-146.

63. Stevens, K. N. J.; Crespo-Biel, O.; van den Bosch, E. E. M.; Dias, A. A.; Knetsch, M. L. W.; Aldenhoff, Y. B. J.; van der Veen, F. H.; Maessen, J. G.; Stobberingh, E. E.; Koole, L. H. The relationship between the antimicrobial effect of catheter coatings containing silver nanoparticles and the coagulation of contacting blood. *Biomaterials* **2009,** *30* (22), 3682-3690.

64. Lu, L.; Sun, R. W.; Chen, R.; Hui, C. K.; Ho, C. M.; Luk, J. M.; Lau, G. K.; Che, C. M. Silver nanoparticles inhibit hepatitis B virus replication. *Antivir. Ther.* **2008,** *13* (2), 253-262.

65. Kim, K. J.; Sung, W. S.; Suh, B. K.; Moon, S. K.; Choi, J. S.; Kim, J. G.; Lee, D. G. Antifungal activity and mode of action of silver nano-particles on Candida albicans. *Biometals* **2009,** *22* (2), 235-242.

66. Esteban-Tejeda, L.; Malpartida, F.; Esteban-Cubillo, A.; Pecharroman, C.; Moya, J. S. The antibacterial and antifungal activity of a soda-lime glass containing silver nanoparticles. *Nanotechnology.* **2009,** *20* (8), 85103.

67. Gajbhiye, M. B.; Kesharwani, J. G.; Ingle, A. P.; Gade, A. K.; Rai, M. K. Fungus-mediated synthesis of silver nanoparticles and their activity against pathogenic fungi in combination with fluconazole. *Nanomedicine.* **2009**.

68. Maki, D. G.; Weise, C. E.; Sarafin, H. W. A semiquantitative culture method for identifying intravenous-catheter-related infection. *N Engl J Med* **1977,** *296* (23), 1305-1309.

69. Sondi, I.; Salopek-Sondi, B. Silver nanoparticles as antimicrobial agent: a case study on E. coli as a model for Gram-negative bacteria. *J Colloid Interface Sci* **2004,** *275* (1), 177-182.

70. Morones, J. R.; Elechiguerra, J. L.; Camacho, A.; Holt, K.; Kouri, J. B.; Ramirez, J. T.; Yacaman, M. J. The bactericidal effect of silver nanoparticles. *Nanotechnology* **2005,** *16* (10), 2346-2353.

71. Pal, S.; Tak, Y. K.; Song, J. M. Does the Antibacterial Activity of Silver Nanoparticles Depend on the Shape of the Nanoparticle? A Study of the Gram-Negative Bacterium Escherichia coli. *Appl. Environ. Microbiol.* **2007,** *73* (6), 1712-1720.

72. Bragg, P. D.; Rainnie, D. J. The effect of silver ions on the respiratory chain of Escherichia coli. *Can. J Microbiol.* **1974,** *20* (6), 883-889.

73. Feng, Q. L.; Wu, J.; Chen, G. Q.; Cui, F. Z.; Kim, T. N.; Kim, J. O. A mechanistic study of the antibacterial effect of silver ions on Escherichia coli and Staphylococcus aureus. *J Biomed. Mater. Res* **2000,** *52* (4), 662-668.

74. Furr, J. R.; Russell, A. D.; Turner, T. D.; Andrews, A. Antibacterial activity of Actisorb Plus, Actisorb and silver nitrate. *J Hosp. Infect.* **1994,** *27* (3), 201-208.

75. Gupta, A.; Matsui, K.; Lo, J. F.; Silver, S. Molecular basis for resistance to silver cations in Salmonella. *Nat Med* **1999,** *5* (2), 183-188.

76. Clement, J. L.; Jarrett, P. S. Antibacterial silver. *Met. Based. Drugs* **1994,** *1* (5-6), 467-482.

77. Elechiguerra, J.; Burt, J.; Morones, J.; Camacho-Bragado, A.; Gao, X.; Lara, H.; Yacaman, M. Interaction of silver nanoparticles with HIV-1. *Journal of Nanobiotechnology* **2005,** *3* (1), 6.

78. Nel, A. Air Pollution-Related Illness: Effects of Particles. *Science* **2005,** *308* (5723), 804-806.

79. Semeykina, A. L.; Skulachev, V. P. Submicromolar Ag+ increases passive Na+ permeability and inhibits the respiration-supported formation of Na+ gradient in Bacillus FTU vesicles. *FEBS Lett* **1990,** *269* (1), 69-72.

80. Hayashi, M.; Miyoshi, T.; Sato, M.; Unemoto, T. Properties of respiratory chain-linked Na(+)-independent NADH-quinone reductase in a marine Vibrio alginolyticus. *Biochim. Biophys. Acta* **1992,** *1099* (2), 145-151.

81. Dibrov, P.; Dzioba, J.; Gosink, K. K.; Hase, C. C. Chemiosmotic mechanism of antimicrobial activity of Ag(+) in Vibrio cholerae. *Antimicrob. Agents Chemother.* **2002,** *46* (8), 2668-2670.

82. Yamanaka, M.; Hara, K.; Kudo, J. Bactericidal actions of a silver ion solution on Escherichia coli, studied by energy-filtering transmission electron microscopy and proteomic analysis. *Appl. Environ. Microbiol.* **2005,** *71* (11), 7589-7593.

83. Castellano, J. J.; Shafii, S. M.; Ko, F.; Donate, G.; Wright, T. E.; Mannari, R. J.; Payne, W. G.; Smith, D. J.; Robson, M. C. Comparative evaluation of silver-containing antimicrobial dressings and drugs. *Int Wound. J* **2007,** *4* (2), 114-122.

84. Sondi, I.; Salopek-Sondi, B. Silver nanoparticles as antimicrobial agent: a case study on E. coli as aámodel for Gram-negative bacteria. *Journal of Colloid and Interface Science* **2004,** *275* (1), 177-182.

85. Lok, C. N.; Ho, C. M.; Chen, R.; He, Q. Y.; Yu, W. Y.; Sun, H.; Tam, P. K. H.; Chiu, J. F.; Che, C. M. Proteomic Analysis of the Mode of Antibacterial Action of Silver Nanoparticles. *J. Proteome Res.* **2006,** *5* (4), 916-924.

86. Kim, J. S.; Kuk, E.; Yu, K. N.; Kim, J. H.; Park, S. J.; Lee, H. J.; Kim, S. H.; Park, Y. K.; Park, Y. H.; Hwang, C. Y.; Kim, Y. K.; Lee, Y. S.; Jeong, D. H.; Cho, M. H. Antimicrobial effects of silver nanoparticles. *Nanomedicine: Nanotechnology, Biology and Medicine* **2007,** *3* (1), 95-101.

87. Choi, O.; Hu, Z. Size dependent and reactive oxygen species related nanosilver toxicity to nitrifying bacteria. *Environ Sci Technol* **2008,** *42* (12), 4583-4588.

88. Pal, S.; Tak, Y. K.; Joardar, J.; Kim, W.; Lee, J. E.; Han, M. S.; Song, J. M. Nanocrystalline silver supported on activated carbon matrix from hydrosol: antibacterial mechanism under prolonged incubation conditions. *J Nanosci. Nanotechnol.* **2009,** *9* (3), 2092-2103.

89. Ayello, E. A.; Cuddigan, J. E. Conquer chronic wounds with wound bed preparation. *Nurse Pract.* **2004,** *29* (3), 8-25.

90. Tomaselli, N. The role of topical silver preparations in wound healing. *J Wound. Ostomy. Continence. Nurs.* **2006,** *33* (4), 367-378.

91. Gray, M.; Ratliff, C. R. Is hyperbaric oxygen therapy effective for the management of chronic wounds? *J Wound. Ostomy. Continence. Nurs.* **2006,** *33* (1), 21-25.

92. Bowler, P. G. Wound pathophysiology, infection and therapeutic options. *Ann Med* **2002,** *34* (6), 419-427.

93. Ip, M.; Lui, S. L.; Poon, V. K.; Lung, I.; Burd, A. Antimicrobial activities of silver dressings: an in vitro comparison. *J Med Microbiol.* **2006,** *55* (Pt 1), 59-63.

94. Ehrlich, H. P. The physiology of wound healing. A summary of normal and abnormal wound healing processes. *Adv. Wound. Care* **1998,** *11* (7), 326-328.

95. Tian, J.; Wong, K. K.; Ho, C. M.; Lok, C. N.; Yu, W. Y.; Che, C. M.; Chiu, J. F.; Tam, P. K. Topical delivery of silver nanoparticles promotes wound healing. *ChemMedChem.* **2007,** *2* (1), 129-136.

96. Olson, M. E.; Wright, J. B.; Lam, K.; Burrell, R. E. Healing of porcine donor sites covered with silver-coated dressings. *Eur J Surg* **2000,** *166* (6), 486-489.

97. Wiegand, C.; Heinze, T.; Hipler, U. C. Comparative in vitro study on cytotoxicity, antimicrobial activity, and binding capacity for pathophysiological factors in chronic wounds of alginate and silver-containing alginate. *Wound. Repair Regen.* **2009,** *17* (4), 511-521.

98. Sibbald, R. G.; Contreras-Ruiz, J.; Coutts, P.; Fierheller, M.; Rothman, A.; Woo, K. Bacteriology, inflammation, and healing: a study of nanocrystalline silver dressings in chronic venous leg ulcers. *Adv. Skin Wound. Care* **2007,** *20* (10), 549-558.

99. Paquet, P.; Pierard, G. E. Invasive atypical fibroxanthoma and eruptive actinic keratoses in a heart transplant patient. *Dermatology* **1996,** *192* (4), 411-413.

100. Biswas, P.; Delfanti, F.; Bernasconi, S.; Mengozzi, M.; Cota, M.; Polentarutti, N.; Mantovani, A.; Lazzarin, A.; Sozzani, S.; Poli, G. Interleukin-6 induces monocyte chemotactic protein-1 in peripheral blood mononuclear cells and in the U937 cell line. *Blood* **1998,** *91* (1), 258-265.

101. Wright, J. B.; Lam, K.; Burrell, R. E. Wound management in an era of increasing bacterial antibiotic resistance: a role for topical silver treatment. *Am J Infect. Control* **1998,** *26* (6), 572-577.

102. Wright, J. B.; Lam, K.; Buret, A. G.; Olson, M. E.; Burrell, R. E. Early healing events in a porcine model of contaminated wounds: effects of nanocrystalline silver on matrix metalloproteinases, cell apoptosis, and healing. *Wound. Repair Regen.* **2002,** *10* (3), 141-151.

103. Vachon, D. J.; Yager, D. R. Novel sulfonated hydrogel composite with the ability to inhibit proteases and bacterial growth. *J Biomed. Mater. Res A* **2006,** *76* (1), 35-43.

104. Walker, M.; Bowler, P. G.; Cochrane, C. A. In vitro studies to show sequestration of matrix metalloproteinases by silver-containing wound care products. *Ostomy. Wound. Manage.* **2007,** *53* (9), 18-25.

105. Rogers, A. A.; Burnett, S.; Moore, J. C.; Shakespeare, P. G.; Chen, W. Y. Involvement of proteolytic enzymes--plasminogen activators and matrix metalloproteinases--in the pathophysiology of pressure ulcers. *Wound. Repair Regen.* **1995,** *3* (3), 273-283.

106. Kahari, V. M.; Saarialho-Kere, U. Matrix metalloproteinases and their inhibitors in tumour growth and invasion. *Ann Med* **1999,** *31* (1), 34-45.

107. Bhol, K. C.; Alroy, J.; Schechter, P. J. Anti-inflammatory effect of topical nanocrystalline silver cream on allergic contact dermatitis in a guinea pig model. *Clin Exp. Dermatol.* **2004,** *29* (3), 282-287.

108. Bhol, K. C.; Schechter, P. J. Topical nanocrystalline silver cream suppresses inflammatory cytokines and induces apoptosis of inflammatory cells in a murine model of allergic contact dermatitis. *Br. J Dermatol.* **2005,** *152* (6), 1235-1242.

109. Nadworny, P. L.; Wang, J.; Tredget, E. E.; Burrell, R. E. Anti-inflammatory activity of nanocrystalline silver in a porcine contact dermatitis model. *Nanomedicine.* **2008,** *4* (3), 241-251.

110. Suska, F.; Svensson, S.; Johansson, A.; Emanuelsson, L.; Karlholm, H.; Ohrlander, M.; Thomsen, P. In vivo evaluation of noble metal coatings. *J Biomed. Mater. Res B Appl. Biomater.* **2009**.

111. Wong, K. K.; Cheung, S. O.; Huang, L.; Niu, J.; Tao, C.; Ho, C. M.; Che, C. M.; Tam, P. K. Further evidence of the anti-inflammatory effects of silver nanoparticles. *ChemMedChem.* **2009,** *4* (7), 1129-1135.

112. Bhol, K. C.; Schechter, P. J. Effects of nanocrystalline silver (NPI 32101) in a rat model of ulcerative colitis. *Dig. Dis Sci* **2007,** *52* (10), 2732-2742.

113. Squier, M. K.; Sehnert, A. J.; Cohen, J. J. Apoptosis in leukocytes. *J Leukoc. Biol* **1995,** *57* (1), 2-10.

114. Savill, J.; Dransfield, I.; Hogg, N.; Haslett, C. Vitronectin receptor-mediated phagocytosis of cells undergoing apoptosis. *Nature* **1990,** *343* (6254), 170-173.

115. Henson, P. M.; Johnston, R. B. Tissue injury in inflammation. Oxidants, proteinases, and cationic proteins. *J Clin Invest* **1987,** *79* (3), 669-674.

116. Anderson, B. O.; Brown, J. M.; Harken, A. H. Mechanisms of neutrophil-mediated tissue injury. *Journal of Surgical Research* **1991,** *51* (2), 170-179.

117. Dive, C.; Gregory, C. D.; Phipps, D. J.; Evans, D. L.; Milner, A. E.; Wyllie, A. H. Analysis and discrimination of necrosis and apoptosis (programmed cell death) by multiparameter flow cytometry. *Biochim Biophys Acta* **1992,** *1133* (3), 275-285.

118. Squier, M. K.; Sehnert, A. J.; Cohen, J. J. Apoptosis in leukocytes. *J Leukoc. Biol* **1995,** *57* (1), 2-10.

119. Tautenhahn, J.; Meyer, F.; Buerger, T.; Schmidt, U.; Lippert, H.; Koenig, W.; Koenig, B. Interactions of neutrophils with silver-coated vascular polyester grafts. *Langenbecks Arch. Surg.* **2008**.

120. Marchi, E.; Vargas, F. S.; Teixeira, L. R.; Acencio, M. M.; Antonangelo, L.; Light, R. W. Intrapleural low-dose silver nitrate elicits more pleural inflammation and less systemic inflammation than low-dose talc. *Chest* **2005,** *128* (3), 1798-1804.

121. Gumpel, J. M. Radioactive colloids in the treatment of arthritis. Review of published and personal results. Criteria for selection of patients. *Ann. Rheum. Dis.* **1973,** *32 Suppl 6*, Suppl-33.

122. Visuthikosol, V.; Kumpolpunth, S. Intra-articular radioactive colloidal gold (198 Au) in the treatment of rheumatoid arthritis. *J. Med. Assoc. Thai.* **1981,** *64* (9), 419-427.

123. Eisler, R. Chrysotherapy: a synoptic review. *Inflamm. Res* **2003,** *52* (12), 487-501.

124. Jessop, J. D. Gold in the treatment of rheumatoid arthritis -- why, when and how? *J Rheumatol Suppl* **1979,** *5*, 12-17.

125. Khlebtsov, N. G.; Dykman, L. A. Optical properties and biomedical applications of plasmonic nanoparticles. *Journal of Quantitative Spectroscopy and Radiative Transfer* **2009,** *In Press, Corrected Proof.*

126. Schrand, A. M.; Braydich-Stolle, L. K.; Schlager, J. J.; Dai, L.; Hussain, S. M. Can silver nanoparticles be useful as potential biological labels? *Nanotechnology* **2008,** *19* (23), 235104.

127. Hu, R.; Yong, K. T.; Roy, I.; Ding, H.; He, S.; Prasad, P. N. Metallic Nanostructures as Localized Plasmon Resonance Enhanced Scattering Probes for Multiplex Dark-Field Targeted Imaging of Cancer Cells. *The Journal of Physical Chemistry C* **2009,** *113* (7), 2676-2684.

128. Kyriacou, S. V.; Brownlow, W. J.; Xu, X. H. N. Using Nanoparticle Optics Assay for Direct Observation of the Function of Antimicrobial Agents in Single Live Bacterial Cells. *Biochemistry* **2004,** *43* (1), 140-147.

129. Qian, X. M.; Nie, S. M. Single-molecule and single-nanoparticle SERS: from fundamental mechanisms to biomedical applications. *Chem Soc Rev* **2008,** *37* (5), 912-920.

130. Jia, X.; Qian, W.; Wu, D.; Wei, D.; Xu, G.; Liu, X. Cuttlebone-derived organic matrix as a scaffold for assembly of silver nanoparticles and application of the composite films in surface-enhanced Raman scattering. *Colloids and Surfaces B: Biointerfaces* **2009,** *68* (2), 231-237.

131. Stoddart, P. R.; Cadusch, P. J.; Boyce, T. M.; Erasmus, R. M.; Comins, J. D. Optical properties of chitin: surface-enhanced Raman scattering substrates based on antireflection structures on cicada wings. *Nanotechnology* **2006,** *17* (3), 680-686.

132. Lansdown, A. B. Silver in health care: antimicrobial effects and safety in use. *Curr Probl. Dermatol.* **2006,** *33*, 17-34.

133. Larese, F. F.; D'Agostin, F.; Crosera, M.; Adami, G.; Renzi, N.; Bovenzi, M.; Maina, G. Human skin penetration of silver nanoparticles through intact and damaged skin. *Toxicology* **2009,** *255* (1-2), 33-37.

134. Um, H. D.; Orenstein, J. M.; Wahl, S. M. Fas mediates apoptosis in human monocytes by a reactive oxygen intermediate dependent pathway. *J Immunol* **1996,** *156* (9), 3469-3477.

135. Talley, A. K.; Dewhurst, S.; Perry, S. W.; Dollard, S. C.; Gummuluru, S.; Fine, S. M.; New, D.; Epstein, L. G.; Gendelman, H. E.; Gelbard, H. A. Tumor necrosis factor alpha-induced apoptosis in human neuronal cells: protection by the antioxidant N-acetylcysteine and the genes bcl-2 and crmA. *Mol. Cell Biol* **1995,** *15* (5), 2359-2366.

136. Zamzami, N.; Marchetti, P.; Castedo, M.; Decaudin, D.; Macho, A.; Hirsch, T.; Susin, S. A.; Petit, P. X.; Mignotte, B.; Kroemer, G. Sequential reduction of mitochondrial transmembrane potential and generation of reactive oxygen species in early programmed cell death. *J Exp. Med* **1995,** *182* (2), 367-377.

137. Lin, M. T.; Beal, M. F. Mitochondrial dysfunction and oxidative stress in neurodegenerative diseases. *Nature* **2006,** *443* (7113), 787-795.

138. Ott, M.; Gogvadze, V.; Orrenius, S.; Zhivotovsky, B. Mitochondria, oxidative stress and cell death. *Apoptosis.* **2007,** *12* (5), 913-922.

139. Braydich-Stolle, L.; Hussain, S.; Schlager, J. J.; Hofmann, M. C. In Vitro Cytotoxicity of Nanoparticles in Mammalian Germline Stem Cells. *Toxicol. Sci.* **2005,** *88* (2), 412-419.

140. Carlson, C.; Hussain, S. M.; Schrand, A. M.; Braydich-Stolle, L. K.; Hess, K. L.; Jones, R. L.; Schlager, J. J. Unique cellular interaction of silver nanoparticles: size-dependent generation of reactive oxygen species. *J Phys. Chem. B* **2008,** *112* (43), 13608-13619.

141. Foldbjerg, R.; Olesen, P.; Hougaard, M.; Dang, D. A.; Hoffmann, H. J.; Autrup, H. PVP-coated silver nanoparticles and silver ions induce reactive oxygen species, apoptosis and necrosis in THP-1 monocytes. *Toxicol. Lett* **2009**.

142. Hsin, Y. H.; Chen, C. F.; Huang, S.; Shih, T. S.; Lai, P. S.; Chueh, P. J. The apoptotic effect of nanosilver is mediated by a ROS- and JNK-dependent mechanism involving the mitochondrial pathway in NIH3T3 cells. *Toxicol. Lett* **2008,** *179* (3), 130-139.

143. Hussain, S. M.; Hess, K. L.; Gearhart, J. M.; Geiss, K. T.; Schlager, J. J. In vitro toxicity of nanoparticles in BRL 3A rat liver cells. *Toxicol In Vitro* **2005,** *19* (7), 975-983.

144. Kim, S.; Choi, J. E.; Choi, J.; Chung, K. H.; Park, K.; Yi, J.; Ryu, D. Y. Oxidative stress-dependent toxicity of silver nanoparticles in human hepatoma cells. *Toxicol. In Vitro* **2009,** *23* (6), 1076-1084.

145. Singh, N.; Manshian, B.; Jenkins, G. J. S.; Griffiths, S. M.; Williams, P. M.; Maffeis, T. G. G.; Wright, C. J.; Doak, S. H. NanoGenotoxicology: The DNA damaging potential of engineered nanomaterials. *Biomaterials* **2009,** *30* (23-24), 3891-3914.

146. Arora, S.; Jain, J.; Rajwade, J. M.; Paknikar, K. M. Cellular responses induced by silver nanoparticles: In vitro studies. *Toxicol. Lett* **2008,** *179* (2), 93-100.

147. Van Den, P. D.; De, S. K.; Lens, D.; Sollie, P. Differential cell death programmes induced by silver dressings in vitro. *Eur J Dermatol.* **2008,** *18* (4), 416-421.

148. Burd, A.; Kwok, C. H.; Hung, S. C.; Chan, H. S.; Gu, H.; Lam, W. K.; Huang, L. A comparative study of the cytotoxicity of silver-based dressings in monolayer cell, tissue explant, and animal models. *Wound. Repair Regen.* **2007,** *15* (1), 94-104.

149. Sionov, R. V.; Haupt, Y. The cellular response to p53: the decision between life and death. *Oncogene* **1999,** *18* (45), 6145-6157.

150. Polster, B. M.; Fiskum, G. Mitochondrial mechanisms of neural cell apoptosis. *J Neurochem.* **2004,** *90* (6), 1281-1289.

151. Mihara, M.; Erster, S.; Zaika, A.; Petrenko, O.; Chittenden, T.; Pancoska, P.; Moll, U. M. p53 has a direct apoptogenic role at the mitochondria. *Mol. Cell* **2003,** *11* (3), 577-590.

152. Ahamed, M.; Karns, M.; Goodson, M.; Rowe, J.; Hussain, S. M.; Schlager, J. J.; Hong, Y. DNA damage response to different surface chemistry of silver nanoparticles in mammalian cells. *Toxicol. Appl. Pharmacol.* **2008,** *233* (3), 404-410.

153. Djordjevic, V. B. Free radicals in cell biology. *Int Rev Cytol.* **2004,** *237*, 57-89.

154. Gilca, M.; Stoian, I.; Atanasiu, V.; Virgolici, B. The oxidative hypothesis of senescence. *J Postgrad. Med* **2007,** *53* (3), 207-213.

155. Simon, H. U.; Haj-Yehia, A.; Levi-Schaffer, F. Role of reactive oxygen species (ROS) in apoptosis induction. *Apoptosis.* **2000,** *5* (5), 415-418.

156. Cha, K.; Hong, H. W.; Choi, Y. G.; Lee, M. J.; Park, J. H.; Chae, H. K.; Ryu, G.; Myung, H. Comparison of acute responses of mice livers to short-term exposure to nano-sized or micro-sized silver particles. *Biotechnol. Lett* **2008,** *30* (11), 1893-1899.

157. Lubick, N. Nanosilver toxicity: ions, nanoparticles--or both? *Environ Sci Technol* **2008,** *42* (23), 8617.

158. Paz-Elizur, T.; Sevilya, Z.; Leitner-Dagan, Y.; Elinger, D.; Roisman, L. C.; Livneh, Z. DNA repair of oxidative DNA damage in human carcinogenesis: potential application for cancer risk assessment and prevention. *Cancer Lett* **2008,** *266* (1), 60-72.

159. Chen, M.; von, M. A. Formation of nucleoplasmic protein aggregates impairs nuclear function in response to SiO2 nanoparticles. *Exp. Cell Res* **2005,** *305* (1), 51-62.

160. Geiser, M.; Rothen-Rutishauser, B.; Kapp, N.; Schurch, S.; Kreyling, W.; Schulz, H.; Semmler, M.; Im, H., V; Heyder, J.; Gehr, P. Ultrafine particles cross cellular membranes by nonphagocytic mechanisms in lungs and in cultured cells. *Environ. Health Perspect.* **2005,** *113* (11), 1555-1560.

161. Nabiev, I.; Mitchell, S.; Davies, A.; Williams, Y.; Kelleher, D.; Moore, R.; Gun'ko, Y. K.; Byrne, S.; Rakovich, Y. P.; Donegan, J. F.; Sukhanova, A.; Conroy, J.; Cottell, D.; Gaponik, N.; Rogach, A.;

Volkov, Y. Nonfunctionalized nanocrystals can exploit a cell's active transport machinery delivering them to specific nuclear and cytoplasmic compartments. *Nano Lett* **2007,** *7* (11), 3452-3461.

162. Yang, W.; Shen, C.; Ji, Q.; An, H.; Wang, J.; Liu, Q.; Zhang, Z. Food storage material silver nanoparticles interfere with DNA replication fidelity and bind with DNA. *Nanotechnology.* **2009,** *20* (8), 85102.

163. Bar-Ilan, O.; Albrecht, R. M.; Fako, V. E.; Furgeson, D. Y. Toxicity assessments of multisized gold and silver nanoparticles in zebrafish embryos. *Small* **2009,** *5* (16), 1897-1910.

164. Rahman, M. F.; Wang, J.; Patterson, T. A.; Saini, U. T.; Robinson, B. L.; Newport, G. D.; Murdock, R. C.; Schlager, J. J.; Hussain, S. M.; Ali, S. F. Expression of genes related to oxidative stress in the mouse brain after exposure to silver-25 nanoparticles. *Toxicol. Lett* **2009,** *187* (1), 15-21.

165. Chen, D.; Xi, T.; Bai, J. Biological effects induced by nanosilver particles: in vivo study. *Biomed. Mater.* **2007,** *2* (3), S126-S128.

166. Alt, V.; Bechert, T.; Steinrucke, P.; Wagener, M.; Seidel, P.; Dingeldein, E.; Domann, E.; Schnettler, R. An in vitro assessment of the antibacterial properties and cytotoxicity of nanoparticulate silver bone cement 9. *Biomaterials* **2004,** *25* (18), 4383-4391.

167. Wen, H. C.; Lin, Y. N.; Jian, S. R.; Tseng, S. C.; Weng, M. X.; Liu, Y. P.; Lee, P. T.; Chen, P. Y.; Hsu, R. Q.; Wu, W. F.; Chou, C. P. Observation of Growth of Human Fibroblasts on Silver Nanoparticles. *Journal of Physics: Conference Series* **2007,** *61*, 445-449.

168. Bosetti, M.; Masse, A.; Tobin, E.; Cannas, M. Silver coated materials for external fixation devices: in vitro biocompatibility and genotoxicity. *Biomaterials* **2002,** *23* (3), 887-892.

169. Bianchini, A.; Bowles, K. C.; Brauner, C. J.; Gorsuch, J. W.; Kramer, J. R.; Wood, C. M. Evaluation of the effect of reactive sulfide on the acute toxicity of silver (I) to Daphnia magna. Part 2: toxicity results. *Environ. Toxicol. Chem.* **2002,** *21* (6), 1294-1300.

170. Wood, C. M.; McDonald, M. D.; Walker, P.; Grosell, M.; Barimo, J. F.; Playle, R. C.; Walsh, P. J. Bioavailability of silver and its relationship to ionoregulation and silver speciation across a range of salinities in the gulf toadfish (Opsanus beta). *Aquat. Toxicol.* **2004,** *70* (2), 137-157.

171. Wang, W. X. Comparison of metal uptake rate and absorption efficiency in marine bivalves. *Environ. Toxicol. Chem.* **2001,** *20* (6), 1367-1373.

172. Choi, O. K.; Hu, Z. Q. Nitrification inhibition by silver nanoparticles. *Water Sci Technol.* **2009,** *59* (9), 1699-1702.

173. Griffitt, R. J.; Luo, J.; Gao, J.; Bonzongo, J. C.; Barber, D. S. Effects of particle composition and species on toxicity of metallic nanomaterials in aquatic organisms. *Environ. Toxicol. Chem.* **2008,** *27* (9), 1972-1978.

174. Colvin, V. L. The potential environmental impact of engineered nanomaterials. *Nat Biotech* **2003,** *21* (10), 1166-1170.

175. Hoet, P. H.; Nemmar, A.; Nemery, B. Health impact of nanomaterials? *Nat. Biotechnol.* **2004,** *22* (1), 19.

176. Oberdorster, G.; Maynard, A.; Donaldson, K.; Castranova, V.; Fitzpatrick, J.; Ausman, K.; Carter, J.; Karn, B.; Kreyling, W.; Lai, D.; Olin, S.; Monteiro-Riviere, N.; Warheit, D.; Yang, H. Principles for characterizing the potential human health effects from exposure to nanomaterials: elements of a screening strategy. *Part Fibre. Toxicol.* **2005,** *2*, 8.

177. Wieder, M. E.; Hone, D. C.; Cook, M. J.; Handsley, M. M.; Gavrilovic, J.; Russell, D. A. Intracellular photodynamic therapy with photosensitizer-nanoparticle conjugates: cancer therapy using a 'Trojan horse'. *Photochemical & Photobiological Sciences 5* (8), 727-734.

178. Zharov, V. P.; Mercer, K. E.; Galitovskaya, E. N.; Smeltzer, M. S. Photothermal nanotherapeutics and nanodiagnostics for selective killing of bacteria targeted with gold nanoparticles. *Biophys. J.* **2005,** biophysj.

179. Liong, M.; Lu, J.; Kovochich, M.; Xia, T.; Ruehm, S. G.; Nel, A. E.; Tamanoi, F.; Zink, J. I. Multifunctional Inorganic Nanoparticles for Imaging, Targeting, and Drug Delivery. *ACS Nano* **2008,** *2* (5), 889-896.

180. Balogh, L. P.; Tse, C.; Lesniak, W.; Ye, J.; O'Donnell, M.; Khan, M. K. Photomechanical therapy: destruction of nanocomposite labeled cells by laser induced optical breakdown. *Nanomedicine: Nanotechnology, Biology and Medicine* **2007,** *3* (4), 350.